

THE RECOVERY OF SODIUM HYDROXIDE FROM COTTON SCOURING EFFLUENTS

by



Alison Elizabeth Simpson BSc(Hons)


Submitted in fulfilment of the academic requirements for the degree of
Doctorate of Philosophy in the Department of Chemical Engineering,
University of Natal

Pollution Research Group
Department of Chemical Engineering
University of Natal
Durban

December 1994

DECLARATION

I, Alison Elizabeth Simpson, declare that the work embodied in this thesis is my own original work, except as otherwise acknowledged in the text, and has not been submitted for degree purposes at any other University or Institution.


.....
15 December 1994

ACKNOWLEDGEMENTS

I acknowledge, with gratitude, the tireless support, encouragement and efforts of my supervisor, Professor Chris Buckley.

This thesis results from a three year contract, awarded in 1983, by the Water Research Commission, to the Pollution Research Group, in the Chemical Engineering Department, of the University of Natal, Durban. The contract was extended for a year in 1986, and for a further six months, in 1987. Additional financial support was provided by Da Gama Textiles in Zwelitsha, the then Ciskei Republic.

The efforts and contributions of the many people in the Textile Industry, the Pollution Research Group, the Department of Chemical Engineering, the Department of Chemistry, and the Water Research Commission are gratefully acknowledged.

I would also like to express my appreciation to others who assisted:

Dr OO Hart, chairman of the steering committee for the Water Research Commission Project, for his guidance and interest over the years;

Prof Ferdinand Neytzell-de Wilde, Dr Carol Kerr, Mr David Cohen, Mr Praveen Naicker and Mr Bruce Townsend of the Pollution Research Group, for their contributions to laboratory and pilot-plant studies;

Dr John Durrans, Mr Lindela Klaus and other staff at Da Gama Textiles for their enthusiasm, hospitality, assistance and support;

Dr Lingham Pillay and Mr Quentin Hurt for their assistance in regression and drawing respectively;

Dr Carol Kerr and Mr Chris Brouckaert for their advice on speciation modelling and membrane transport respectively;

Mrs Loveena Kissoon for administrative assistance;

Without the encouragement of my parents, my husband and my work colleagues, this thesis may not have developed beyond the requirements of a Masters degree. I appreciate their efforts.

ABSTRACT

This dissertation describes the characterisation of, and development of a novel integrated waste management strategy for, hydroxide scouring effluents produced during cotton processing. Such effluents are typical of mineral salt-rich waste waters which are not significantly biodegradable in conventional treatment plants. The proposed strategy focuses on two complementary concepts: **process-oriented waste minimisation** adopts a systematic approach to identifying potential problems and solutions of waste reduction in the manufacturing process itself; while **add-on controls** reduce the impact of the waste after it has been generated, by recycling and treatment.

The basic procedures for ensuring effective water and chemical management within the scouring process are described. Examples are given of factory surveys, which have resulted in significant chemical and water savings, reduced effluent discharge costs, maximum effluent concentration, and minimum pollutant loading and volume.

Pilot-plant investigations demonstrate the technical and economic feasibility of a four stage treatment sequence of neutralisation (using carbon dioxide gas), cross-flow microfiltration, nanofiltration and electrochemical recovery to remove colour and impurities from the scouring effluent and produce directly reusable sodium hydroxide and water. Fouling and scaling of the cross-flow microfiltration, nanofiltration and electrochemical membranes are minimal and reversible if the operation is carried out under carefully selected conditions. A long anode coating life is predicted. Current efficiencies for the recovery of sodium hydroxide (up to 20 % concentration) are 70 to 80 % and the electrical power requirements are 3 500 to 4 000 kWh/tonne of 100 % NaOH.

Pilot-plant trials are supplemented by extensive laboratory tests and semi-quantitative modelling to examine specific aspects of the nanofiltration and electrochemical stages in detail. Electromembrane fouling and cleaning techniques, and other anode materials are evaluated. The effects of solution speciation chemistry on the performance of the nanofiltration membrane is evaluated using a combination of speciation and membrane transport modelling and the predicted results are used to explain observed behaviour.

Based on the results of pilot-plant trials and supplementary laboratory and theoretical work, a detailed design of an electrochemically-based treatment system and an economic analysis of the electrochemical recovery system are presented. The effects of rinsing variables, processing temperatures, and background rinse water concentrations on the plant size requirements and capital costs are determined.

The implementation of the waste management concepts presented in this dissertation will have significant impact on water and sodium hydroxide consumption (decreasing these by up to 95 and 75 % respectively), as well as effluent volumes and pollutant loadings.

TABLE OF CONTENTS

SECTION 1

INTRODUCTION

1.1.	Water Resources	1-1
1.1.1.	Water Supply	1-1
1.1.2.	Water Quality	1-2
1.2.	Management of Industrial Pollutants	1-2
1.3.	Management of Textile Waste Water	1-2
1.4.	Specific Objectives	1-3
1.5.	General Comments	1-5

SECTION 2

THE TEXTILE INDUSTRY - AN OVERVIEW OF ENVIRONMENTAL LEGISLATION, MANUFACTURING OPERATIONS AND SCOURING

2.1.	Water Use in Textile Processing	2-1
2.2.	The Need for Water Pollution Control in Textile Processing	2-2
2.3.	Regulatory Control of Water Use and Wastewater Discharge	2-3
2.3.1.	The Water Act	2-3
2.3.2.	Strategy and Policy Guidelines	2-4
2.3.3.	Industry-Based Recycling and Reclamation	2-7
2.4.	Textile Processing	2-8
2.4.1.	Textile Fibres	2-8
2.4.2.	Textile Processing Operations	2-8
2.4.3.	Textile Mill Classification	2-11
2.5.	Scouring Technology	2-13
2.5.1.	Identification of Potentially Most Polluting Scouring Processes	2-14
2.5.2.	Scouring of Cotton and Cotton-Blends	2-14
2.6.	Characterisation of Cotton Scouring Effluents	2-19
2.6.1.	Batch vs Continuous Rinsing	2-19
2.6.2.	Chemical Composition	2-20
2.6.3.	Pollutant Loading	2-20

SECTION 3

ENVIRONMENTAL MANAGEMENT OPTIONS FOR POLLUTION CONTROL IN SCOURING PROCESSES

3.1.	Waste Management by Waste Avoidance and Minimisation	3-2
3.1.1.	Process Redesign	3-3
3.1.2.	Process Optimisation	3-4
3.1.3.	Equipment Selection	3-8
3.1.4.	Housekeeping	3-8
3.2.	Waste Management by Treatment, Recovery and Disposal	3-10
3.2.1.	Review of Options for Recovery and Reuse of Scouring Effluents	3-12
3.2.2.	Review of Treatment Options Prior to Discharge of Scouring Effluents	3-18

SECTION 4

CHEMICAL, WATER AND WASTE WATER MANAGEMENT IN SCOURING PROCESSES

4.1.	Analysis of Sodium Hydroxide Consumption	4-1
4.1.1.	Survey Results	4-2
4.1.2.	Discussion of Survey Results	4-4
4.1.3.	Recommendations for Improved Chemical Management	4-6
4.2.	Analysis of Rinsing Water Use	4-6
4.2.1.	Rinsing and Washing Theory	4-7
4.2.2.	Batch Rinsing	4-7
4.2.3.	Continuous Rinsing	4-8

4.2.4.	Development of a General Matrix for Analysis of Rinsing Ranges.....	4-14
4.2.5.	Analysis of Four-Bowl Counter-Current Scour Rinsing Range.....	4-15
4.3.	Practical Application of Rinsing Theory to Scouring.....	4-23
4.3.1.	Description of Scouring Operation.....	4-23
4.3.2.	Empirical Verification of Predicted Rinsing Parameters	4-23
4.3.3.	Influence of Rinsing Variables on Operation of Proposed Recovery Plant.....	4-24
4.3.4.	Recommendations for the Operation of the Scouring Range.....	4-24

SECTION 5

DEVELOPMENT, DESCRIPTION AND THEORY OF RECOVERY PROCESS

5.1.	Description of Process Sequence	5-1
5.2.	Novelty and Advantages of Process Sequence.....	5-3
5.3.	Process Chemistry.....	5-4
5.4.	Description of Individual Process Stages.....	5-7
5.4.1.	Neutralisation.....	5-7
5.4.2.	Cross-Flow Microfiltration.....	5-7
5.4.3.	Nanofiltration.....	5-9
5.4.3.1.	Applications	5-10
5.4.3.2.	Membrane Characteristics	5-11
5.4.3.3.	Osmotic Pressure Predictions	5-14
5.4.3.4.	Membrane Transport Theories.....	5-15
5.4.3.5.	System Specific Features.....	5-23
5.4.3.6.	Membrane Transport Modelling for Carbonate Solutions	5-24
5.4.4.	Electrochemical Recovery	5-27
5.4.4.1.	Electrochemical Cell.....	5-29
5.4.4.2.	Kinetic Overpotential	5-31
5.4.4.3.	Concentration Polarisation	5-31
5.4.4.4.	Cell Resistance.....	5-33
5.4.4.5.	Exchange Current	5-35
5.4.4.6.	Current Efficiency and Power	5-35
5.4.4.7.	Electrodes	5-38
5.4.4.8.	Electromembranes	5-39
5.4.4.9.	Cell Design.....	5-45
5.5.	Chemical Recovery Potential of the Process Sequence.....	5-46

SECTION 6

EXPERIMENTAL PROCEDURES

6.1.	Pilot-Plant Design.....	6-1
6.1.1.	Neutralisation Unit.....	6-1
6.1.2.	Cross-Flow Microfiltration Unit	6-1
6.1.3.	Nanofiltration Unit	6-4
6.1.4.	Electrochemical Recovery Unit	6-5
6.2.	Experimental Procedures and Trials	6-7
6.3.	Supplementary Investigations of Nanofiltration	6-9
6.3.1.	Effect of Electrolyte Characteristics on Nanofilter Performance	6-9
6.3.2.	Effect of Chelating Agents on Nanofilter Performance.....	6-11
6.3.3.	Chemical Speciation Modelling of Nanofiltration.....	6-11
6.3.4.	Transport Modelling of Nanofiltration.....	6-13
6.3.5.	Supplementary Experimentation for Quantitative Explanation of Membrane Performance and PREMSEP Development.....	6-15
6.4.	Supplementary Investigations of Electrolysis.....	6-16
6.4.1.	Electromembrane Fouling.....	6-16
6.4.2.	Electromembrane Cleaning.....	6-19
6.4.3.	Other Electrodes.....	6-21

SECTION 7

RESULTS AND DISCUSSION OF PILOT PLANT TRIALS

7.1.	Effect of Treatment Sequence on Scouring Effluent.....	7-2
7.2.	Neutralisation	7-2
7.3.	Cross-Flow Microfiltration.....	7-3
7.4.	Nanofiltration.....	7-4
7.5.	Electrochemical Recovery	7-6
7.5.1.	Current Efficiency	7-6
7.5.2.	Power Consumption and Cost.....	7-8
7.5.3.	Flow Distribution.....	7-10
7.5.4.	Limiting Current Densities	7-11
7.5.5.	Effects of Anolyte Concentration.....	7-12
7.5.6.	Temperature Effects.....	7-13
7.5.7.	Dimensionally Stable Anode Performance.....	7-14
7.5.8.	Electromembrane Performance	7-15
7.5.9.	Recovery of Sodium Salts	7-17
7.5.10.	Water Transport	7-18
7.5.11.	Background Concentration Closed-Loop Recycle.....	7-18

SECTION 8

RESULTS AND DISCUSSION OF SUPPLEMENTARY INVESTIGATIONS OF NANOFILTRATION

8.1.	Effect of Electrolyte Characteristics on Nanofilter Performance	8-1
8.1.1.	Effect of pH and Concentration of Sodium Salts on Membrane Retention.....	8-2
8.1.2.	Effect of pH and Concentration of Sodium Salts on Membrane Flux ...	8-4
8.1.3.	Effect of pH on Membrane Retention of Divalent Ions.....	8-5
8.2.	Effect of Chelating Agents on Nanofilter Performance.....	8-6
8.3.	Chemical Speciation Modelling of Nanofiltration.....	8-7
8.3.1.	Pure Sodium Carbonate Solutions.....	8-8
8.3.1.1.	Equilibrium Speciation Concentrations.....	8-8
8.3.1.2.	Mass Distribution of System Components	8-10
8.3.1.3.	Charge Distribution of Equilibrium Species	8-14
8.3.2.	Impure Sodium Carbonate Solutions.....	8-16
8.3.2.1.	Equilibrium Species Concentration	8-17
8.3.2.2.	Equilibrium Mass Distribution.....	8-19
8.3.2.3.	Saturated Solids and Precipitation	8-23
8.4.	Semi-Quantitative Explanation of Nanofiltration Performance.....	8-25
8.4.1.	Osmotic Pressure Variations.....	8-26
8.4.2.	Concentration Polarisation	8-27
8.4.3.	Determination of Water Permeability Constant, A	8-28
8.4.4.	Water Flux Dependence on Solution Characteristics.....	8-30
8.4.5.	Solute Flux Dependence on Solution Characteristics.....	8-32
8.4.6.	pH Variation Across the Membrane	8-34
8.4.7.	Impure Sodium Carbonate Solutions.....	8-37
8.4.7.1.	Solutions Without EDTA Complexation.....	8-38
8.4.7.2.	Solutions With EDTA Complexation	8-39
8.5.	Transport Modelling of Nanofiltration	8-40

SECTION 9

RESULTS AND DISCUSSION OF SUPPLEMENTARY INVESTIGATIONS OF ELECTROLYSIS

9.1.	Electromembrane Fouling.....	9-1
9.1.1.	Electromembrane Area-Resistance.....	9-1
9.1.2.	Effect of Hardness-Ion Concentration on Area-Resistance	9-2
9.1.3.	Current Efficiencies	9-7
9.1.4.	Restoration of Cell Performance	9-8
9.1.5.	Scale Characterisation and Mechanism of Deposition.....	9-10
9.2.	Electromembrane Cleaning.....	9-11
9.2.1.	Scale Characterisation.....	9-12

9.2.2.	Comparison of Effectiveness of Cleaning Techniques	9-13
9.2.3.	Selection of a Suitable Scale Control Technique.....	9-15
9.3.	Other Electrodes.....	9-17
9.3.1.	Stainless Steel Anodes.....	9-17
9.3.2.	Nickel Anodes.....	9-18

SECTION 10

DESIGN OF A PLANT FOR THE ELECTROCHEMICAL RECOVERY OF STRONG SCOURING EFFLUENTS

10.1.	Design Example	10-1
10.2.	General Considerations.....	10-2
10.2.1.	Textile Processing Considerations	10-3
10.2.2.	Pretreatment Requirements	10-3
10.2.3.	Scaling Prevention.....	10-4
10.2.4.	Membrane Selection and Module Arrangement	10-4
10.3.	Design Basis	10-5
10.4.	Specification of Batch Neutralisation Unit.....	10-6
10.4.1.	Equipment	10-6
10.4.2.	Sizing.....	10-8
10.5.	Specification of Batch Cross-Flow Microfiltration Unit.....	10-9
10.5.1.	Equipment	10-9
10.5.2.	Sizing.....	10-11
10.5.3.	Design Configuration	10-12
10.5.4.	Overall Performance.....	10-12
10.6.	Specification of Batch Nanofiltration Unit	10-12
10.6.1.	Equipment	10-12
10.6.2.	Sizing.....	10-15
10.6.3.	Design Configuration	10-17
10.6.4.	Overall Performance.....	10-18
10.7.	Specification of Electrochemical Recovery Unit.....	10-18
10.7.1.	Equipment	10-18
10.7.2.	Sizing.....	10-23
10.8.	Synopsis of Design Specifications and Performance.....	10-23
10.9.	Economic Evaluation	10-24
10.9.1.	Capital Cost Estimate.....	10-27
10.9.2.	Operating Costs.....	10-28
10.9.3.	Savings.....	10-29

SECTION 11

CONCLUSIONS AND RECOMMENDATIONS

REFERENCES

NOMENCLATURE

APPENDIX 1: Candidate's Publications List

APPENDIX 2: Modifications of Rinsing Equations for Four-Bowl Counter-Current Rinse Range

APPENDIX 3: Dependence of Rinsing Performance on Nip Expression Combination and Specific Water Use in a Four-Bowl Counter-Current Rinse Range

APPENDIX 4: Washing Characteristics and Performance Dependence on Wash Water Concentration for Three Drag-Out Combinations in a Four-Bowl Counter-Current Rinse Range

APPENDIX 5: Comments on Analytical Methods and Operational Procedures for Individual Pilot-Plant Experiments

APPENDIX 6: Pilot-Plant Investigations

APPENDIX 7: Supplementary Investigations into Performance, Speciation and Modelling of Nanofiltration

APPENDIX 8: Supplementary Investigations into Electromembrane Fouling

APPENDIX 9: Supplementary Investigations into Electromembrane Cleaning

APPENDIX 10: Supplementary Investigations into Other Anode Materials

APPENDIX 11: Spread Sheet for Design Calculations

LIST OF TABLES

Table 2.1	The South African Water Act, 1956 (Act 54 of 1956), General and Specific Standards for Discharge	2-5
Table 2.2	Target Guideline Ranges for Specific Water Quality Variables, Textile Industry	2-7
Table 2.3	Examples of Typical Compositions of Strong Scouring Effluents	2-20
Table 2.4	Relative Pollutant Loadings from Individual Textile Unit Operations	2-21
Table 3.1	Results of Cascade Trials at a Cotton Processing Mill	3-7
Table 3.2	Options for Improving Effluent Characteristics	3-12
Table 4.1	Survey Data Summary	4-3
Table 4.2	Overall Sodium Hydroxide Balance	4-3
Table 4.3	Selected Drag-Out Combinations	4-18
Table 4.4	Predicted Rinsing Efficiency and Effluent Concentration for Nip Expression Configuration Cases	4-18
Table 4.5	Results of Rinsing Trials	4-24
Table 5.1	Comparison of Electrochemical Process with Conventional Chlor-Alkali Processes	5-28
Table 5.2	Properties of Nafion® Membranes	5-42
Table 6.1	Summary of Pilot-Plant Specifications	6-2
Table 6.2	Nanofiltration Membranes: Manufacturer's Specifications	6-4
Table 6.3	Characterisation of Scouring Effluent	6-8
Table 6.4	Summary of Experimental Conditions for Nanofiltration Modelling Experiments	6-15
Table 6.5	Summary of Experimental Procedure for Electromembrane Cleaning	6-21
Table 7.1	Average Composition of Scouring Effluent After Each Stage of the Treatment Sequence	7-2
Table 7.2	Point Retentions for Cross-Flow Microfiltration (%)	7-4
Table 7.3	Point Retentions for Nanofiltration (%)	7-5
Table 7.4	Summary of Electrolysis Results	7-7
Table 7.5	Summary of Power Consumptions and Costs for Sodium Hydroxide Recovery	7-9
Table 7.6	Recovery of Sodium and Inorganic Carbon Species from Anolyte	7-17
Table 7.7	Water Transport Numbers	7-19
Table 8.1	Summary of Calculated Flux, pH and Effective Pressure Values for Experiments 6, 7 and 8	8-26
Table 8.2	Water Fluxes: Correlation of Discontinuities in Water Flux with Speciation Trends	8-31

Table 8.3	Solute Fluxes: Correlation of Discontinuities in Water Flux with Speciation Trends	8-33
Table 8.4	Gradient in Hydrogen Ion Concentration Across the Membrane During Nanofiltration of Sodium Carbonate Solutions at Varying pH and Concentration	8-36
Table 9.1	Mass Balance for Divalent Cations	9-6
Table 9.2	Summary of Cleaning and Performance Results	9-12
Table 9.3	Summary of Results of Pilot-Plant Tests Using Nickel Anodes	9-20
Table 9.4	Summary of Results of Laboratory Tests Using Anodes	9-20
Table 10.1	Comparison of Rinsing Processes	10-2
Table 10.2	Design Data for Treatment Sequence	10-5
Table 10.3	Batch Neutralisation Equipment Requirements	10-7
Table 10.4	Batch Cross-Flow Microfiltration Equipment Requirements	10-9
Table 10.5	Cross-Flow Microfiltration: Design Specifications, Calculations and Performance	10-13
Table 10.6	Batch Neutralisation Equipment Requirements	10-14
Table 10.7	Nanofiltration: Design Specifications, Calculations and Performance	10-16
Table 10.8	Characteristics of Bipolar Cells in Comparison With Monopolar Cells	10-19
Table 10.9	Batch Electrochemical Unit Specifications	10-20
Table 10.10	Electrochemical Unit Specifications and Operating Characteristics	10-23
Table 10.11	Design Example: Process Data on a Dry Fabric Basis, Variable Rinse Water Concentration	10-25
Table 10.12	Typical Costs of Chemicals and Utilities	10-26
Table 10.13	Capital Cost Estimation	10-29
Table 10.14	Operating Costs Estimation	10-30
Table 10.15	Potential Savings	10-30

LIST OF FIGURES

Figure 1.1	Success Cycle	1-6
Figure 2.1	Production of Fabric	2-9
Figure 2.2	Textile Industry Categorisation by Fibre Processed	2-11
Figure 2.3	Woven Cotton Fabric Finishing Mill	2-12
Figure 2.4	Knit Fabric Finishing Mill	2-13
Figure 2.5	Stock Yarn Dyeing and Finishing Mill	2-13
Figure 2.6	Schematic of a Rope or J-Box Rinsing Range	2-17
Figure 2.7	Schematic of an Open-Width Rinsing Range	2-18
Figure 2.8	Acceptable Saponification Limits of Polyester as a Function of Sodium Hydroxide Concentration, Temperature and Contact Time	2-18
Figure 3.1	Effluent Management options for Scouring Process	3-2
Figure 3.2	Dependence of Impurity Removal on Specific Water Use for Three Rinsing Ranges	3-7
Figure 3.3	Schematic of Electro-Oxidation Process	3-14
Figure 4.1	Sodium Hydroxide Distribution System Within Factory	4-2
Figure 4.2	Sodium Hydroxide Balance at a Particular Factory	4-4
Figure 4.3	Sodium Hydroxide Losses at a Particular Factory	4-5
Figure 4.4	Comparison of Water Uses of Various Rinse Machines	4-8
Figure 4.5	Dependence of Impurity on Specific Water Use	4-10
Figure 4.6	Rinsing Water Dilution vs Rinse Ratio for a Counter-Current Multi-Unit Rinse Range	4-12
Figure 4.7	Dependence of Recovery Potential on Rinse Ratio	4-13
Figure 4.8	Determination of Chemical Concentration of First Rinse Bowl	4-13
Figure 4.9	Dependence of Impurity Removal on Specific Water Use for Counter-Current and Cross-Flow Rinsing Ranges where $k = 0,3$	4-14
Figure 4.10	Schematic of Material Flows in a Multi-Unit Counter-Current Rinse Range	4-14
Figure 4.11	Mass Balance for a Four-Bowl Counter-Current Rinse Range	4-16
Figure 4.12	Determination of Rinsing Parameter, k	4-17
Figure 4.13	Dependence of Rinsing Efficiencies on Nip Expression and Specific Water Use	4-19
Figure 4.14	Dependence of Effluent Concentration on Nip Expression and Specific Water Use	4-20
Figure 4.15	Dependence of Rinsing Efficiency on Rinsing Water Impurity Level	4-21
Figure 4.16	Dependence of Effluent Concentration on Rinsing Water Impurity Level	4-22
Figure 4.17	Dependence of Effluent Mass Loading on Rinsing Water Impurity Level	4-22

Figure 4.18	Dependence of Cloth Mass Loading on Rinsing Water Impurity Level	4-23
Figure 5.1	Process Sequence for the Recovery and Recycle of Scouring Effluents	5-1
Figure 5.2	Schematic of Electrochemical Membrane Cell	5-2
Figure 5.3	Distribution of Carbonate Species with pH at 20 °C	5-4
Figure 5.4	Number of papers on Nanofiltration Listed in Chemical Abstracts	5-9
Figure 5.5	Spectrum of Application of Membrane Separation Processes	5-12
Figure 5.6	Illustration of Three Types of Transport Showing Increased Concentration of Solute in the Boundary Layer with Decreasing the Membrane Surface	5-17
Figure 5.7	Relationship Between Conductivity, Concentration and Temperature of Sodium Bicarbonate in Solution	5-34
Figure 5.8	Relationship Between Conductivity, Concentration and Temperature of Sodium Hydroxide in Solution	5-34
Figure 5.9	Nafion® Membrane Performance	5-42
Figure 6.1	Schematic Diagram of Neutralisation Unit	6-3
Figure 6.2	Schematic Diagram of Cross-Flow Microfiltration Unit	6-3
Figure 6.3	Schematic Diagram of Nanofiltration Unit	6-5
Figure 6.4	Schematic Diagram of Electrochemical Unit	6-6
Figure 6.5	Schematic Diagram of Laboratory Nanofiltration Rig	6-10
Figure 6.6	Schematic Diagram of Fouling Apparatus	6-17
Figure 6.7	End and Side View of Flow-Through Cell Showing Position of Platinum Probes	6-18
Figure 6.8	Schematic Diagram of Laboratory Apparatus for Electromembrane Cleaning	6-28
Figure 7.1	Relationship Between Anolyte Flow Rate and Volt Drop	7-11
Figure 7.2	Experimentally Observed Relationship Between Achievable Current Density and Anolyte Concentration	7-12
Figure 7.3	Relationship Between the Anolyte Concentration and pH	7-13
Figure 7.4	Initial Current Density for Each Experiment	7-15
Figure 7.5	Effect of Anolyte Sodium Concentration on Water Transport Numbers	7-20
Figure 7.6	Closed-Loop Recycle of Rinse Water with a Background Concentration	7-21
Figure 8.1	Distribution of Inorganic Carbon Species Between Nanofiltrate Permeate and Feed Over a Range of pH Values	8-2
Figure 8.2	Dependence of Membrane Na Retention on Feed pH and Salt Concentration	8-3
Figure 8.3	Dependence of Membrane Anion Retentions on Feed pH and Salt Concentration	8-4
Figure 8.4	Dependence of Membrane Flux on Feed and Salt Concentration	8-5

Figure 8.5	Dependence of Membrane Retention of Divalent Cations on pH of Sodium Carbonate/Bicarbonate Solution (10 g/l Na)	8-5
Figure 8.6	pH Effect of a Sodium Carbonate/Bicarbonate Solution (10 g/l Na) on Na:Ca and Na:Mg Retention Ratios	8-7
Figure 8.7	Equilibrium Concentrations of Dominant Species Present in Sodium Carbonate Solutions of Varying Strength and pH	8-9
Figure 8.8	Equilibrium Composition Showing Mass Distribution Between Dissolved Species of Inorganic Carbon Present in Sodium Carbonate Solutions of Varying Strength and pH	8-11
Figure 8.9	Equilibrium Composition Showing Mass Distribution Between Dissolved Species of Sodium Present in Sodium Carbonate Solutions of Varying Strength and pH	8-13
Figure 8.10	Distribution of Total Charge in Sodium Carbonate Solutions of Varying Strength and pH	8-15
Figure 8.11	Equilibrium Concentration of Ca- and Mg-Containing Species in a Sodium Carbonate Solutions Containing 10 g/l Na, and at Different pH Values	8-17
Figure 8.12	Equilibrium Concentration of Ca- and Mg-Containing Species in a Sodium Carbonate Solutions Containing 10 g/l Na and 100 mg/l EDTA, and at Different pH Values	8-20
Figure 8.13	Mass Distribution of Ca and Mg Between the Species at Equilibrium in a Sodium Carbonate Solution Containing 10 g/l Na	8-21
Figure 8.14	Mass Distribution of EDTA, Ca and Mg Between the Species at Equilibrium in a Sodium Carbonate Solution Containing 10 g/l Na	8-22
Figure 8.15	Correlation Between Predicted and Experimental Osmotic Pressures in Sodium Carbonate Solutions of Varying Strength and pH	8-27
Figure 8.16	Water Flux as a Function of Effective Pressure for Three Different Feed Velocities	8-28
Figure 8.17	Variability of Water Permeability Parameter, A, with pH and Concentration of Sodium Carbonate Solutions Containing 1, 10 and 30 g/l Na	8-29
Figure 8.18	Variation of Water Fluxes with pH in Sodium Carbonate Solutions Containing 1, 10 and 30 g/l Na	8-30
Figure 8.19	Variation in Permeate Na and IC Concentrations with pH and Concentration of Sodium Carbonate Solutions	8-32
Figure 8.20	Variation in Solute Fluxes with pH and Concentration of Sodium Carbonate Solutions	8-33
Figure 8.21	Relationship Between Feed and Permeate pH Values for Different Water Fluxes in Sodium Carbonate Solutions of Varying Concentration	8-35
Figure 8.22	Gradient in Hydrogen Ion Concentration Across the Membrane During Nanofiltration of Sodium Carbonate at Varying pH and Concentration	8-36
Figure 8.23	Predicted Permeate Flux as a function of Feed Pressure and Flow Rate (Nanofiltration Experiment 9)	8-41
Figure 8.24	Predicted Permeate Total Carbonate Concentration as a Function of Feed Pressure and Flow Rate (Nanofiltration Experiment 9)	8-41

Figure 8.25	Predicted Permeate Total Hydrogen Ion Concentration as a Function of Feed Pressure and Flow Rate (Nanofiltration Experiment 9)	8-42
Figure 8.26	Predicted Permeate Total Sodium Concentration as a Function of Feed Pressure and Flow Rate (Nanofiltration Experiment 9)	8-42
Figure 8.27	Predicted Permeate Flux as a Function of Feed pH (Nanofiltration Experiment 7)	8-43
Figure 8.28	Predicted Permeating Concentrations of Total and Individual Carbonate Species as a Function of Feed pH (Nanofiltration Experiment 7)	8-43
Figure 8.29	Predicted Permeating Concentrations of Total and Individual Hydrogen Ion Species as a Function of Feed pH (Nanofiltration Experiment 7)	8-44
Figure 8.30	Predicted Permeating Concentrations of Nitrate, and Total and Individual Sodium Species as a Function of Feed pH (Nanofiltration Experiment 7)	8-44
Figure 9.1	Dependence of Membrane Area-Resistance on Current Passed	9-4
Figure 9.2	Dependence of Membrane Area-Resistance on Anolyte Sodium Concentration	9-4
Figure 9.3	Relationship Between Membrane Area-Resistance and Total Magnesium	9-5
Figure 9.4	Relationship Between Membrane Area-Resistance and Total Calcium	9-5
Figure 9.5	Incremental Change in Current Efficiencies	9-7
Figure 9.6	Rate of Calcium Removal for Three Acid Cleaning Techniques	9-14
Figure 9.7	Rate of Magnesium Removal for Three Cleaning Techniques	9-15
Figure 9.8	Potential-pH Equilibrium Diagram for the System Iron-Water, at 25 °C	9-19
Figure 9.9	Theoretical Conditions for Corrosion, Immunity and Passivation of Iron	9-20
Figure 9.10	Potential-pH Equilibrium Diagram for the System Nickel-Water, at 25 °C	9-22
Figure 9.11	Theoretical Conditions for Corrosion, Immunity and Passivation of Nickel in Chloride-Free Solutions	9-23
Figure 9.12	Dependence of Anode Mass Loss on Electricity Passed and Anolyte pH	9-23
Figure 10.1	Mass Balance Basis for Recovery Process Using Background Sodium Concentration	10-6
Figure 10.2	Schematic of Batch Neutralisation Unit	10-8
Figure 10.3	Schematic of Batch Cross-Flow Microfiltration Unit	10-10
Figure 10.4	Schematic of Batch Nanofiltration Unit	10-15
Figure 10.5	Basic Configuration of Spiral Elements Showing Flows in Arbitrary Units	10-17
Figure 10.6	Schematic of Batch Electrochemical Unit	10-21
Figure 10.7	Design Example: Dependence of Electromembrane Area Requirements on Rinse Water Concentration (at 60 °C)	10-26
Figure 10.8	Design Example: Dependence of Sodium Losses on Rinse Water Concentration	10-27
Figure 10.9	Design Example: Dependence of Electromembrane Area Requirements on Temperature	10-27

LIST OF ABBREVIATIONS

BOD	Biological Oxygen Demand
CD	Current Density
COD	Chemical Oxygen Demand
CP	Cost Period
DC	Direct Current
DSA	Dimensionally Stable Anode
DWAF	Department of Water Affairs and Forestry
EDTA	Ethylenediamine Tetra-Acetic Acid
IR	Ohmic (drop)
PP	Pollution Prevention (approach to water quality management)
PVC	Polyvinyl Chloride
RSA	Republic of South Africa
RWQO	Receiving Water Quality Objectives (approach to water quality management)
SS	Suspended Solids
TC	Total Carbon
TDS	Total Dissolved Solids
TIC	Total Inorganic Carbon
TOC	Total Organic Carbon
TS	Total Solids
US EPA	United States Environmental Protection Agency
WRC	Water Research Commission

SECTION 1

INTRODUCTION

1.1. Water Resources

Water is the key to the continued overall development of the Republic of South Africa (RSA) (Olivier, 1980). The critical factor for economic and industrial survival is the availability of water at a quality suitable for a range of urban and industrial uses. Two issues are threatening this survival: water supply and water quality. In order that water remain both a renewable and a sustainable resource, water quality must be preserved and the limited water supplies must be used effectively.

1.1.1 Water Supply

Southern Africa is, for the most part, a semi-arid, water deficient region of the world, which is subject to variable rainfall, droughts, floods, and high evaporation losses. Annual rainfall amounts to only 58 % of the world average; run-off is unfavourably distributed; the availability of underground water is limited; and the quality of the water resources is deteriorating (Department of Water Affairs, 1986). It was estimated in 1986 that the average annual run-off into rivers in the RSA is 52 000 million m³/a (143 million m³/d), of which 40 %, or 20 800 million m³/a (57 million m³/d), is the assured portion which can be made available for use through the provision of storage facilities. It is anticipated that future developments will increase this portion to 50 %. A conservative estimation of potential groundwater availability, based on 1986 abstraction, is 3 million m³/d, bringing the potential availability of natural resources to 27 400 million m³/a (75 million m³/d).

It was also estimated that, if the present increase in demand materialises, then the total water needs by early next century will be 29 270 million m³/a (80 million m³/d), which exceeds the maximum anticipated yields.

Solutions to the problem are being sought.

- 1) Methods are being developed to improve the efficiency of use of natural water resources.
- 2) Techniques are being implemented to raise the effectiveness of the current use of developed supplies, such as the reuse of waste water from industrial operations, and the improved use of water for irrigation in the agricultural sector.

- 3) Technologies are being considered for the creation of new water sources, such as the desalination of sea water, tapping of icebergs, interbasin transfer and weather modification.

1.1.2 Water Quality

In addition to the problem of limited water supplies, rapidly declining water quality, and the consequences of such a decline, has become a matter of major concern both in the RSA, and world-wide. The increasing salinity of the RSA's water resources is the most significant water quality problem facing the country (Stander, 1987), and the future of Industry is largely dependent on the control of this problem. A further concern is that, since Southern Africa is a water deficient region, the industrial effluent return flow forms a considerable supplementary source of water, adding to the mineralisation process.

Mineralisation may be controlled by minimising pollutants in industrial discharges, and encouraging water and chemical reclamation and recycling by Industry. Both minimisation, and reclamation and recycling, are addressed as part of the Department of Water Affairs' strategy and policy toward the use of water for industrial purposes (see Section 2.3.2). This policy requires that effluent production is minimised, and that, where effluent is produced, it is of suitable quality for return to the environment, thus constituting a reusable supplementary source of water. The policy also aims to ensure that the mineralisation process, and water quality deterioration, are reduced or eliminated. This can only be achieved by efficient management of potential pollutants from industrial sources.

1.2. Management of Industrial Pollutants

Pollution may be defined as the release of any substance causing damage to targets in the environment (Holdgate, 1979). It follows from this definition that the emission of a potential pollutant to the environment does not necessarily constitute pollution if it is rendered harmless by transformation, or dilution, before reaching the target. Therefore, elimination of pollution by an industrial discharge, does not require that emissions be restricted to zero, but rather that emissions be controlled within acceptable criteria, and that the release of these emissions into the environment be effectively managed.

1.3. Management of Textile Waste Water

Waste waters produced during textile processing are typically non-biodegradable in conventional wastewater treatment plants and contain high concentrations of mineral salts. These waste waters pose a pollution threat to the environment, in particular the water

environment, unless they are carefully managed. The authorities have identified the need to develop techniques to minimise, control, treat and dispose of potentially harmful pollutant streams from the Textile Industry. As a result, the Water Research Commission (WRC) contracted the Pollution Research Group, of the Department of Chemical Engineering, at the University of Natal, Durban, to investigate waste management procedures and techniques that would be suitable for application to waste waters generated during textile scouring and bleaching operations. This investigation was entitled *Water and Effluent Management in the Textile Industry: Treatment of Scouring and Bleaching Effluents*, and was assigned the WRC Project Number 122.

This research project consisted of several broad tasks.

- 1) Examination of the compositions, volumes and pollutant emission rates of waste waters from the processing of wool, cotton, and polyester fibres and their blends, and identification of the processes which were most significant in terms of their pollution potential. In the case of wool, carbonising and bleaching effluents were considered, while in the case of cotton and polyester, scouring and bleaching effluents were considered.
- 2) Development and implementation of within-process procedures and techniques, including closed-loop recycle, to minimise waste generation at source.
- 3) Development, testing and evaluation of potentially suitable end-of-pipe treatment options for each of the waste waters of concern.
- 4) Development of the basic design criteria for the implementation of selected treatment options.

A three year contract was awarded to the Pollution Research Group in 1983. An extension, for one year, was granted in 1986, and for a further six months in 1987. The final project report, and a technical guide for the planning, design and implementation of relevant waste water treatment plants, were published by the WRC in 1990 and 1991 respectively.

1.4. Specific Objectives

During the WRC project, strong scour waste waters, or effluents, produced from the scouring of cotton and cotton blends using hot, concentrated sodium hydroxide solutions, were identified to be the most potentially polluting of all the waste waters considered.

Investigations focused on the development of an economically, technically, and environmentally effective wastewater management strategy, that would eliminate or minimise the impact of this type of textile effluent on the environment. Technologies and combinations of technologies, were considered and tested, including conventional and dynamic membrane techniques, electro-oxidation, electrochemical recovery, and evaporation. The most effective combination investigated was an electrochemical process which enabled recovery of water, heat and sodium hydroxide.

The subject of the present dissertation is the development of an effective, functional and usable wastewater management strategy for sodium hydroxide scouring of textile blends, from conception, to evaluation, testing and implementation. Specifically, this involves the:

- 1) Characterisation of strong scouring effluents and determination of their contribution to total factory waste water and environmental degradation;
- 2) Description of the regulations governing the discharge of waste waters in general, and textile wastewaters specifically, in South Africa;
- 3) Review and evaluation of suitable approaches for the management of scouring effluents, considering both process-oriented pollution prevention and waste minimisation as well as end-of-pipe solutions;
- 4) Development and testing of modifications to the scouring process, such that the effluent produced is of minimum volume and maximum concentration, while cloth quality is unaltered;
- 5) Development and testing of an electrochemical-based treatment sequence which allows the recovery (for reuse) of chemicals and water from scouring effluents;
- 6) Design and costing of a full-scale treatment plant.

In addition, a semi-quantitative explanation was developed of the performance of the nanofiltration component of the process to the chemical system consisting of sodium, carbonate, nitrate, protons, calcium, magnesium and EDTA.

This work results mainly from a study undertaken at Da Gama Textiles, in Zwelitsha, the then Ciskei, between 1985 and 1987.

This dissertation consists of eleven sections. While the current section places the subject of the thesis in the context of the overall water situation in the RSA, and more specifically, WRC Project No 122, Sections 2 to 5 present a literature review and a theoretical discussion of various aspects relevant to subsequent work. **Section 2** overviews the Textile Industry, describing the framework of environmental regulations within which textile processes in the

RSA must operate. It also describes the context of scouring within the overall textile manufacturing sequence, the theory of scouring and the nature of strongly caustic scouring effluents. **Section 3** is a theoretical discussion of environmental management options for pollution control, and the development of an overall chemical, water and effluent management strategy for application specifically within the scouring operation. This management strategy clearly distinguishes two main aspects: in-plant control, to prevent and minimise waste water generation; and the implementation of end-of-pipe treatment and recycling. **Section 4** and **Section 5**, expand on **Section 3**. **Section 4** discusses the theory and practice of in-plant control of water and waste water, specifically where this is relevant to the generation of a waste water stream most amenable to electrochemical treatment and recovery. **Section 5** discusses the development of the electrochemical treatment and recovery process, describing the treatment sequence and its advantages, and providing theoretical details relating to the unit operations within the sequence. Experimental details of pilot plant and other supplementary work are described in **Section 6**, while **Section 7**, **Section 8** and **Section 9** present and discuss the results of the pilot plant, supplementary work on nanofiltration and the supplementary work on electrolysis respectively. **Section 10** discusses technical and economical aspects of the commercial implementation of the treatment and recycle process, providing basic design criteria for a full-scale plant. The conclusions and recommendations of the study are presented in **Section 11**.

1.5 General Comments

The present work arose from the need to solve a real and pressing environmental problem of industrial interest. From a technical point of view, the problem is a complex one, to which no acceptable solution was commercially available. Further, aside from the work described in this dissertation, no other researchers have been able to formulate, develop and implement an effective solution, even on a reduced scale. To be effective, while meeting industrial needs, the solution must be functional, usable, legally compliant, compatible with industrial processing, and technically, financially and environmentally sound. Early in this programme of work, it became evident that all these requirements could not be met by using any one conventional approach, process or operation, or by considering, in isolation, any one aspect of the entire situation. Rather, to achieve the overall objectives, the final solution had to integrate carefully a series of processing and treatment sub-solutions. Clearly:

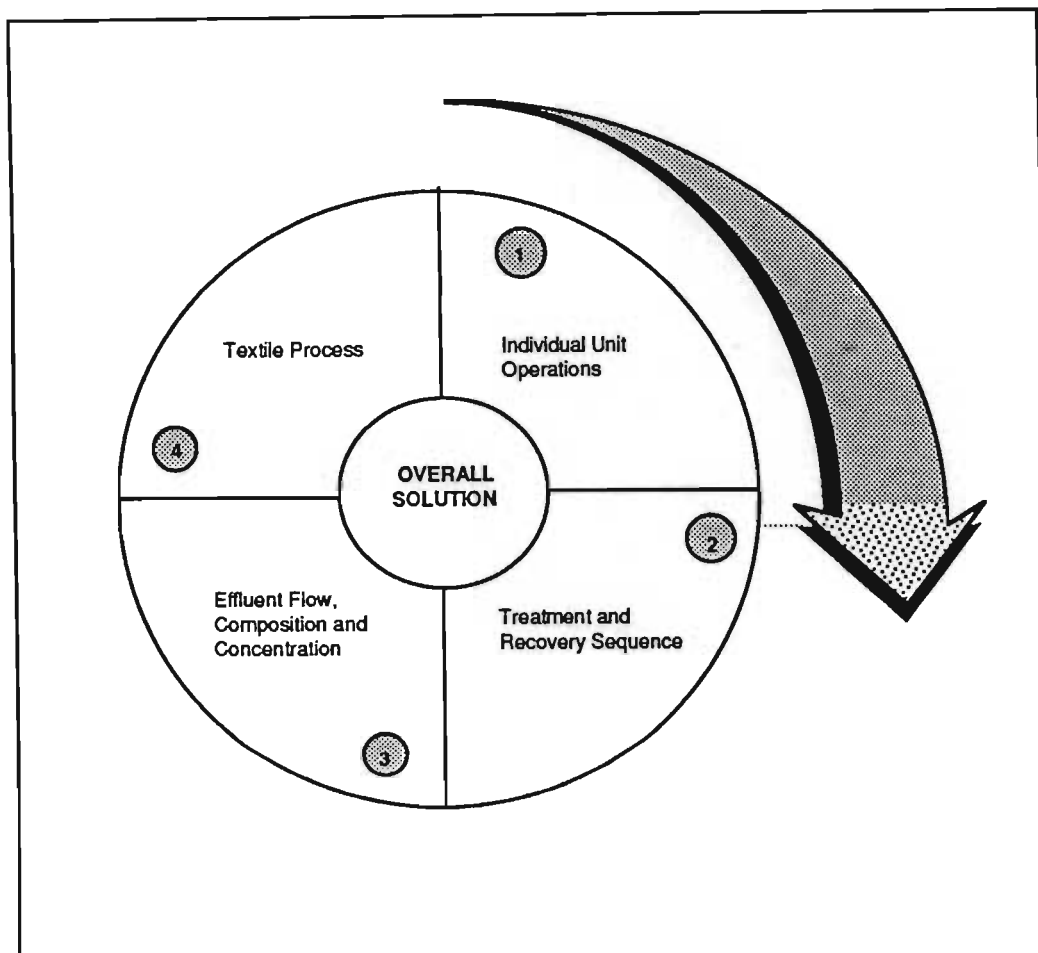
- 1) Individual unit operations needed to be integrated systematically into the sequence which facilitated the treatment and recovery of resources from scouring effluent. Although measured relationships of process variables within each unit operation needed definition,

the effect of these variables on subsequent unit operations within the sequence, and ultimately on the success of the entire sequence, needed evaluation.

- 2) The treatment and recovery sequence alone could not provide a single solution. Its success is critically dependent on the nature of the effluent from the scouring process, which in turn is defined by the processing variables governing the textile operations.

Figure 1.1 illustrates the interdependency of the parameters affecting the success of the overall solution.

Figure 1.1
Success Cycle



As a result of the nature of the multi-faceted approach necessary to address the problem, and the complex dependency of the successful solution on a series of tailored engineering sub-solutions, the scope of the work presented in this dissertation is broad. In fact, the main strength of the work lies in this broadness, particularly in the innovative and systematic combination of selected engineering principles, unit operations and processing techniques, which individually do not resolve the problem, but which together combine into a workable

and acceptable solution. Not only is this particular combined approach novel, but many aspects of the work involved original thought and contributed to various areas in the science of pollution prevention, waste water treatment, and membrane processes. For example:

- 1) The treatment and recovery sequence is the first published process which successfully recovers pure chemicals and water of high quality from cotton scouring effluents. The sequence was granted full international patents in ten countries between 1987 and 1991. These patents are as follows:

- C.A. BUCKLEY and A.E. SIMPSON, Effluent Treatment, SA Patent No. 87/4406, 18 June 1987.
- C.A. BUCKLEY and A.E. SIMPSON, Effluent Treatment, Canadian Patent No. 539,772.3, 16 June 1987.
- C.A. BUCKLEY and A.E. SIMPSON, Effluent Treatment, Australian Patent No. 590,852, 15 June 1987.
- C.A. BUCKLEY and A.E. SIMPSON, Effluent Treatment, Japanese Patent No. 62,155646, 24 June 1987.
- C.A. BUCKLEY and A.E. SIMPSON, Effluent Treatment, United States of America Patent No. 4752363, 21 June 1987.
- C.A. BUCKLEY and A.E. SIMPSON, Effluent Treatment, German Patent No. 87305644.4, 27 June 1990.
- C.A. BUCKLEY and A.E. SIMPSON, Effluent Treatment, Austrian Patent No. 87305644.4, 27 June 1987.
- C.A. BUCKLEY and A.E. SIMPSON, Effluent Treatment, Greek Patent No. 87305644.4, 17 Oct. 1990.
- C.A. BUCKLEY and A.E. SIMPSON, Effluent Treatment, French Patent No. 87305644.4, 17 Oct. 1990.
- C.A. BUCKLEY and A.E. SIMPSON, Effluent Treatment, Dutch Patent No. 87305644.4, 17 Oct. 1990.

In addition to numerous reports for internal use by the WRC, industry and researchers, the work also resulted in the publishing of seven refereed papers, ten conference proceedings and two books. The refereed papers are as follows:

- BUCKLEY, C.A., BINDOFF A.L., KERR, C.A., KERR, A., SIMPSON A.E. and COHEN D.W., The Use of Speciation and X-Ray Techniques for Determining Pretreatment Steps for Desalination. *Desalination*, **66**, 409 - 429, 1987.
- SIMPSON, A.E. and BUCKLEY, C.A., The Treatment of Industrial Effluents Containing Sodium Hydroxide to Enable the Reuse of Chemicals and Water. *Desalination*, **67**, 305 - 319, 1987.
- SIMPSON, A.E., KERR, C.A. and BUCKLEY, C.A., The Effect of pH on the Nanofiltration of the Carbonate System in Solution. *Desalination*, **64**, 305 - 319, 1987.

- SIMPSON, A.E. and BUCKLEY, C.A., The Recovery of Caustic Soda from Caustic Effluents. *ChemSA*, 76 - 80, March 1988.
- SIMPSON, A.E. and BUCKLEY, C.A., The Recovery and Reuse of Sodium Hydroxide from Industrial Effluents, *Advances in Reverse Osmosis and Ultrafiltration*, pp 335 - 346, Published by the National Research Council of Canada, Editors - T. Matsuura and S. Sourirajan, 1989.
- BUCKLEY, C.A., KERR, C.A. and SIMPSON, A.E., Small Scale Tests to Determine the Feasibility of Reverse Osmosis and Ultrafiltration for the Treatment of Industrial Effluents. *Water SA*, 18(1), 63 - 67, January 1992.
- VOORTMAN, W.J., SIMPSON, A.E., KERR, C.A., and BUCKLEY, C.A., Application of Electromembrane processes to the Treatment of Aqueous Effluent Streams. *Water Science and Technology*, 25(10), 291 - 298, 1992, ISSN 0273-1223.

The conference proceedings are as follows:

- SIMPSON, A.E. and BUCKLEY, C.A., The Recovery and Recycling of Sodium Hydroxide Containing Effluents. Institute of Water Pollution Control Biennial Conference, Port Elizabeth, Republic of South Africa, 12 to 15 May 1987.
- SIMPSON, A.E. and BUCKLEY, C.A., The Recovery of Caustic Soda from Caustic Effluents. Technology Forum on Effluent Treatment and Chemical Recovery by Electrically Driven Membrane Processes, CSIR Conference Centre, Pretoria, Republic of South Africa, 29 June 1987.
- BUCKLEY, C.A., BINDOFF A.L., KERR, C.A., KERR, A. and SIMPSON A.E., The Use of Speciation and X-Ray Techniques for Determining Pretreatment Steps for Desalination. Presented at the Third World Congress on Desalination and Water Reuse, Cannes, 14 to 17 September 1987.
- SIMPSON, A.E. and BUCKLEY, C.A., The Treatment of Industrial Effluents Containing Sodium Hydroxide to Enable the Reuse of Chemicals and Water. Presented at the Third World Congress on Desalination and Water Reuse, Cannes, 14 to 17 September 1987.
- SIMPSON, A.E., KERR, C.A. and BUCKLEY, C.A., The Effect of pH on the Nanofiltration of the Carbonate System in Solution. Presented at the Third World Congress on Desalination and Water Reuse, Cannes, 14 to 17 September 1987.
- SIMPSON, A.E. and BUCKLEY, C.A., The Recovery and Reuse of Sodium Hydroxide from Industrial Effluents. Presentation at the American Chemical Society, Division of Industrial and Engineering Chemistry Meeting: Symposium on Advances in Reverse Osmosis and Ultrafiltration. Third Chemical Congress of the North American Continent, Toronto, Canada, 5 to 10 June 1988.
- SIMPSON, A.E., Electrolysis and Facilitated Transport. Contribution to the Workshop on Desalination and Membrane Processes, Ohristad, 24 - 26 August 1988
- BUCKLEY, C.A. and SIMPSON, A.E., Practical Methods in Attaining Reductions in Chemical, Water and Effluent Loads. Presented at New Technologies for Textiles Symposium, University of Port Elizabeth, 15 to 16 October 1990.
- BUCKLEY, C.A. and SIMPSON, A.E., Closed Loop Treatment Options for Scouring Effluent. Presented at New Technologies for Textiles Symposium, University of Port Elizabeth, 15 to 16 October 1990.

- VOORTMAN, W.J., SIMPSON, A.E. and BUCKLEY, C.A., Application of Electrochemical Membrane Processes to the Treatment of Aqueous Effluent Streams. IAWPRC Specialised Conference on Membrane Technology in Wastewater Management, The Cape Sun Hotel, Cape Town, 2 - 5 March 1992.

The books are as follows:

- Pollution Research Group, Department of Chemical Engineering, WRC Project No 122, Final Report, Water Management and Effluent Treatment in the Textile Industry: Scouring and Bleaching Effluents. WRC, Pretoria, ISBN 0 947447 91 1 (1990).
- Pollution Research Group, A Guide for the Planning, Design and Implementation of Waste Water Treatment Plants in the Textile Industry, Part III, Closed Loop Treatment/Recycle Options for Textile Scouring and Bleaching Effluents. WRC Project No 122, Report No TT48/90, ISBN 0 947447 80 0 (1990).

Aspects of the sequence were adapted to facilitate application of the principles to wastewater from other industrial sectors. As a result, patents were filed and granted on two further related processes for the electrochemical treatment of waste waters in the mining and chemicals industries. These are as follows:

- C.A. BUCKLEY and A.E. SIMPSON, The Removal of Sulphuric Acid from Aqueous Medium Containing the Acid, SA Patent No.88/5487, 27 July 1988.
- C.A. BUCKLEY and A.E. SIMPSON, The Removal of Sulphuric Acid from Aqueous Medium Containing the Acid, Australian Patent No. 20399/88, 23 August 1988.
- C.A. BUCKLEY and A.E. SIMPSON, The Removal of Sulphuric Acid from Aqueous Medium Containing the Acid, Canadian Patent No. 573,738-9, 3 August 1988.
- C.A. BUCKLEY and A.E. SIMPSON, The Removal of Ammonium Salts from Aqueous Medium Containing the Salt, SA Patent No. 88/8898, 28 November 1988.
- C.A. BUCKLEY and A.E. SIMPSON, The Removal of Ammonium Salts from Aqueous Medium Containing the Salt, Australian Patent No. 26329/88, November 1988.
- C.A. BUCKLEY and A.E. SIMPSON, The Removal of Ammonium Salts from Aqueous Medium Containing the Salt, Canadian Patent No. 584,427.4, November 1988.
- C.A. BUCKLEY and A.E. SIMPSON, The Removal of Ammonium Salts from Aqueous Medium Containing the Salt, European Patent No. 88311324.9, November 1988.
- C.A. BUCKLEY and A.E. SIMPSON, The Removal of Ammonium Salts from Aqueous Medium Containing the Salt, United States of America Patent No. 07/276,626, November 1988.

A full list of the candidate's publications resulting from this work is presented in Appendix 1. Also listed are publications on related work in other sectors undertaken by the candidate.

- 2) At the time that this work was carried out, cross-flow microfiltration, one of today's prominent membrane techniques for water and waste water treatment, was in its initial development phase. This work was one of the original studies concerning the use of the woven cloth arrangement of this membrane technique for treating industrial effluents. Woven cloth cross-flow microfiltration has been commercially available since the mid-to-late 1980's and is marketed internationally for a wide range of waste water and water applications.
- 3) The first experimental nanofiltration membranes became available to researchers in the mid-1980's and the Pollution Research Group were offered samples for evaluation. These samples were used in this study, which became one of the first studies ever undertaken of this membrane process. In fact, the first paper reported in Chemical Abstracts dealing with nanofiltration resulted from this work. This paper was published in 1987, and is still one of the most authoritative references on the subject. Its details are as follows:
 - SIMPSON, A.E., KERR, C.A. and BUCKLEY, C.A., The Effect of pH on the Nanofiltration of the Carbonate System in Solution. *Desalination*, 64, 305 - 319, 1987.
- 4) Since nanofiltration membranes become commercially available, researchers world-wide have failed to model successfully its transport characteristics in real applications. The current work uses new developments in combining chemical speciation theory and ion transport modelling to contribute to the understanding of the nanofiltration process. This dual approach to understanding membrane performance has not been used by other researchers, but is an exciting new tool for predicting the transport characteristics of solution components in membrane systems.
- 5) The adaptation and application of conventional electrochemical techniques, widely used for chemical manufacture, to textile waste water treatment and chemical recovery is novel. In addition, the use of sodium carbonate/bicarbonate salts in place of sodium chloride salts for sodium hydroxide generation, is a previously unexplored diversion from conventional practice. This work contributes to the understanding of chemical reactions during electrolysis of non-conventional, complex and impure solutions, and precipitate formation (and control and prevention) on the electromembrane surface during electrochemical processing of these solutions.

SECTION 2

THE SOUTH AFRICAN TEXTILE INDUSTRY - AN OVERVIEW OF ENVIRONMENTAL LEGISLATION, MANUFACTURING OPERATIONS AND SCOURING

The Textile Industry is a group of related sectors which use natural and synthetic fibre raw materials to produce a wide range of finished products. The Industry in the RSA supports 90 000 people and has total sales of R 6 535 million (Textile Federation, 1993). Because of the wide array of activities it is difficult to determine the number of textile enterprises in the RSA (Department of Water Affairs and Forestry, 1993). However, it is a major industry with over 300 textile factories, of which 50 are concerned with the weaving of cotton and cotton/synthetic fibre cloths (Water Research Commission, 1976). Approximately 65 000 tonnes of cotton were consumed by the Textile Industry in 1992, which accounted for one quarter of raw fibre consumed (Textile Federation, 1993). The Textile Industry uses 5 % of the energy requirements of the manufacturing sector (Department of Planning and the Environment, 1978).

Two factors influence the environmental performance of the Textile Industry. Firstly, statutory environmental controls influence the nature of the discharges and the final impact of the textile operations on the environment. To develop a pollution control strategy, it is essential to understand the regulatory background and statutory requirements with which Industry must comply. Secondly, the type of the fibre processed and the characteristics and conditions of the unit processing operations largely determine the extent and nature of the potential pollution from a process or the overall site. This dissertation is concerned with pollution control in scouring processes, especially those processes where strong sodium hydroxide solutions are used to scour cotton and cotton blends. Since scouring is an integral part of manufacturing, this process cannot be studied in isolation, but must be considered within the overall textile manufacturing operation.

To provide a basic understanding of the textile manufacturing operation, the remainder of this section overviews water requirements (Section 2.1), the regulatory framework for environmental control (Sections 2.2 and 2.3), textile processing (Section 2.4), in particular scouring technology (Section 2.5), and characteristics of scouring effluent (Section 2.6).

2.1. Water Use In Textile Processing

The Textile Industry requires water for:

- 1) Processing;
- 2) Product, equipment and floor washing;

- 3) Cooling systems;
- 4) Steam generation;
- 5) Air conditioning;
- 6) Transport of material;
- 7) Personnel consumption and sanitation.

Steam generation, air conditioning, human consumption, and certain stages of the production process require water of potable, or higher, quality, while a water of lower quality is suitable for other uses.

The volume of water used depends on the fibre, manner of processing, processing sequence and processing equipment. Typical quantities used are 150 to 1 400 l/kg of product, and hence large volumes of textile effluent require treatment and disposal (WIRA, 1973 and CDTRA, 1971).

Of particular significance to the Textile Industry is the strong correlation between water and energy use (Pollution Research Group, 1990). Since many wet processing operations are carried out at elevated temperature, water savings measures automatically result in energy savings.

2.2. The Need for Water Pollution Control In Textile Processing

Amendments to the Water Act of 1956 (see Section 2.3) have placed considerable responsibility on industries to optimise their water use, and to treat their waste waters to the prescribed standards, as determined by the receiving water quality objectives (RWQO) approach. The Textile Industry, because of the nature of its waste waters, is faced with a particularly serious set of problems.

Textile plants use a wide variety of dyes and other chemicals, such as acids, alkalis, salts, detergents, wetting agents, sizes and finishes. Many of these chemicals are not retained in the final product, but are discharged in the effluent. Since textile waste waters are generally non-biodegradable, their discharge to sewage systems, or to the environment, presents a problem. Mills discharging to sewage works may be responsible for colour and chemical oxygen demand (COD) problems, while those discharging directly to the environment need to pretreat their waste water to remove high percentages of colour, COD and mineral salts.

Unless appropriate and adequate care is exercised, the discharge of textile waste waters to the water environment may have serious and long-lasting consequences for the following reasons.

- 1) Solid wastes, including fibre, are unsightly and may result in the deposition of anaerobic sludge layers in receiving waters.
- 2) Many organic contaminants, including dyes, synthetic sizes, and detergents, are only semi-biodegradable. Furthermore, they may be potentially damaging to the performance of municipal sewage works and to the environment if returned to water sources. Other organic compounds with high biological oxygen demand (BOD), such as starches, may increase the cost of sewer discharge, or cause anaerobic conditions if discharged to a water body.
- 3) The presence of inorganic contaminants in the form of salts, acids, or alkalis in high concentrations, will cause a gradual deterioration of the receiving water, making it unsuitable for subsequent use as domestic, industrial, agricultural, recreational and environmental water.

2.3. Regulatory Control of Water Use and Wastewater Discharge

Regulatory control of water use and waste water discharge within the Textile Industry is achieved by means of the legislation discussed below.

2.3.1 The Water Act

The use of water for industrial purposes, together with control over effluent production and water pollution, is regulated in the RSA by the Water Act, 1956 (Act 54 of 1956) as amended. In the case of the former Republics of Transkei, Venda, Bophuthatswana, and Ciskei, the Water Act and its amendments at the time of independence, were adopted. Subsequent amendments to the Water Act in the RSA have not necessarily been adopted in these independent republics.

The Water Act vests the necessary powers to exercise control over the management of water resources in the Department of Water Affairs and Forestry (DWAF). These resources include inland ground and surface waters, as well as the coastal-marine environment.

The Water Act originally served its purpose well (Best, 1984). It enabled water demand to be regulated in keeping with the portion of the national budget allocated to the development of additional water supplies. In addition, it safeguarded the available, but limited, water resources from catastrophic levels of pollution, without seriously constraining industrial development.

In view of the general decline in the quality of many of the RSA's water sources, the initial Water Act could no longer effectively control water pollution and industrial water use. Therefore, the Water Act and effluent standards were amended during 1984. The main requirements of this Water Amendment Act of 1984 retained the basic requirements of the Water Act of 1956.

2.3.2 Strategy and Policy Guidelines

Following the Water Amendment Act of 1984, the DWAF defined its approach to the effective management of water resources in a policy document (Department of Water Affairs, 1986). This document attempted to increase the awareness of all water managers, scientists, and consumers to the opportunities and limitations associated with water use and effluent disposal in the RSA. More recently, the DWAF has again reviewed its water quality management policy and has implemented a new approach to water pollution control which forms an integral part of water quality management (Department of Water Affairs and Forestry, 1991). This new approach encompasses three separate concepts of integrated catchment management, pollution prevention and receiving water quality objectives. The overall major goal of the DWAF, the maintenance of the fitness for use of the RSA's water on a sustained basis, is reflected in these policy documents. The fitness for use concept implies the evaluation of water quality in terms of the requirements of a particular user or category of users (domestic, industrial, agricultural, environmental and recreational).

Section 21 of the Water Act prescribed three uniform effluent standards (Government Gazette, 1984):

- 1) General standard for discharge into most rivers and streams in the RSA;
- 2) Special standard (Schedule I) for discharge into rivers in catchment areas, the so-called 'mountain and trout streams';
- 3) Special standard (Schedule II) for discharge into specified catchments sensitive to phosphorus and prone to eutrophication.

This Uniform Effluent Standards approach to water pollution control was applied until recently. To counter continuing water quality deterioration, the DWAF has changed its approach to the Receiving Water Quality Objectives (RWQO) approach for non-hazardous substances and to the Pollution Prevention (PP) approach for hazardous substances. The RWQO approach focuses on the fundamental policy objective of maintaining fitness for use, and permits integration of factors affecting water quality, conferring greater flexibility on water quality management. PP aims to minimise or prevent the release of hazardous pollutants to the water environment (Department of Water Affairs and Forestry, 1993). Until the new approaches are fully operational, the current general and special effluent standards serve as minimum effluent standards (Table 2.1).

Table 2.1
The South African Water Act, 1956 (Act 54 of 1956)
General and Specific Standards for Discharge

Parameter	Units	General Standard	Special Standard Schedule I	Special Standard Schedule II
Colour, odour, taste		nil	nil	nil
pH		5,5 to 9,5	5,5 to 7,5	5,5 to 9,5
Dissolved oxygen	%	not less than 75	not less than 75	not less than 75
Temperature	°C	not more than 35	not more than 25	not more than 35
Typical faecal coliforms	/100 ml	nil	nil	nil
Chemical oxygen demand	mg/l	not more than 75	not more than 30	not more than 75
Oxygen absorbed	mg/l	not more than 10	not more than 5	not more than 10
Conductivity	mS/m	not to increase more than 75 mS/m above intake, max. 250	not to increase more than 15% above intake, max. 250	not to increase more than 75 mS/m above intake, max. 250
Suspended solids	mg/l	not more than 25	not more than 10	not more than 25
Sodium	mg/l	below 90 above intake	below 50 above intake	below 90 above intake
Soap, oil and grease	mg/l	not more than 2,5	nil	not more than 2,5
Residual chlorine, as Cl	mg/l	not more than 0,1	nil	not more than 0,1
Free & saline ammonia, as N	mg/l	not more than 10	not more than 1	not more than 10
Nitrate, as N	mg/l	not specified	not more than 1,5	not specified
Arsenic	mg/l	not more than 0,5	not more than 0,1	not more than 0,5
Boron	mg/l	not more than 1	not more than 0,5	not more than 1
Chromium, total	mg/l	not more than 0,5	not more than 0,05	not more than 0,5
Chromium VI	mg/l	not more than 0,05	not specified	not more than 0,05
Copper	mg/l	not more than 1	not more than 0,02	not more than 1
Phenol	mg/l	not more than 0,1	not more than 0,01	not more than 0,1
Lead	mg/l	not more than 1	not more than 0,1	not more than 1
Copper	mg/l	not more than 0,5	not more than 0,02	not more than 0,5
Sulphides, as S	mg/l	not more than 1	not more than 0,05	not more than 1
Fluorine	mg/l	not more than 1	not more than 1	not more than 1
Zinc	mg/l	not more than 5	not more than 0,3	not more than 5
Phosphate, total as P	mg/l	not specified	not more than 1	not more than 1
Iron	mg/l	not specified	not more than 0,3	not specified
Manganese	mg/l	not more than 0,4	not more than 0,1	not more than 0,4
Cyanide, as CN	mg/l	not more than 0,5	not more than 0,5	not more than 0,5
Total Cadmium, Chromium, Copper, Mercury and Lead	mg/l	not more than 1	not more than 1	not more than 1
Cadmium	mg/l	not more than 0,05	not more than 0,05	not more than 0,05
Mercury	mg/l	not more than 0,02	not more than 0,02	not more than 0,02
Selenium	mg/l	not more than 0,05	not more than 0,05	not more than 1

As presently applied in the RSA, the RWQO approach involves compilation of water quality guidelines based on the requirements of recognised water uses; formulation of water quality management objectives which recognise the water quality requirements of water users, as well as economic, social, legal and technological considerations; and imposition of site-specific effluent standards to ensure that water quality management objectives are met for particular water bodies.

The DWAF has combined the RWQO approach with water quality management goals, which embody the precautionary principle of source reduction, as well as the application of minimum effluent standards. These goals are summarised as follows:

- 1) Source reduction, recycling, detoxification and neutralisation of wastes. Voluntary action is promoted.
- 2) If there is no alternative to the discharge of an effluent, it should meet minimum standards, which may be uniform or industry-related. The current general and special effluent standards (Table 2.1) are adapted to serve as minimum standards.
- 3) If the application of minimum effluent standards is not sufficient to maintain the fitness for use of the receiving water body, then standards stricter than the minimum standards will be enforced. These standards will be site-specific and in accordance with the RWQO approach.
- 4) Exemptions from compliance with minimum effluent standards will be considered as a last resort and only if the receiving water body has sufficient assimilative capacity.

To ensure consistency in the application of these goals to individual cases, decision-making guidelines are being developed by adaptation of the general and special effluent standards.

Currently, guidelines for addressing the quality of intake water have been developed for six industrial categories of major water users (Department of Water Affairs and Forestry, 1993). These are leather and tanning; power generation; iron and steel; pulp and paper; petrochemical; and textiles. In addition, only those water quality variables are considered which are fundamental to the main water related problems experienced in each industry, and which can be controlled to some extent by effective catchment management. The information used to develop these guidelines was gathered from local sources, in conjunction with a review of international literature. The guidelines reflect the situation that occurs in a typical example in each industry, and are used in site-specific assessments.

The industrial guidelines describe the impacts of water quality change in terms of four norms: the overall cost of water; the level of water treatment technology required to make the quality of the water supply fit for its intended use; the level of supervision required to operate and maintain water treatment plant; and the complexity of waste handling.

Guidelines for specific water quality variables relevant to the textile industry are presented in a series of tables in a recent publication (Department of Water Affairs and Forestry, 1993).

These variables are evaluated at different concentration levels in terms of their effects on the norms used to measure the fitness for use of water for industrial purposes. The target guideline ranges for specific water quality variables are summarised in Table 2.2. Non-target ranges are not listed here.

Table 2.2
Target Guideline Ranges for Specific Water Quality Variables, Textile Industry

Variable	Target Guideline Range	Norms			
		Increase in Water Costs	Technology	Supervision	Waste Handling Problems
pH	7,0 - 8,5	None (0%)	None	None	None
Electrical conductivity	10 - 70 mS/m	None (0%)	Standard	Unskilled	Slight
SS	0 - 5 mg/l	None (0%)	Low	Routine	None
Total hardness	0 - 25 mg/l	None (0%)	Standard	Unskilled	Sight
Alkalinity	0 - 100 mg/l	None (0%)	Low	Routine	None
Sulphate	0 - 250 mg/l	None (0%)	Low	Routine	Slight
Iron	0.0 - 0.2 mg/l	None (0%)	Standard	Routine	Slight
Manganese	0.0 - 0.1 mg/l	None (0%)	Standard	Routine	Slight
COD	0 - 10 mg/l	None (0%)	Low	Routine	Slight

2.3.3 Industry-Based Recycling and Reclamation

The DWAF relies on the co-operation of both research and industrial organisations to develop other approaches, which will ensure the industrial and economic future of the RSA. It is the Department's policy to encourage industrialists to implement improved in-plant control as the first option to water quality management.

Industry-based recycling and reclamation is desirable in that pollutants may be removed, at source, from segregated, purer streams. In addition, heat energy, water, and chemical

savings are often achieved. Industry-based recycling includes the reuse of process water, contaminated by low levels of pollutants, from one process, in another subsequent process. Reclamation measures include primary treatment, to enable the water to be reused, or advanced treatment, to allow for the separation, recovery, and direct reuse of waste water constituents.

2.4. Textile Processing

The raw materials supplied to a textile processing operation are fibre, water, energy and chemicals. The outputs from the operation are textile product and wastes, including liquid effluent, solid wastes, atmospheric emissions, waste heat, exhausted chemicals, and fabric impurities. A brief description of fibre type, textile processing and mill classification follows.

2.4.1 Textile Fibres

The fibres of interest in the current dissertation are cotton and polyester.

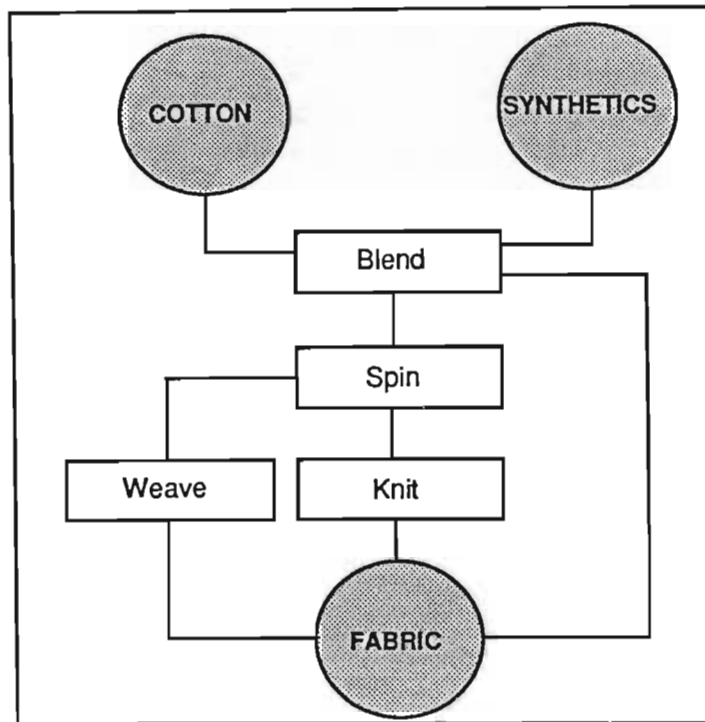
Cotton is the seed hair of a wide variety of plants of the *Gossypium* family. Cotton fibres consist mainly of cellulose. Natural cotton is contaminated by oil and wax (0,5 %). Pectic acid, which is soluble in hydroxide solutions, but insoluble in water, is present in the form of calcium or magnesium salts. Cotton may also contain small amounts (1 to 2 %) of mineral matter, composed of silicon, iron, aluminium, calcium, magnesium, potassium, sodium, chloride and sulphate. Nitrogen containing impurities, such as polypeptides or proteins, and natural colouring matter are also present.

Polyester is a synthetic fibre, and is the product of a commercial chemical process involving the condensation of ethylene glycol and terephthalic acid. Polyester fibres are produced by melt spinning and, being thermoplastic, can be easily shaped to produce textured effects. The fibres exhibit marked crystallinity, and the closely packed, highly-oriented molecules make polyester strongly hydrophobic.

2.4.2 Textile Processing Operations

Various processing operations are involved in the transformation of the raw fibre into the finished textile product, as presented in Figure 2.1. The conditions under which each operation is carried out depend on the type of raw fibre used. Processing operations are either dry, as in blending, spinning, weaving, and knitting; or wet, as described below where certain properties are imparted to the prepared fibre or fabric by treatment in various solutions.

Figure 2.1
Production of Fabric



The wet processing section of a textile mill processing cotton and polyester commences with desizing. The subsequent operations prepare the textile material for dyeing, printing, and finishing. Impurities are made soluble, dissolved or dispersed, and removed by washing (with chemical addition) or rinsing (with water only). Adequate washing/rinsing capacity and optimum water flows are essential at each stage of wet processing to ensure production of high quality textiles. In addition, accurate control of the chemical concentration, and the reaction time and temperatures are essential during wet processing. The order in which dry and wet processing operations are carried out depends on the specific production programme of the mill, and on equipment availability. The unit operations are described briefly below.

- 1) *Opening.* This mechanical operation opens the bales of raw fibres, blending together various components, and allowing for the removal of contaminants.
- 2) *Carding and spinning.* During carding, the long axes of the fibres are aligned, the short fibres are removed, and further blending occurs. In spinning the fibres are drawn and twisted into a yarn. Where the yarn is to be used for weaving, it is divided into the warp (longitudinal threads) and the weft (lateral threads).

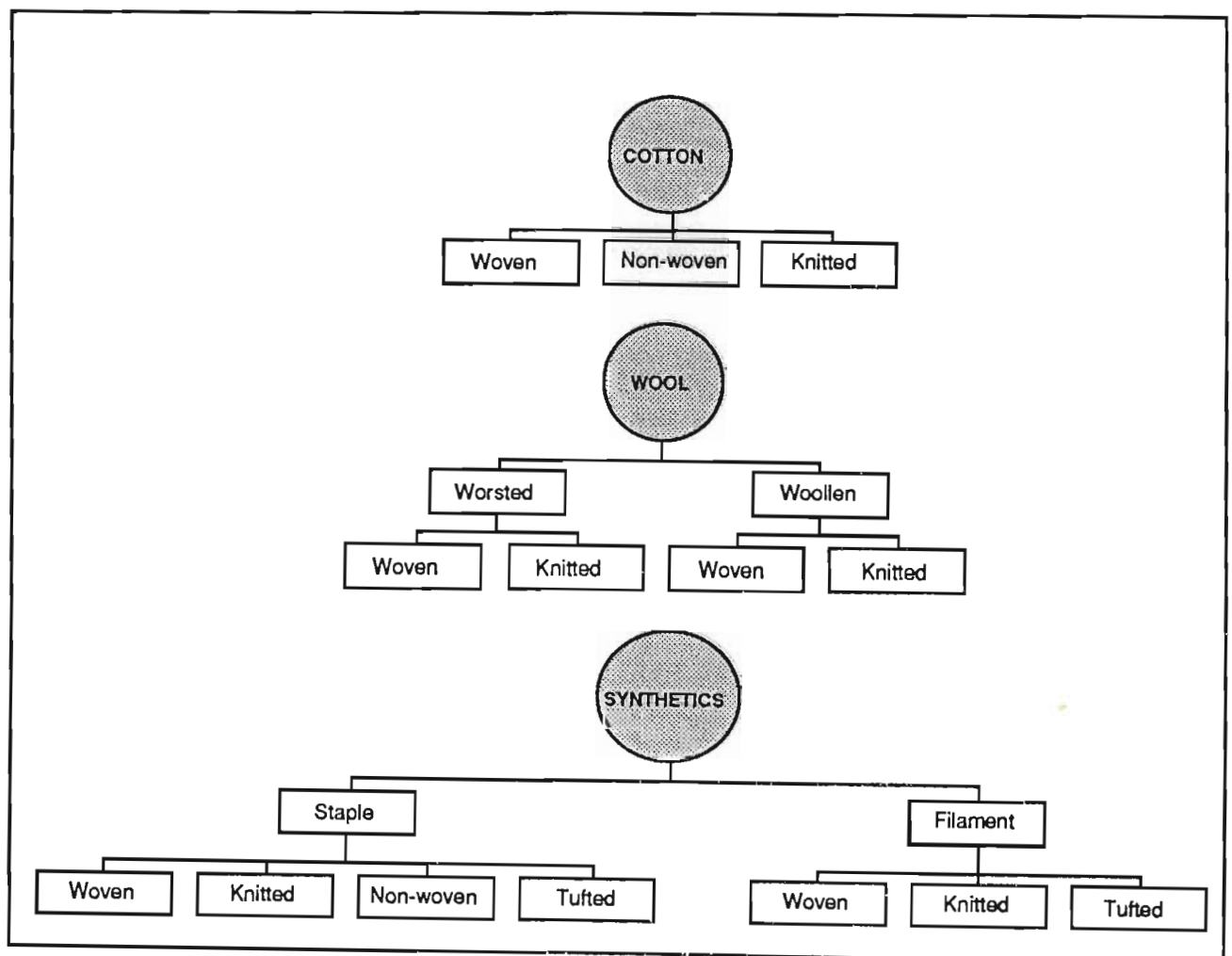
- 3) *Warping.* During warping, parallel yarns are wound onto a back beam. The back beams are combined during sizing to form a weaver's beam. In the case of coloured woven fabrics, the yarn is dyed prior to warping.
- 4) *Sizing.* The sizing operation coats the individual warp yarns with a protective film of size. The size strengthens the yarn, allowing it to resist the abrasive action of the loom, and reduces the hairiness of the threads.
- 5) *Weaving.* Weaving is a dry process, in which the weft is inserted into the warp, but is carried out under humid conditions. Under these conditions, the size film is flexible, and warp breaks on the loom can be minimised. After weaving the greige cloth is inspected for faults, and may be cropped and singed to remove excess hairiness.
- 6) *Knitting.* Knitting involves forming a fabric by the interlooping of successive series of loops of yarn or thread and is carried out with the continuous addition of lubricating oil to the yarn to minimise fibre breaks.
- 7) *Desizing.* During desizing the size is washed from the cloth. The technology used depends on the properties of the sizing agents.
- 8) *Scouring.* During this process, oils, fats, waxes, soluble impurities, and particulate and solid dirt adhering to the fibres are removed. Scouring usually involves treatment with a detergent, with or without the addition of an alkali, depending on the type of fibre and the degree of contamination.
- 9) *Bleaching.* Bleaching serves to whiten the fibre by removing the natural colouring matter. Bleaching is carried out using oxidising or, less often, reducing bleaching agents.
- 10) *Mercerising.* Mercerising refers to the treatment of fibres, usually cotton, under tension with concentrated sodium hydroxide. Mercerising imparts a sheen to the fibre and improves its uptake of dyes.
- 11) *Dyeing and printing.* Stock, yarn, or fabric is coloured to the customers requirements by the uniform or localised application of colouring matter during dyeing or printing respectively.

- 12) *Finishing*. Final processing operations impart special properties to the textile material, such as easy handling, mothproofing, antistatic, non-slip, and anti-piling.

2.4.3 Textile Mill Classification

Individual textile mills tend to concentrate on one method of textile manufacture, such as knitting or weaving, and on one fibre or its blends, such as wool, cotton or nylon and wool-acrylics, cotton-polyester or polyester-viscose. A detailed classification of the Textile Industry is difficult, but these two methods are commonly used, that is by fibre processing and by mill operation. Figure 2.2 presents the classification of finished products by the fibre processed.

Figure 2.2
Textile Industry Categorisation by Fibre Processed



The principle types of mill operations are presented in Figures 2.3 to 2.5 (ATMI, 1973, US EPA, 1974, NCWQ, 1975) and include:

- 1) Wool scouring and finishing;
- 2) Dry processing;
- 3) Woven fabric finishing;
- 4) Knitted fabric finishing;
- 5) Carpet manufacture;
- 6) Stock and yarn dyeing and finishing.

The last four classes may involve scouring, where cotton and polyester-cotton blends are processed.

Figure 2.3
Woven Cotton Fabric Finishing Mill

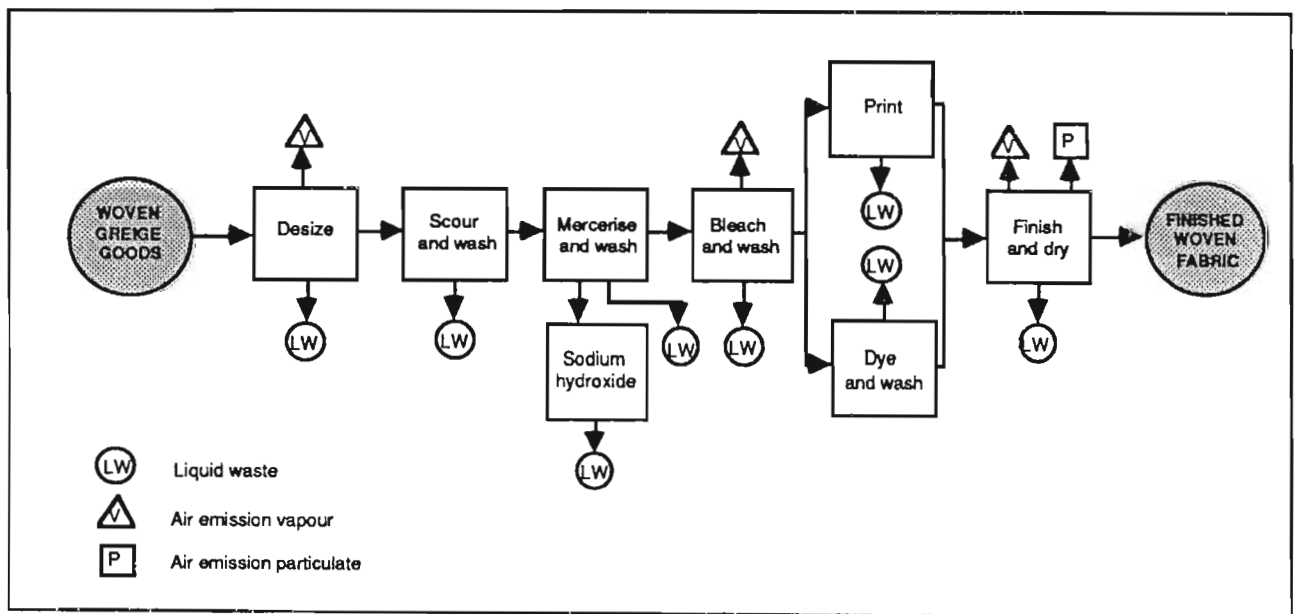


Figure 2.4
Knit Fabric Finishing Mill

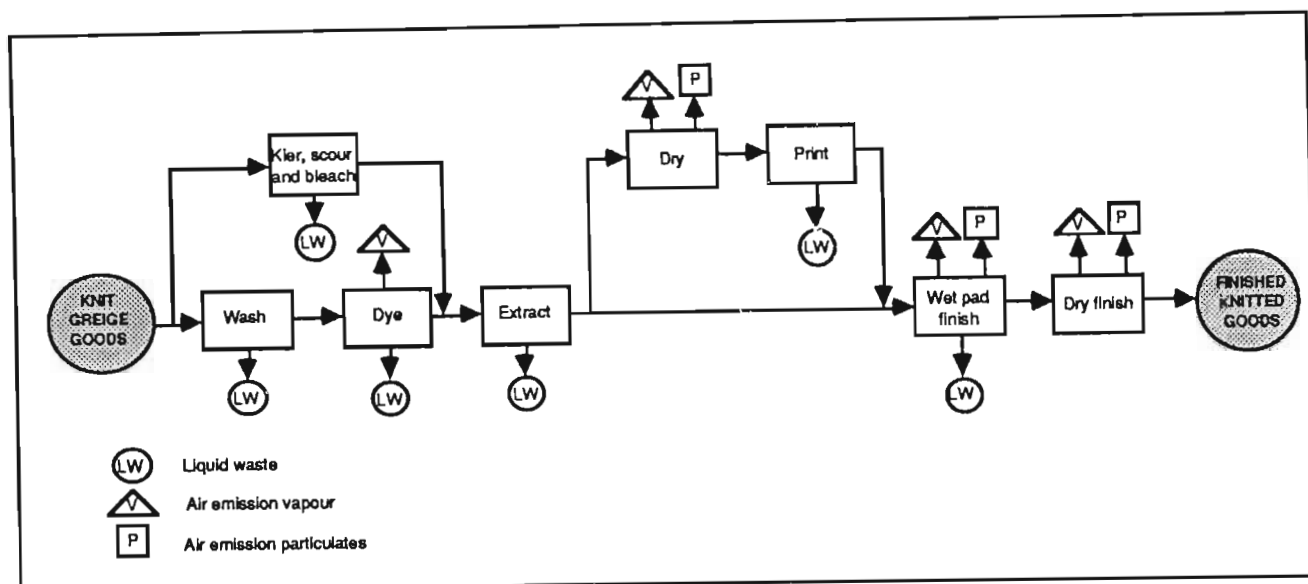
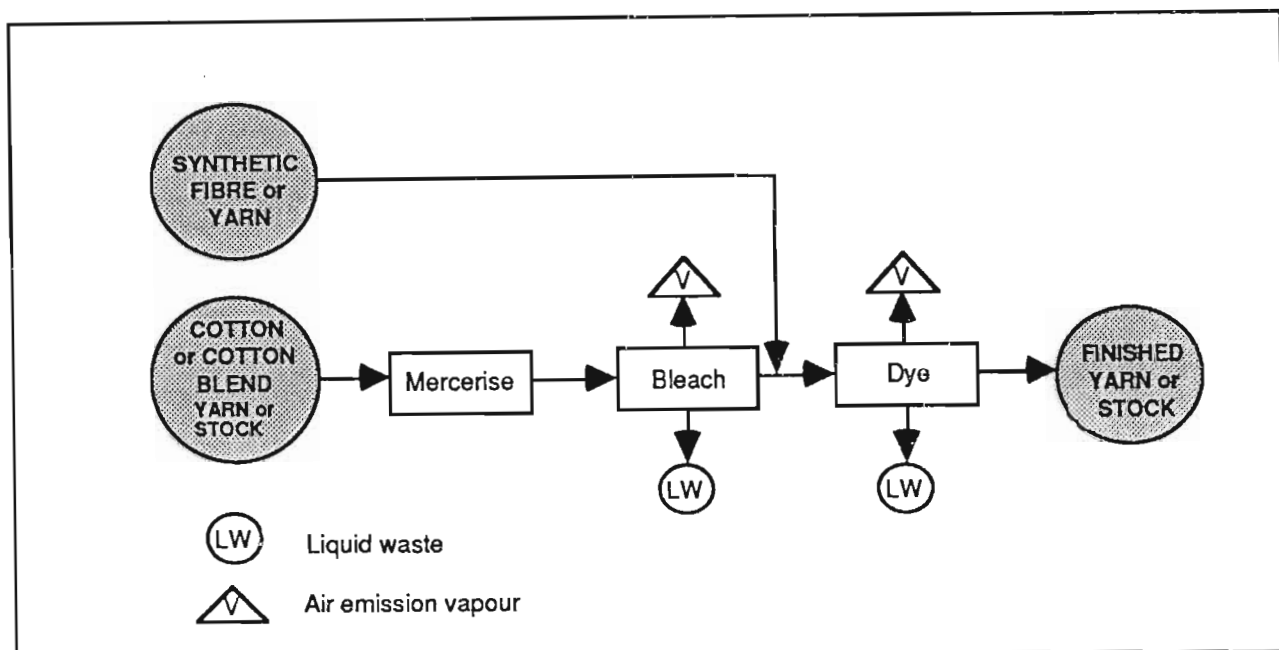


Figure 2.5
Stock and Yarn Dyeing and Finishing Mill



2.5. Scouring Technology

Scouring is a wet processing operation, designed to cleanse the raw fibres, leaving them in a condition suitable for subsequent processing. It is usually the first wet processing operation, where sizing is not carried out. Where sizing is carried out, scouring is preceded by desizing. Scouring consists of contacting the fibre with the appropriate chemical solution, allowing it to

react under the appropriate conditions of temperature and pressure, and then rinsing the unreacted chemicals and contaminants from the fibre.

2.5.1 Identification of Potentially Most Polluting Scouring Processes

The conditions of scouring depend on the fibre type and the degree of contamination. Clean or synthetic fibres are scoured in relatively mild conditions by comparison to the conditions required for the scouring of contaminated and natural fibres.

For example, scouring of polyester is usually undertaken in warm (60 °C), mildly alkaline conditions (1 g/l sodium carbonate), with a combination of non-ionic and anionic detergents, to remove oils and other minor contaminants that have been incorporated into the textile material during spinning, weaving, or knitting operations. Typically, the effluents produced vary in pH from 8 to 12, are warm (40 to 60 °C) and, for a water use of 20 l/kg fibre and a wet pick-up of 100 %, contain 0,2 g/l sodium (Buckley, 1983). These weak scouring effluents are not the concern of this dissertation.

By comparison, the scouring of cotton and cotton-polyester blends is carried out under severe conditions of temperature, pressure, pH and chemical concentration. Since the effluents produced are very alkaline, and contain high concentrations of inorganic salts and organic compounds, their discharge is potentially threatening to the environment. It is these so-called strong scouring effluents which are the subject of this dissertation.

2.5.2 Scouring of Cotton and Cotton-Blends

Scouring Action

Although cotton is not as contaminated as some other natural fibres, such as wool, it contains waxes of a high molecular mass, which are not easily removed. In addition, it contains protein impurities, which are located within the lumen of the fibre, making them resistant to chemical attack. The impurities may be removed from carded, woven, or knitted cotton, by treatment in boiling sodium hydroxide, in the presence of suitable auxiliary chemicals. During this severe alkaline scouring process, various chemical reactions occur, including the:

- 1) Conversion of pectins and pectoses to soluble pectic salts;
- 2) Degradation of the proteins into soluble amino acids or ammonia;
- 3) Solution of mineral matter;
- 4) Removal of adventitious dirt;

- 5) Hydrolysis of the saponifiable matter to form salts, which emulsify the unsaponifiable oils and retain the dirt particles in suspension;
- 6) Improvement of the hydrophilic properties of the fibre, which determine the water absorbability, and the evenness of dye and chemical uptake.

The fraction of sodium hydroxide consumed in the scouring process varies from 10 to 80 %, depending on the temperature and the reaction time of the process.

Cotton can be scoured equally effectively with other strong alkalis, such as potassium hydroxide, in place of sodium hydroxide. For the sake of clarity, reference is made only to sodium hydroxide in this dissertation. However, it should be noted that the principles, procedures and technologies applicable to sodium hydroxide scouring are also applicable to, for example, potassium hydroxide scouring.

Description of Scouring Process

Cotton scouring processes are batch or continuous. Batch scouring produces a sequence of effluents of decreasing concentration. Continuous scouring produces a single effluent, because the scouring solution is padded onto the textile material at high concentration and is removed in a subsequent rinsing process.

- * Batch scouring is generally carried out in cylindrical vessels, or kiers, made of cast iron or stainless steel. These may be open, where the liquor boils at atmospheric pressure (boil-off), or closed, where the liquor boils under pressures, at temperatures above 100 °C (kier-boil). In both instances, the operation commences when the textile fibre and chemicals are charged to the equipment. Steam is then used to heat the solution and circulate the sodium hydroxide through the textile material. The process continues for a predetermined period of time, and under the specified conditions of temperatures and pressures. Thereafter, the liquor is drained from the textile fibre, and the fibre is rinsed with water, either hot or cold, and either by drop-fill or overflow method.

Boil-off is an archaic method, which has been largely replaced by more effective scouring methods. A reducing agent is always added to prevent the oxidative degradation of the cellulose fibre, caused by the combination of atmospheric oxygen and alkali.

Typical boil-off conditions would be:

For cloth (BASF, 1977)

sodium hydroxide	10 to 20 g/l
wetting agent/detergent	1 to 2 g/l
liquor ratio	3 to 7 kg/kg cloth
processing temperature	95 to 98 °C
batch time	4 to 6 h

For cotton wool (Buckley, 1983 and Buckley *et al*, 1979)

sodium hydroxide	10 to 50 g/l
wetting agent/detergent	2 to 3 g/l
liquor ratio	20 kg/kg cloth
processing temperature	98 °C
batch time	4 to 6 h

Typical kier-boil conditions (Groves and Anderson, 1977) would be:

potassium hydroxide	40 g/l
(or sodium hydroxide equivalent)	
wetting agent/detergent	1 to 2 g/l
liquor ratio	10 kg/kg cloth
processing temperature	100 kPa at 135 °C
batch time	3 to 4 h

Continuous scouring involves the continuous passage of a length of textile material through a bath containing the so-called padding solution, usually sodium hydroxide, under specific conditions of temperature, pressure and concentration. Typical material speeds would be 30 to 80 m/min. The impregnated textile material is then subjected to a specific temperature and pressure regime, for a certain time, which allows the scouring action to proceed.

Thereafter, the textile material is rinsed free of dissolved impurities and unreacted processing chemicals by continuous passage through rinsing equipment, typically consisting of a multi-stage, counter-current sequence, operating with single- or multiple-water input, under boiling conditions. Continuous scouring is generally conducted in campaigns, consisting of a series of process batches; each of which is carried out under similar padding and processing conditions. When a campaign is completed, the padding solution and processing conditions are changed or adjusted, and the next campaign is commenced.

Continuous scouring is generally achieved in one of three types of units: J-boxes; caravans; or open-width reaction chambers.

J-boxes can be used to process fabric in either rope form, or in open-width form. Figure 2.6 is a schematic of a J-box machine. Scouring is achieved by impregnating the cloth with sodium hydroxide; heating it to elevated temperatures (93 to 99 °C); and allowing it to pass through the J-box, with a reaction time of approximately one hour.

In the caravan system, fabric is first padded with a solution of sodium hydroxide containing a reducing agent. It is then steamed and wound onto a roller, within a sealed vessel or caravan. The caravan is rotated, in a steam atmosphere at 90 °C, for one to two hours to allow scouring to proceed.

Open-width reaction chambers, such as the Vaporloc Unit, by Mather and Platt, are designed to operate under pressures of 200 kPa, with temperatures above 130 °C. The fabric is padded with a sodium hydroxide solution and scouring is achieved in periods of one to two minutes. Figure 2.7 is a schematic of an open-width rinsing range.

Typical compositions of the padding solution (Buckley, 1983) are:

sodium hydroxide	40 to 70 g/l
wetting agent	2 g/l
reducing agent	20 g/l
liquor ratio	0,7 to 1 kg/kg cloth

Figure 2.6
Schematic of a Rope or J-Box Rinsing Range

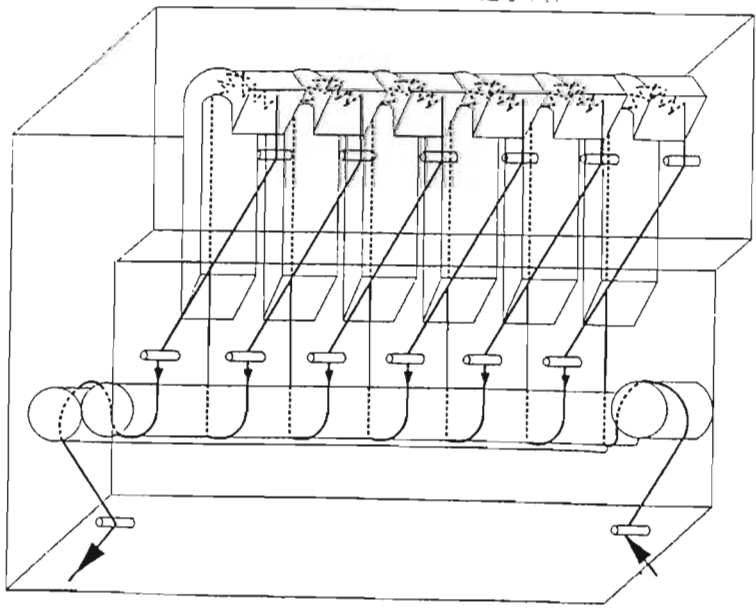
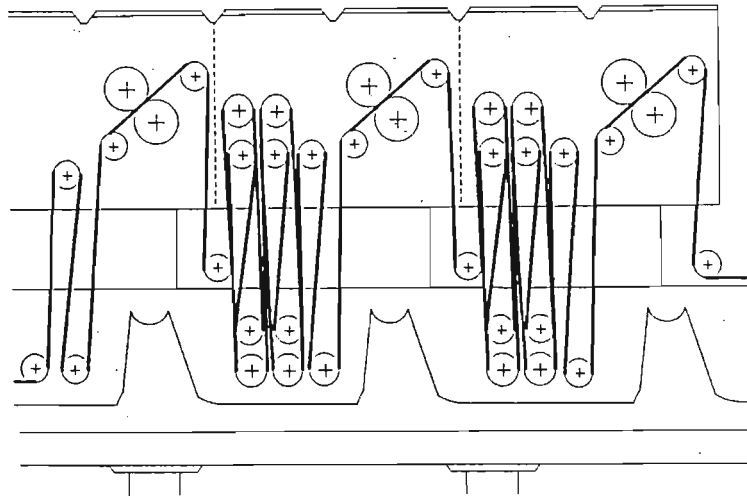


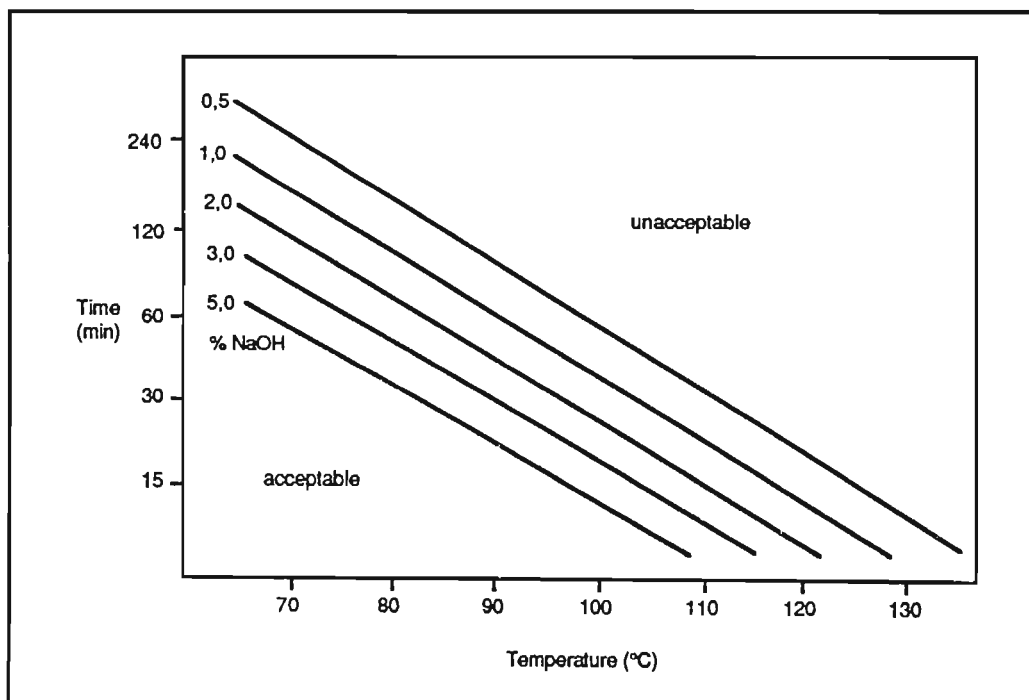
Figure 2.7
Schematic of an Open-Width Rinsing Range



Cotton-Polyester Blends

Cotton-polyester blends are treated either as heavily contaminated polyesters or mildly contaminated cottons, and are scoured accordingly. The alkali concentration, reaction time and temperature is controlled to minimise tendering, or saponification, of the polyester fibre. Figure 2.8 (BASF, 1977) presents the conditions under which the rate of saponification is unacceptably high. Scouring should be carried out under conditions of temperature and time which lie below the sodium hydroxide concentration lines.

Figure 2.8
Acceptable Saponification Limits of Polyester as a Function of Sodium Hydroxide Concentration, Temperature and Contact Time



Source: BASF, 1977

2.6. Characterisation of Cotton Scouring Effluents

Some empirical data on the characteristics of cotton scouring effluents are presented in this subsection. Section 4 discusses the theory of rinsing operations, relating the characteristics of scouring effluent to the design, configuration and operational parameters of the rinsing equipment.

2.6.1 Batch vs Continuous Rinsing

Scouring effluent results when the textile fibre is rinsed after padding and processing. As with padding and scouring processes, rinsing operations may be batch or continuous.

In a batch operation, rinsing will be conducted by overflow rinse or drop-fill methods. Overflow rinsing consists of adding water to a batch of cloth, in a confined vessel, with continuous overflow for a certain period of time, or until the overflow rinse water meets some predetermined quality criteria. Drop-fill rinsing consists of the repetitive draining and refilling of a confined vessel, allowing a dwell time after refilling, until the desired removal efficiency is attained. In general, the impurity concentration of each drop will be 10 to 20 % of the concentration of the previous drop. Elevated temperature enhances the rinsing efficiency.

Batch rinsing methods are inefficient, consume large quantities of water, and produce effluents of high volume and low concentration (0,5 to 2,5 g/l NaOH). Typical water use is 20 to 25 l/kg fibre (Pollution Research Group, 1989), and the effluent is produced at temperatures above 80 °C.

In a continuous operation, there is a continuous flow of water and textile fabric through the machine. The machine may be a single compartment rinsing range, or a multi-unit range, usually in a counter-current, with or without fabric neutralisation (using acid) in the final wash bowl, depending on subsequent operations. Typical water use is 4 to 5 l/kg fibre, effluent temperature is near boiling, and sodium hydroxide concentrations in the effluent are high (typically 6 to 20 g/l NaOH).

The subject of this dissertation is strong effluents from the continuous scouring of cotton and cotton-polyester blends, since the treatment process developed is technically and economically applicable to effluents containing high concentrations of sodium hydroxide.

2.6.2 Chemical Composition

The chemical composition of effluents from scouring operations varies from plant to plant.

The concentration shows great variance, and is determined by several factors, including the:

- 1) Impurity concentration of the raw fibre prior to wet processing;
- 2) Use of batch or continuous processing systems;
- 3) Use of batch or continuous rinsing operations;
- 4) Chemical concentration in the padding solution;
- 5) Efficiency and configuration of the rinse range;
- 6) Liquor-to-fibre ratio, and wash water flow.

As a guide to the range of characteristics of strong scouring effluents, Table 2.3 presents approximate concentrations of a selection of traditional parameters. The data in this table has been extracted from various surveys, and can be used to predict the effluent characteristics of a scouring operation.

Table 2.3
Examples of Typical Compositions of Strong Scouring Effluents

Fibre ¹	Form	Process ²	Effluent (l/kg)	pH	Cond. (mS/m)	TS (g/l)	Na (g/l)	Ca (g/l)	Mg (g/l)	NaOH (g/l)	TOC (g/l)	COD (g/l)
cotton	fibre	boil-off b	20,0	11-12	1 700		2,3			2,4	2,1	
		kier-boil b	17,0	10-13	1 500		1,9			2,7	1,4	
cotton	fibre	boil-off b	20,0	12-13	1 300		2,9			4,2	3,4	
cotton	woven	kier-boil b	30,0	10-13	<3 400	7	1,8	0,03	0,02	1,5	1,2	
cotton	woven	kier-boil b	18,0	9-12		4	1,1				1,5	3,3
cot-PE	woven	caravan c	3,8	13,5	7 400	51	17	0,08	0,02	26	10	32
cot-PE	woven	J-box c	2,3	13,0						9		
cot-PE	woven	open width c	3,1	13,5	8 200	30	11	0,03	0	19	4	10
cot-PE	woven	open width c	7,3	13,0						6		
cot-PE	woven	open width c	2,5	10-12		24					5,3	12
cot-PE	knit	b	21,0	9,0	100	2,7	0,1	0,02	0,02		1,1	

Note: ¹ cot-PE denotes cotton-polyester blends

² b denotes batch, c denotes continuous

Source: Buckley, 1983; Buckley *et al*, 1979; Groves and Anderson, 1977; Pollution Research Group, 1989

2.6.3 Pollutant Loading

The emission rates, or loading, of a selection of traditional pollutants from typical scouring processes are as follows (Pollution Research Group, 1983; Buckley, 1983; Buckley *et al*, 1979; Groves and Anderson, 1977; Pollution Research Group, 1989):

biological oxygen demand (BOD)	10,8 kg/tonne fibre
chemical oxygen demand (COD)	4 to 122 kg/tonne fibre
suspended solids (SS)	5 kg/tonne fibre
total dissolved solids (TDS)	9,8 kg/tonne fibre
total solids (TS)	30 to 200 kg/tonne fibre
oil and grease	20 kg/tonne fibre
sodium	1 to 60 kg/tonne fibre
sodium hydroxide	18 to 100 kg/tonne fibre
calcium	0,1 to 0,8 kg/tonne fibre
magnesium	0 to 0,6 kg/tonne fibre

For comparative purposes, the pollutant loadings of singeing, desizing, scouring, bleaching, and mercerising effluents from a particular mill, processing cotton and cotton-polyester blends, are presented in Table 2.4. At this mill, the scouring effluent contributed over 25 % of the chemical oxygen demand (COD), and over 36 % of the total solids (TS) loadings of the wet preparation section. On an overall mill basis, both the COD and TS constituted 10 % of the total mill waste water pollutant load.

Table 2.4
Relative Pollutant Loadings from Individual Textile Unit Operations

Process	Effluent Volume (%)	Chemical Oxygen Demand (mass %)	Total Solids (mass %)	Oxygen Absorbed (mass %)	Total Carbon (mass %)
Singeing	2,1	8,2	5,7	7,0	6,4
Desizing	33,9	57,0	44,0	47,9	61,6
Scouring	22,2	25,6	35,8	25,8	26,6
Bleaching	22,2	5,9	7,2	13,3	3,3
Mercerising wash 1	0,8	0,1	0,4	0,1	0,1
Mercerising wash 2	19,8	3,2	5,9	5,9	2,0
Total emission rate (g/kg cloth)		130	186	21	55
Concentration (mg/l)		10,4	14,3	1,6	4,4

Source: Buckley et al, 1979

SECTION 3

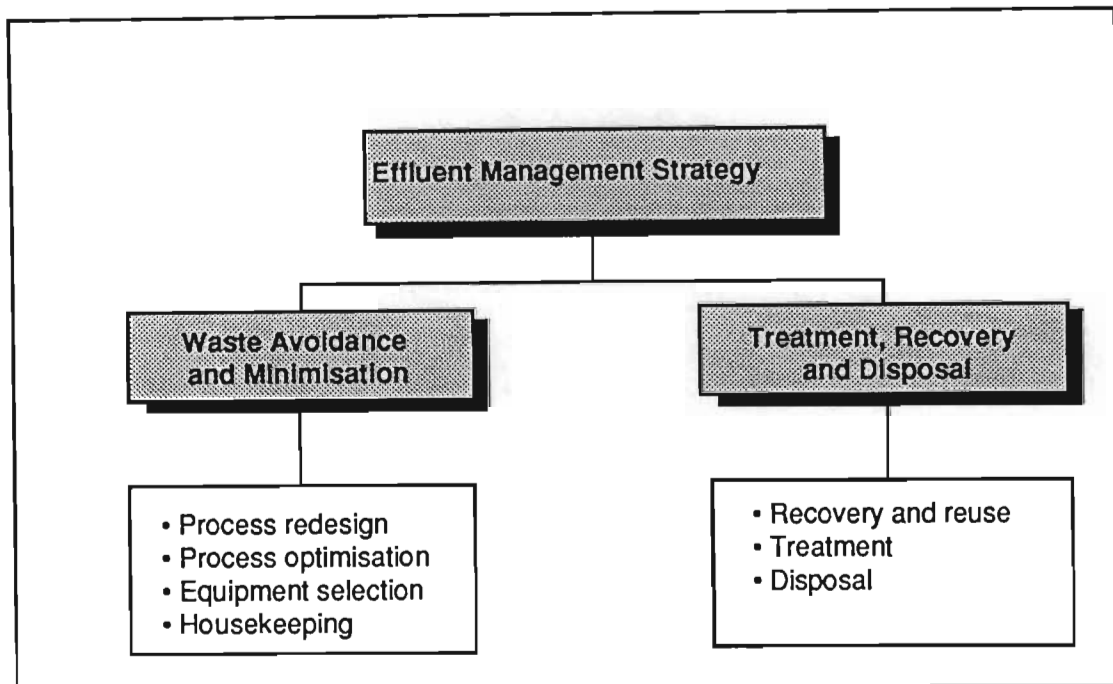
ENVIRONMENTAL MANAGEMENT OPTIONS FOR POLLUTION CONTROL IN SCOURING PROCESSES

The overall management of the scouring process from a pollution control aspect is essential because of the serious environmental impact associated with the disposal of the effluents, either neutralised, or in their alkaline state, and because of the escalating costs associated with purchasing new chemicals and disposing of waste chemicals (Buckley and Simpson, 1990a). In considering and developing a management strategy for pollution control of cotton scouring processes, a factory should implement a phased programme of waste prevention, minimisation (Section 3.1) and treatment (Section 3.2) with a suitable basis or incentive for decision making. For example, this basis may be economics, the reduction of water use, the lowering of pollutant loadings, or the elimination of environmentally unacceptable chemicals.

There are two approaches to addressing waste management, and the most acceptable solution may be a combination of the two approaches. The first approach, **process-oriented waste prevention and minimisation**, involves the reduction, elimination or recycling of pollutant discharges. In the second, or traditional, approach, industry relies on **add-on controls or treatments**, which reduce the impact of waste after it has been generated. In recent years, the limitations to this second approach have been recognised and legislative authorities in many countries have increasingly enacted regulations which favour a process-oriented approach to waste management. The need to develop process-oriented pollution control measures has resulted indirectly in an initiation of ideas in waste management. The generation of waste is increasingly regarded as a loss of resources, and efforts are being concentrated on the integration of waste minimisation procedures into the process at source. By adopting a systematic approach to identifying potential problems and solutions of waste reduction throughout the manufacturing process, considerable savings accrue with minimal expenditure, improved public attitude towards the company and relieved regulatory burden, while being of benefit to the environment (Pearson, 1991; Benforado et al, 1991).

The overall strategy for the implementation of an effluent management system for scouring processes involves, on the one hand, process-oriented waste avoidance and minimisation and, on the other hand, waste recycling/recovery, treatment and disposal. These options, and their applications, are summarised in Figure 3.1 and reviewed in Sections 3.1 and 3.2. The development and practical implementation of an appropriate waste management strategy for one particular site is described in the remaining part of this dissertation.

Figure 3.1
Effluent Management Options for Scouring Processes



3.1. Waste Management by Waste Avoidance and Minimisation

Process-oriented waste management options, in order of preference, include avoiding the use of unacceptable chemicals and waste minimisation.

Although *avoidance* is the preferred option, the chemistry of the cotton scouring process requires the use of traditional combinations of chemicals, in certain concentrations and under specific conditions, for which there is no effective alternative. *Waste minimisation* places emphasis on prevention at source, with the reduction of waste volumes, concentrations and pollutant loadings, and on measures to avoid catastrophic levels of emissions resulting from breakdowns. Waste minimisation is the first phase in reducing the environmental impact of a process, and addresses aspects such as process design and optimisation, equipment selection, and housekeeping procedures (Chemex, 1991). By minimising the generation of waste, subsequent requirements for downstream processing, handling and treatment are eliminated or reduced. Waste minimisation often involves procedural, operational or material changes, without necessitating serious equipment changes, or sophisticated technology. They are usually inexpensive relative to their potential long-term economic benefit, and can be implemented without disruption of the manufacturing process (Nichols, 1988). Some relevant process-oriented waste management strategies are presented below.

3.1.1 Process Redesign

The design of a process is an important aspect of waste minimisation. In the past, at any given facility, the same technology and procedures have tended to be used over the lifetime of a process. Environmental, safety and quality assurance considerations now necessitate re-evaluation of existing processes, to allow improvements to be made which ensure that processes become more environmentally-compatible. Such improvements may involve changes in raw materials, process sequence, processing chemicals, and process controls as follows.

- 1) Changes in raw materials may result in reduced effluent discharge problems. For example, synthetic fibres, or higher quality natural fibres, with lower concentrations of impurities, may be used (Pollution Research Group, 1990).
- 2) Reductions in the overall number of processes in the manufacturing sequence can lower the number of padding and washing operations required. For example, oxidative-desize allows desizing, scouring, and bleaching to be carried out in a single stage. Scouring-bleaching and desizing scouring are further examples of reduced stage operations.
- 3) Changes to processing chemicals may influence the pollution characteristics of emissions. Solvent scouring has found limited application as an alternative to aqueous scouring (Pollution Research Group, 1990). In this system, water and scouring chemicals are replaced by an organic solvent, which is recovered by distillation. Water pollution is reduced, but unrecovered solvent and solvent residues often present greater disposal problems than waste water streams. In addition, air pollution during solvent recovery and product drying is usually unavoidable.

High-COD organic acids, such as acetic acid, used in neutralising the fibre after scouring and rinsing, may be replaced with stronger mineral acids. In such cases, reliable pH control equipment is required to prevent over-acidification and subsequent degradation of the cotton fibre.

- 4) Stricter processing controls allow processes to proceed uniformly and reproducibly, thus reducing the potential for fluctuations both in processing conditions and in effluent characteristics. Added benefits include the reduced cost of quality control and assurance (Patel, 1988). Examples of improved control include the installation of fully computerised processing; automated chemical dosing systems to prevent excess use of chemicals; and instrumentation to ensure the uniformity of chemical application and temperature control.

3.1.2 Process Optimisation

In the context of the current dissertation, the most relevant aspect of process optimisation refers specifically to a chemical, water and effluent management strategy addressed at the scouring process, and aimed at preventing waste by ensuring that minimal quantities of chemicals and water are used. The successful development and implementation of a subsequent, but effective, treatment and recovery system for cotton scour effluents depends on a complete understanding of this water and chemical flow regime, both within the scouring process and in relation to the overall factory water and chemical consumption and distribution. Process optimisation may involve (Buckley and Simpson, 1990b) various procedures:

- 1) Modifying established recipes, which are usually designed to be fail-safe under the most extreme conditions, and result in the excess use of chemicals, increased pollution and higher effluent concentrations;
- 2) Conducting water, heat energy, chemical, and effluent emission rate balances over the scouring process;
- 3) Identifying the minimum water quality requirements for scouring;
- 4) Minimising the use of water during scouring;
- 5) Investigating the direct use of other factory effluents as rinse water in the scouring process;
- 6) Minimising sodium hydroxide carry-over from padding to rinsing;
- 7) Minimising rinse water flow;
- 8) Modifying, or replacing, inefficient textile equipment;
- 9) Improving existing control equipment to ensure that targets are attained.

Case studies from the Pollution Research Group's files (Buckley and Simpson, 1990b) indicate how significant savings can be achieved by process optimisation, which simultaneously reduces water and chemical consumption, and pollutant emission rates. A recurring conclusion from such investigations is that there is often no immediate need for the installation of effluent treatment equipment (Buckley and Simpson, 1990a), since substantial savings in water and chemical consumption, and reductions in effluent emission rate, could be achieved through in-house water and effluent management programmes which aim to optimise the process. In the past, these savings have often been adequate to meet regulatory requirements at the time of the study, but as stricter environmental legislation is introduced the development of treatment facilities is unavoidable. Additional published literature is available on process optimisation (ATMI, 1973; US EPA, 1978; Lockwood Greene

Engineers Inc., 1975; Cooper, 1978). Although all these studies may not relate specifically, or totally, to the scouring process, the philosophy and approach taken is directly applicable to waste minimisation during scouring. For this reason several examples are summarised below.

Example 1: Chemical and effluent balance

Sodium hydroxide is the major bulk chemical consumed by the Textile Industry and substantial amounts are discharged in textile effluents. Approximately 6 000 tonnes/a (2 % of the South African market) was consumed by the South African Textile Industry in 1987 and sodium hydroxide may account for up to 15 % of the total cost of dyes and chemicals (Pollution Research Group, 1990). The efficient use of sodium hydroxide lowers raw material requirements and effluent discharge costs. To establish the efficiency of sodium hydroxide use, the following parameters are relevant:

- 1) Sodium hydroxide purchases and transfers to production processes;
- 2) Cloth production at individual processes consuming sodium hydroxide;
- 3) Variation in the specific sodium hydroxide use (i.e., in relation to fibre throughput) by individual processes;
- 4) Theoretical (calculated from recipes) specific sodium hydroxide use;
- 5) Mass of recycled sodium hydroxide;
- 6) Potential maximum mass of sodium hydroxide that could be recycled.

Sodium hydroxide surveys and balances over individual processes, and over the entire factory can lead to substantial benefits. One such survey was carried out at a textile mill processing cotton, in order to evaluate the effectiveness to which sodium hydroxide was being used. The factory personnel had kept routine records of sodium hydroxide purchases and recoveries, process water and chemical consumption of individual machines, and cloth production rates. The survey involved the collation and analysis of data logged over a 12-month period from 1986 to 1987. Results were obtained which gave information on the specific water and chemical consumption (in relation to cloth processed) of individual processes and machines, and average sodium hydroxide concentration in the effluent. There were several conclusions from the study.

- 1) Comparison of the actual specific sodium hydroxide consumption on each machine with the theoretical consumption calculated from recipes and batch data indicated that there was considerable over-consumption. The main reasons for this observed over-consumption were the variations in wet pick-up of chemicals onto the fabric after impregnation of sodium hydroxide from the padding solution, and poor control in the mixing station, which resulted in padding solutions of higher-than-required concentration. The excess consumption of sodium hydroxide over the 12-month period amounted to 289 tonnes as 100 % NaOH, which translated to an overexpenditure of R180 000 (1986) for the period.
- 2) There was a significant monthly variation in specific sodium hydroxide consumption, reported in g/kg cloth, for various processes. It was assumed that the fabric quality during the month with the lowest specific sodium hydroxide consumption for each process was acceptable, although these figures were below the theoretical consumption calculated from recipes. On this basis, the annual consumption of sodium hydroxide would produce acceptable quality cloth was calculated to be 941 tonnes lower than the actual consumption and 652 tonnes lower than the theoretical consumption. These translated to potential annual savings of R600 000 and R420 000 (1986) respectively.
- 3) Less than 45 % of the sodium hydroxide used in mercerising was being recovered, since only the most concentrated rinsing water, that from the first rinse bowl, was being recycled to the evaporator for recovery. The sodium hydroxide discharged in the rinse water from the remaining bowls constituted 34 % of the total sodium hydroxide used at the site, and represented an annual replacement cost of R375 000 (1986). If this sodium hydroxide were recovered along with that from the most concentrated rinse stream, chemical consumption would be decreased and environmental benefit would be significant.

Example 2: Water balance

The water requirements of each manufacturing operation, in the context of the overall water balance, is an important aspect of water management. To establish an overall water balance and a process water flowsheet, the following parameters must be determined (Pollution Research Group, 1990):

- 1) The total water consumption from flow meters on the mains water reticulation;
- 2) The quality of the mains water and pretreatment requirements for use in processing;
- 3) The process water distribution to each section or process in the factory;
- 4) A detailed plan of process water, storm water, domestic waste streams, steam and effluent distribution pipelines and drains;
- 5) Effluent flows, expressed in cubic meters per hour and litres per unit of fibre, either by meter or kilogram.

A spreadsheet was developed to enable a particular textile mill to compute water use and effluent production on a weekly basis, for each individual process, utilities and the overall site. The balance indicated that about 30 % of the water intake could not be accounted. It also identified areas for investigation, and provided a means of establishing excess or unusual water use or effluent discharge volumes.

Example 3: Water and chemical reticulation

Since large volumes of water are used in rinsing processes the resulting effluents are often dilute. The possibility exists for the reuse of certain waste water streams in other textile operations as process water, with or without the addition of chemicals; rinse water, where low quality water is acceptable; and rinse water for direct reuse in successively dirtier bowls of continuous counter-current rinsing systems, as already discussed. In a closed loop recycle, a constant bleed-off may be required to maintain the concentrations below an predetermined level. The segregation and reuse of effluent streams reduces final effluent volume, and results in energy, water and chemical savings. As the cost of these raw materials has increased, the cascading of effluents has become popular, as illustrated below.

- 1) Spent bleaching streams have been successfully cascaded to scouring, where the residual chemicals and auxiliaries actually improved the efficiency of scouring (Water Resources Research Institute, 1982).
- 2) Rinsing and padding solutions from chlorine bleaching have been used to increase the degradation and removal rate in desizing, where the size to be removed is starch (Water Resources Research Institute, 1982).
- 3) Effluents from bleaching processes are clean, and have been used as rinse water in scouring (ATMI, 1973; Pollution Research Group, 1989).
- 4) Effluents from kiering, although highly contaminated by soap, emulsified waxes, and lubricants, may be reconstituted and reused (Pollution Research Group, 1989).
- 5) Mercerising effluent and impregnator overflows contain only low concentrations of impurities, and are usually concentrated by evaporation, for reuse as process sodium hydroxide in mercerising. These streams could contain between 50 and 300 g/l NaOH, depending on the equipment configuration and operational procedures and conditions. Where no evaporative recovery unit is available, these streams could be used for kier boiling, prescouring or dyeing (Water Resources Research Institute, 1982). Mercerising effluents of higher concentrations may also be used as padding solutions in scouring (ATMI, 1973). Alternatively, this effluent may be used as an ion exchange regenerant, in water softening systems on the site.

Cascading trials at a textile mill processing cotton and cotton blends, have indicated that substantial savings in water, effluent discharge and energy costs can result from the reuse of effluents from one process in another process (Pollution Research Group, 1989). In each trial, a minimum length of 10 000 m of cloth was processed under stable conditions. Weak effluent from the second mercerising rinse range was successfully reused as rinsing water in scouring, oxidative desizing and the first rinsing stage of mercerising, with no detrimental effect on final cloth quality. The results of the trials are summarised in Table 3.1.

Table 3.1
Results of Cascade Trials at a Cotton Processing Mill

Source Effluent	Destination Process	Comment
mercerising second rinse stage	scour rinsing range	<ul style="list-style-type: none"> • no difficulties experienced in subsequent processing • residual NaOH on cloth increased from 20 to 40 g/l • residual TOC on cloth increased by 25%
mercerising second rinse stage	oxidative desize rinsing range	<ul style="list-style-type: none"> • no difficulties experienced in subsequent processing • residual NaOH on cloth lower than when rinsed with fresh water • residual TOC on cloth increased by 25%
mercerising second rinse stage	mercerising first rinse stage	<ul style="list-style-type: none"> • no difficulties experienced in subsequent processing • no increase in residual NaOH on cloth • residual TOC and TDS increased by 50%

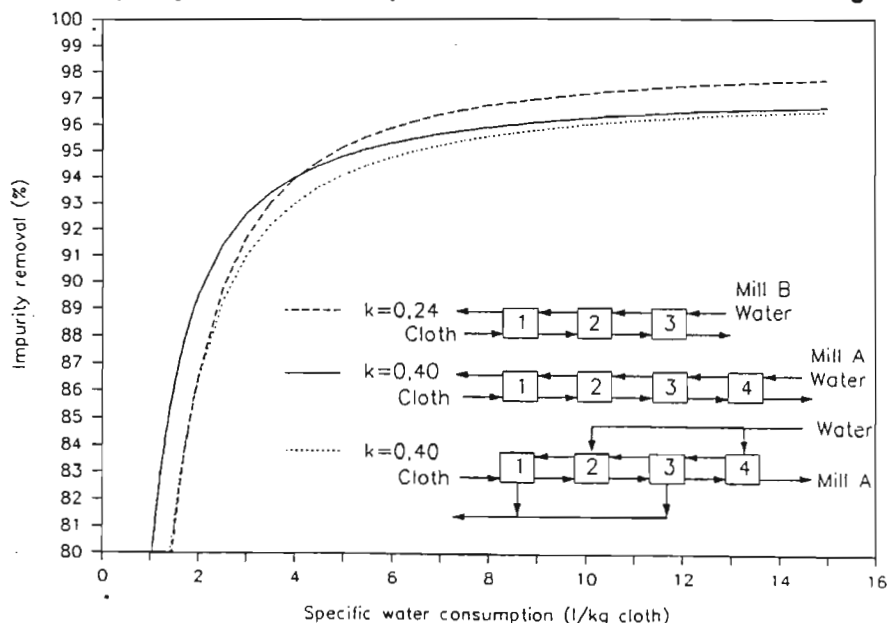
Source: Pollution Research Group, 1990

Example 4: Water use during rinsing.

The theory of rinsing is discussed in Section 4. Impurity removal increases with an increase in specific water consumption, but this increase is minimal at high specific water uses. A comparison of rinsing ranges at two mills was carried out (Pollution Research Group, 1988), to illustrate the effect of specific water use on impurity removal. Other variables considered were rinsing parameter, k , and equipment configuration. The results of this comparison are presented in Figure 3.2. Mill A had an open-width washing unit, operated in a combined of cross-flow, counter-current configuration, with rinse water entering at bowls two and four, and effluent leaving at bowls one and three. The rinsing parameter, k , for this range was 0,4. The effect of converting this unit to a full counter-current range ($k = 0,4$) is illustrated in the figure. Mill B had a counter-current three-bowl unit with $k = 0,24$. Several conclusions can be made.

- 1) For Mills A and B, very little increase in impurity removal occurs with a specific water use above approximately 8 to 10 l/kg cloth. The ideality of the rinse ranges, ie., their k values, limit the maximum achievable impurity removal as discussed in Section 4.
- 2) If the unit at Mill A were to be converted to a full counter-current unit, then the specific water use could be decreased by 20 % while achieving the same impurity level on the fabric.
- 3) For Mill B, impurity removals were comparable to, and above, those of Mill A at specific water uses of 5 l/kg cloth and above 5 l/kg cloth respectively. This is because the washer at Mill B was more ideal, ie., k was smaller.

Figure 3.2
Dependence of Impurity Removal on Specific Water Use for Three Rinsing Ranges



3.1.3 Equipment Selection

The influence of the design of processing equipment on scouring effluent characteristics and process performance has been discussed in Section 2.5. For example, the distinction can be made between batch and continuous processing equipment, and between largely physical conditions of scouring (high temperatures and pressures, long times) and largely chemical conditions of scouring (high reagent concentrations). The influence of the design and operation of the rinse equipment on the efficiency of the rinsing process and on the effluent characteristics is discussed in more detail in Section 4. For example, an equipment modification that could significantly reduce chemical consumption, carry-over, waste and discharge from continuous scouring processes, is the installation of high efficiency squeeze rollers after padding, and between each rinsing stage. Similarly, the use of additional drying cylinders preceding a padding bath, ensures that minimum dilution water is carried into the process on the fibre. This eases the load on recovery systems, or eliminates the need for such systems.

Although benefits are to be obtained from equipment replacement or modification aimed to reduce pollution, this is often expensive, not always cost-effective, and in many cases cannot be justified from purely environmental considerations. Several industries, such as the fine chemicals and pharmaceutical industries are replacing existing equipment and facilities with those which have been designed to comply with the concept known as containment - separating the process chemicals from the operators, and from the environment, for the protection of both (Semenenko, 1991). This concept provides complete isolation and integrity of material balances, providing full environmental protection, minimising fugitive loss, reducing chemical handling requirements and improving yields. There are various approaches to containment, and the degree to which it is practised varies between sites and industries. The concept is relatively new, and has been applied principally in industries where sensitive or highly toxic materials are processed. No applications in the Textile Industry are known.

3.1.4 Housekeeping

Housekeeping, commonly termed *good manufacturing practice*, is an integral, and often inexpensive, element of pollution prevention. It implies improved procedural or institutional policies and practices (Randall, 1992). There are several important aspects of housekeeping as it relates to scouring processes.

- 1) *Waste handling and segregation*, which involves the identification, segregation, and separate treatment of high strength and environmentally-detrimental effluents, and avoids dilution with weaker and more environmentally-compatible effluents.
- 2) *Procedural measures*, to facilitate better documentation, and improved materials handling and storage, material tracking and inventory control. This includes careful and regular inspection and auditing of equipment, with annual emission balances to measure consistency and improvement, and to identify potential areas for pollution control. The imposition of a strict material control policy is essential in preventing the excessive use, and waste, of chemicals and auxiliaries. Central to waste minimisation is the implementation of an efficient management data acquisition and reporting system. This will ensure that current data is available to management in an immediately usable form. This data acquisition process will be aided by the installation of chemical, water and effluent flow meters (US EPA, 1978; Funke, 1969; Etablissements Emile Degremont, no date).
- 3) *Loss prevention*, to provide better awareness of spill prevention and in-house preventative maintenance programmes. The development of procedures for containing and handling accidental releases of large quantities of scouring chemicals, and sodium hydroxide specifically, will limit the consequences of adverse effects to personnel and the environment. For example, dry clean-up of chemical spills is preferable to dilution and flushing. The use of hose-pipes for spill control or equipment and floor washing should be discouraged. Closely related to the handling of spills, is the identification of shock discharges characterised by high emission rates, and a means to distribute such discharges evenly into the overall factory discharge. Examples of such a discharge would be the release of a bath of padding solution (say 20 to 70 g/l NaOH) at the completion of a campaign of batch-continuous processing runs; the discharge of the boil-off or kier-boil liquor at the completion of a batch scour; or the indiscriminate disposal of residual chemicals and spent liquors at other stages in the process.
- 4) *Effective maintenance*, which is both thorough and routine. Pipes, drains, sumps, flow meters, dripping taps and automatic valves should be given special attention.
- 5) *Staff motivation and training*, since considerable benefits are accrued if staff understand the process and are aware of the need for resource conservation and pollution control. In addition, upper management initiatives, and incentives and training offered to staff, often result in improved production and minimum waste.

- 6) *Accounting practices*, to incorporate a better apportionment of waste management costs to the departments that generate wastes.

3.2. Waste Management by Treatment, Recovery and Disposal

Waste minimisation procedures are rarely effective enough to result in zero discharge. Wastes are produced and may require *treatment*, preferably with *recovery and recycling*, to meet the particular requirements of the site. Recycling allows the waste to be put to good use, but should only be considered after process-oriented management options have been implemented. With increasingly stringent regulatory requirements, tailor-made treatment and recycle solutions need to be developed, which consider the individual clean-up requirements, and technical, economic and environmental aspects. Increasingly, these solutions involve a combination of unit processes into an effective, economically viable treatment sequence, which performs to the required specifications. Unavoidable and untreatable wastes may be produced, either directly from the production process or as a consequence of a treatment process. Thus, adequate *waste disposal* is required, which either dilutes or immobilises the waste, in a manner which renders it harmless to the environment.

There are three principal policy options applicable to the handling of strong scouring effluents. These are, in order of increasing desirability, as follows:

- 1) *Direct discharge* to a sewer, disposal at sea, or discharge to solar evaporation ponds, without treatment or reuse, are the most commonly practised techniques of management of strong scouring effluents in Southern Africa. These techniques result in considerable impact on the environment, as a medium sized textile mill will discharge between 0,8 and 1,2 tonnes/d of sodium hydroxide, in the form of scouring effluent. They are viewed as short term solutions, and more environmentally-acceptable, on-site treatment options are preferred.
- 2) *Partial or extensive in-plant and end-of-pipe treatment* of the effluent prior to discharge, to render harmless any specific components which are potentially harmful to the environment. This improves the quality of the effluent, particularly with regard to pH, COD, suspended matter and organic contaminants. The trend towards combined treatment at source and end-of-pipe is increasing in developed countries (Chemex, 1991), since legislation is requiring guarantees on pollution control.

- 3) *Industry-based recycle* of effluents for reclamation of reusable components, such as water and chemicals, on an end-of-pipe or closed-loop recycle basis. This option is the most preferable since it ensures maximum simultaneous resource conservation and environmental protection.

The selection of treatment or recycle operations and their combination in an effective sequence, which is economically, technically and environmentally viable, is a complex procedure. There are several stages involved in the selection process (Chemex, 1991).

- 1) Surveying the facilities and available operating data.
- 2) Defining all design criteria, such as the technical requirements, discharge standards, utility costs, and the impact of individual waste streams on the total factory waste.
- 3) Conceptualising a series of potentially applicable treatment sequences.
- 4) Conducting pilot trials to determine potential average, maximum and minimum emission rates, optimum combinations of unit operations and operating costs. These trials decrease the risk factor, and enable the capacity and performance of the process sequence to be guaranteed.
- 5) Developing a conceptual design and costs for several technically viable sequences.
- 6) Developing the basic engineering for the selected option.

Treatment or recycling plants can be designed to meet almost any quality, performance or discharge criteria, if the cost is not the determining factor. A cost-effective environmentally-compatible, and technically feasible solution needs to take into consideration particular site constraints. The final process selected will depend on site-specific discharge regulations and possible amendments; effluent discharge costing formulae; cost of steam (heat), water pretreatment, and alternative water supplies; company preferences for self-sufficiency in pollution control; availability of an external treatment plant; and site expansion plans.

Table 3.2 summarises conventional options for generally improving effluent characteristics with respect to volume, colour, soluble organic compounds, soluble inorganic compounds and settleable and suspended solids, with or without recovery of resources.

Table 3.2
General Options for Improving Effluent Characteristics

Effluent Characteristic	Methodology	Technical Options
volume	see Section 4	
colour	segregation and treatment	flocculation, adsorption, hyperfiltration
organic compounds	segregation and treatment; process selection; control of chemical use	biological treatment, flocculation, adsorption, microfiltration, ultrafiltration, hyperfiltration
inorganic compounds	segregation and treatment; process selection; control of chemical use	hyperfiltration, electrodialysis, electrolysis
settleable and suspended solids	separation	screening, settling, flocculation, dissolved air flotation, microfiltration

Source: Pollution Research Group, 1990

With increasingly stringent environmental requirements, conventional systems are not generally capable of treating industrial effluents to meet anticipated lower limits (Smart, 1990). Furthermore, technologies are not universally applicable, and often a combination is required of two or more mechanical, chemical, biological or thermal processes in a sophisticated economically and environmentally-acceptable system.

The problem of selecting a process for the treatment or recycle of scour effluent is complicated by the fact that conventional primary and secondary treatment methods of screening, filtration, sedimentation, flotation and biological treatment are not usually applicable. In addition, tertiary and advanced water treatment operations of coagulation, multi-media filtration, activated carbon adsorption, ozonation and chemical or wet oxidation are not suitable. For the treatment or recycle of scouring effluents, it is necessary to apply a combination of, often sophisticated, chemical and physical techniques. Treatment and recycle systems which have either been considered, or found application, in the past are reviewed below.

3.2.1 Review of Options for Recovery and Reuse of Scouring Effluents

Six recycle techniques are reported in the literature which may allow partial recovery and reuse of water or chemicals from scouring effluents. Most of these techniques have been tested on a laboratory-scale only, and few are available commercially. These are listed below.

Causticising with sodium hydroxide recovery

Causticising is used in the pulp and paper industry as a means of recovering pulping chemicals for reuse in the preparation of new pulping liquor (Cooper, 1978). It is potentially applicable to the recovery of sodium hydroxide from scouring effluents which are sufficiently

concentrated with respect to both sodium and organic compounds. The dilute waste liquor is concentrated by evaporation prior to regeneration. Regeneration entails burning the concentrate for heat recovery, to leave a residual sodium-based salt, or mixture of salts, depending on the pulping process. Where the residue contains sodium carbonate, calcium oxide is added to convert the sodium salt to sodium hydroxide. This technology is not known to have been used commercially for the treatment of scour effluents.

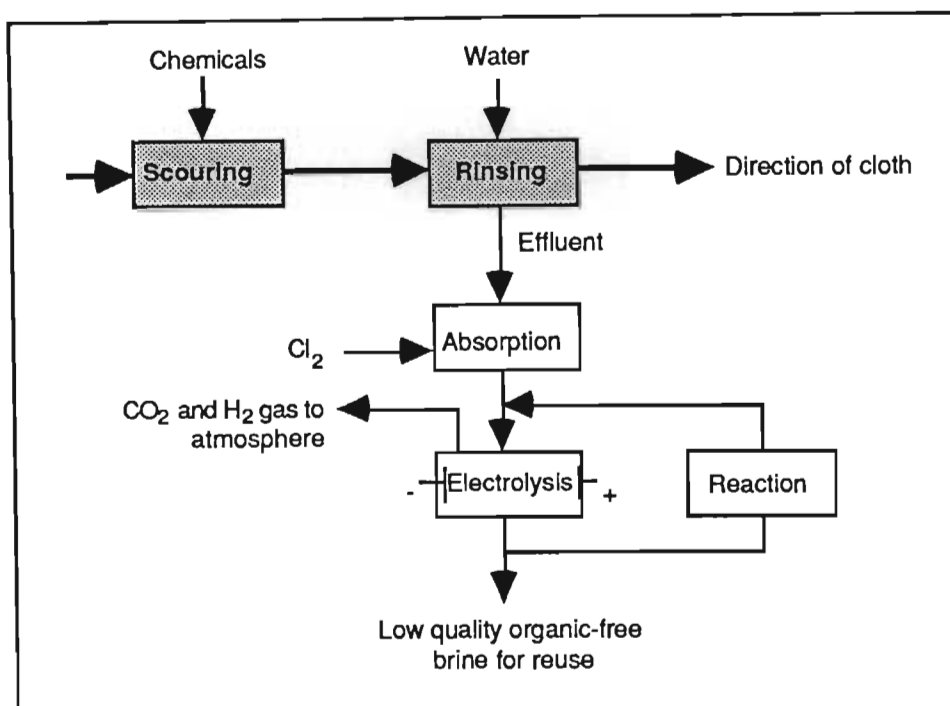
Neutralisation and electro-oxidation with low quality water recovery

Trials indicate that electro-oxidation of organic material in scouring effluent is technically feasible, and can neutralise the effluent and lower the COD concentration considerably (Pollution Research Group, 1989 and 1990). This has a significant impact on factory discharge, since scouring effluents can contribute up to 25 % of the COD in the overall discharge. Electro-oxidation was achieved using hypochlorous acid, which was generated from the effluent components during electrolysis in an electro-oxidation cell. The typical composition of scouring effluent used in the trials was: pH 13,7; TS 64 000 mg/l; TOC 7 700 mg/l; COD 26 000 mg/l, Na 15 400 mg/l; Cl 1 mg/l; and total Ca and Mg 100 mg/l. Figure 3.3 is a schematic of the treatment process, which consists of:

- 1) Neutralisation of the sodium hydroxide in the effluent using chlorine to produce sodium chloride;
- 2) Electrolysis of the sodium chloride in an undivided electro-oxidation cell to generate hypochlorous acid;
- 3) Oxidation of the organic compounds in a reaction vessel with a suitable residence time.

The process produces a colourless slightly alkaline, and mildly oxidising brine solution, which may be reused in bleaching or as low quality water. Hydrogen gas from the cathode reaction, and carbon dioxide gas from the oxidation of organic compounds, are also produced. Typical results indicate that initial current efficiencies for the removal of easily oxidisable COD is near 100 %. As the COD concentration decreases, the resistance to oxidation increases, with overall COD removal efficiencies dropping to 90 % current efficiency, at 70 % COD removal, and to 40 % current efficiency, at 95 % COD removal. The major causes of reduced efficiencies are the side reactions which produce oxychlorides, under conditions of high temperature, low chloride concentration, high hypochlorite concentration, and high current densities. Optimum pH values for maximum current efficiencies are 5,5 to 6,5, where 85 % of the COD is removed at 85 % current efficiency. Colour and turbidity removal are complete, while the Na, Mg and Ca concentrations are unchanged. The concentrations of chloride and hypochlorite in the treated effluent are 16 000 and 5 300 mg/l respectively. This stream may be reused as low quality water.

Figure 3.3
Schematic of Electro-Oxidation Process



The process described above is similar to one developed for the purification of alkaline solutions after the bleaching of cotton fabrics (Gorzka *et al*, 1991). Organic impurities were electro-oxidised using a Ti electrode coated with ruthenium and titanium oxide, at 600 to 1 000 mV (1 A/dm²). Sodium hydroxide solutions treated in this way could be reused.

Additional literature is limited with respect to the use of electro-oxidation to treat alkaline textile waste waters. Studies of the application of this technology in the textile industry appear to be restricted mainly to the reduction of COD, colour and organic matter content in waste waters containing dyes (Wilcock *et al*, 1992; Uhrich *et al*, 1988; Kennedy, 1991; Shifin *et al*, 1975; and Svetashova *et al*, 1976). Furthermore, as a technique for the destruction of organic compounds in general industrial waste waters, electro-oxidation is currently a popular area of research and development. Useful reviews of the potential applications are given by Savall and Comninellis (1992); Sequeira and Araujo (1991); Meissner and Haertel (1992); and Scott (1992).

Membranes processing with water and chemical recovery

Membrane separation techniques, such as microfiltration, ultrafiltration and reverse osmosis, are pressure driven techniques, capable of separating solution components on the basis of molecular size and shape, and involve neither a phase change, nor interphase mass transport. Membrane techniques have been used in the Textile Industry for treatment of

various waste waters (Brandon and Gaddis, 1977; Brandon *et al*, 1981; Brandon and Samfield, 1978; Porter and Goodman, 1984; Treffry-Goatley *et al*, 1983; El-Nashar, 1977). A combination of ultrafiltration and reverse osmosis, which is technically capable of purifying and concentrating, was proposed for alkaline effluents from the Textile Industry (Bechtold *et al*, 1985), but the principle could not be put to practice at the time because of the instability of polymeric membranes to sodium hydroxide. However, more recently, membranes have been produced that are capable of effective separation over extreme ranges of pH (0.5 to 14) and at temperatures over 60 °C. For example, Gaddis *et al* (1989) describe the recovery of sodium hydroxide from textile finishing waste waters by ultrafiltration, and the reuse of this hydroxide solution in dyeing processes at the site.

Dynamic (formed-in-place) membranes, laid down on porous stainless steel supports, are capable of treating effluents under extreme conditions (Johnson *et al*, 1972; Groves *et al*, 1983a and 1983b). Dynamic membranes have been used in several textile applications (Brandon *et al*, 1980). Such systems are robust and have high temperature stability, long service life, and the ability to replace the dynamic membrane *in situ* using solution chemistry. However, they are expensive.

Laboratory tests (Brown and Buckley, 1983), using dynamically-formed ultrafiltration membranes, have successfully treated scouring effluent, to produce a concentrate of organic material and a permeate stream of sodium hydroxide. It is feasible that the permeate may be concentrated by evaporation, to enable both rinse water and chemicals to be recycled to the scouring process. Typical upper limits of composition of scouring effluent used in the ultrafiltration trials were: pH 14; TS 89 000 mg/l; Na 10 000 mg/l; NaOH 14 000 mg/l; TOC 26 000 mg/l; and COD 44 000 mg/l. Composite permeate (recovered sodium hydroxide) concentrations, at 90 % volume recovery, contained 13 600 mg/l NaOH. Inorganic species point rejections were 10 to 20 %, while the organic carbon point rejection was 60 to 80 %. Temperature corrected fluxes (20 °C) at 5 MPa were 20 to 30 l/m²h after 40 days of operation. This process has not been fully developed, piloted or commercialised.

Evaporation and centrifugation with water and chemical recovery

The evaporation of mercerising effluent, after centrifugation to remove suspended solids, is accepted technology in the Textile Industry for recovering sodium hydroxide for reuse in the mercerising process (Hong *et al*, 1985; Sharma, 1983; Fosberg and Claussen, 1982). Multi-stage circulation evaporators are commonly used (Bechtold *et al*, 1985), and operated under partial vacuum with heating in the first stage. Heat is recovered from the condensate. Since evaporators are more cost-effective where the feed is concentrated, multi-stage counter-current rinse ranges are used in mercerising to produce a concentrated effluent.

In the past, scouring effluents have been considered to be too contaminated and too weak for recovery and reuse by evaporation (ATMI, 1973). Pilot trials, using a falling film evaporator rated at an evaporative capacity of 25 l/h of water for a feed of 80 to 180 l/h, indicated that scouring effluent could be successfully concentrated and reused in the scouring process, with no adverse effects on subsequent factory processes or on final cloth quality (Pollution Research Group, 1989 and 1990). Since the chemical consumption of sodium hydroxide during scouring is low, the ratio of non-hydroxide sodium to hydroxide sodium in the effluent is also low (Buckley and Simpson, 1990a). Typical effluent concentrations into the evaporator were: pH 14; TDS 40 000 mg/l; TOC 4 500 mg/l; Na 8 000 mg/l; total Ca and Mg 50 mg/l; and NaOH 16 400 mg/l. Typical concentrations of recovered sodium hydroxide solution were TDS 172 000 mg/l; TOC 12 300 mg/l; Na 57 500 mg/l; total Ca and Mg 120 mg/l; and NaOH 96 000 mg/l. Maximum concentrations achieved were 40 % NaOH. The condensate was clean, pH 8 and TDS 100 mg/l, and suitable for reuse directly in the process as hot rinsing water.

The application of evaporative techniques to the treatment of scouring effluents results in the concentration of the recoverable chemicals, as well as the contaminants. The pilot trials indicated that these contaminants did not present a problem since a significant portion (up to 30 % TS, 30 % COD, 25 % Ca and 10 % Mg) were concentrated above their solubility limit during evaporation, and removed from the product, as a sludge, by settling or centrifugation. The sludge characteristics were dependent on the degree of evaporation, and the sodium hydroxide concentration of the concentrate. Those impurities that remained in the recycled sodium hydroxide solution did not inhibit the scouring action or impair the final cloth quality.

The fundamental obstacle limiting the use of evaporation is energy consumption. Practical limitations include scaling, corrosion, entrainment and foaming. During the above pilot trials, fouling of the heat exchange surfaces was negligible, and foaming and entrainment could be avoided by the use of anti-foam.

Evaporation is not known to be used commercially for the treatment and recovery of scouring effluent.

Electro-osmose with chemical recovery

A process was proposed during the early 1920's (Bleachers Association Ltd, 1920), which was aimed at recovering sodium hydroxide from kier liquors by a combination of electrolysis and *electro-osmose*. During laboratory trials, the kier liquid was placed inside a porous pot containing a suitable electrode, which was made the anode. Lead was found to be the most

suitable anode material. The porous pot was surrounded by a vessel containing water and a nickel gauze cathode. Approximately 50 % of the sodium present in the effluent could be recovered as sodium hydroxide, and the liberated organic acids were readily sedimented. It was proposed that this process would be *successful in dealing with large volumes and would be more economical than the established process of evaporation to dryness, ignition and lixiviation.*

Electrolysis with water, chemicals and heat recovery

This process is the subject of this dissertation and is concerned with the electrochemical recovery of sodium hydroxide from strong scouring effluents using the four stage treatment sequence consisting of:

- 1) Neutralisation with carbon dioxide to convert the sodium hydroxide to sodium bicarbonate;
- 2) Cross-flow microfiltration to remove suspended, colloidal and waxy contaminants from the neutralised effluent;
- 3) Nanofiltration to separate the soluble organic and divalent metal contaminants from the sodium bicarbonate;
- 4) Electrochemical treatment in a membrane cell to split the sodium bicarbonate into sodium hydroxide, carbon dioxide and a dilute brine.

The treatment sequence produces:

- 1) Two concentrates containing organic material and divalent metal ions from the filtration stages, and comprising, between them, 10 % of the initial scouring effluent volume;
- 2) Hydrogen and oxygen gases from the electrochemical unit;
- 3) A dilute brine solution from the anode compartment of the electrochemical unit, which is suitable for reuse as rinsing water in the scouring rinse range;
- 4) A concentrated, pure sodium hydroxide stream for recycling to the electrochemical process.

In total, 17 refereed papers and conference proceedings have resulted from this work (the most relevant being Simpson and Buckley, 1987a, 1987b, 1987c, 1988; Simpson et al, 1986). Furthermore, full international patents on the process have been filed and granted in 18 countries. Section 5 describes the development and theory of this treatment sequence. Sections 6 to 9 describe the practical application of this sequence at pilot-plant scale.

3.2.2 Review of Treatment Options Prior to Discharge of Scouring Effluents

An extensive literature search has identified six treatment options which have been applied to scouring effluents to improve their quality prior to discharge from the facility. These options do not result in recovery of any sort, and are discussed below.

Neutralisation

This is one of the simplest pretreatment options available. Sulphuric acid is usually used to adjust the alkalinity of scouring effluents to an acceptable value prior to discharge to the sewer, or disposal at sea. The sensible admixture of acidic and alkaline effluents within a site will minimise additional chemical requirements, although there is usually an excess of alkali in textile mills which process cotton fibres.

Review of the literature shows a limited number of publications with respect to the use of flue gases as a low cost treatment of alkaline textile effluents (Majumdar, 1993; Schwarzmüller, 1991). Carbonation, using waste boiler combustion products, is a technically and economically viable technique for neutralising alkaline wastes (CDTRA, 1971; Franklin *et al*, 1969). Socha (1989) describes a full-scale installation in Poland, in which alkaline waste waters from the finishing of cotton textiles, and containing detergents, dye residues, fibrous suspensions and sodium hydroxide, are neutralised by flue gases from the combustion of coal in the textile plant. Best results are obtained in a three-stage saturation process with 50, 30 and 20 % of the flue gases being directed to the first, second and third stages respectively. The pH value of the waste water is consistently lowered to below 8. Also in Poland, Wieslaw and Andrzej (1987a and b) have studied the kinetics of the carbon dioxide reaction with hydroxide ions and have designed reactors for the neutralisation of textile waste water with flue gases.

Segregation and dilution

Segregation and dilution of a concentrated or potentially harmful effluent may be achieved by controlled release of the stream into the main factory discharge. Balancing and holding tanks need to be installed.

Biological treatment

Biological degradation is applicable where the pH is not too high, and where appropriate nutrients are available. General textile effluents may be effectively treated in admixtures with domestic sewage (CDTRA, 1971; US EPA, 1974 and 1978; Lockwood Greene Engineers Inc, 1975; Olthof and Eckenfelder, 1976; Jones, 1973; Jones 1974; Van Leeuwen *et al*,

1981). The extended aeration activated sludge process has consistently demonstrated its value as the most effective form of biological treatment (Porter, 1971; Jones *et al*, 1962).

Traditionally, biological plants have not been considered effective in treating strong scouring effluents, since the hydroxide alkalinity, fatty matter and inorganic compounds inhibit biological growth. Using the activated sludge process, it is possible to treat admixtures of strong scouring effluents with other textile effluents or domestic sewage. For example, a 95 % reduction on the BOD concentration of batch kiering liquors, fortified with ammonium phosphates, has been achieved (Sharma, 1983). However, only small volume ratios of scouring effluent may be used (CDTRA, 1971). Using percolating filters, it is possible to partially treat scouring liquors in admixture with dyehouse waste (CDTRA, 1971). BOD removals for combined kiering and dyehouse effluents were 8 to 48 %, compared to 24 to 92 % for the treatment of dyehouse effluents on their own.

Carliell (1993) reviewed the literature with respect to the degradation of cotton scouring and desizing effluents by adapted microbial associations. Few publications existed, and most were the products of only two scientists, working in collaboration to adapt anaerobic micro-organisms to degrade textile finishing effluents (from desizing, scouring and bleaching operations). Carliell, in her own work on the biodegradation of azo dyes in anaerobic systems, used organic-rich textile scouring effluents as carbon sources during decolourisation of the dye. These scouring effluents provided organic carbon for anaerobic microbial metabolism and indirectly aided decolourisation. At the same time the COD and colour content of the effluent were reduced; the high pH was neutralised by carbon dioxide production in the digester; and energy was produced in the form of methane which could be used to heat the digester, or utilised elsewhere in the factory. Carliell also concluded that anaerobic digestion of finishing effluents could be achieved following enrichment of an adapted microbial population, but that the varied compositions of these effluent streams could necessitate spatial segregation of specific microbial populations in a multistage digester to ensure efficient removal of organic carbon.

Flocculation

Flocculation of scouring effluents may be achieved by acidification to between pH 2 and 7, where large amounts of dispersed suspended matter are formed. The resulting solids are sticky, and difficult to consolidate or separate. Sedimentation trials have been unsuccessful in concentrating this solid matter (CDTRA, 1971).

Flotation

This technology uses finely dispersed gas bubbles to raise dispersed impurities to the surface, where the resultant scum can be removed mechanically. The gas bubbles can be generated mechanically, by air nozzles and turbines; electrolytically; or chemically from gas-forming chemicals. A single stage chemical flotation technique has been developed to purify concentrated sodium hydroxide effluents under oxidising conditions, with the removal of lint, dispersed matter, fatty and waxy components, residual sizes, surfactants, dissolved impurities and natural dyes (Bechtold, 1985) on a merceriser recycle stream in Germany. Electro-flotation was shown by Shifin et al (1976) to be effective in treating waste water from dyeing and finishing textile operations, to remove 80 % of the surfactants present, 97 % of the colour and 80 % of the COD. Although this process may have application to scouring effluent under certain conditions, no specific trials are reported in the literature.

Wet air oxidation

This is a process in which organic compounds in aqueous wastes are oxidised exothermally in the liquid phase, using a combination of elevated temperature and pressure (Kenox, 1989). This technique is particularly applicable to the treatment of effluents containing concentrations of oxidisable material between 2 and 20 %. The system was first commercialised by Zimpro Inc (Zimmerman, 1958; Zimmerman and Diddams, 1960; Maddern, 1980; Randall and Knopp, 1980; Morgan and Soul, 1968), but is currently marketed by several other companies. It is claimed that the destruction of waste contaminants in the presence of water, by wet oxidation, is as effective as evaporation and subsequent incineration of the residue. Although wet oxidation of alkaline wastes has been principally applied to pulp and paper effluents, it may be applicable to other caustic effluents.

SECTION 4

CHEMICAL, WATER AND WASTE WATER MANAGEMENT IN SCOURING PROCESSES

Section 3 examined general environmental management options available for pollution control in scouring processes, stressing the need for an integrated practical approach encompassing process-oriented waste minimisation and closed-loop waste recycling or, less preferably, end-of-line treatment prior to disposal. Although the main emphasis of this dissertation is on the development of a process to allow recovery of sodium hydroxide from strong scouring effluents, such development cannot be carried out in isolation from process-oriented waste minimisation considerations, since such considerations have a bearing on the technical, environmental and economic performance of the recovery process. This section examines the practical application of selected process-oriented waste minimisation considerations to the textile scouring process at the factory of concern. Both the consumption of sodium hydroxide (Section 4.1) and rinsing water (Section 4.2), in the context of rinsing theory, (Section 4.3) are examined, since these factors are most likely to influence scouring effluent characteristics.

4.1. Analysis of Sodium Hydroxide Consumption

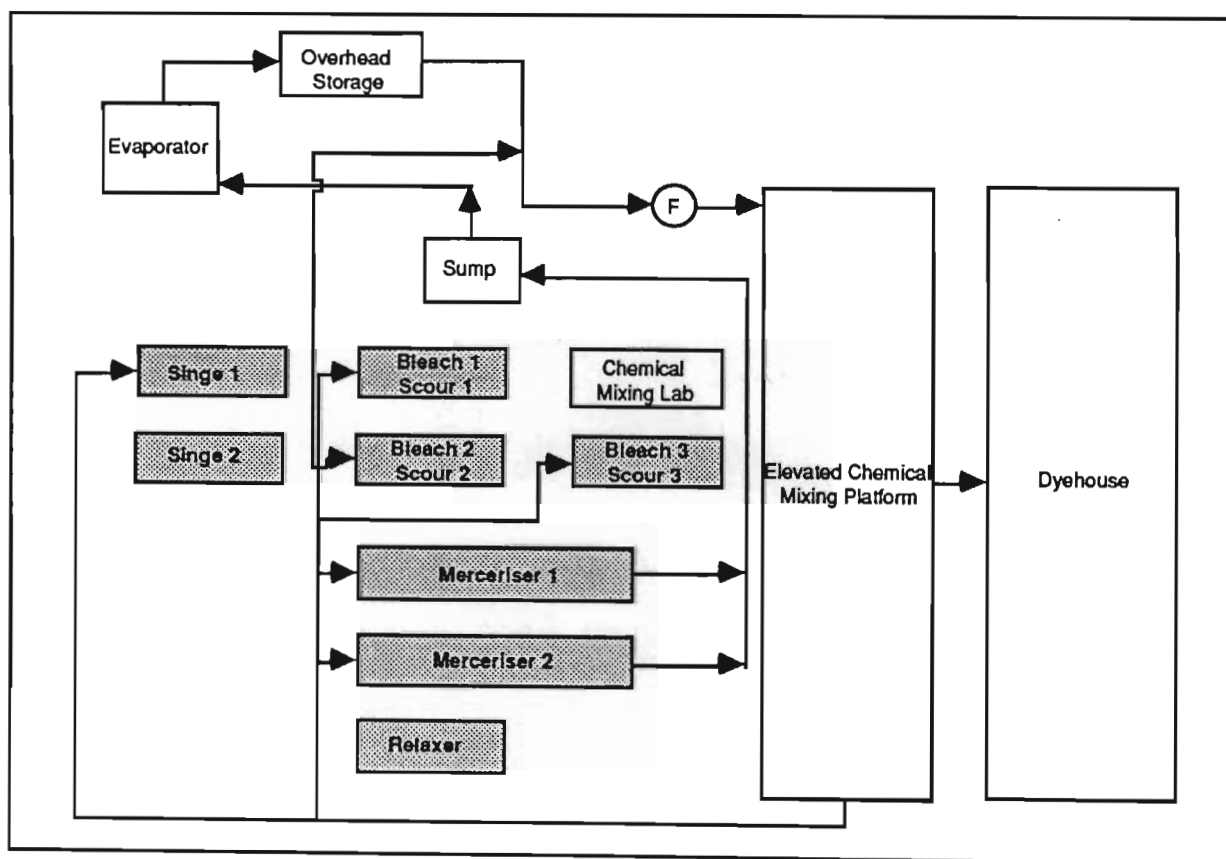
Consideration of overall sodium hydroxide reticulation within a total manufacturing process establishes a balance of consumption, recovery and loss, and allows major areas of over-consumption or loss to be identified and addressed prior to the development and implementation of an effluent recovery or treatment strategy. It also puts into perspective the consumption of sodium hydroxide in the scouring process, with total consumption on a site.

Prior to the pilot-scale testing of the process for recovering sodium hydroxide from strong scouring effluents (Section 5), a survey was conducted at the textile factory to establish a sodium hydroxide balance and to offer recommendations on minimising consumption and maximising reuse opportunities (Pollution Research Group, 1989). This survey involved the collation and manipulation of mass, volume and flow data routinely gathered and logged by the factory personnel in process logbooks, delivery and store records, chemical mixing data documentation, and production records over seven cost periods (each equivalent to approximately one calendar month in duration). Wet pick-up data for each machine and chemical recipes for batch make-up were also used.

The distribution network of sodium hydroxide within the wet preparation section of the factory is shown in Figure 4.1, where each individual machine is indicated. The textile processes which use sodium hydroxide are mercerising, scouring, bleaching and dyeing. Sodium

hydroxide is distributed from an overhead storage tank either directly to user processes, or indirectly via chemical mixing stations. Monthly sodium hydroxide consumption for the period under consideration was approximately 200 tonnes (as 100 % NaOH). For the most part, sodium hydroxide consumed in processing is discharged from the respective processes as rinsing effluent. Mercerising effluent is either evaporated to allow recovery of chemicals or, during periods of evaporator malfunction and reduced or inadequate capacity, is discharged, together with scouring effluent, to evaporation dams. All other process effluents are discharged from the site in the main effluent stream.

Figure 4.1
Sodium Hydroxide Distribution System Within Factory



4.1.1. Survey Results

Table 4.1 summarises the collated data for the seven cost periods (CP) considered in the survey. All figures, unless otherwise indicated, are reported as 100 % NaOH.

Comparisons of predicted, calculated and actual figures for sodium hydroxide consumption from various independent sources allowed cross-checking of results and identification of the most accurate figures for use in establishing the overall balance of inflow and outflow, which is summarised for the period in Table 4.2.

A detailed explanation of the data in the tables is presented in the original report (Pollution Research Group, 1989).

Table 4.1
Survey Data Summary

Parameter/Source	CP1	CP2	CP3	CP4	CP5	CP6	CP7
<u>Purchases</u> (kg NaOH)							
delivery book	71 335	99 187	99 224	91 368	64 428	93 814	76 712
stores records	110 760	88 099	103 968	101 770	83 059	89 146	87 456
<u>Recovered NaOH</u> (kg NaOH)							
evaporator log book	37 183	121 605	152 906	85 004	127 095	132 939	116 809
<u>Consumption</u> (kg NaOH)							
dyehouse	3 000	6 100	6 100	6 100	6 100	6 100	6 100
scour machine 1	2 562	9 150	8 418	7 686	6 222	4 758	8 784
scour machine 2	7 878	20 258	30 012	23 259	28 136	32 638	24 384
scour machine 3	1 125	2 626	6 002	3 752	2 626	3 752	1 501
mercerise machine 1	69 569	107 516	139 138	94 867	130 706	168 652	118 057
mercerise machine 2	0	46 278	47 428	29 511	37 558	54 997	41 583
bleach machine 1	226	875	958	818	632	708	891
bleach machine 2	182	386	325	363	219	348	416
bleach machine 3	0	137	110	27	55	0	55
bleach machine 4	648	1 537	1 883	1 492	1 582	2 079	1 748
<u>Analysis of Mercerising</u> (kg NaOH)							
total NaOH consumption	69 569	153 794	186 566	124 378	168 264	4 143	159 640
NaOH to dams	-	1 295	13 195	9 135	4 935	237	2 380
NaOH to main effluent	1 391	3 076	3 731	2 488	3 365	3 906	3 193
NaOH to evaporator							
• theoretical	68 178	149 425	169 640	112 755	159 964	223 649	154 067
• actual	56 700	52 255	243 005	110 565	101 115	945	103 670
NaOH lost to condensate	1 554	1 274	6 670	3 007	2 662	4 473	2 753
<u>Analysis of Mercerising</u> (m ³)							
effluent volume to evaporator	1 620	1 493	6 943	3 159	2 889	218 231	2 962
volume of recovered NaOH (560g/l)	66	219	273	152	227	145 005	209
volume of condensate (1g/l)	1 554	1 274	6 670	3 007	2 662	3 906	2 753
<u>Scouring</u> (kg NaOH)							
total NaOH consumption	11 565	32 034	44 432	34 697	36 984	41 148	34 669
NaOH to dams	10 409	28 831	39 989	31 227	33 286	37 033	31 202
NaOH to main effluent	1 157	3 203	4 443	3 470	3 698	4 115	3 467

Table 4.2
Overall Sodium Hydroxide Balance

Component (kg NaOH)	CP1	CP2	CP3	CP4	CP5	CP6	CP7	CP1-CP7
<u>Inflow</u>								
Purchases	71 335	99 187	99 224	91 368	64 428	93 814	76 712	599 068
<u>Outflow</u>								
Loss in mercerising circuit	11 478	97 168	-73 365	2 190	58 849	73 226	50 397	219 943
Loss in evaporator condensate	1 554	1 274	6 670	3 007	2 662	3 906	2 753	21 826
Loss to evaporation dams	10 409	30 126	53 184	40 362	38 221	37 978	33 522	243 802
Loss to main effluent	6 604	15 314	17 550	4 758	15 651	17 823	15 870	103 570
Total outflow	30 045	143 882	14 039	60 317	115 383	132 933	102 542	589 141
Variance (kg NaOH)								9,9
Variance (%)								0,002

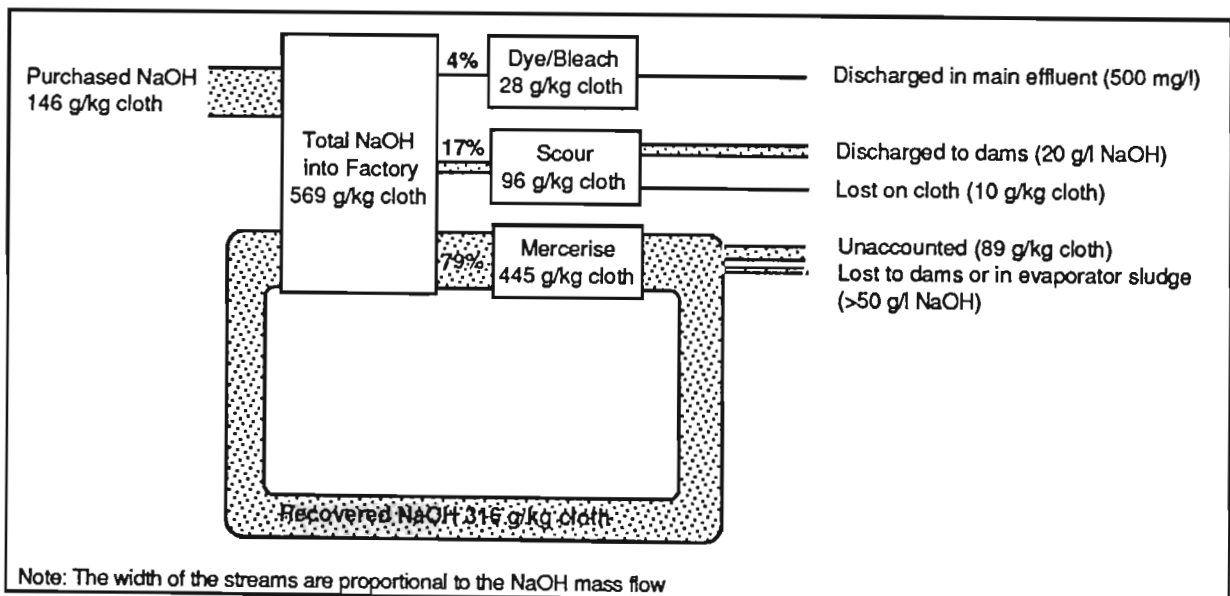
4.1.2. Discussion of Survey Results

Sodium hydroxide balance

The specific sodium hydroxide use over the complete textile process is illustrated in Figure 4.2. The textile processes consuming NaOH are:

- 1) *Mercerising.* Of the total factory consumption of 1 374 tonnes, 79 % (or 445 g NaOH/kg cloth) was consumed in mercerising. The sodium hydroxide contained on the fabric after mercerising was almost completely (98 %) washed off and was recovered by evaporation. Approximately 5 % was lost in the evaporator condensate and sludge streams. Note that approximately 20 % of the NaOH used in the mercerising process could not be accounted for after mercerising (it was used in mercerising, but was not pumped to the the evaporator), while a further 4 % was known to be discharged to the evaporation dams during periods when the evaporator was overloaded.
- 2) *Scouring.* This process accounted for 17 % (or 96 g NaOH/kg cloth) of the total factory NaOH consumption. The sodium hydroxide carried over on the cloth after scouring was almost completely (90 %) washed off and discharged to the evaporation dams. Note that the remaining 10 % was discharged to the main effluent.
- 3) *Dyeing and bleaching.* Together, these processes used only 4 % (or 28 g NaOH/kg cloth) of the total sodium hydroxide consumed at the site. The sodium hydroxide used in these processes is discharged in the main effluent stream.

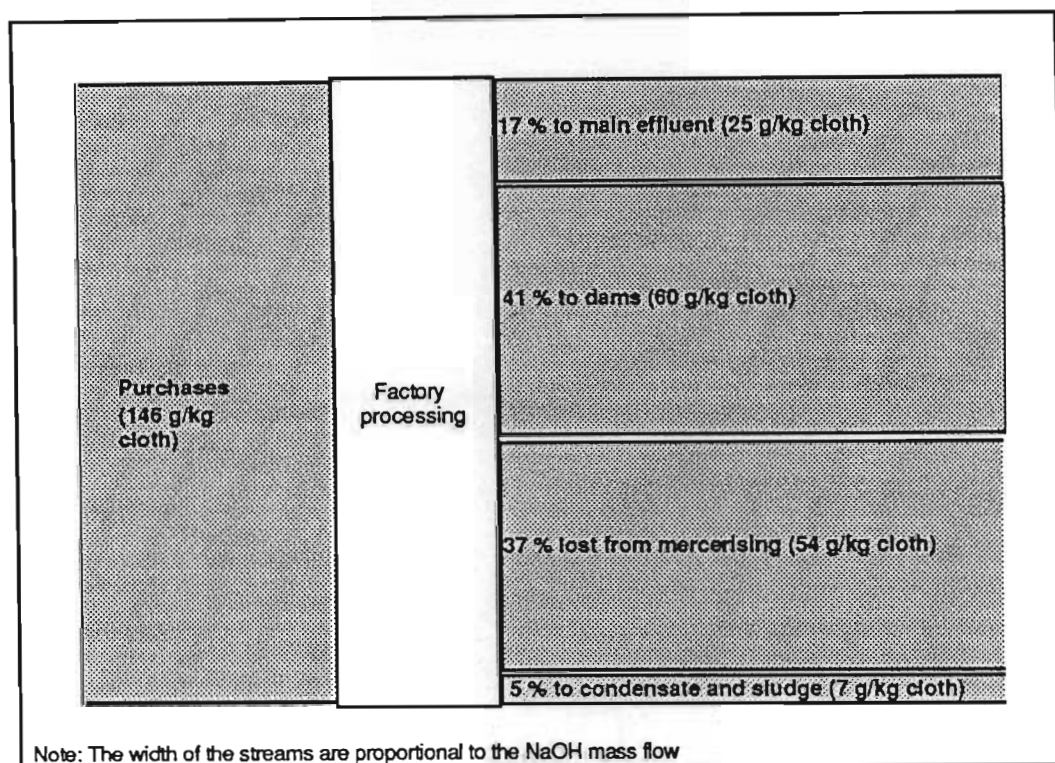
Figure 4.2
Sodium Hydroxide Balance at a Particular Factory



Sodium hydroxide losses

The areas of sodium hydroxide loss were established and are set against total inflow (or purchases) in Figure 4.3. Of the net sodium hydroxide entering the factory, 17 % was discharged with the main effluent stream, 41 % was pumped to the solar evaporation dams and 5 % was lost in evaporator condensate and sludge. A large loss of 37 % comprised sodium hydroxide which was unaccounted for after mercerising i.e., it was *lost* from the reticulation system between the mercerising processes and the evaporator. This stream may have been discharged either with the main effluent or to the evaporation dam.

Figure 4.3
Sodium Hydroxide Losses at a Particular Factory



Because of environmental pressures, the long term strategy of the factory had been to discontinue the use of solar evaporation dams for effluent disposal. It had been assumed that the implementation of a treatment system which would enable recovery and reuse of scouring effluents would achieve this objective. However, the results of the survey indicated that, of the NaOH discharged to the evaporation dams, 15 % originated from the mercerising process. The inability of the evaporator to meet the demand required of it in terms of evaporative capacity resulted in 4 % of the mercerising effluent by-passing the evaporator. Clearly, implementation of a treatment/recovery system for scouring effluent alone would not eliminate the need to use evaporation dams, and the performance of the evaporation system became of primary importance in the total management strategy.

Furthermore, the amount of sodium hydroxide *lost* from the mercerising process was equivalent to the amount of sodium hydroxide discharged in scouring effluent. The value of the sodium hydroxide in each of these cases translated to approximately R300 000 per annum (1986). Clearly, any attempt to implement a scouring effluent recovery system must be preceded by an exercise to properly understand the mercerising effluent-evaporator system and to identify and reduce losses.

4.1.3. Recommendations for Improved Chemical Management

Recommendations were made to:

- 1) Eliminate the major losses, especially in the mercerising-evaporator system;
- 2) Improve the performance of the evaporator and increase its throughput by optimising the concentration of recovered sodium hydroxide;
- 3) Maximise the reuse of sodium hydroxide by the scheduling of streams and cascading of effluents from scouring and mercerising for use in the dyeing, bleaching and scouring processes;
- 4) Improve the control of sodium hydroxide concentrations and flow, thereby reducing the potential for fluctuations in the mercerising process and achieving consistency in final cloth quality;
- 5) Facilitate the use of a computerised spreadsheet to maintain an accurate and current indication of the status of the factory sodium hydroxide balance.

Only after the above recommendations had been adequately addressed was it considered appropriate for the factory to proceed with plans for the implementation of treatment and recovery systems for the control of scouring effluent.

4.2. Analysis of Rinsing Water Use

Washing or rinsing is a frequent operation in textile processing which needs to be carried out efficiently for maximum benefit. The impurity level on the fabric must be reduced to an acceptable, predetermined level, and this should be achieved using minimal amounts of water. Water savings measures do not affect the pollution loading of an effluent, in fact decreased water consumption increases the effluent concentrations. Apart from the obvious environmental benefits associated with reduced water use, such reductions are beneficial to treatment/recycle processes: the size, and thus the cost, of effluent treatment/recovery plants is often proportional to the volume of effluent to be treated, while the technical and

economic performance of chemical recovery and closed-loop recycle often improves as the concentration of recoverable materials in the incoming effluent increases. The theory of washing and rinsing are discussed in this Section. The practical considerations of optimising water use during scouring on a particular machine at the factory of concern are discussed in Section 4.3.

4.2.1. Rinsing and Washing Theory

Although the terms washing and rinsing are used interchangeably, washing is taken to imply an operation that involves the use of chemicals to remove impurities from cloth, whereas rinsing implies a purely physical removal of impurities from the cloth by the use of water. The principles of both operations are similar, and for the sake of clarity, the term rinsing will be used in this dissertation.

The volume of water required during a rinsing operation, and to a large extent the concentration of scouring effluent, depends on a number of factors. These include the:

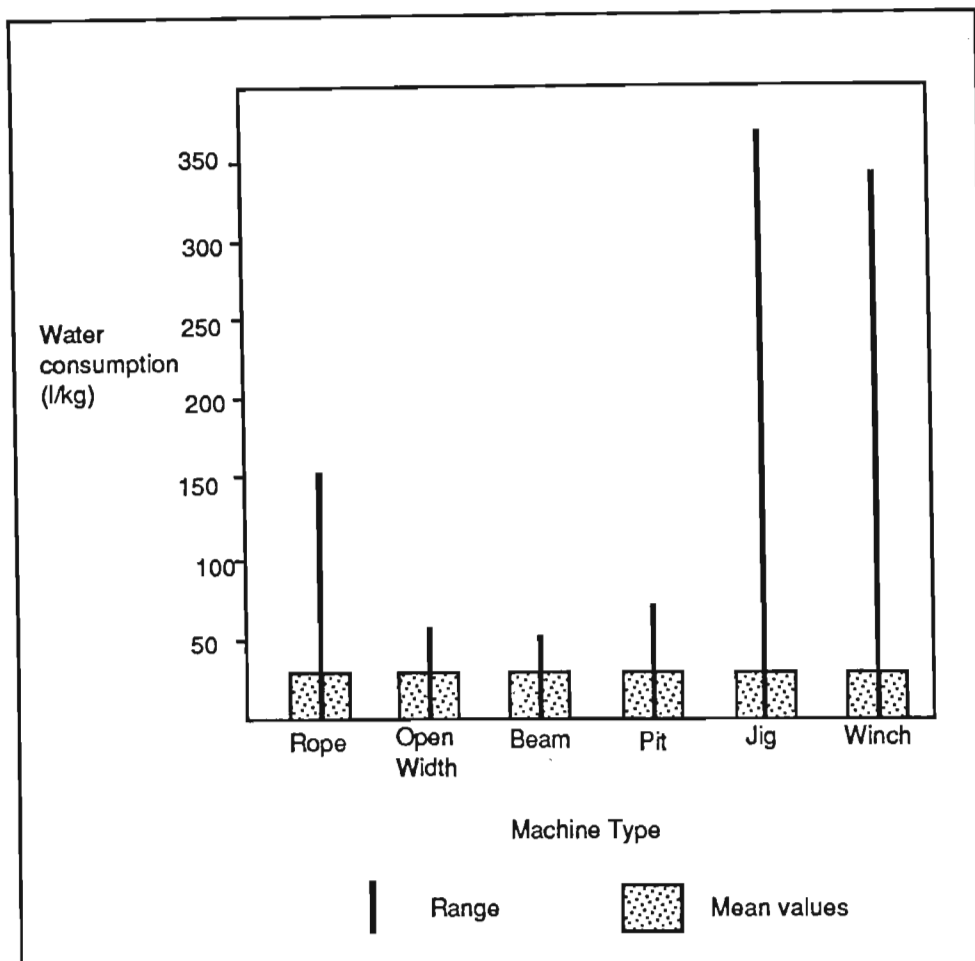
- 1) Type and concentration of impurity on the cloth;
- 2) Volume, concentration and nature of the chemical solution carried over on the textile material from the padding solution;
- 3) Type of rinsing equipment and machine speed;
- 4) Rinsing temperature;
- 5) Final concentration of impurities permissible on the cloth after rinsing, which depends on subsequent unit operations;
- 6) Cloth characteristics, such as construction and weight and fibre type.

Figure 4.4 (Water Resources Research Institute, 1982) compares the specific water use of a range of batch and continuous rinsing machines.

4.2.2. Batch Rinsing

In batch rinsing there is a predetermined liquor-to-goods ratio, and a fixed volume of water per batch for batches of the same mass. Batch rinsing machines include: jigs, which are versatile in that they can process a range of fabrics, the water use showing large variation and being a function of the technique employed (drop-fill or overflow); winches, which have a high water consumption and are used for processes with many steps where frequent washes are required; jets; and beams. The simplified theoretical basis for batch rinsing has been presented elsewhere (Pollution Research Group, 1988).

Figure 4.4
Comparison of Water Uses of Various Rinse Machines



Source: Water Resources Research Institute, 1982

4.2.3. Continuous Rinsing

In continuous rinsing, a continuous stream of rinsing water and fabric is supplied to the washers. Steady-state conditions prevail, in which the rate of inflow of impurities on the fabric is balanced by the rate of outflow of impurities in the effluent and on the rinsed cloth. Continuous rinsing machines include rope ranges and open-width ranges. Rope ranges process cloth which is twisted into a loose 'rope', and are particularly applicable for handling long lengths of cloth. They consist of one or more boxes, separated from one another by squeeze rollers. These ranges have high specific water use for light clothes; in such cases two or more ropes are often processed in parallel to reduce specific water use. Open-width ranges process the cloth in its expanded form and are usually more efficient in their water use. Both rope and open-width ranges may be single compartment or multi-unit.

Single rinsing units

Theoretical analysis of rinsing operations (Parish, 1965; Buckley and Groves, 1977; Prabhu, 1972) has shown that the rinsing efficiency, expressed as the ratio of the impurity concentration on the fabric before and after a single washing bowl, is given by:

$$\frac{C_{in}}{C_{out}} = \frac{1 - k + (fk) / m}{1 - k + f / m} \quad (4.1)$$

where C_{in} = impurity concentration on the fabric entering the rinse bowl
 C_{out} = impurity concentration on the fabric leaving the rinse bowl
 k = rinsing parameter
 f = specific water use in l/kg cloth
 m = fabric moisture content entering and leaving the rinse bowl in g/kg cloth

This relationship assumes that all the impurities present are dissolved in the fabric moisture. The rinsing parameter, k , ranges from 0 (complete impurity removal) to 1 (no impurity removal), and is influenced by several factors as follows.

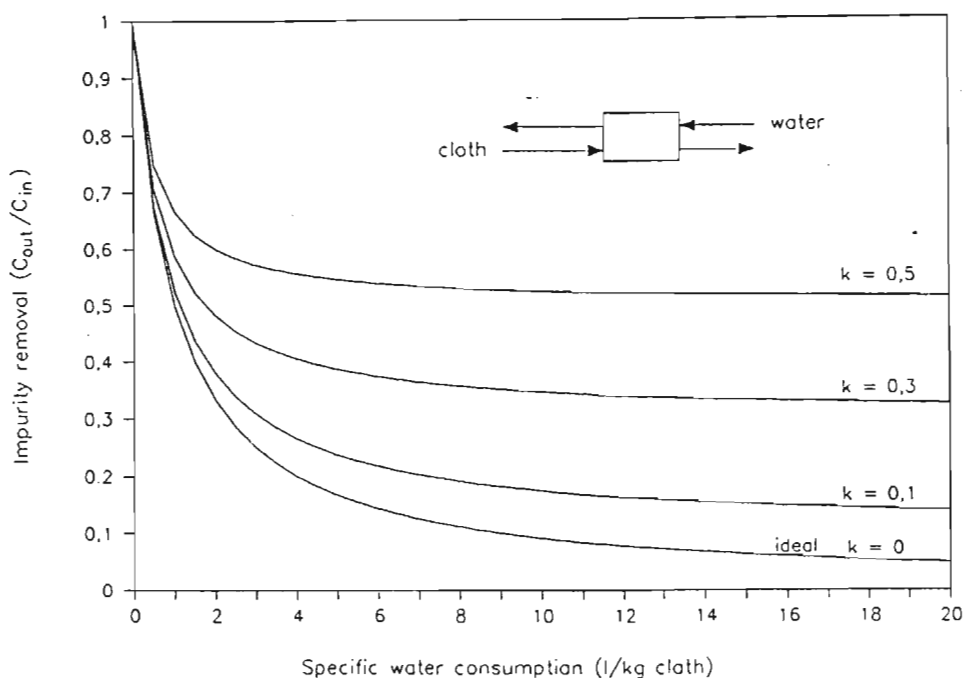
- 1) *Cloth speed.* At slow cloth speeds, impurities redistribute themselves between the cloth and the water, reducing the efficiency of rinsing, while at higher cloth speeds, turbulence at the cloth surface improves rinsing efficiency.
- 2) *Rinsing temperature.* Impurity removal increases with temperature, because of higher rates of impurity diffusion and lower viscosities.
- 3) *Rinsing unit design.* Desirable design features would include surface turbulence promotion, long retention times, prevention of the short circulation of the rinsing water from the inlet to the outlet, and a high roller nip expression to minimise the final moisture content of the cloth leaving the unit.
- 4) *Fabric type.* Light, open-weave fabrics are more easily rinsed than heavy, close-weave fabrics.

Figure 4.5 presents the impurity removal in a single rinsing unit as a function of specific water use. Several conclusions can be drawn.

- 1) At fixed specific water use, f , impurity removal decreases as the washer becomes less ideal.

- 2) For any given rinsing range, the rinsing parameter, k , is fixed and determines the maximum effective specific water use. There is a maximum limit to impurity removal; increases in specific water use above that which correlates with the maximum impurity removal, effects no increase in impurity removal.
- 3) As the washer becomes less ideal, ie., as k increases, the maximum effective specific water use decreases. This has various implications. Firstly, for optimum operation, a less ideal washer should be run at a lower specific water use than an efficient washer. Secondly, the rinsing efficiency of a less ideal washer cannot be improved merely by increasing the rinsing water flow.

Figure 4.5
Dependence of Impurity Removal on Specific Water Use



Multi-unit rinsing range

There are three modes in which multi-unit rinsing ranges can be operated: cross-flow; counter-current; or a combination of the two. A cross-flow rinsing range consists of several units in series, each fed by the same flow rate of rinsing water. For n units in series, the rinsing efficiency is:

$$\frac{C_n}{C_0} = \left(\frac{C_1}{C_0}\right)^n \quad (4.2)$$

where C_1 = impurity concentration on the fabric after the first rinse bowl
 C_0 = impurity concentration on the fabric before the first rinse bowl
 C_n = impurity concentration on the fabric after the final rinse bowl

The efficiency of cross-flow rinsing units can be greatly increased by partial or full conversion to allow counter-current flow of water. In this way the cloth leaving the range is contacted with the cleanest water. The concentration of impurities in the effluent is maintained at a maximum, by withdrawing it from the most contaminated bowl through which the cloth passes first.

Typically two to five bowls are employed in counter-current operation.

The washing efficiency depends on the amount of water which is carried over from the rinsing range, the so-called drag-out, and the washing parameter of the rinsing range. The ratio of the rinsing water flow to the drag-out is defined as the rinse ratio, r (US EPA, 1979).

Figure 4.6 presents the relationship between the rinse ratio, the number of rinse tanks, and the resulting dilution in the rinsing bowls. This figure enables the water requirements to be predicted and is based on the following equation:

$$\frac{C_s}{C_n} = r^n = \frac{Q_r}{Q_d} \quad (4.3)$$

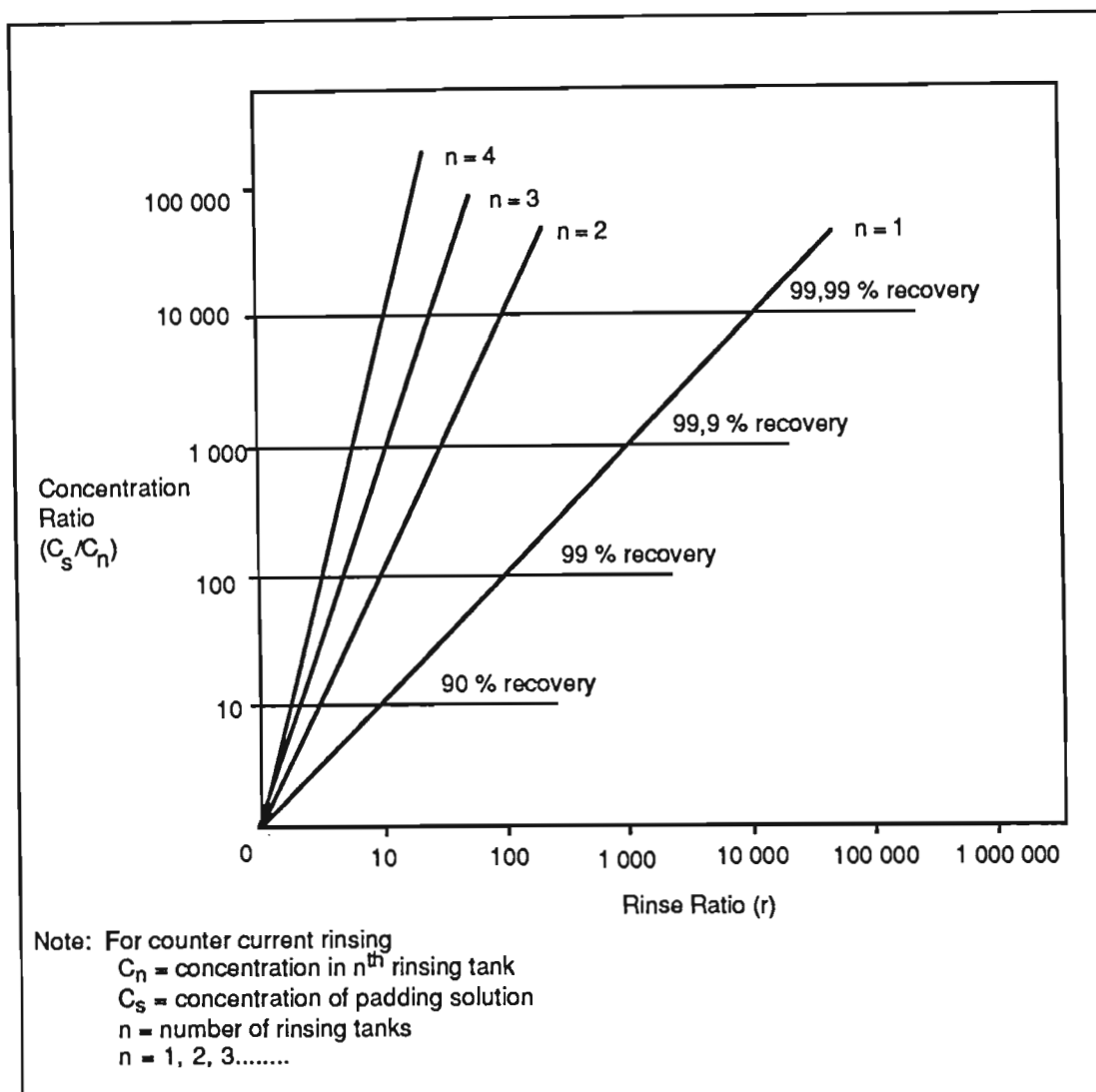
where n = the number of rinsing bowls ($n = 1, 2, 3 \dots$)
 C_s = the concentration of chemicals in the padding solution
 C_n = the chemical concentration in the n^{th} rinsing bowl
 r = the rinse ratio
 Q_r = the flow of rinsing water
 Q_d = the drag-out

Figure 4.6 also compares the amount of chemicals actually removed into the rinsing water and the amount of chemicals carried into the rinsing range on the cloth, ie., the maximum possible amount that could be removed. The chemicals removed are potentially available for recovery, which can be defined as:

$$\text{potential recovery (\%)} = \left(1 - \frac{C_n}{C_s}\right) \times 100 \quad (4.4)$$

For example, in a two-bowl system, if the rinse ratio is 10, C_s/C_n would be 100. A closed loop system would enable a maximum potential recovery of 99 % of the chemicals carried into the rinsing range on the fabric.

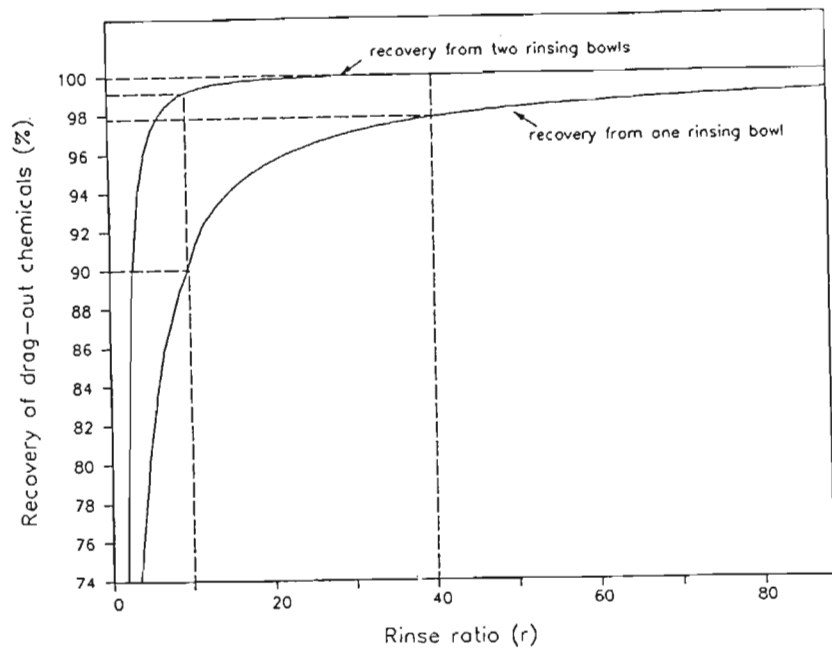
Figure 4.6
Rinsing Water Dilution vs Rinse Ratio for a Counter-Current Multi-Unit Rinse Range



Source: US EPA, 1979

Figure 4.7 shows different levels of maximum potential chemical recovery over a range of rinse ratios, for rinsing systems configured with one and two bowls. For example, if one rinsing bowl is considered, and the rinse ratio is 10, then it is potentially possible to recover 90 % of the chemicals carried in on the cloth. If the rinse ratio is increased to 40, only an additional 7.5 % of the chemicals is potentially recoverable. By comparison, if a two-bowl system were used, then for rinse ratios of 10 and 40, maximum potential recovery would be 99 and 99.9 % respectively.

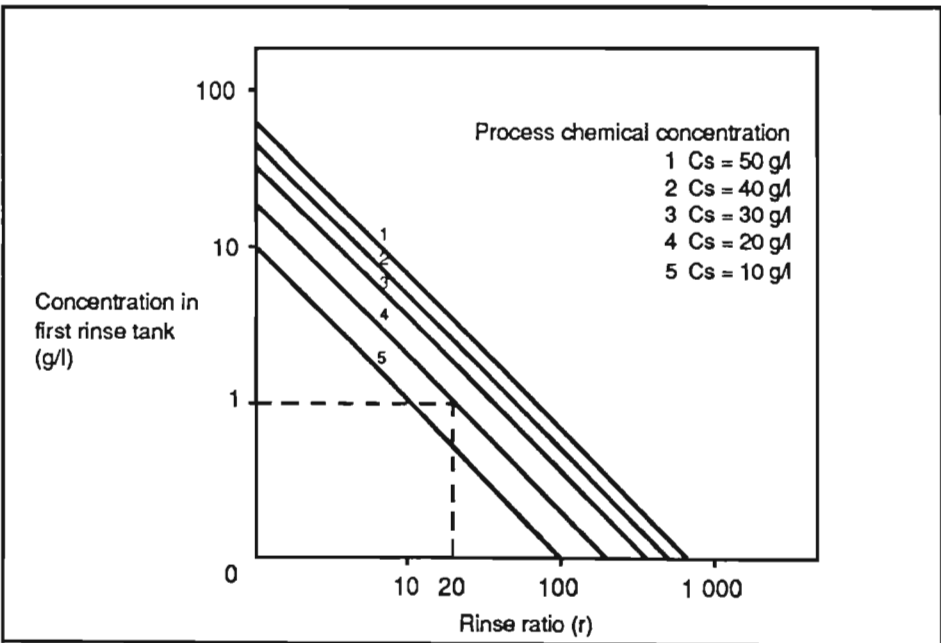
Figure 4.7
Dependence of Recovery Potential on Rinse Ratio



Source: US EPA, 1979

Figure 4.8 illustrates, for a range of padding solution concentrations, the relationship between the rinse ratio and the concentration in the first bowl of a three-bowl counter-current rinsing unit, ie., the final effluent concentration. For example, if the padding solution (C_s) contains 20 g/l, and the rinse ratio is 20, the concentration of the effluent will be 1 g/l.

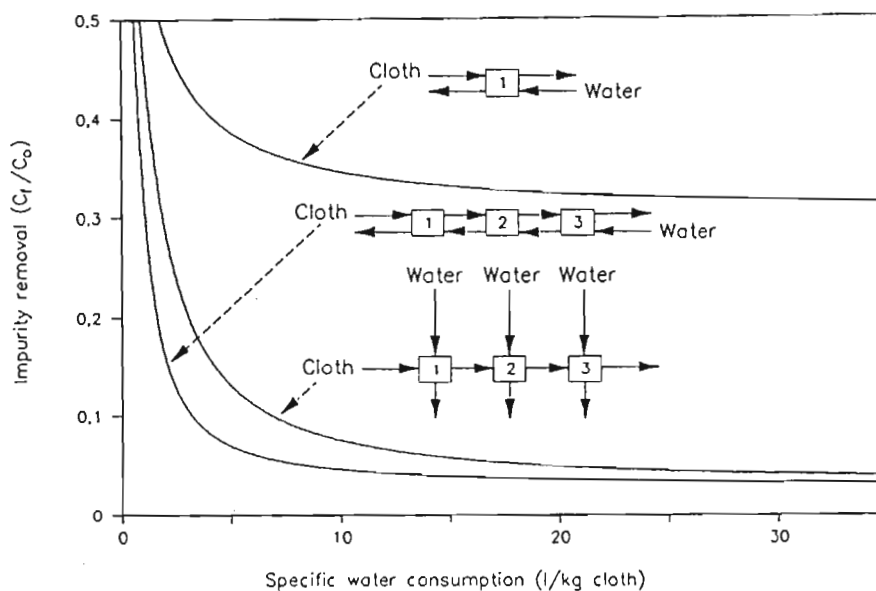
Figure 4.8
Determination of Chemical Concentration of First Rinse Bowl



Source: US EPA, 1979

Figure 4.9 compares the final impurity levels on the cloth, C_n , as a function of the specific water use, for various configuration rinsing ranges, where $k = 0.3$. The configurations are a single rinsing unit, and two three-bowl units, one connected in cross-flow and the third in counter-current. The figure effectively illustrates the improvement of rinsing efficiency with more bowls, and more bowls assembled in a counter-current configuration.

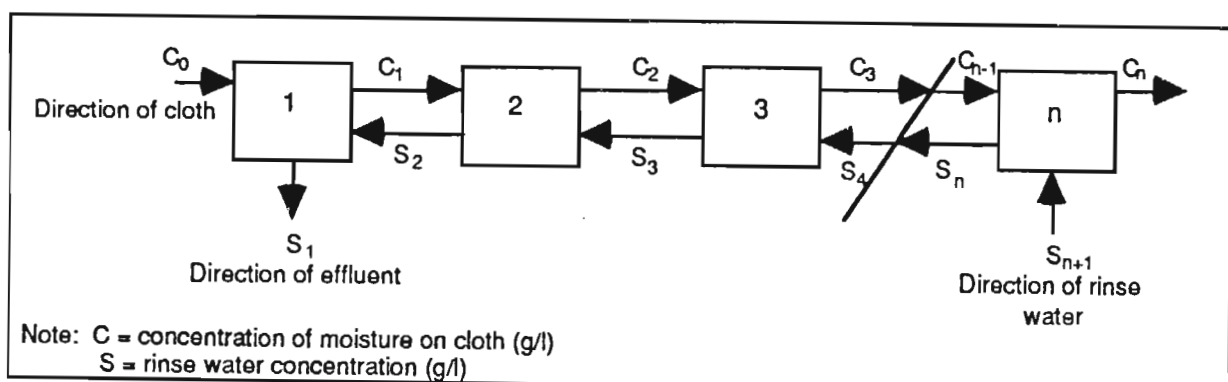
Figure 4.9
Dependence of Impurity Removal on Specific Water Use for Counter-Current and Cross-Flow Rinsing Ranges where $k = 0.3$



4.2.4. Development of a General Matrix for Analysis of Rinsing Ranges

The operation of the rinsing range was predicted by developing a matrix which took into consideration all the variables of the process. In the development of this matrix for a typical counter-current rinsing range (Figure 4.10), each bowl is treated as a single bowl.

Figure 4.10
Schematic of Material Flows In a Multi-Unit Counter-Current Rinse Range



For each bowl, an impurity mass balance is set up according to the equation:

$$C_{n-1} + (f/m_n) S_{n+1} = C_n + (f/m_n) S_n \quad (4.5)$$

- where m_n = moisture content of the squeezed cloth (kg solution/kg cloth) leaving bowl n
- C_1 to C_n = concentration of impurity in the moisture on the cloth leaving rinse bowls 1 to n (g/l)
- C_0 to C_{n-1} = concentration of impurity in the moisture on the cloth entering rinse bowls 1 to n (g/l)
- f = specific water use (l/kg cloth)
- S_1 to S_n = concentration of impurity in effluent leaving rinse bowls 1 to n (g/l)
- S_2 to S_{n+1} = concentration of impurity in rinsing water entering bowls 1 to n (g/l)

To compensate for the non-ideality of the rinsing operation, a rinsing parameter, k (also referred to in equation 4.1), is introduced into equation 4.5 as follows. If:

$$k = \frac{C_1 - S_1}{C_0 - S_1} \text{ then, for any rinse bowl } i: \quad (4.6)$$

$$S_i = \frac{k C_{i-1} - C_i}{k-1} \text{ Hence,} \quad (4.7)$$

$$\frac{S_i}{S_{i-1}} = \frac{k (C_{i-1}/C_0) - C_i/C_0}{k - C_{i-1}/C_0} \quad (4.8)$$

Substitution of equation 4.7 into 4.5 and condensing terms using

$$\begin{aligned} x &= (k - 1fk/m) \\ y &= (1 - k + f/m) \\ z &= (fk/m + 1 - k + f/m) \end{aligned} \quad (4.9)$$

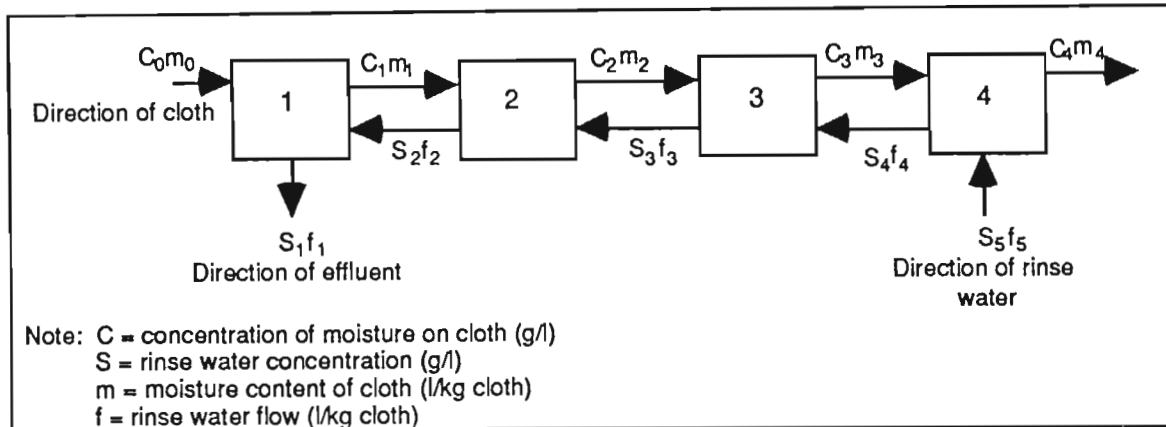
allows the following matrix to be obtained:

$$\begin{bmatrix} z & -f/m & 0 & 0 & C_1/C_0 \\ x & z & -f/m & 0 & C_2/C_0 \\ 0 & x & z & -f/m & C_3/C_0 \\ 0 & 0 & x & y & C_4/C_0 \end{bmatrix} = \begin{bmatrix} -x \\ 0 \\ 0 \\ 0 \end{bmatrix} \quad (4.10)$$

4.2.5. Analysis of Four-Bowl Counter-Current Scour Rinsing Range

Figure 4.11 is a schematic of the scouring rinsing range of concern.

Figure 4.11
Mass Balance for Four-Bowl Counter-Current Rinse Range



The theoretical analysis was conducted in five stages, as follows.

- 1) Determination of rinsing parameter, k ;
- 2) Modification of equation 4.10 to accommodate variations in the drag-out, m , from each rinse bowl, as well as the situation where the rinsing water concentration is zero;
- 3) Determination of the dependence of the rinsing efficiency and final effluent concentration, S_1 , on the specific rinsing water flow, f_5 , and on the nip expressions m_0 and m_4 ;
- 4) Selection of the most favourable configuration of m_0 to m_4 in combination with a selected rinsing water flow, f_5 , to facilitate efficient rinsing while minimising water and chemical use;
- 5) Determination of the dependence of the rinsing efficiencies and effluent concentrations on the initial rinsing water concentration, S_5 , at the selected nip expression combination, and on the specific rinsing water flow, f_5 .

These five stages are discussed below.

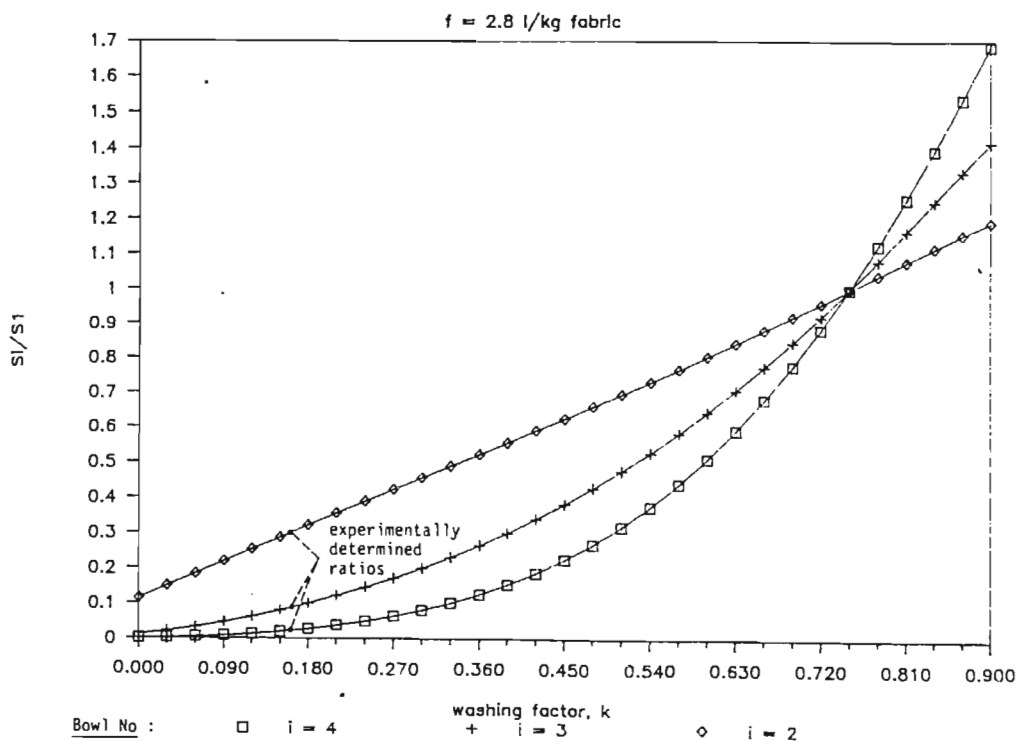
Determination of rinsing parameter, k

A computer spreadsheet was set up in which the moisture content, m , and the specific water use, f , were specified and assumed constant over the entire rinsing range. Equation 4.10 was solved for k in the range of 0 to 1 to yield values for cloth impurity ratios, C_i/C_o . It was assumed that:

- | | | |
|-------------|---|-------------------------|
| m | = | 0,8 l moisture/kg cloth |
| C_o | = | 50 g/l |
| cloth speed | = | 50 m/min |
| cloth mass | = | 250 g/linear m. |

Using equation 4.8, the values for the rinse ratios, S_i/S_1 , were determined and plotted against k for a selection of specific water uses. Figure 4.12 is a sample plot for $f = 2.8$ l/kg cloth. Using rinse ratios determined experimentally from conductivity and sodium concentration measurements (Pollution Research Group, 1989) of rinsing waters from the rinsing range, the rinsing parameter was determined at each specific water use. The average k value was 0.15. It was assumed that k was consistent through the wash range, and the value of 0.15 was used for all subsequent calculations.

Figure 4.12
Example of the Determination of Rinsing Parameter, k



Modification of mass balance parameters

Appendix 2 details the modifications to equation 4.10 in the case where the drag-out for each bowl is individually specified, and in the case where the rinsing water concentration, S_5 , is not zero. The modified matrix equation is:

$$\begin{bmatrix} -kf_2 - a_1 & f_2 & 0 & 0 \\ b_1 & kf_3 + a_2 & -f_3 & 0 \\ 0 & b_2 & kf_4 + a_3 & -f_4 \\ 0 & 0 & b_3 & a_4 \end{bmatrix} \begin{bmatrix} C_1 \\ C_2 \\ C_3 \\ C_4 \end{bmatrix} = \begin{bmatrix} C_0 b_0 \\ 0 \\ 0 \\ -f_5 S_5 (k - 1) \end{bmatrix} \quad (4.12)$$

$$\text{where } a_n = -m_n k + m_n + f_n$$

$$b_n = m_n k - m_n - f_{n+1} k$$

Determination of rinsing efficiency and effluent concentration

Having determined k and modified the computer spreadsheet to accommodate equation 4.12, a series of calculations were performed in which the rinsing water concentration, S_5 , was set at zero and the nip expressions, m_0 to m_4 , were set at the selected combinations given in Table 4.3.

Table 4.3
Selected Drag-out Combinations

Case Number	Nip Expression (l/kg cloth)				
	m_0	m_1	m_2	m_3	m_4
1	0,8	0,8	0,8	0,8	0,8
2	0,65	0,65	0,65	0,65	0,65
3	0,5	0,5	0,5	0,5	0,5
4	0,5	0,8	0,8	0,8	0,5
5	0,8	0,8	0,8	0,8	0,5
6	0,5	0,8	0,8	0,8	0,8

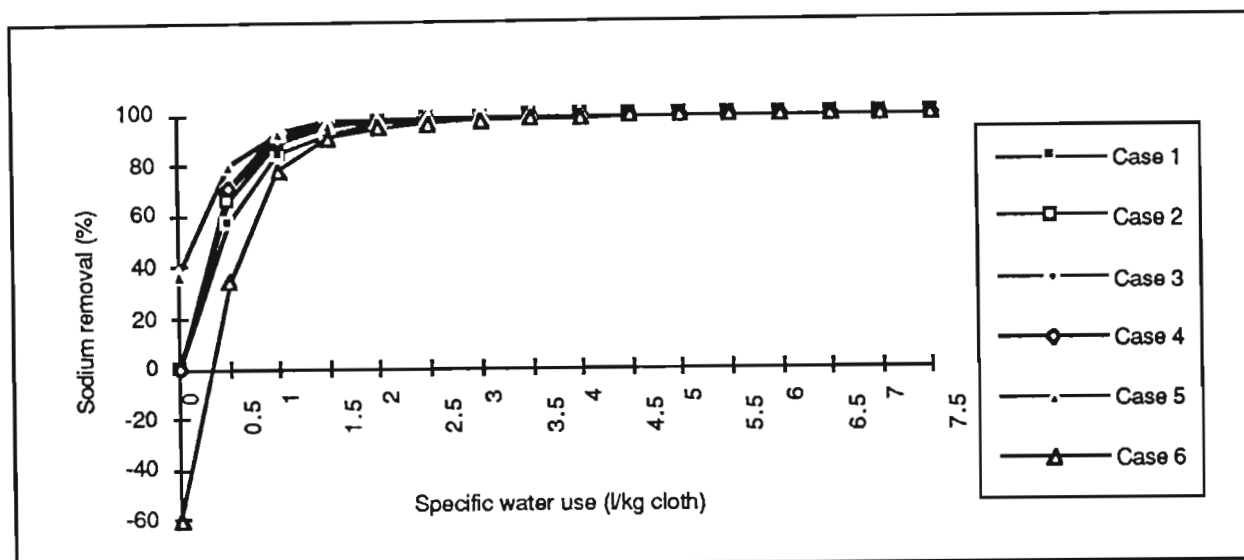
The existing factory configuration is case 5. Appendix 3 calculates the percent removal of sodium from the cloth for each of the cases, and through a range of specific water uses from 0 to 7,5 l/kg cloth. Table 4.4 summarises the results of Appendix 3, presenting the nip expression configurations in order with respect to decreasing sodium removal through the range of specific water uses. The sodium balance is also presented as sodium entering the rinsing range; and sodium distribution between the cloth and effluent leaving the range. In order to minimise chemical loss from the system, the total amount of sodium entering the rinsing range, and hence m_0 , should be maintained as low as possible. Examination of Table 4.4 indicates that sodium losses may be reduced by 37 % where m_0 is reduced from 0,8 to 0,5 l/kg cloth.

Table 4.4
Predicted Rinsing Efficiency and Effluent Concentration for Nip Expression Configuration Cases

Case Number	m_0 l/kg cloth	m_1 l/kg cloth	m_2 l/kg cloth	m_3 l/kg cloth	m_4 l/kg cloth	Removal %	Effluent Concentration g/l Na	Total Na to Rinsing g/kg cloth	Mass Na on Cloth g/kg	Mass Na in Effluent g/kg
3	0,5	0,5	0,5	0,5	0,5	94,2-99,8	13,5-1,9	14,4	0,8-0,02	13,5-14,4
5	0,8	0,5	0,8	0,8	0,5	92,9-99,8	16,4-2,9	23,0	1,6-0,04	21,4-23,0
4	0,5	0,8	0,8	0,8	0,5	90,4-99,7	13,0-1,9	14,4	1,4-0,04	13,0-14,3
2	0,65	0,65	0,65	0,65	0,65	89,8-99,7	16,8-2,5	18,7	1,9-0,04	16,8-18,6
1	0,8	0,8	0,8	0,8	0,8	84,7-99,8	19,5-3,0	23,0	3,5-0,07	19,5-22,9
6	0,5	0,8	0,8	0,8	0,8	78,8-99,6	16,2-2,0	14,4	3,5-0,06	11,3-14,3

Figure 4.13 plots the predicted rinsing efficiency against specific water use for the six cases of nip expression combinations.

Figure 4.13
Dependence of Rinsing Efficiencies on Nip Expression and Specific Water Use

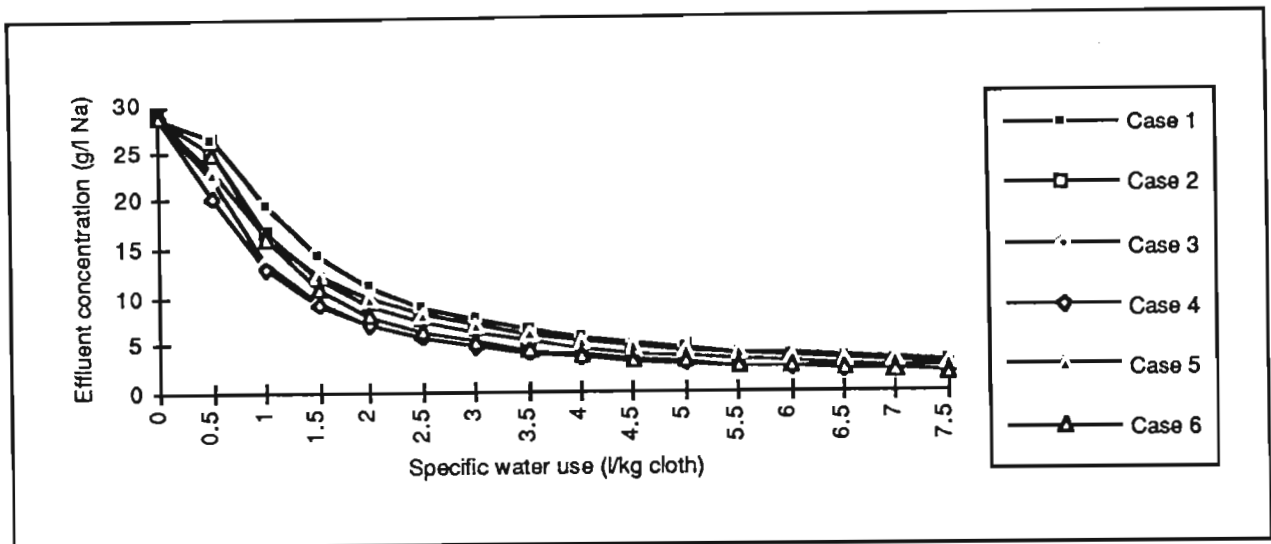


The following observations can be made.

- 1) Case 3, in which carry over from each bowl was minimal (m_0 to $m_4 = 0,5$ l/kg cloth), showed greatest rinsing efficiency at all values of specific water use. A comparison of the rinsing efficiencies of cases 4 and 5 ($m_4 = 0,5$ l/kg cloth), and cases 1, 2 and 6 ($m_4 = 0,8$ l/kg cloth), indicate that efficiencies are higher in cases where the drag-out from the final bowl is minimised.
- 2) At specific water use exceeding 1,5 l/kg cloth, the improvement in rinsing efficiency is relatively small. At the time this analysis was conducted, the rinsing range was being operated at a specific water use of 6,5 l/kg cloth using a nip expression configuration equivalent to case 5. Although rinsing efficiencies are predicted to be 99,8 %, water use is considered excessive. For example, if specific water use is reduced by 62 %, to 2,5 l/kg cloth, rinsing efficiency is only decreased by 2,6 %. Since subsequent processing includes both mercerising and bleaching, exceptionally high removals of sodium are not considered to be essential after scouring; 97,2 % is acceptable.

Figure 4.14 is a plot of the predicted final effluent concentrations, as a function of specific water use, for the six cases under analysis. Effluent concentrations decrease from case 1, in which drag-out from all bowls is high (0,8 l/kg cloth), to cases 3, 4 and 6 where m_0 is low at 0,5 l/kg cloth, ie., where the amount of chemicals entering the rinsing range on the cloth is minimised.

Figure 4.14
Dependence of Effluent Concentration on Nip Expression and Specific Water Use



Selection of most favourable rinsing parameters

The analysis above shows that the most favourable conditions are achieved where:

- 1) High expression nip rollers are installed before the first rinse bowl and after the last rinse bowl to minimise chemicals dragged into the range, reduce effluent pollution loads and lower impurity levels on exiting cloth;
- 2) Specific water use is decreased to 2 l/kg cloth, or less, while acceptable rinsing efficiency is maintained and final cloth quality is not impaired.

Based on the above considerations, cases 3, 4 and 5 ($m_0 = 0,5$ l/kg cloth) were selected for examination in the final stages of the analysis. The most favourable conditions of specific water use (1,5 l/kg cloth) were assumed, for which rinsing efficiencies ranging between 95,7 and 97,6 % have been predicted for the three cases.

Effect of impurities in rinsing water on rinsing performance

In cases where an effluent is to be treated for recovery, it is not always feasible or possible to remove all traces of impurities from the stream prior to reuse. The effect that residual concentrations of impurities in recycled rinsing water have on rinsing performance has been examined for the three most favourable scenarios selected above. The computer spreadsheet was adjusted to allow predictions to be made in cases where rinsing water concentration (ie S_5) was above zero. Appendix 4 presents the results, which are summarised in Figures 4.15 to 4.18. Examination of Figures 4.16 and 4.17 shows the

substantial effect that nip expression before the first bowl (m_0) has on effluent characteristics (concentration and loading). The principal conclusions are as follows.

- 1) The rinsing efficiency (Figure 4.15) decreases as the level of impurities in the rinsing water increases. At impurity levels of 5 g Na/l, rinsing efficiencies decrease from above 95 % for all three cases to between 79 and 86 %.
- 2) Effluent concentrations (Figure 4.16) increase as the level of impurities in the rinsing water increases, but at a slower rate. For example, at impurity levels of 5 g Na/l, the effluent concentration is only increased by approximately 3 g Na/l.
- 3) Effluent mass loading (Figure 4.17) is increased by up to 39 % as the level of impurities in the rinsing water is increased from 0 to 5 g Na/l.
- 4) Cloth mass loading, or carry-over of chemicals after rinsing, (Figure 4.18) is increased by approximately 2 g Na/kg cloth, or 500 % as the level of impurities in the rinsing water is increased from 0 to 5 g Na/l.

Figure 4.15
Dependence of Rinsing Efficiency on Rinsing water Impurity Level

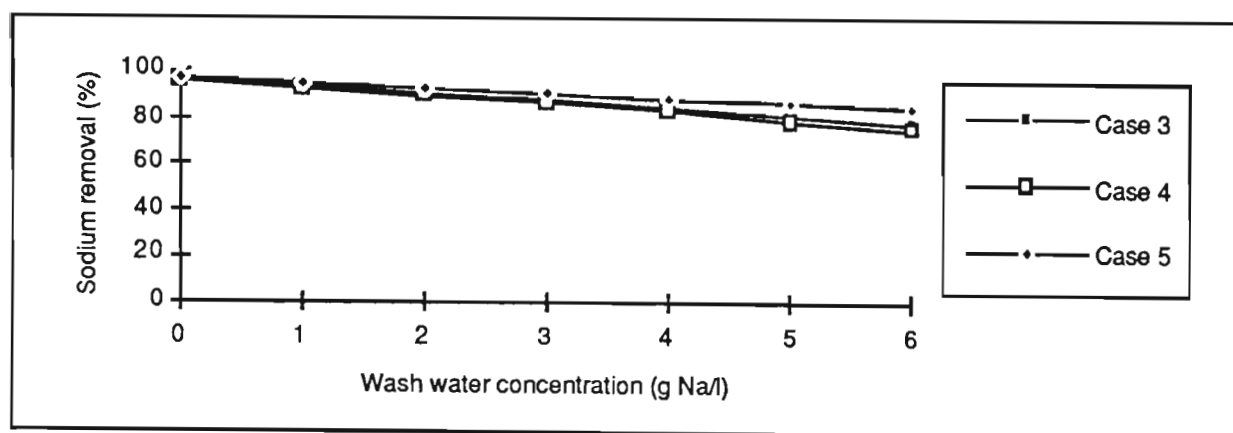


Figure 4.16
Dependence of Effluent Concentration on Rinsing Water Impurity Level

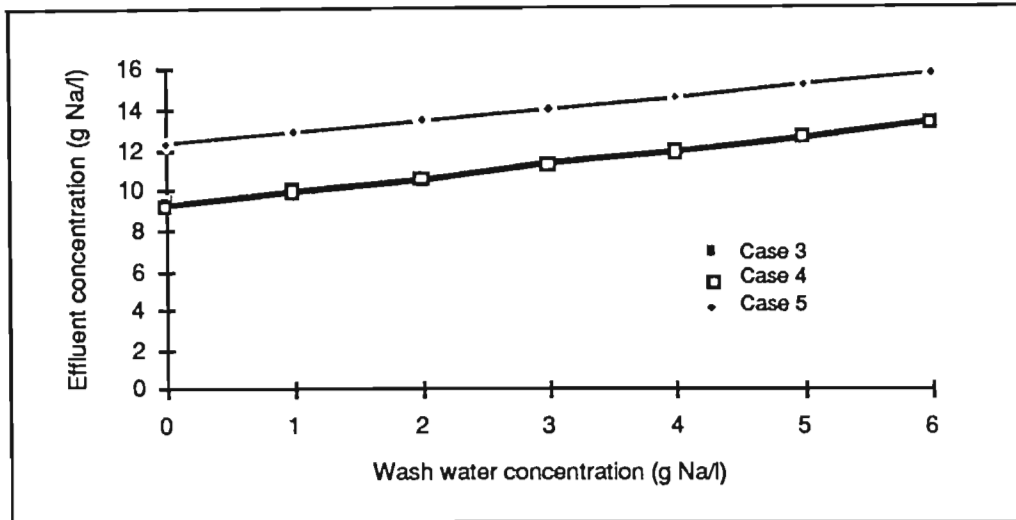


Figure 4.17
Dependence of Effluent Mass Loading on Rinsing Water Impurity Level

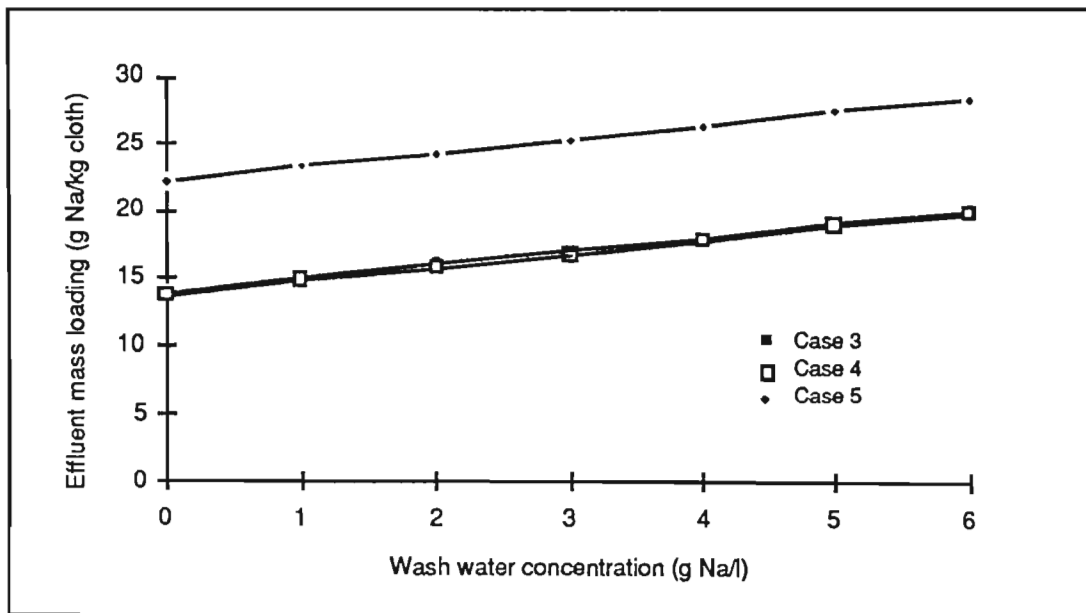
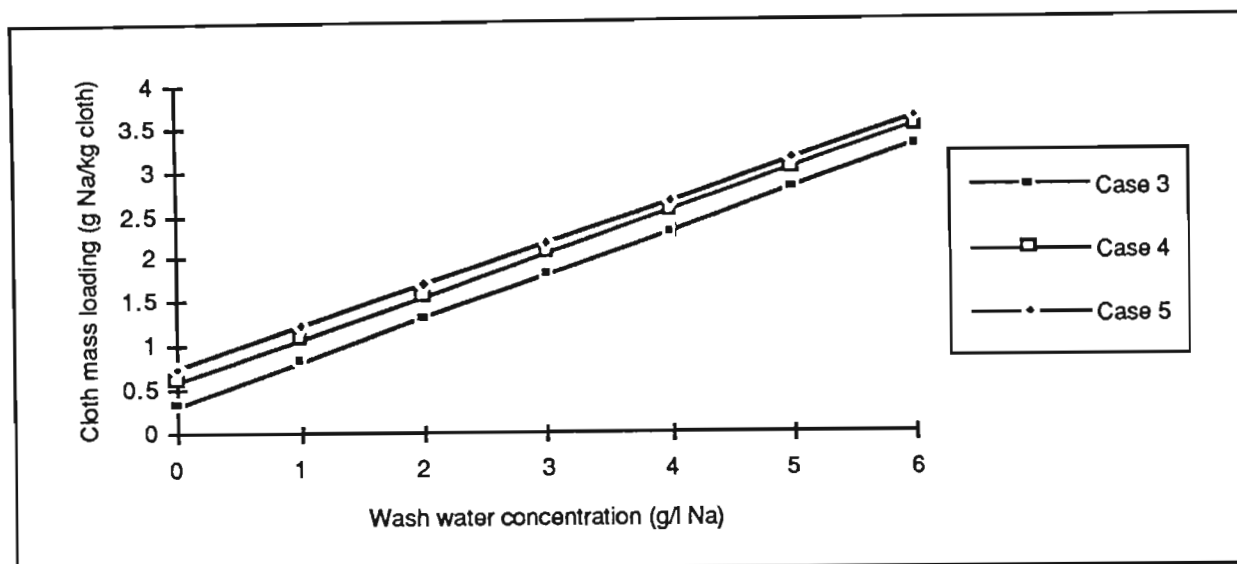


Figure 4.18
Dependence of Cloth Mass Loading on Rinsing water Impurity Level



4.3. Practical Application of Rinsing Theory to Scouring

Rinsing theory was used to predict the interdependence of rinsing variables during a typical scouring operation. The accuracy of this theory was then assessed by comparing predicted data with empirical data.

4.3.1. Description of Scouring Operation

The wet preparation section of the factory under consideration carried out scouring in an open-width Vaporloc machine using a sodium hydroxide padding solution at 50 g/l for a fabric speed of 50 m/min. The Vaporloc temperature was 100 to 110 °C, while the effluent discharged from the first rinse bowl was at 100 °C. A continuous counter-current four-bowl rinsing range was employed with a water flow of 4 to 5 m³/h. The average specific water use was 6,5 l/kg cloth. The rinsing water used was a mixture of mains water and effluent from a bleaching machine at a volume ratio of 7:3.

4.3.2. Empirical Verification of Predicted Rinsing Parameters

Three trials were conducted to verify the theoretical predictions presented in Section 4.2.5. The yarn type used in the trials contained cotton and polyester, blended in equal proportions (250 g/linear m). The rinse flow was adjusted on the rotameter situated on the mains water line entering the fourth bowl of the rinsing range. Trials were conducted at water flows equivalent to specific water uses of 1,7; 2,6 and 3,8 l/kg cloth. The process was allowed to equilibrate at the set water flow for 5 to 6 h before sampling. Thereafter, liquid in the saturator and each of the four rinse bowls, and cloth before and after the saturator, after the Vaporloc and after rinsing were sampled. Table 4.5 summarises the results of the trials.

Table 4.5
Results of Rinsing Trials

Specific Water Use l/kg cloth	Saturator Concentration g Na/l	Rinsing Efficiency %		Effluent Concentration g Na/l	
		Measured	Predicted	Measured	Predicted
3,8	54	99,1	99,4	8,2	6,2
2,6	80	98,5	98,9	11,5	11,4
1,7	63	97,9	97,7	13,9	13,6

Theoretical predictions compare favourably with experimental data. Furthermore, the results verified that specific water use may be significantly reduced (from the normal 6,5 l/kg cloth) while maintaining rinsing performance at acceptable levels.

4.3.3. Influence of Rinsing Variables on Operation of Proposed Recovery Plant

Optimisation and control of the rinsing variables, in particular the nip expression on the roller at the entrance to the rinsing range, the specific water use and the background rinsing water concentration, are critical in determining the characteristics of the effluent, and hence the size requirements and operational costs of effluent treatment or recovery plant. The ultimate selection of rinsing variables is a balance between capital expenditure (plant size and hence effluent characteristics) and operational costs (power and sodium hydroxide make-up requirements). The inter-relationship between the above rinsing variables and potential viability of the recovery system is discussed in Section 10.

4.3.4. Recommendations for the Operation of the Scouring Range

Considering the options, it was recommended that:

- 1) An additional high expression nip roller be placed at the entrance to the rinsing range (m_0 and $m_4 = 0,5$ l/kg cloth; m_1 , m_2 and $m_3 = 0,8$ l/kg cloth);
- 2) The specific water use be reduced to 1,5 l/kg cloth.

Under these conditions, it was predicted that the rinsing range would operate at 96,7 % impurity removal efficiency, and produce an effluent with a sodium hydroxide concentration of 21 g/l at a rate of 1,2 m³/h. These recommended changes were predicted to have no effect on the final quality of the cloth since the scoured cloth is usually subjected to further treatment with sodium hydroxide during mercerising and bleaching.

SECTION 5

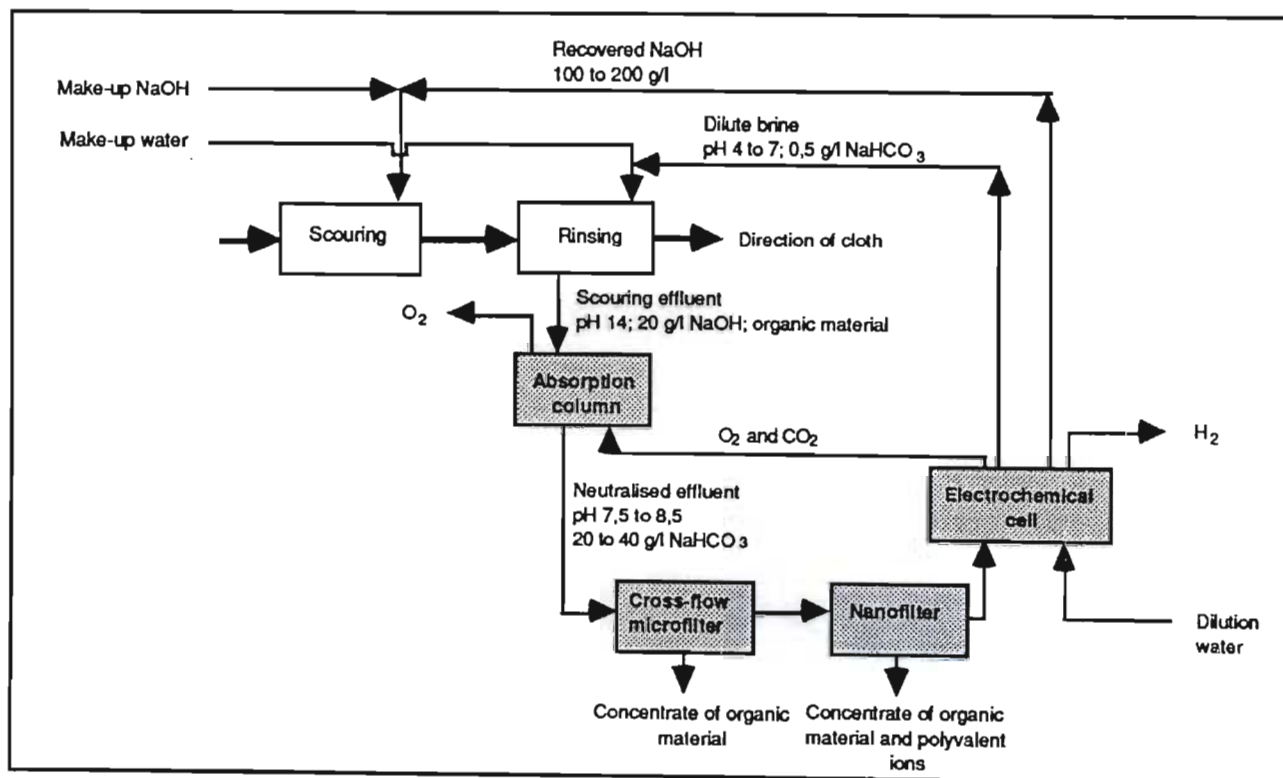
DEVELOPMENT, DESCRIPTION AND THEORY OF RECOVERY PROCESS

The disposal of scouring effluents is governed by effluent discharge regulations and is problematic because of high ionic concentration and alkalinity. Discharge to the sea or solar evaporation dams, and irrigation, are regarded as short-term measures. Possible treatment or recovery technologies for scouring effluents are discussed in Section 3.2.2. No processes are commercially available or proven which allow for the closed-loop recycle of the components of scouring effluent within the scouring process, thereby allowing resource conservation and waste elimination. This section discusses the development of a recovery system (Sections 5.1 and 5.2) which will enable the recycle of heat energy, water and sodium hydroxide within the scouring process. The process chemistry (Section 5.3) and the theory and applications of the individual unit operations comprising the recovery system are reviewed (Section 5.4). The mass balance relationships describing the chemical recovery potential of the processes are given in Section 5.5.

5.1. Description of Process Sequence

The process sequence is shown in Figure 5.1.

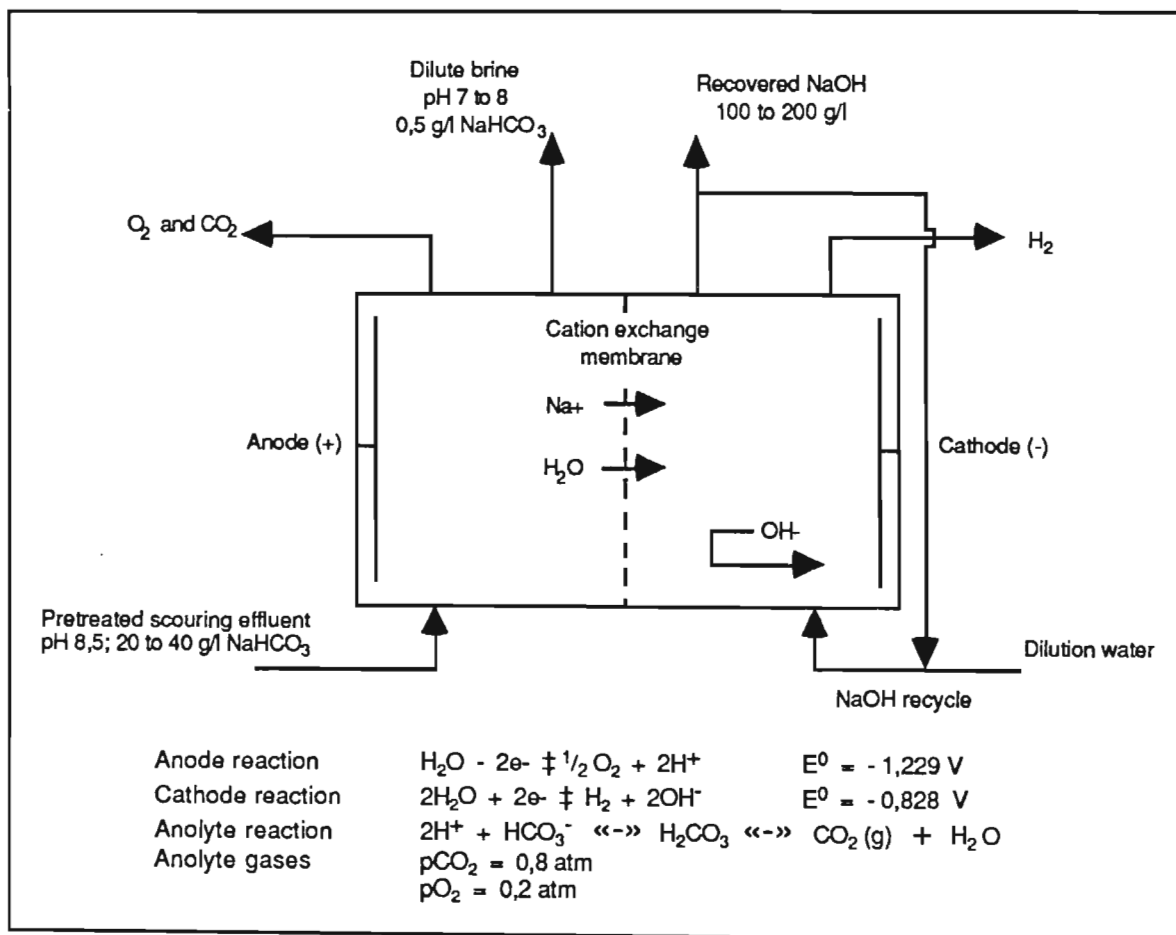
Figure 5.1
Process Sequence for the Recovery and Recycle of Scouring Effluents



It consists of a three-stage pretreatment sequence, followed by a chemical recovery stage as follows:

- 1) Neutralisation of the effluent with carbon dioxide to convert the sodium hydroxide to sodium bicarbonate;
- 2) Cross-flow microfiltration to remove suspended, colloidal and waxy contaminants from the neutralised effluent;
- 3) Nanofiltration to separate the sodium bicarbonate from the soluble organic and divalent metal contaminants;
- 4) Electrochemical treatment in a membrane cell (Figure 5.2) to split the sodium bicarbonate into sodium hydroxide, carbon dioxide and a dilute brine solution.

Figure 5.2
Schematic of Electrochemical Membrane Cell



The technologies used increase in sophistication from Stage 1 to Stage 4, and have been carefully selected at each stage to impart specific properties to the effluent such that it is amenable to treatment in the subsequent stage.

The principal objective of the three pretreatment stages is to separate the recoverable chemicals from the impurities, while the electrochemical stage recovers and concentrates the sodium by the desired amount.

The products of the treatment sequence include the following streams.

- 1) Two concentrate streams containing organic material and divalent metal ions from the filtration stages. These streams comprise up to 10 % of the initial volume of the scouring effluent and require disposal.
- 2) Hydrogen and oxygen from the electrochemical unit.
- 3) Dilute brine from the anode compartment of the electrochemical unit, which is suitable for reuse in the rinsing range of the scouring operation.
- 4) A concentrated sodium hydroxide stream for recycling to the scouring process.
- 5) Reusable heat energy, in the form of hot recovered brine and sodium hydroxide.

5.2. Novelty and Advantages of Process Sequence

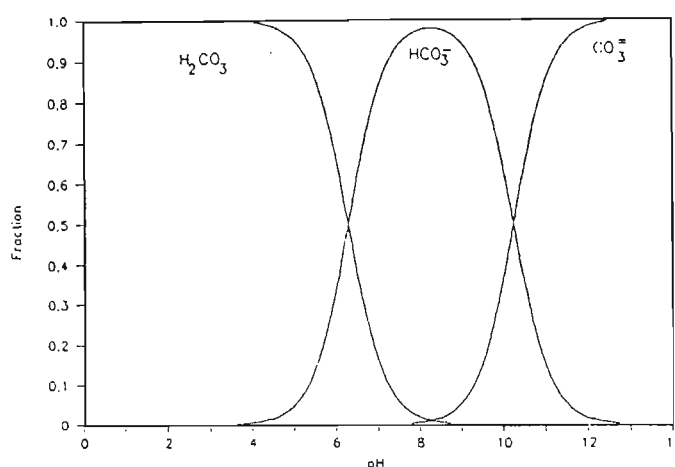
The innovation of the process lies not only in the novel way in which four now-commercially available technologies are adapted and applied, but also in the unique way in which they are combined. The chemistry of the individual process stages is inter-related and interdependent, and each stage uses simple adaptations of standard equipment, in some cases operated under non-standards conditions, to achieve the desired treatment and recovery. A combination of cross-flow microfiltration and nanofiltration is used for brine purification, in place of conventional lime softening and ion exchange. Although these membrane pretreatment techniques have, in the late 1980's, become commercially available, widely accepted and proven for applications similar to those for which they are proposed in this dissertation, at the time that the work was carried out, neither technique was fully developed nor commercialised. Indeed, while the experimental data from cross-flow microfiltration tests conducted in this study contributed to the preliminary understanding of the application of this technology to industrial effluents, the work done on nanofiltration pioneered the use of this technology for treating both pure solutions and industrial effluents, and remains an authoritative reference study. Furthermore, the electrochemical stage, as used here, involves novel adaptation of conventional applications. The standard equipment and principles used for the electrolytic production of chlorine and sodium hydroxide from sodium chloride brine are adapted for producing carbon dioxide and sodium hydroxide from carbonate solutions, and operated successfully with unique solution chemistry and under unusual conditions of electrolyte concentration and composition.

Besides the obvious benefits associated with pollution abatement, the process facilitates savings in water, heat energy, chemical and effluent discharge costs. In addition, the process is tailored to the requirements of the individual site. The sodium hydroxide may be recovered in concentrations up to 45 % NaOH, although there are considerable entropy savings involved in the generation of sodium hydroxide at the concentration required for scouring (10 to 20 %). Poorer current efficiencies may be tolerated than in commercial electrolysis, since chemical savings are generated from a waste which would otherwise be discharged, at cost, to the environment.

5.3. Process Chemistry

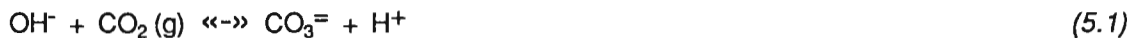
The success of the process is dependent on the careful control of the solution chemistry, in particular the equilibrium which exists between the various forms of inorganic carbon in solution. To achieve the process objectives and maximise recovery, it is essential to ensure that the desired species of inorganic carbon predominates at each stage. Figure 5.3 shows the pH dependence of the equilibrium between carbonate components, bicarbonate components and carbonic acid (carbon dioxide in water) at 20 °C.

Figure 5.3
Distribution of Carbonate Species with pH at 20 °C



Source: Harned and Davies, 1943; Harned and Scholes, 1941; Wissburn et al, 1954

As alkaline solutions absorb carbon dioxide, hydroxide ions are converted to carbonate ions. Hydrogen ions are released in the process, thereby reducing the pH value of the solution as follows:



At pH values above 12,8, only carbonate ions and hydroxide ions can co-exist in any significant concentration. As the solution absorbs more carbon dioxide, it becomes more acid and bicarbonate ions are formed by an equilibrium shift as follows:



Bicarbonate and carbonate ions predominate in solution in the pH range 8,6 to 12,8. The position of the equilibrium is determined by the pH of the solution, with carbonate ions predominating above pH 10,5 and bicarbonate ions predominating at lower values. Below pH 8,6 carbonate ions cease to exist at any significant concentration, and bicarbonate ions are transformed into carbonic acid:



Below pH 4,6 bicarbonate ions cannot exist in significant concentration, and carbon dioxide may be lost from the system as carbonic acid exists in equilibrium with carbon dioxide and water:



The amounts of hydroxide, hydrogen, bicarbonate and carbonate ions, carbon dioxide and carbonic acid present are regulated by the equilibrium constants (Loewenthal and Marais, 1983). The first and second stage ionisation constants, K_1 and K_2 respectively, are given by the following equations (20 °C):

$$K_1 = \frac{\{\text{H}^+\} \{\text{HCO}_3^-\}}{\{\text{CO}_2\}} = 4,15 \times 10^{-7} \quad (5.5)$$

$$K_2 = \frac{\{\text{H}^+\} \{\text{CO}_3^{2-}\}}{\{\text{HCO}_3^-\}} = 4,20 \times 10^{-11} \quad (5.6)$$

where $\{\text{CO}_2\}$ represents the sum of the activities of the carbonic acid and carbon dioxide in solution. The ratios of the activities of the components are constant at any given pH value and the predominant ionic component depends wholly on the pH value.

In practice, the solution chemistry of the inorganic carbon system described here is complicated by the fact that, for each determinand or component, a variety of chemical species exist at equilibrium. For example, a pure sodium carbonate solution will contain:

- | | |
|------------------------------|---|
| 1) Four free ion species | H^+ , Na^+ , CO_3^{2-} and OH^- ; |
| 2) Two soluble ion complexes | NaCO_3^- and HCO_3^- ; |
| 3) Two ion pairs | H_2CO_3 and NaHCO_3 . |

These eight species will all be present at equilibrium, the nature and concentration of each being dependent on the pH and composition of the solution. The addition of small amounts of chemical impurities, such as magnesium or calcium salts, further complicates the solution chemistry, creating an often surprisingly large number of dissolved, gaseous and/or solid species. Similarly, the presence of organic complexing agents, such as EDTA, also changes the behaviour of the ions and the distribution of the species in solution.

A knowledge of the species present at equilibrium and their behaviour under changing conditions of pH can assist in understanding observed chemical characteristics of solutions, defining optimum processing conditions, and modelling the movement of species within aqueous systems. Identifying and quantifying chemical species present in an inorganic carbon solution may be achieved by various methods. While *chemical analysis* of aqueous solutions provides information on the main determinands of a system, only very sophisticated analytical techniques can accurately define the forms or species of each of these determinands that might be present in solution. *Numerical techniques* can be used to find the distribution of species in simple chemical solutions, for example, by making reasonable assumptions, approximate concentrations can be calculated without solving equilibrium equations (Kerr and Buckley, 1993). Alternatively *graphical representations* of equilibrium relationships, such as Figure 5.3, can be drawn to give an overview of the system and its sensitivity to changes in pH. However, these techniques are often not applicable to complex solutions because they require specialist knowledge in the field of physical chemistry. In addition, a few user-friendly *computer equilibrium chemical speciation programs* are now available which are designed to be operated by non-specialists with sound scientific grounding. The use of one such program for speciating sodium carbonate solutions at different strengths and pH values is described in Section 6.4. This program, MINTEQA2, developed for the US Environmental Protection Agency, requires only water quality data on the input side, and is supplemented by an extensive thermodynamic database and a preprocessor which facilitates the input of information.

5.4. Description of Individual Process Stages

The theory of the individual stages is reviewed below. Since the development, testing and optimisation of the nanofiltration and electrolysis stages were considered to be the most important components of the work undertaken, this dissertation emphasises the theoretical and practical aspects of these two techniques. Neutralisation and cross-flow microfiltration are addressed in less detail.

5.4.1. Neutralisation

The characteristics of scouring effluents are discussed in Section 2.6. The principal contaminants are sodium hydroxide, hardness ions and dissolved or suspended organic material. The neutralisation stage serves to reduce the pH of the effluent to a level suitable for membrane treatment by conversion of the hydroxide ions to a salt (sodium bicarbonate). The reduction in pH also results in the precipitation of a fine floc containing impurities such as sizing agents, waxes, pectins and divalent ions.

Neutralisation is achieved by contacting the effluent with carbon dioxide gas, most effectively in counter-current flow mode. Equations 5.1 and 5.2 above apply, and the pH of the scouring effluent is lowered to the pH value of 8.6. At this pH value, monovalent bicarbonate ions predominate. The control of the final pH is critical. At lower pH values, the potential exists for the loss of carbon dioxide from the solution. At higher values, the inorganic carbon is present as divalent carbonate ions, which will be retained in the concentrate from the nanofiltration membrane (see Section 5.4.3), thereby reducing the recovery potential of the carbon (and sodium) species.

5.4.2. Cross-Flow Microfiltration

Cross-flow microfiltration is a solid-liquid separation technique in which the direction of filtrate flow is perpendicular to the direction of flow of the feed. The feed suspension sweeps across the face of a filter membrane, while the pressure differences cause the liquid to pass through the membrane, leaving the solids to be carried away in the residual flow. The accumulation of solids on the membrane is controlled by the shearing action of the flow. The process removes suspended solids only (down to submicron sizes) and may use particles present in the effluent to act as filter medium. Alternatively, a filtration aid (such as diatomaceous earth) or flocculating agent (such as limestone) may be used to aid filtration. Initially, effluent is circulated around the microfilter to deposit a layer of particles on the supporting filter membrane. Once a certain level of deposit has been achieved, a clean liquid stream is

produced (Martin, 1991). The filter tubes may be constructed from porous plastic, fibre glass, sintered ceramics, metal, carbon or woven fabric.

In the process sequence which has been developed for the treatment of scouring effluent, the main functions of the cross-flow microfiltration stage are to pretreat the neutralised effluent to remove suspended solids, including lint, colloidal solids, and the fine floc material which consists of waxes, pectins and divalent metal ions. This is particularly important as a pretreatment to nanofiltration where spiral wrap modules are used, since the presence of suspended matter will cause blockages within the module structure.

Cross-flow microfiltration produces two products: a high volume, clear permeate; and a low volume, turbid concentrate containing mostly suspended and colloidal organic contaminants of the effluent and sequestered divalent cations.

In cross-flow microfiltration, the concentrate and permeate flows, Q_C and Q_P respectively, and concentrations, C_C and C_P respectively, are functions of water recovery, feed characteristics and membrane point retention performance. The following relationships hold (Pollution Research Group, 1990):

$$Q_C = Q_f (1 - WR) \quad (5.7)$$

$$Q_P = Q_f - Q_C \quad (5.8)$$

$$C_P = \frac{C_f (1 - (1 - WR)^{1-s})}{WR} \quad (5.9)$$

$$C_C = \frac{Q_f C_f - Q_P C_P}{Q_C} \quad (5.10)$$

where Q = flow (m^3/h)

C = concentration (kg/m^3)

WR = water recovery (%) = $\frac{Q_P}{Q_f} \times 100$

s = membrane point retention (%) = $1 - \frac{C_P}{C_f} \times 100$ (5.11)

and subscripts c = concentrate stream

p = permeate stream

f = feed stream

Cross-flow microfiltration is a developing technology which is rapidly finding application for the removal of a range of contaminants from water and domestic and industrial waste waters. It is

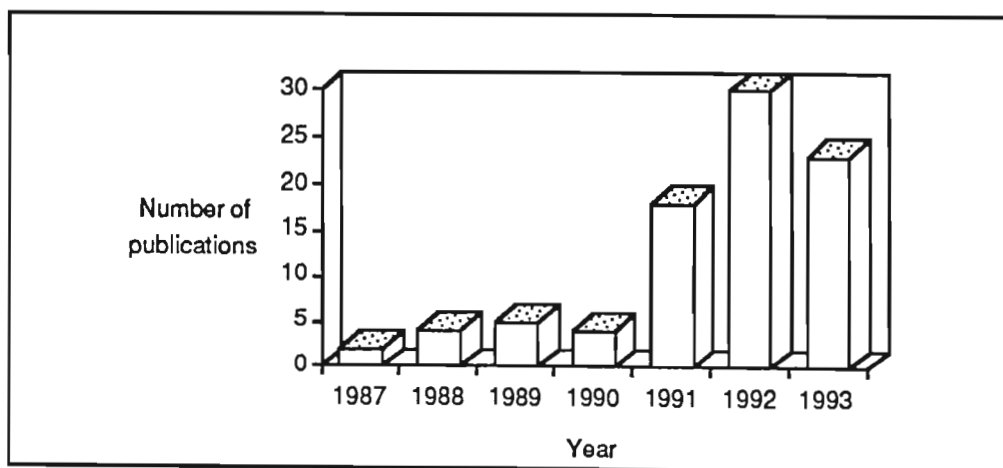
used in place of conventional clarification. The advantages of this system above conventional clarification and sand filtration are that:

- 1) The process can remove all particles larger than $0.1\ \mu\text{m}$ and this produces a very high standard of waste water for many applications. On the other hand, clarification and sand filtration cannot capture fine particles, and this results in a poor quality treated waste water.
- 2) Only chemical addition sufficient to flocculate impurities is needed. Additional chemicals are not necessary to encourage coagulation of particles to a size where they can be settled.

5.4.3. Nanofiltration

Nanofiltration is the latest development in membrane applications, and promises to significantly widen the application of membranes in liquid-phase separations. The first nanofiltration membranes were produced by FilmTec in the mid 1980's, the name deriving from the minimum size of particles or solutes that are rejected by more than 95 %. The growth of interest in nanofiltration is evidenced in Figure 5.4 by the increasing number of literature references listed in Chemical Abstracts since the first paper was published on the subject in 1987 (this paper resulted from the current work).

Figure 5.4
Number of Papers on Nanofiltration Listed In Chemical Abstracts



Peterson (1993) provides an overview of the historical development of nanofiltration membranes and discusses the properties of membranes currently on the market.

In the process sequence which has been developed for the treatment of scouring effluent, the main function of nanofiltration is to pretreat the effluent to separate the sodium salt from divalent metal ions and soluble organic material, of molecular mass greater than 200 to

400 daltons. This separation is essential for prolonging the life of the electrochemical membrane used in the recovery stage. The feed to nanofiltration is the cross-flow microfiltration permeate, from which two streams are produced: a high volume, sodium bicarbonate stream and a low volume concentrate containing high molecular mass compounds and divalent and polyvalent ions.

Since the chemistry of inorganic carbon is pH dependent, the relative amounts of monovalent and divalent species may be controlled by varying the pH value of the solution. This in turn will modify the retention characteristics of nanofiltration membranes against inorganic carbon species, thereby controlling the osmotic pressure, ionic strength and composition of the permeate. The mass balance relationships derived for cross-flow microfiltration in equations 5.7 to 5.10 above apply to nanofiltration.

5.4.3.1 Applications

Nanofiltration, also called *charged ultrafiltration*, *loose reverse osmosis* or *low pressure reverse osmosis* (Eriksson, 1988), is now a commercialised pressure-driven membrane process. It is applicable to the processing of streams where high retention or removal of monovalent ions is not necessary or desired. At the time when this work was undertaken, FilmTec had two membranes, NF 40 and NF 70, emerging from development. The NF 40 membrane was used in the current work, but was replaced on the market in 1991 by the NF 45 membrane, which has improved alkali resistance, higher fluxes and improved retention of sulphate ions (Lomax, 1994).

Since commercialisation, the principal applications of the NF 40 membranes have been in the separation of organic compounds in the molecular mass range of 300 to 1 000 daltons from salts containing monovalent anions (Eriksson, 1988). Examples include cheese whey fractionation, antibiotic processing, chemical processing, and sulphate removal from seawater (de Witte, 1992; Bilstad, 1992; Timmer *et al*, 1993; Raman *et al*, 1994; and Tsuru *et al*, 1994). Other applications are in various stages of development for waste water treatment in the pulp and paper industry (Zaidi *et al*, 1992; Nuortila-Jokinen *et al*, 1993); the chemicals industry (Von Eysmond *et al*, 1993); mining (Awadalla *et al*, 1994); metal processing (Fane *et al*, 1992); and textile dyeing (Schirg and Widmer, 1992; Bonomo *et al*, 1992; Gaeta and Fedele, 1991).

The NF 70 membrane has found principal application for water purification, where the permeate does not have to be of the quality produced by reverse osmosis. It successfully removes heavy metals, hardness ions, silica, pesticides, bacteria, viruses, trihalomethanes and colour from water and is used mostly in home water purification and municipal water

treatment works (Hart *et al*, 1991; Pedersen *et al*, 1991; Lozier and Carlson, 1991; Hofman *et al*, 1993; Kopp *et al*, 1993; Anselme *et al*, 1993; Yahya *et al*, 1993).

To date, the largest application of nanofiltration has been in removing hardness ions and organic materials for water supply (Raman, *et al* 1994). As a potential softening technique, and in cases where only selective softening and partial ion removal are required, nanofiltration holds the potential to achieve a similar performance, at lower power and pretreatment costs, and with smaller capital investment, than the other processes of reverse osmosis and lime/soda ash precipitation. In fact, the removal of sulphates from sea water in the North Sea oil rigs represents the largest single application of nanofiltration, with plants sized up to 16 000 m³/d. The first commercial nanofiltration plant was actually installed for this application, in 1987.

5.3.4.2 Membrane Characteristics

Nanofiltration membranes possess properties lying between those of reverse osmosis and ultrafiltration, and may be considered as high charge density ultrafiltration membranes with the ability to retain low molecular mass substances. Molecules with a molecular mass greater than 200 to 400 daltons, for example glucose, are retained and inorganic ions are selectively excluded according to their charge densities (Simpson, Kerr and Buckley, 1987). Since low molecular mass salts such as monovalent species permeate the membrane, the osmotic pressure difference is much less than that for reverse osmosis membranes. Thus nanofiltration membranes require lower pressures (say 1,4 MPa) than reverse osmosis, which requires pressures above 4 MPa. Figure 5.5 compares the spectrum of application of nanofiltration with older, and better known, filtration processes.

Composite nanofiltration membranes consist of a hydrophobic substrate, similar to those of conventional ultrafiltration membranes, onto which is incorporated hydrophilic groups which are negatively charged such that the original ultrafiltration properties are selectively enhanced for certain species. The ultrathin barrier layer, which provides the properties for controlling permeability, is supported by a base layer of reinforcing fabric overcoated with a microporous, usually polysulphone, polymer.

Nanofiltration membranes are believed to be porous, with an average pore diameter of 1 to 2 nm (Bhattacharyya and Williams, 1989; Raman *et al*, 1994). The unique features of the charged membrane result from the interaction of the charged groups with aqueous ionic species (Mickley, 1985) leading to the following properties:

Figure 5.5
Spectrum of Application of Membrane Separation Processes

Particle size (μm)	0,0001	0,001	0,01	0,1	1	10	100
Molecular mass (dalton)	100	1 000	10 000	100 000	500 000		
Particle characteristic	ionic	molecular	macromolecular		cellular and microparticulate		
Typical components	ions salts	vitamins	proteins		fats bacteria	aggregates	yeasts
Separation process	reverse osmosis	nanofiltration			ultrafiltration	microfiltration	traditional filtration

Source: Jelen, 1991

- 1) Improved membrane antifouling. Colloidal, oily and proteinaceous materials are generally hydrophobic in nature and are the main cause of fouling of conventional desalination membranes. At pH values below 8, these materials possess residual negative charge and are repelled from the nanofiltration membrane surface by the charged groups. This makes nanofiltration competitive with reverse osmosis in high-fouling applications such as dye concentration and paper waste treatment.
- 2) Increased fluxes. This results from the more favourable orientation of the water dipoles.
- 3) Enhanced and selective retentions of some electrolytes.

Whereas the retention of neutral species is by size, salt retention by nanofiltration is mainly a result of electrostatic interaction between the ions and the membrane. The charged membrane repels ions of like charge, or co-ions. The counter-ions are retained simultaneously because of the requirements of electroneutrality. The retention of ions depends on the charge density of the species, their concentration and their ability to either repel or shield charges on the membrane. For solutions containing different free ions, an unequal distribution of these ions results across the membrane, and transport rates change as ion concentrations change, known as the Donnan effect. Ion exclusion decreases in the presence of counter-ions of low valence, since charge shielding is weaker, but increases in the presence of co-ions of high valence, which are more effectively repelled by the

membrane. At high electrolyte concentrations, the membrane charges are more effectively neutralised or shielded by the counter-ions, resulting in reduced membrane selectivity.

A few papers have been published on the effects of solute-solute interactions on the relative permeability of charged species, and are reviewed by Nielsen and Jonsson (1994). The general trend is that, in a mixture of more and less permeable ions, rejection of the more permeable ions decreases and that of the less permeable ions increases. Researchers have found that membrane adsorption of permeable ions is substantially increased by the addition of impermeable salts to the solution, and vice versa. In fact, negative rejections of permeable salts are possible under certain conditions.

The practical significance of the membrane properties is that nanofiltration will not achieve high separation of monovalent ions in salt solutions, such as sodium bicarbonate or sodium chloride. Retentions will be highest for salts containing divalent anions and monovalent cations, such as sodium sulphate and sodium carbonate. Salts containing monovalent anions and divalent cations, such as calcium chloride, will be least effectively retained by charged membranes (Simpson, Kerr and Buckley, 1987). Furthermore, membrane retention of a monovalent species (more permeable) is influenced by the presence of divalent ions (less permeable). For example, if the solution contains Na_2SO_4 and NaHCO_3 , the membrane preferentially retains SO_4^{2-} ions over HCO_3^- . The retention of HCO_3^- decreases as the concentration of SO_4^{2-} increases. At high SO_4^{2-} concentrations, retentions of the monovalent species can even be negative, resulting in a higher concentration of the salt in the permeate than in the feed.

The preferential passage for common anions is $\text{NO}_3^- > \text{Cl}^- > \text{HCO}_3^- > \text{SO}_4^{2-}$, while for cations it is $\text{Na}^+ > \text{K}^+ > \text{Ca}^{++} > \text{Mg}^{++}$ (de Witte, 1992). For example, the retentions of NaNO_3 , NaCl and Na_2SO_4 are 15,8; 18,7 and 94 % respectively under the specific experimental conditions used by Bhattacharyya and Williams (1989), while retention of the salts K_2SO_4 , Na_2SO_4 , Na_2CO_3 , KCl , LiCl , NH_4Cl , MgSO_4 and CaCl_2 decreases in this order from 85 to 10 % (Rudie *et al*, 1993). While preferential passage through nanofiltration membranes is predictable, quantifying the passage of individual ions is complicated by the fact that this passage is determined by the presence of the highest retained species. Furthermore, there is a complex relationship between the membrane's surface chemistry and steric exclusion character and membrane performance for specific separations. Even today, the mechanism of transport through nanofiltration membranes is not well understood and no researcher has successfully modelled this process for complex solutions in commercial applications (Lomax, 1994).

5.4.3.3 Osmotic Pressure Predictions

The osmotic pressure of a solution is a key variable in the consideration of its treatment using a membrane separation process, such as nanofiltration. Specifically, in carbonate solutions, the osmotic pressure is not only a function of component concentration, but also of pH, since the number of species present in any solution depends on the pH of the solution. Although osmotic pressure can be measured experimentally, it may be predicted from a knowledge of the chemical species present. Brouckaert *et al* (1993) describe the method for undertaking such predictions, based on the use of the speciation program, MINTEQA2, for determining the equilibrium speciation of the solution to be modelled. A correlation based on the Gibbs-Duhem and Davies equations was found to give accurate predictions (within 10 %) of the osmotic pressure up to 2 000 kPa. In their derivation, osmotic pressure, π , is calculated from the activity of water:

$$\pi \text{ (kPa)} = -\frac{RT}{v_w} \ln a_w \quad (5.12)$$

where R = universal gas constant (8,314 l.kPa.mol⁻¹.K⁻¹)
 T = absolute temperature (K)
 v_w = molar volume of water (0,018067 l.mol⁻¹ at 25 °C)
 a_w = activity of water
 and subscript w = water

An expression for the activity of water was derived by integrating the Gibbs-Duhem equation, which for constant temperature and pressure is:

$$\text{moles}_w d \ln a_w = - \sum_j \text{moles}_j d \ln a_j \quad (5.13)$$

where a = activity
 j = jth solute species

The boundary condition for the integration is pure water, where $a_w = 1$.

To perform the integration, the activity coefficients of all solute species must be known as functions of concentration. The Davies equation, a simplified version of the extended Debye-Huckel equation was used to predict the activity coefficient, γ , of charged species, q :

$$\log \gamma_q = -G c_q^2 \frac{\sqrt{I}}{(1 + B \rho_q \sqrt{I})} + b_q I \quad (5.14)$$

where

- G = function of dielectric constant and temperature ($0,509 \text{ kg}^{1/2} \cdot \text{mol}^{-1/2}$)
- c = charge number
- B = function of dielectric constant and temperature ($\text{kg}^{1/2} \cdot \text{cm}^{-1} \cdot \text{mol}^{-1/2}$)
- ρ = ion size parameter (cm)
- b = ion specific parameter (kg/mol)
- I = ionic strength $1/2 \sum_q c_q^2 m_q$ (mol/kg)
- m = molality (mol/kg)

For neutral species, u, activity coefficients are modelled by the equation:

$$\ln \gamma_u = \alpha I \quad (5.15)$$

where α = constant

Substituting these into the Gibbs-Duhem equation and integrating from pure water to the solution equilibrium yields:

$$55,52 \ln a_w = - \sum_j m_j - \sum_q m_q + 4,606 G (1 + \sqrt{I} - 2 \ln (1 + \sqrt{I}) - \frac{1}{(1 + \sqrt{I})}) - 2,303 G b I^2 \quad (5.16)$$

The first two terms give the total concentration of solute species, the third gives the electrostatic contribution, and the fourth is empirical. All data required in this equation is part of the MINTEQA2 speciation modelling program output (see Section 5.3). Using this output, predictions can be made of the osmotic pressures of solutions. This is particularly useful in predicting effective driving forces for mass transport in pressure driven membrane processes, and therefore evaluating the direction of flux change.

5.4.3.4 Membrane Transport Theories

As with all membrane processes, nanofiltration performance may be evaluated in terms of membrane retention, permeate flux and water recovery. Theories relating to membrane transport aim to predict these parameters, both in simple single-salt solutions and in mixed systems, and indicate the separation dependency on feed concentration, permeate volume flux and membrane charge density (if applicable). Generally, they do this by predicting the solute and solvent fluxes, from which the performance parameters of interest are computed.

While there are various theories reported in the literature for transport through reverse osmosis membranes, the mechanism of mass transport specifically for nanofiltration is less clear. This results from the unique structure and properties of the membrane itself. For example, using affinity chromatographic methods to characterise pore size and surface character of nanofiltration membranes, Rudie et al (1993) suggest that a complex combination of both steric exclusion and surface force interactions is responsible for the unusual selectivity behaviour of the charged membrane towards ionic species. This view is confirmed by Jelen (1991) who, in reviewing the principles of pressure-driven membrane processes, states that, for nanofiltration of simple solutions, permeation of salts appears to be governed by both diffusion through the membrane material (similar to the ideal RO process) and by the convective pore flow (as accepted for conventional UF processes). He also acknowledges that separation performance of nanofiltration for mixtures of ionic species is complicated by Donnan exclusion effects, causing substantial differences in retention of the same species, depending on solution concentration and composition.

This Section reviews the major theories for membrane transport, which may be used to describe the performance of the system under consideration, namely the nanofiltration of sodium carbonate/bicarbonate solutions at different concentrations and over a range of pH values. This system is a complex and interesting one, not only because of the unique membrane properties, but also because of the complicated inter-relationships between the eight individual species, of four different charges, which co-exist at equilibrium in any sodium carbonate/bicarbonate solution.

Reviews of membrane transport theories by the Pollution Research Group summarise state-of-the-art knowledge and recent developments in this field (Brouckaert, 1994; and Wadley, 1994a). The two most applicable membrane transport theories are the solution diffusion model and the preferential sorption-capillary flow model. Both assume the three types of transport shown in Figure 5.6, that is water and solute transport through the membrane pores, and mass transfer away from the membrane on the high pressure side of the membrane as a result of the concentration gradient which develops between the more concentrated boundary layer and the less concentrated bulk feed solution. The transport equations used in each theory take different forms, and each has its own area of utility.

If the cross-flow velocity at the membrane surface is significantly high, then the thickness of the boundary layer is sufficiently small to assume that the concentration of the solute at the membrane-liquid interface approaches that in the bulk solution. At low flows, the boundary layer thickness increases, as does the difference between the concentrations of solute at the

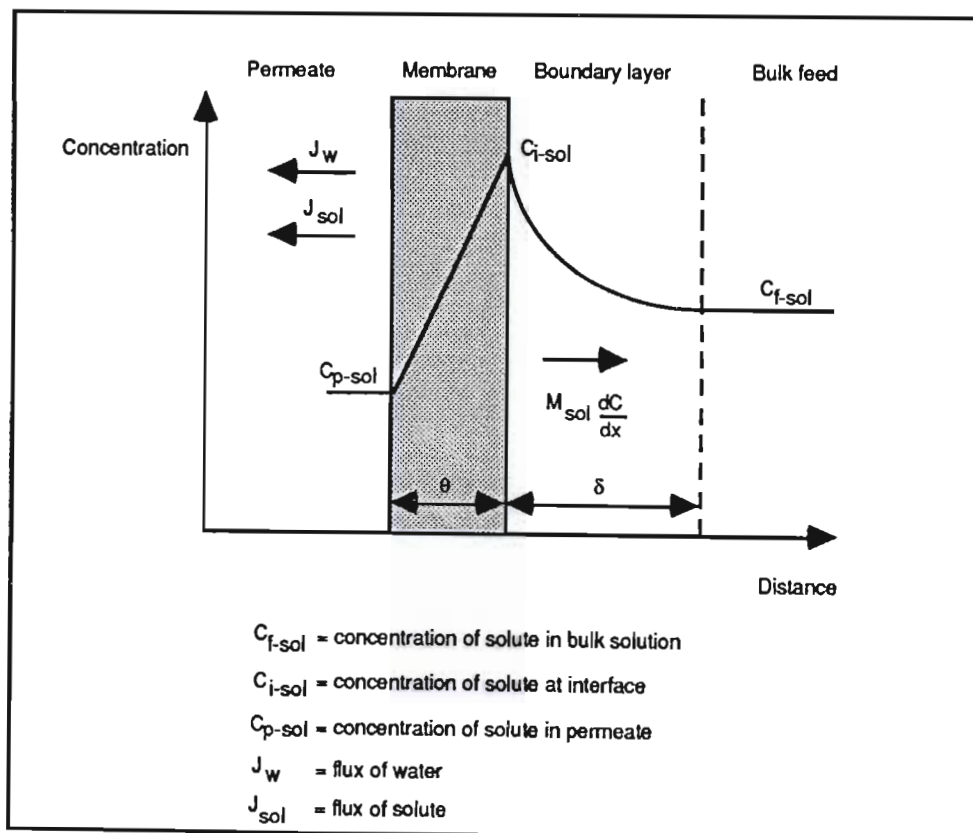
interface and in the bulk solution. Flux reduction may occur as a result of concentration polarisation in the vicinity of the membrane surface, which leads to an increase in the osmotic pressure. Clearly, in these cases, the hydrodynamic environment near the membrane surface is of great significance to membrane flux. Transport of neutral molecules in the boundary layer is described by expressions for diffusion in a liquid. Where ions are present, the Nernst-Planck equation proper may be used as the basis for predicting the transport of solute in the boundary layer:

$$J_{sol} = -D_{sol} \frac{dC_{sol}}{dx} - D_{sol} z_{sol} C_{sol} \psi + J_v C_{sol} \quad (5.17)$$

where

- J_{sol} = solute flux (mol/m²s)
- J_v = permeate volume flux (mol/m²s)
- D_{sol} = diffusion coefficient of the solute
- x = membrane thickness (m)
- C_{sol} = concentration of solute (mol/m³)
- z_{sol} = valence of species
- ψ = electric potential (V)

Figure 5.6
Illustration of Three Types of Transport Showing Increased Concentration of Solute In the Boundary Layer with Decreasing Distance from the Membrane Surface



Although the various theories differ in the physical interpretation of the transport mechanism within the membrane, the predictions of each have been shown to be almost identical in practice (Muldowney and Punzi, 1988). The solution diffusion theory considers the solution within the membrane to be in hydrological continuity with the solution outside the membrane, while the sorption-capillary theory considers the membrane and solution to be discontinuous phases, across which an equilibrium distribution exists.

The basic features of both theories, especially those relating to transport through the membrane itself, are described below.

Solution Diffusion Theory

According to the solution diffusion theory (summarised by Timmer *et al*, 1993), concentration and pressure gradients are the driving forces for solvent and solute flow through the membrane. The principle driving force for solvent flow is the pressure gradient across the membrane, with a linear dependence of flow on the pressure gradient:

$$J_w = A (\Delta P - \Delta \pi) = J_v \quad (5.18)$$

where

- J_w = solvent flux (m/s)
- J_v = permeate volume flux (m/s)
- ΔP = transmembrane pressure (Pa)
- $\Delta \pi$ = osmotic pressure difference across the membrane (Pa)
- A = solvent (pure water) permeability (m/s.Pa)

and subscript

- w = water
- v = permeate volume

The pure water permeability, A , describes the general resistance of a membrane to water transport as a result of, for example, compaction under pressure and the viscosity of water. A is determined empirically and, in the absence of effects such as fouling or compaction, should be constant for any solute. For simplicity, the theory assumes that the solvent flux, J_w , is equal to the permeate volume flux, J_v . The theory also assumes a negligible concentration gradient for the solvent, and neglects the concentration dependence of solvent flow in the equations. Conversely, according to the solution diffusion model, pressure dependence of solute transport is considered to be negligible. Solute transport is driven mainly by the concentration gradient of solute across the membrane and a linear relationship is assumed between solute flux, J_{sol} (mol/m²s), and concentration gradient:

$$J_{sol} = M_{sol} (C_{m-sol} - C_{p-sol}) \quad (5.19)$$

where M_{sol} = mass transfer (by diffusion) co-efficient of solute in membrane phase
 C_{m-sol} = concentration of solute at membrane interface (mol/m³)
 C_{p-sol} = concentration of solute in permeate (mol/m³)

Equation 5.19 is the simplest form of solution diffusion theory for membrane transport. Further terms have been added by various researchers to yield the extended Nernst-Planck equation, which, in addition to solute transport by diffusion, accounts for this transport by coupling between solute and solvent, and by electrostatic concentration gradients (as described by Tsuru *et al*, 1991). This extended equation is:

$$J_{sol} = -C_{m-sol} u_{sol} R T \frac{d}{dx} \ln a_{sol} - z_{sol} C_{m-sol} u_{sol} F \frac{d}{dx} \psi + \beta_{sol} C_{m-sol} J_v \quad (5.20)$$

where u_{sol} = mobility of the solute (C/m².J.s)
 x = membrane thickness (m)
 a_{sol} = activity of solute
 z_{sol} = valence of species
 ψ = electric potential (V)
 β_{sol} = convective coupling co-efficient of solute

The right hand side of the equation expresses the diffusion term, migration term in an electric field, and convection term respectively.

The membrane point retention, σ , defined in equation 5.11 above, is a measure of the extent of solute separation and is a function of the water and solute fluxes. It may also be defined as:

$$\sigma (\%) = 1 - \frac{J_{sol}}{J_w C_{f-sol}} \cdot 100 \quad (5.21)$$

where C_{f-sol} = concentration of solute in the feed (mol/m³)

Primary separation of solutes occurs at the thin film barrier layer. The solute flux, J_{sol} , is a function of feed concentration, membrane charge density, ion charge and the diffusion coefficients of ions in the membrane. Because this flux depends on the concentration gradient of solute molecules near the membrane surface, it also depends on operating parameters. Since increased cross-flow velocities and reduced operating pressures lower

polarisation, high velocities and low pressures provide the highest solute separation/pressure ratio (Rudie *et al*, 1993).

Conditions which cause increased solute flux also reduce the difference in solute concentration across the membrane. The resultant decrease in osmotic pressure increases available effective pressure, defined as the difference between applied and osmotic pressures, which in turn results in increased water fluxes.

For systems containing charged components, the electroneutrality condition must be met:

$$\text{In the external solution:} \quad \sum z_{sol} C_{f-sol} = 0 \quad (5.22)$$

$$\text{In the membrane:} \quad \sum z_{sol} C_{m-sol} = -Z_m \quad (5.23)$$

where C_{f-sol} = solute concentration in feed (mol/m³)
 Z_m = charge density of membrane (mol/m³)

The constraint of zero electric current through the membrane is given as:

$$\sum z_{sol} J_{sol} = 0 \quad (5.24)$$

At steady state:

$$\frac{dJ_{sol}}{dx} = 0 \quad (5.25)$$

J_{sol} is constant under a particular set of operating conditions, and the reverse osmosis condition (or mass balance) is:

$$J_{sol} = C_{p-sol} J_v \quad (5.26)$$

This condition reflects the requirement that, at equilibrium, there is no depletion or accumulation of solute in the membrane. The boundary conditions are:

$$x = 0$$

$$C_{f-sol} = C_{m-sol}$$

$$x = \theta$$

$$C_{f-sol} = C_{p-sol}$$

In the case where charged membranes are used, the membrane charge density, Z , must be modified to account for the effect of the electric interaction of the external solution with the ionic groups in the membranes. The effective charge density, ϕZ , takes into account the ratio of the dissociated functional groups of the membrane with the stoichiometrically fixed ones.

Preferential Sorption-Capillary Flow Theory

This theory has resulted mainly from the work of Sourirajan and co-workers over the last 30 years (Sourirajan and Matsuura, 1985). Sourirajan has proposed two theories, the simple case resembling the diffusion term of equation 5.19. In some respects, Sourirajan's theories can be simplified for computer modelling purposes by using the Spiegler-Kedem theory, which is based on non-equilibrium thermodynamics and the assumptions of the friction model of membrane transport processes, but which does not consider concentration polarisation (Spiegler and Kedem, 1966). The Spiegler-Kedem theory is responsible for the introduction of the reflection (coupling/convection) term in the extended Nernst-Planck equation (5.20).

Sourirajan's preferential sorption-capillary flow theory assumes preferential adsorption of water at the membrane-feed interface and no solute accumulation in the membrane pores. The continuous withdrawal of interfacial water through the pores results in the formation of a boundary layer between the interfacial region and the bulk feed solution, which is more concentrated than the feed solution. It is also assumed that water is transported by viscous flow and solutes by pore diffusion, and that the effective mass transport co-efficient on the high pressure side of the membrane can be determined by *film theory*. The theory is formulated in terms of four basic transport equations, not dissimilar to those of the solution diffusion theory, as follows:

- 1) *Pure water permeability, A*. This is proportional to the transmembrane pressure difference, and is equivalent to that described in equation 5.18. It is defined as:

$$A = \frac{Q_w}{18 \cdot \text{area} \cdot \Delta P} \quad (5.27)$$

where Q_w = flow rate of permeate (m^3/s)
 18 = molar mass of water
 area = effective membrane area (m^2)

- 2) *Water flux, J_w* . For solutions in which the viscosities are close to that of pure water, this is proportional to the effective transmembrane pressure difference and resembles equation 5.18:

$$J_w = A (\Delta P - \pi_i + \pi_p) \quad (5.28)$$

where π_i = osmotic pressure in the boundary layer
 π_p = osmotic pressure in the permeate

- 3) *Solute flux through the membrane pores, J_{sol} .* This is proportional to the concentration difference on either side of the membrane phase and the equation resembles equation 5.19:

$$J_{sol} = \frac{M_{sol}}{\theta} \cdot (c X_{i-sol} - c X_{p-sol}) \quad (5.29)$$

where θ = effective membrane thickness
 c = molar density of the solution (mol/m³)
 X_i = mole fraction of solute in solution in boundary layer
 X_p = mole fraction of solute in permeate

If a linear relationship is assumed between the mole fraction of solute in the solution and in the membrane, and using the relationship $X_{p-sol} = J_{sol}/(J_{sol} + J_w)$, this equation can be expressed in terms of the water flux:

$$J_w = c \frac{M_{sol}}{k \theta} \cdot \frac{1 - X_{p-sol}}{X_{p-sol}} (X_{i-sol} - X_{p-sol}) \quad (5.30)$$

where $\frac{M_{sol}}{k \theta}$ = solute transport parameter
and k = mass transfer coefficient

- 4) *Mass transfer on high pressure side of membrane.* The solute which is retained by the membrane concentrates in the boundary layer at steady state, and must be removed by diffusion back into the bulk solution. Applying standard film mass-transfer theory gives:

$$J_w = c_{f-sol} k (1 - X_{p-sol}) \ln \frac{X_{i-sol} - X_{p-sol}}{X_{f-sol} - X_{p-sol}} \quad (5.31)$$

where the value of k depends on the nature of the solute, its concentration in the bulk feed, and the feed flow rate.

The derivation of these equations is described in detail in Chapter 2 of the publication by Sourirajan and Matsuura (1985); and is summarised by Wadley (1994a).

The expressions associated with the theories discussed refer specifically to single-solute solutions at a single point in a membrane system. Whereas many predictions have been published on the retention of species by membranes in single-solute solutions, in which the salt is normally considered as neutral salt molecules, fewer papers have dealt with solute retention involving mixed solutes in aqueous solutions (Nielsen and Jonsson, 1994). However, analytical techniques have been used for predicting membrane performance in mixed solute systems. These techniques usually involve solving the expressions above for each individual component, along with the required additional equations necessary for overall electroneutrality of the systems. The net result is the summation of the effects of the individual components in a mixed system. An additional important feature of mixed solute retention, is the solute-solute interaction which may be observed by the change of the single-solute retention induced by the presence of a second solute.

While experimental information provides an indication of the performance of the membrane during operation, this information is best interpreted by means of a computer model which simulates the system and applies the theory. The following sections look more specifically at the considerations required in developing and applying the theory of membrane transport to the nanofiltration of carbonate solutions. These sections address the modelling concepts in a qualitative manner. The quantitative analysis and mathematical manipulations inherent in the development of the model are the subject of another post-graduate study being undertaken at the Pollution Research Group by CJ Brouckaert.

5.4.3.5 System Specific Features

There are specific features of the system under consideration which need to be accounted for in developing a model for predicting transport based on the theories described above.

- 1) *The solution chemistry.* The complex interdependence of mass and charge distribution of the system components between eight individual neutral, anionic and cationic species on pH and concentration means that solute-solute interaction in a mixed solute system must be considered. Furthermore, solute species in transport cannot be considered as neutral ion pairs, but must be considered individually, and electrostatic interactions must be accounted for by the introduction of the potential term into the modelling equations.

- 2) *Membrane-solute-solvent interactions.* Because of the charged nature of the nanofiltration membrane, ionic species interact electrostatically with the membrane and, as a result, are selectively permeable. The contribution of coupling and convective forces in mass transport must be considered.

5.4.3.6 Membrane Transport Modelling for Carbonate Solutions

Although membrane literature comprehensively covers membrane properties and theories, performance, and pilot (and even full-scale) plant experience, this information is not readily accessible in usable form (Buckley, 1993). In particular, membrane models are presented as mathematical equations or as rigid vendor-produced computer packages. While these packages may be suitable for well-characterised solutions such as sea water, they are not suitable for the analysis of less common or complex solutions and harsh conditions. While far fewer models are reported in the literature for nanofiltration than for reverse osmosis, these models tend to address single-salt solutions or solutions with two interacting solutes.

Nielsen and Jonsson (1994) have developed an expression for calculating the change in retention of a given ion under nanofiltration conditions when adding other salts to the bulk solution. The expression was derived from the extended Nernst-Planck equation, and provides a simple means of calculating the change in retention from a knowledge of the equivalent conductance and concentrations of ions in the bulk solution. Heyde and Andersen (1975) explained the increase observed in membrane sorption of permeable ions on addition of impermeable salts to the bulk solution, in terms of constrained phase equilibria and the Donnan effect. Negative retentions of permeable species in solutions containing high concentrations of impermeable species have been modelled using solution-diffusion theory in combination with Donnan equilibrium theory (Lonsdale *et al*, 1975). Timmer *et al* (1993) have performed model studies to improve lactic acid separation from fermentation broths by reverse osmosis and nanofiltration. The model was based on the extended Nernst-Planck equation, for the description of mass transport of lactic acid under various pH and pressure conditions of the feed. Tsuru *et al* (1991) successfully applied the extended Nernst-Planck equation to the analysis of experimental data relating to the negative retention of anions in the nanofiltration of mono- and divalent ion mixtures by considering the effective charge density. Retentions of ions in mixed electrolyte solutions were predicted using the transport parameters obtained from single electrolyte experiments.

At the Pollution Research Group, Brouckaert and co-workers (1994) have been involved in assembling computer software and modelling methodology which would support the implementation of membrane separation technology for waste-water treatment using various

modules and membrane configurations. Data have been taken from existing installations to verify modelling results and predictions have been good for a series of commercial plants. Models have been based mainly on the Spiegler-Kedem theory and theories by Sourirajan. Wadley *et al* (1994) describe the implementation of a computer model to simulate nanofiltration applied to the recovery of waste brine at a sugar decolourisation plant. The model is based on the Spiegler-Kedem theory of reverse osmosis and was used to describe system performance and propose suitable module arrangements for a full-scale plant.

While published models describing nanofiltration are scarce and problem-specific, only one model has been identified in the literature which attempts to address the complications of the carbonate system in solution (Hagmeyer, 1993). In this work, simple modelling was done using the solution diffusion model to predict the transport of inorganic carbon species during nanofiltration of drinking water. Although this work is recent, it does not attempt to understand the implications of speciation on carbonate chemistry, and considers only the system components CO_2 , HCO_3^- and CO_3^{2-} . For dilute solutions, such as drinking water, this appears to be a good approximation since these species predominate over ion complexes such as NaCO_3^- and predicted retentions correlate reasonably with empirical data.

For the system under consideration in this thesis, a computerised model has been developed (Brouckaert, Baddock and Wadley, 1994), which predicts the effect of operating conditions and the concentration of each solute species on the permeate flux and solute retention for any solution, including the carbonate system. The model was developed by specialists at the Pollution Research Group with the aid of the program Mathematica for solving the computational complexities. The general concepts of the model are given here.

The model is based on the extended Nernst-Planck equation (5.20), which considers transport as a result of diffusion, and by electrostatic and convective forces in the system. Separate equations are written and solved for each ion, and are summed to give the results for the system as a whole. Consideration is also given to mass transport in the boundary layer, and the computations are simplified by assuming constant potential gradients across the membrane and in the boundary layer.

The mass balance in equation 5.26 and the electroneutrality condition in equation 5.24 are assumed. Because of the charge density of the membrane, for the zero charge condition to apply, equation 5.23 is set to equal $-Z_m$, where Z_m is the effective charge on the membrane.

In order to integrate the transport equation over the thickness of the membrane, θ , the potential gradient, must be known, that is the value of the potential, ϕ , at each point must be

calculated. ϕ is given by the grouping $F \frac{d}{dx} \psi$ in equation 5.20, and may be solved at each point in the membrane by multiplication of both sides of this equation by the charge and summing for all species:

$$\sum J_{sol} z_{sol} = - \sum z_{sol} C_{m-sol} u_{sol} RT \frac{d}{dx} \ln a_{sol} - \sum J_{sol} z_{sol}^2 C_{m-sol} u_{sol} \phi + \sum z_{sol} \beta_{sol} C_{m-sol} J_v \quad (5.32)$$

and

$$\phi = \frac{- \sum z_{sol} C_{m-sol} u_{sol} RT \frac{d}{dx} \ln a_{sol} + \sum z_{sol} \beta_{sol} C_{m-sol} J_v - \sum J_{sol} z_{sol}}{\sum J_{sol} z_{sol}^2 C_{m-sol} u_{sol}} \quad (5.33)$$

To simplify the computation of ϕ at each point in the membrane thickness by equation 5.33, it was considered appropriate to assume an average and constant value of ϕ over the entire membrane. This approach had proved successful for Tsuru (1991).

Once ϕ had been assumed constant, the extended Nernst-Planck equation 5.20 can be integrated over the thickness of the membrane to yield an equation for the first unknown C_{p-sol} :

$$C_{p-sol} = C_{i-sol} \exp \bar{a}_{sol} \frac{J_v C_{p-sol}}{M_{sol} \bar{a}_{sol}} \quad (5.34)$$

where \bar{a} = a constant which includes the reflection/convection co-efficient term and ϕ

The value of ϕ is unknown and may be solved iteratively by combining the equations describing the conditions of electroneutrality and zero charge and applying them at the feed-membrane interface and at the permeate-membrane interface to solve for \bar{a} . The third unknown, J_v , may be solved by equation 5.18, which is adapted by the Spiegler-Kedem theory to consider the effects of concentration and convection on the osmotic pressure.

Thus the unknowns J_v , ϕ and C_{p-sol} can be solved iteratively.

To determine C_{i-sol} from C_{f-sol} , the boundary layer needs consideration. A similar process is used, whereby the Nernst-Planck equation proper (equation 5.17) is integrated over the thickness, δ , of the boundary layer to yield the following relationship:

$$C_{i-sol} = C_{b-sol} \exp q_{sol} \frac{J_v C_{p-sol}}{M_{sol} q_{sol}} \quad (5.35)$$

where q = a constant which includes the reflection/convection co-efficient term and ψ

In a similar manner to that described above, the unknowns J_v , ψ and C_{p-sol} can be solved iteratively.

Section 8.4 discusses the application of this model to the carbonate system in solution.

5.4.4. Electrochemical Recovery

The electrochemical stage is the heart of the treatment sequence and has three main functions, to:

- 1) Recover, from the nanofiltrate, sodium hydroxide at a concentration suitable for reuse in scouring;
- 2) Deplete the nanofiltrate of soluble sodium salts to produce a water of suitable quality for reuse in the scour rinse range;
- 3) Generate acidic gas (carbon dioxide) for recycle to the neutralisation stage of the treatment process.

Electrochemistry is not a commonly used industrial technology. Perhaps the most widely used industrial application is in the production of chlorine, hydrogen and sodium hydroxide by the electrolysis of sodium chloride. Other industrial applications include *in situ* electrolytic generation of chemical reagents, most commonly hypochlorite. For example, sea water may be electrolysed to disinfect sewage. A further application of electrolysis is the electrolytically induced reduction and coagulation of Cr(VI) to form a precipitate of Cr(III) hydroxide.

Some applications of electrochemistry in waste water treatment are discussed in Section 3.2.1 and references are made to literature reviews which provide background information on the subject. The commercial use of electrochemistry as a waste water treatment technology, has only limited application, despite the amount of effort that appears to have been put into the research and development of the technology. This limited application is because, although in many cases, these systems are cost effective, operational demands often offset the advantages gained (Eilbeck and Mattock, 1987). Perhaps the main exception is the anodic oxidation of cyanide in waste water, a process which has been

extensively studied and applied (Ermakov *et al*, 1990). Cathodic reduction of metal ions from waste waters to deposit the metal is another widely investigated process (Van der Vlist, 1989). Most application has been for relatively valuable metals, such as silver and gold. Where metals are present as mixtures, they cannot be adequately separated and this process loses some benefit. Other fields in which electrochemistry is gradually finding commercial acceptance as a waste water treatment technology include the treatment of organic wastes to lower COD levels, or destroy hazardous compounds, such as phenolic materials, and the adaptation of electrolytic processes to generate gas bubbles for flotation applications. Using electroflotation, protein may be recovered from dairy wastes.

Literature with respect to the application of electrochemistry as a wastewater treatment process in the Textile Industry is limited mainly to the electro-oxidation of dyes. Although the principles of the electrochemical process discussed in this dissertation for the treatment of textile scouring effluent closely resemble those used in the chlor-alkali industry, the operational conditions and applied variables differ considerably. While development of the pretreatment sequence was geared toward producing a feed which was amenable to treatment by electrochemical processes, significant attention was given to the development of the electrochemical process to ensure that conventional technology could be successfully adapted to non-conventional application, while remaining economically viable. The principal adaptations required are summarised in Table 5.1.

Table 5.1
Comparison of Electrochemical Process with Conventional Chlor-Alkali Process

Parameter	Conventional Chlor-Alkali Process	Scouring Effluent Recovery Process	Implications
<u>Anolyte</u>			
Chemical	NaCl	Na solutions of inorganic carbon species	Different solution chemistry
Concentration	120 g/l Na ⁺	1 to 20 g/l Na ⁺	Lower conductivity, larger concentration gradients, different optimum applied operating variables and performance
Gas	Cl ₂	CO ₂	Different pH range of operation and materials of construction
Impurities	<0,5 mg/l Ca ⁺⁺ <0,1 mg/l Mg ⁺⁺	20 mg/l Ca ⁺⁺ 3 mg/l Mg ⁺⁺	Potential electromembrane fouling
<u>Catholyte</u>			
NaOH	up to 50 %	10 to 20 % NaOH	Entropy savings
<u>Process</u>	Stand alone	Part of manufacturing process	Integration and interdependence of recovery and processing variables

5.4.4.1. Electrochemical Cell

The electrochemical cell is a device which uses electrical energy to effect a chemical change, and is the converse process of transforming chemical energy into electrical energy in a galvanic cell or battery (Eilbeck and Mattock, 1987). In the simplest form, the electrochemical cell consists of two electrodes, an anode and a cathode, immersed in an electrically conducting solution, or electrolyte, and connected together, external to the solution, via an electrical circuit which includes a current source and control devices. The chemical processes occurring in such cells are reduction-oxidation ones, and take place at the interfaces between the electrodes and the electrolytes. The reactions occurring at the anode and cathode are stoichiometrically equivalent, since the number of electrons being discharged by the cathode is equal to the number being taken up by the anode.

Figure 5.2 is a diagram of the electrochemical cell used in the treatment sequence. The cell is divided into two compartments by the electrochemical membrane, which is a highly selective cation-permeable ion-exchange membrane. The nanofiltrate is circulated through the anode compartment and a weak sodium hydroxide solution is circulated through the cathode compartment. When an electrical potential is applied across the electrodes three distinct processes occur, by which electricity is conducted.

- 1) Metallic conduction occurs in the external circuit, where the current is carried solely by electrons.
- 2) Electrolytic conduction takes place within the bulk of the solution, where the charge carriers are anions and cations. All ionic species will contribute to this process, whether or not they are involved directly in the oxidation or reduction reactions. Their relative contributions are dictated by their concentrations and transport numbers. More specifically in the present system, sodium ions and water of association are transported through the electromembrane towards the cathode, from the anolyte.
- 3) At the electrode interfaces oxidation and reduction processes occur by which the ionic conduction of the solution is coupled to the electronic conduction within the electrode and external circuit. It is by this process that electrical energy is converted to chemical work. Electrical losses occurring elsewhere in the cell appear as ohmic heating. Specifically, water is reduced at the cathode interface with the consumption of electrons:



The hydroxide ions combine with the sodium ions as they are transported through the electromembrane, to produce a concentrated sodium hydroxide solution. The hydrogen gas is vented to the atmosphere. At the anode surface, water is oxidised with the evolution of electrons:



As hydrogen ions are released at the anode, the acidity of the anolyte increases, thereby shifting the inorganic carbon equilibrium in the direction which results in the formation of carbonic acid, free carbon dioxide and water, as presented by equations 5.3 and 5.4. The gases evolved from the anolyte (carbon dioxide and oxygen, which is generated at the anode surface) are recycled to the neutralisation stage of the process, where the carbon dioxide is absorbed by inflowing effluent, while the oxygen passes through the unit and is vented to the atmosphere.

Mass transport of ions and other solution components occurs by one of three mechanisms (Wadley, 1994b):

- 1) Diffusion, by which the species move as a result of a concentration gradient. This mechanism predominates at the electrode/electrolyte interface.
- 2) Convection, by which the species move as a result of external mechanical forces, such as electrolyte flow or electrode rotation. This mechanism is dominant in the bulk solution.
- 3) Migration, by which the species move as a result of an electrical potential.

The electric current which flows through the cell involves the movement of electrons in the electrodes and the movement of ions in the electrolytes and membrane. During their passage through the cell, electrons experience a number of energy reducing steps which can be measured as successive reductions in the electric potential difference between the anode and the cathode. In sequence, these include the anode reaction potential, the anodic overpotential, resistance to ion flow in the anolyte, resistance in the electromembrane, resistance in the catholyte, the cathodic overpotential and the cathode overpotential. Voortman (1992) carried out a theoretical analysis of each of these energy reducing steps to predict the potential drops and to identify processes which consume the most power.

Basic theoretical concepts of electrochemistry which influence the understanding of the operation of the electrochemical process are discussed below.

5.4.4.2. Kinetic Overpotential

The minimum direct-current electrical energy required to produce the desired electrochemical reactions can be deduced from the standard potentials of the reactions occurring at each electrode (equations 5.12 and 5.13) and the Nernst equation, which predicts the equilibrium potential, and is given by:

$$E = E^0 + \frac{R}{n} \frac{T}{F} \ln \frac{\{reactants\}}{\{products\}} \quad (5.38)$$

where E = half cell potential or equilibrium potential

E^0 = standard electrode potential

R = gas constant

T = absolute temperature

n = number of electrons transferred

F = Faraday's constant

$\{ \}$ = activity

When current passes through a cell, a number of irreversible phenomena occur. These may include a slow step in the overall electrode reaction such that the reaction is not able to remove (or supply) electrons as fast as they are supplied (or required). In these circumstances a cathode will develop a potential more negative than the equilibrium potential, while the anode will require a potential more positive than the equilibrium potential and so-called polarisation occurs. The effect of polarisation on practical electrolysis makes it necessary to apply a larger voltage than is calculated from standard electrode potentials before electrolysis can occur. The difference between the actual working potential of an electrode and the equilibrium potential is termed electrode overpotential. The electrode overpotential depends in a complex manner on the electrode materials and the applied current density.

5.4.4.3. Concentration Polarisation

Any reaction at an electrode surface in which solute species are discharged can only be sustained if reactant is transported (by, for example, diffusion, ionic migration and convective mixing) from the bulk solution to the electrode surface so as to replenish those species consumed in the electrochemical reaction. At low overpotentials, mass transport satisfies the demands of the process. However, with increasing overpotential and reaction rate, a point is reached where, regardless of the efficiency of electron transfer, the net reaction rate

becomes limited by mass transport, and the electrode is said to be concentration polarised. This effect can be reduced, but not eliminated, by increased agitation and improved cell geometry.

At steady-state conditions, the concentration of reactants in the layer immediately adjacent to the electrode surface, the diffusion layer, will be lower than that in the bulk solution. In addition, the concentration gradient through this layer is assumed linear. The rate of migration, r_{diff} , of a reactant by diffusion through this layer is given by Fick's Law:

$$r_{diff} = \frac{D (C_b - C_e)}{d} \quad (5.39)$$

where D = diffusion coefficient
 C_b = concentration in the bulk solution
 C_e = concentration at the electrode surface
 d = thickness of the diffusion layer.

The rate of ionic migration, r_{mig} , in the case of cations, is given by the equation:

$$r_{mig} = \frac{t_+ C D}{n F} \quad (5.40)$$

where t_+ = cation transport number (or fraction of total current carried by one cation species)
 CD = current density

Associated with ion transport is water transport, which occurs simultaneously and is caused by hydrostatic and osmotic pressure differences between compartments and by electro-osmosis during electrolysis. The water transport number, n_w , is the number of moles of water transported per mole of, say, sodium ions. In electro-osmosis, water is transferred either as water of hydration of ions or by the momentum imparted to 'free' water molecules by migrating hydrated ions.

Combining equations 5.39 and 5.40 gives the total rate of delivery of an ion to an electrode across the diffusion layer, r_{total} :

$$r_{total} = \frac{CD}{n F} = \frac{t_+ CD}{n F} + \frac{D (C_b - C_e)}{d} \quad (5.41)$$

As the voltage is increased, the current density will increase as long as the concentration gradient across the diffusion layer can increase sufficiently to supply the species at the

required rate. As C_e approaches zero, the rate of the electrode reaction can no longer increase and the reaction becomes diffusion-limited:

$$r_{total} = \frac{t_+ CD_{lim}}{n F} + \frac{D C_b}{d} \quad (5.42)$$

Thus, the diffusion current is proportional to the bulk concentration of the electroactive species, and the reaction rate will decrease as electrolysis proceeds. In the context of waste water treatment, this mass transfer limitation is particularly significant where the electroactive species are present in relatively low concentrations.

Although the above discussion of mass transfer limitation has been given with respect to electrode reactions, similar principles govern the transport of ions across ion-selective electromembranes. Where the current flowing through the electromembrane exceeds the equivalent supply of sodium ions to the electromembrane surface, concentration polarisation occurs at the interface between the anolyte and the electromembrane. The occurrence and control of concentration polarisation at the electromembrane surface is a critical factor in determining the technical and economic feasibility of the process under consideration.

5.4.4.4. Cell Resistance

In addition to overpotentials caused by kinetic and concentration polarisation, a further source of overpotential results from the finite resistance of the system. Ohmic (or 'IR') losses, occur in the electrodes, cell structure, anolyte, catholyte and electromembrane. The ohmic losses give rise to resistive heating, and are directly proportional to the applied current density, and the length and resistivity of the current path.

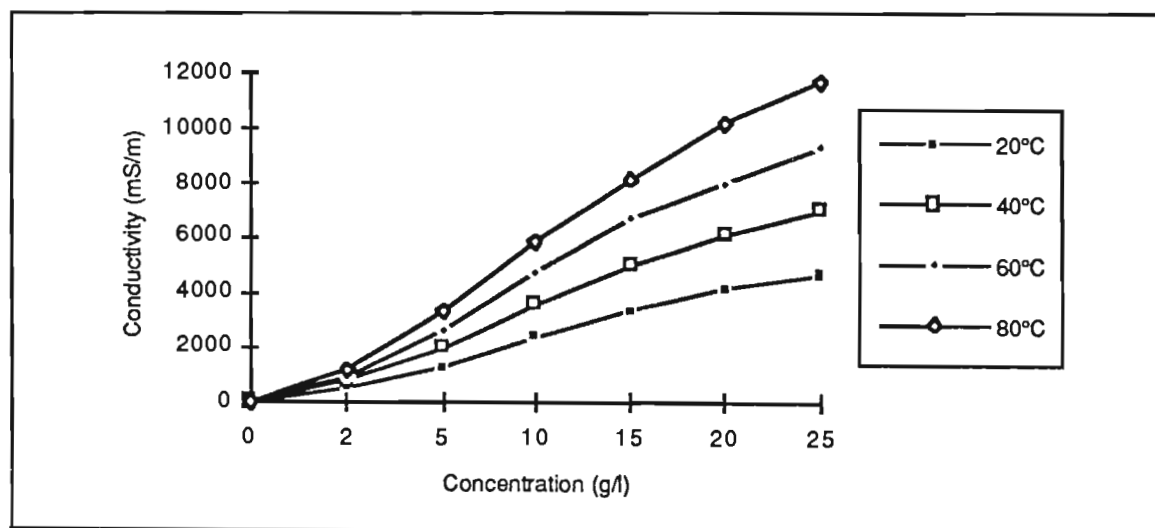
The ohmic losses through an electrolyte are a function of the resistance of the solution, which varies inversely with the concentration, or more precisely, the specific conductivity of the electrolyte. The volt drop through an electrolyte may be calculated from the equation:

$$E_o = \frac{d i}{L a} \quad (5.43)$$

where L = conductivity
 d = distance
 i = current
 a = area

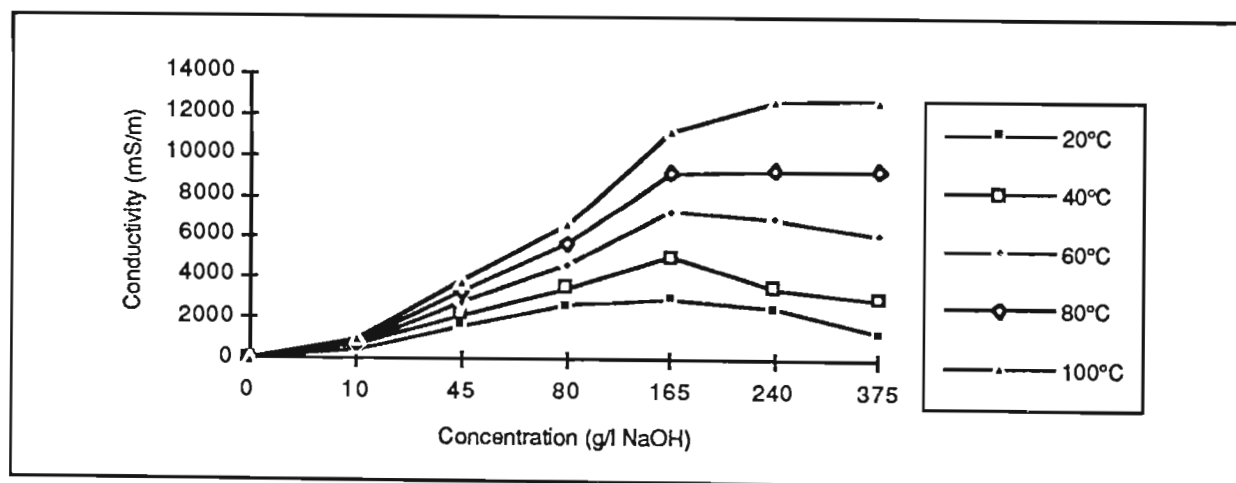
The relationships between the concentration and conductivity of sodium bicarbonate and sodium hydroxide solutions at various temperatures have been derived from the literature (Lobo, 1984; Lobo and Quaresma, 1981) and are given in Figures 5.7 and 5.8.

Figure 5.7
Relationship Between Conductivity, Concentration and Temperature of Sodium Bicarbonate In Solution



Data Source: Lobo, 1984; Lobo and Quaresma, 1981

Figure 5.8
Relationship Between Conductivity, Concentration and Temperature of Sodium Hydroxide In Solution



Data Source: Lobo, 1984; Lobo and Quaresma, 1981

Using these plots, an equation was developed which predicted the conductivity of the analyte solution at any concentration and temperature:

$$L_{\text{NaHCO}_3} = [(7,43 \times 10^{-2}T - 6,3 \times 10^{-5}T^2 + 1,37) \times \text{concentration}] + \\ [(-1,06 \times 10^{-3}T + 2,06 \times 10^{-6}T^2 - 1,78 \times 10^{-2}) + \\ [0,101T - 2,8 \times 10^{-3}T^2 + 2,15 \times 10^{-5}T^3 - 1,21]] \quad (5.44)$$

Thus, before electrolysis can occur, the applied potential must overcome the equilibrium potentials of the anode and cathode, any associated overpotentials, and the ohmic losses of the system. This applied potential has important practical and economic significance in the process under consideration.

5.4.4.5. Exchange Current

At the position of equilibrium there is no nett current flow, since the forward (cathodic) and reverse (anodic) reactions both proceed at equal, but finite, velocities and hence there are associated electron currents (Eilbeck and Mattock, 1987). At equilibrium potential:

$$i_c = -i_a = i_0 \quad (5.45)$$

where i_c is the cathode current, i_a the anode current and i_0 the exchange current. The exchange current provides a measure of the rates at which the cathodic and anodic reactions are occurring at any particular electrode. In any working cell there are anodic and cathodic currents associated both with cathodes and anodes; but $i_c > i_a$ at the cathode whereas at the anode $i_a > i_c$. The exchange current is characteristic of both the particular electrode reaction and the nature of the electrode surface, and is an important parameter in the design of any electrochemical cell.

5.4.4.6. Current Efficiency and Power

The current efficiency, η , of a particular species is based on the charge passed during electrolysis and is given by the equation:

$$\eta = \frac{\text{moles of electrons used in forming the product}}{\text{total moles of electrons consumed}} \quad (5.46)$$

A mole of electrons is a Faraday, which is related to current (A) and time (h) by Faraday's Law:

$$\text{Faraday} = \frac{A \cdot h}{26.8} \quad (5.47)$$

In the electrochemical application under consideration, it is assumed that both the anodic and cathodic reactions, for which water is the primary reactant, proceed at 100 % current

efficiency. However, the current efficiency for sodium hydroxide production and the efficiency for carbon dioxide release are reduced as a result of various factors:

- 1) *Reduced sodium transport number.* This results from the passage of current through the electromembrane by cations other than sodium ions, in particular hydrogen ions. The transport of hydrogen ions both reduces the transport number of sodium, and neutralises hydroxide ions formed at the cathode, thereby lowering the current efficiency for hydroxide production. The passage of current by hydrogen ions is favoured by a high pH gradient across the electromembrane, and can be reduced by maintaining the catholyte hydroxide concentration as low as is practically acceptable, and by ensuring that the pH of the anolyte is not allowed to drop to extremely low pH values. In addition, hydrogen ion migration can be minimised by ensuring that the supply of sodium ions to the electromembrane surface is sufficient to avoid mass transfer limitations. This is achieved by careful control of electrolyte flows, cell geometry and current densities.
- 2) *Back-migration of anions.* This involves the passage of current through the electromembrane by anions, particularly by hydroxide ions, from the catholyte to the anolyte. This reduces the current efficiency of hydrogen ion production in the anolyte compartment, which hinders the chemical equilibrium shift of inorganic carbon from the bicarbonate species to carbon dioxide. Careful control of the catholyte pH ensures that the sodium hydroxide concentration does not exceed the limit for a particular electromembrane, above which the electromembrane loses its selectivity.
- 3) *Concentration polarisation.* This is likely to occur on the anode side of the electromembrane. This may result when there are no cations available in the diffusion layer adjacent to the electromembrane to transport the current. As a consequence, water is split into hydrogen and hydroxide ions at the electromembrane surface. The hydrogen ions transport current, with no desalting effect, while the hydroxide ions inhibit carbon dioxide release and recovery.

To calculate the current efficiency of sodium hydroxide generation, changes in the concentration of cations (sodium ions) and anions (hydroxide ions) in the catholyte, cations (sodium ions) and anions (inorganic carbon-containing anions) in the anolyte, and anions (inorganic carbon-containing anions) in the absorption column liquor may be used. In theory, for each mole of electrons consumed in the process, one mole of:

- 1) Hydroxide ions are produced in the catholyte
- 2) Sodium ions are transferred from the anolyte to the catholyte, increasing the catholyte content by one mole and decreasing the anolyte content by one mole
- 3) Hydrogen ions are produced in the anolyte
- 4) Carbonate ions are converted to one mole of bicarbonate ions in the anolyte **or**
- 5) Bicarbonate ions are converted to one mole of carbon dioxide gas in the anolyte **In which case**
- 6) Hydroxide ions (or one mole of carbonate ions) in the absorption column liquor are converted to one mole of carbonate ions (or bicarbonate ions).

The specific power consumption of an electrochemical process may be expressed in terms of kWh/tonne of sodium hydroxide produced, and is related to the voltage (V), current (A) and time (h) by the equation:

$$\text{power} = \frac{V \times A \times h}{\text{tonne NaOH}} \quad (5.48)$$

In calculating the electrical requirements of a system, the current efficiency (η) is taken into account:

$$\text{Faradays} = \frac{\text{mass of Na to be transferred}}{23 \text{ g/mol} \times \eta} \quad (5.49)$$

Factors affecting current efficiency and power consumption include the following:

- 1) *The rate and uniformity of fluid flow distribution of the electrolytes*, in particular the anolyte, through the cell stack. Sufficient flow prevents gas blinding of the electromembrane and electrode surfaces (ie., reduction of effective area by accumulation of stagnant or slow moving gas zones) and concentration polarisation at the electromembrane surface.
- 2) *The operating current density*. High current densities are desirable in that the duty per unit area of the cell increases, thereby lowering plant size requirements. The maximum current density at which the system may operate efficiently is termed the limiting current density, which depends on the temperature and concentration of the electrolytes, in particular the anolyte. At current densities above the limiting value, the diffusive supply of sodium ions at the electromembrane surface becomes insufficient for the transport of electric current. As a result of concentration polarisation, water in the depleted diffusion layer is decomposed and the electric current is carried by the hydrogen ions, causing a

loss in current efficiency. The combination of limiting current density and current efficiency determines the electromembrane area requirements for a specific duty according to the following relationship:

$$area = \frac{A \times h}{\text{limiting } CD} \times \frac{1}{\eta} \quad (5.50)$$

- 3) *The temperature of the electrolytes.* Elevated temperatures have a beneficial effect on the kinetics of all electrode processes, diffusion coefficients, limiting current density, and rate of chemical reaction. In addition, it significantly affects the cell resistance components, in particular the ohmic loss through the electrolytes.
- 4) *The electromembrane and electrode condition* (also see Sections 5.4.4.7 and 5.4.4.8). Deposits or degradation of electrode or electromembrane surfaces will increase working voltages. Maintaining the correct flow conditions in the cell will ensure that the electromembrane is evenly positioned between the electrodes, and that physical abrasion of the electrode surfaces by the electromembrane is inhibited. Degradation of the electromembrane is minimised by routine flushing of the surface, in particular the surface on the anode side, to remove deposits. In addition, prevention of concentration polarisation at the electromembrane surface prevents the accumulation of hydroxide ions at the anode surface of the electromembrane, thereby reducing the potential for precipitation and scale formation in this area. Furthermore, it is desirable to operate composite electromembranes at a low water transport number to prevent accumulation of water, and subsequent blistering, within the electromembrane.
- 5) *The pH and concentration of the electrolytes*, in particular the anolyte. At high pH and concentration gradients, back-migration of species occurs and the sodium transport number is decreased, both causing loss in efficiency.

5.4.4.7. **Electrodes**

The major considerations in the selection of electrodes are (Buckley, 1984):

- 1) *Stability.* The electrode should be stable towards oxidation and attack by the reactants, products and intermediates which may be formed during electrolysis. Corrosion (most likely to occur with the anode) is unacceptable, since this results in contamination of the electrolytes by polyvalent metal ions and precipitates. When a metal is immersed in an aqueous solution not containing its own ions, the metal will either assume a corrosion potential set up by the kinetically favoured reactions or an equilibrium potential

established by the redox species into the solution. If an electrode is polarised in the anode direction (as in the case of water oxidation and oxygen discharge) its stability can be predicted from potential-pH diagrams. Since oxygen discharge occurs at large potentials positive to the hydrogen electrode, there is a tendency for most non-oxidic metallic compounds to become converted into oxides. For this reason, the most suitable anode materials are simple or mixed oxides which exhibit metallic conductivities. Mixed oxides existing in their highest valence state and forming solid solutions exhibit remarkable stability in environments encountered during evolution. Precious metal coated titanium anodes, such as those coated with ruthenium and titanium oxides and commonly called dimensionally stable anodes (DSA), are specifically suited for oxygen generation. The disadvantages of such electrodes are their expense, and the fact that the coating life is limited by passivation, preceded by a gradual dissolution of the precious metal oxide coating. Increased resistance, and therefore increased power consumption, occurs as a result of the accumulation of non-conducting oxides in the interfacial region between the titanium base metal and the oxide coating. Recoating costs are high.

- 2) *Overpotential.* Electrodes must be specifically selected to have low overpotentials for the favoured reaction. DSA's are designed for low overpotential oxygen generation, while cathode coatings such as Raney nickel, molybdenum nickel alloy, aluminium alloy or zinc nickel alloy result in a low overpotential for hydrogen generation (Brown, 1983). However, mild or stainless steel cathodes are commonly used.
- 3) *Conductivity.* The electrode coating should exhibit metallic conductivities in order to minimise voltage losses associated with ohmic drop across the coating and the formation of insulating layers. The conductivity of the surface layers formed on the electrodes must remain high. The formation of insulating films reduces the surface conductivity.
- 4) *Electrocatalysis.* Electrocatalytic activity reduces the electrode overpotential.

5.4.4.8. Electromembranes

Chemical and Physical Properties

Electromembranes are manufactured by companies such as Du Pont, Asahi Glass, Tokuyama Soda, and Asahi Chemicals. The present application uses a sodium-selective cation exchange membrane to separate the anolyte from the catholyte. Besides being water resistant and anionic, the electromembrane should exhibit the following properties (Buckley, 1984):

- 1) *Chemical and thermal stability.* The electromembrane should not deteriorate in the presence of the reactants, products and intermediates, even at high temperatures.
- 2) *Dimension stability.* The dimension tolerance specifications of the electromembrane, such as the size and flatness, in highly oxidising environments at elevated temperature should be minimal.
- 3) *Selectivity.* To maintain high current efficiencies, the electromembrane should be highly selective to sodium, even at high sodium hydroxide concentrations. It should be impermeable to anions and non-polar compounds.
- 4) *Low electrical resistance.* The resistance should be low to minimise ohmic loss across the electromembrane, allowing the easy passage of current and hydrated ions.
- 5) *High current density tolerance.* Because of the high cost of the electromembrane, it should be able to operate at high current densities to minimise surface area requirements.
- 6) *Mechanical strength.* Strong mechanical properties are required to endure handling and to maintain performance under electrolysis in extreme conditions.

Three literature reviews (Simmrock et al, 1981; Yeager, 1982; and Asawa, 1989) provide useful background information on the nature and properties of cation exchange electromembranes. In general, cation exchange electromembranes suitable for the application are composed of a thin film of copolymerised tetrafluoroethylene and sulphonated or carboxylated perfluorovinyl ether. The properties of these electromembranes result mainly from the hydrophilic nature of the polymers, and vary with the equivalent weight (concentration of anionic groups per unit polymer weight) of the polymer. For example, a high equivalent weight polymer will absorb less water and therefore exclude anions more efficiently, resulting in higher current efficiencies.

A number of anionic groups may be employed as side chains, and the choice alters the characteristics of the electromembrane. In practice, only sulphonic and carboxylic groups are common, although more recently substituted sulphonamide polymers are being used. Unfortunately, because of their high conductivity, sulphonic groups attract water, thereby increasing the water content of the electromembrane, promoting back-migration of hydroxide ions and lowering its selectivity. (The swelling behaviour of cation exchange electromembranes, in relation to the nature of the perfluorinated polymer used and the anionic groups attached, is discussed by Yeo *et al*, 1981). These electromembranes are only

suitable for the production of low concentrations of sodium hydroxide. On the other hand, carboxylic groups are less hydrophilic, consequently exhibiting higher current efficiencies, but at the expense of higher electrical resistance leading to higher power requirements. In order to minimise these conflicting effects, most manufacturers adopt a two layer electromembrane such as that described by Miyake *et al* (1987). A thin, high equivalent weight, carboxylic layer on the cathode side has a low water content to give high efficiency, while a thicker, lower equivalent weight, sulphonic layer on the anode side provides low electrical resistance and mechanical strength. Reinforcement is provided by Teflon cloth, which is laminated between the two polymer layers to form a electromembrane which has a thickness of 0,1 to 0,2 mm. This construction also avoids a further difficulty encountered with carboxylic-based electromembranes, namely the repression of ionisation of the carboxylic groups when the anolyte is acid, thereby increasing resistance. Substituted sulphonamide polymers are formed by reaction of the surface of the polymer in the sulphonyl fluoride form with substances such as ammonia, methylamines and diamines, to form a surface layer of sulphonamide groups. This modified barrier possesses excellent anion retention properties and is most suitable for the production of concentrated sodium hydroxide (30 to 40 %). More recently, electromembrane properties have been enhanced by alternative techniques. For example, Hiyoshi and Kasiwada (1992) describe the development of a cation exchange membrane for electrolysis of alkali metal chlorides which comprises a carboxylate-containing fluorocarbon polymer layer with an inorganic coating on the cathode side and a sulphonate and/or carboxylate-containing fluorocarbon polymer layer on the anode side. Such electromembranes are suitable for producing sodium hydroxide in concentrations of 45 to 55 % from saline solutions containing 150 to 200 g/l sodium chloride with reduced energy consumption.

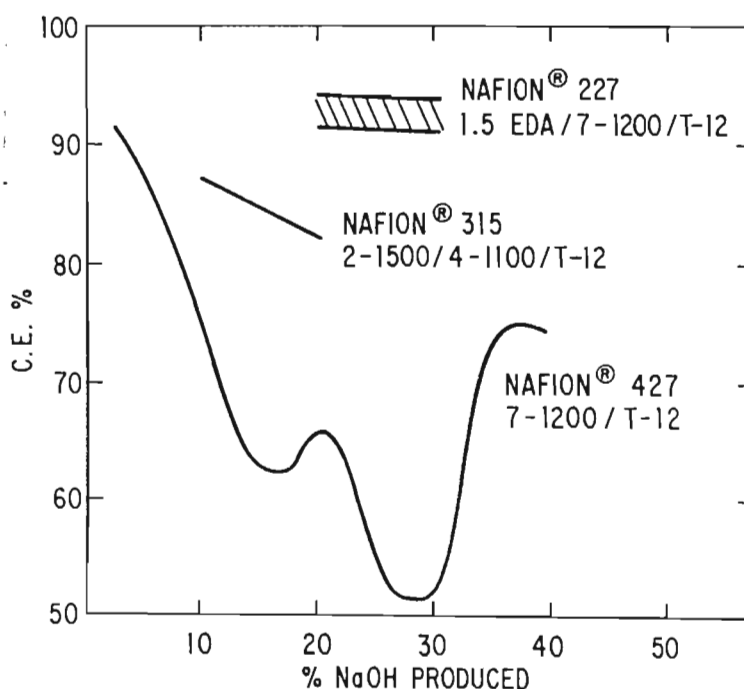
As an example of the variation in electromembrane properties and applications with the nature of the polymers, Table 5.2 summarises the properties of a selection of Nafion® electromembranes, which are manufactured by Du Pont (Pollution Research Group, 1989). In addition, Figure 5.9 compares the performance of Nafion® 427 (perfluorosulphonic acid), Nafion® 315 (composite), and Nafion® 227 (sulphonamide) electromembranes (Hora and Maloney, 1977).

Table 5.2
Properties of Nafion® Membranes

Parameter	100 series (eg No. 117)	300 series (eg No. 324)	400 series (eg No. 423)	900 series (eg no. 901)
Description	sulphonic films (no reinforcement)	reinforced composite of two sulphonic films of different equivalent weights	reinforced sulphonic films	reinforced bimembranes comprising carboxylic and sulphonic groups
Applications	low hydroxide concentration, fuel cells, acid and water hydrolysis	10 to 20% NaOH, metal ion recovery, swimming pool chlorination	KOH and 8-10% NaOH production, spent acid regeneration	30 to 45% NaOH
Ionic form	H ⁺	H ⁺	K ⁺	K ⁺
Resistance (ohm-cm) in 0,6 N KCl 24% NaCl	1,5	4,5	4,7	2,8
Mass (g/dm ²)	3,4	4,8	4,2	5,7
Equivalent weight	1 100	1 500 and 1 100	1 200	
Standard widths (m)	0,61; 0,75; 1,2; 1,5	0,61; 0,75; 1,2; 1,5	0,61; 0,75; 1,2; 1,5	0,61; 0,75; 1,2; 1,5
Standard length (m)	0,61 to 2,5	0,61 to 2,5	0,61 to 2,5	0,61 to 2,5

Source: Pollution Research Group, 1989

Figure 5.9
Nafion® Membrane Performance



Note: C.E. represents current efficiency

Source: Hora and Maloney, 1977

Degradation and Membrane Life

The ageing of electromembranes is attributed to the deposition of large clusters of insoluble metal compounds within the electromembrane structure, especially calcium and magnesium

hydroxides, but also aluminium, silica and any other metal ions which form insoluble hydroxides. These deposits often cause irreversible physical destruction of the electromembrane structure and polymer morphology. They also shield parts of the electromembrane, which causes local stresses and reduced available electromembrane area. The effect of deposition is increased electromembrane resistance and ohmic loss. Under normal circumstances, even temporarily high concentrations are detrimental since the effect is cumulative. For this reason, chlor-alkali processes which use electromembrane cells are equipped with primary (soda ash/caustic softening) and secondary (ion exchange) pretreatment units to lower calcium and magnesium concentrations in the brine to below 50 and 10 µg/l respectively. Molnar and Dorio (1977) examined the interactions of hardness ions with Nafion® electromembranes. Brines containing 20 mg/l each of calcium and magnesium ions were shown to have a deleterious effect on Nafion® 315, with current efficiencies falling from 82 % in the control case to between 74 and 78 % and voltages increasing from 4,5 to 5,5 V within 20 days of operation at current densities of 3 200 A/m². Prolonged operation with excessive precipitation within the electromembrane resulted in ruptures of the barrier layer. Orthophosphate addition up to 370 mg/l was found to be partly effective as a complexing agent for hardness ions. Precipitation was reduced significantly by removing the hardness ions from solution via the orthophosphate route. Current efficiencies were reduced from 95 % to 88 % after 120 days of operation, while the voltage remained steady around 4,5 V for a current density of 3 200 A/m². Orthophosphate retards the migration of hardness ions into the electromembrane by forming a loose, highly conductive gel-like material on the surface of the electromembrane. Partial recovery of performance could be achieved if fouled electromembranes were washed with distilled water or solutions of ethylenediamine tetra-acetic acid (EDTA).

The concept of chelation, or the ability of a compound to form a metal complex, is an important aspect of the current investigation, since the presence of chelating agents can alter both the retention performance of the nanofilter (Strathmann and Kock, 1979) and the lifetime of the electromembrane. The latter is particularly important in considering the commercial viability of the treatment sequence, since one of the criteria necessary to ensure success is a long electromembrane life.

Derivatives of chemicals such as gluconic acid, EDTA, citric acid, succinic acid, polyphosphates and borax are sold commercially as scale inhibitors to increase the solubility of calcium and magnesium ions by complex formation. The retarding power of most chelating agents available commercially is correlated to the degree of ionisation of the agent. Therefore, performance is dependent on pH, with most agents being effective in basic environments. For example, the degree of ionisation of polyacrylic acid increases from 10 to 90 % as the pH

is increased from 3 to 11. In the presence of strong acid, ionisation is suppressed and chelating ability inhibited.

Burney and Gantt (1983) describe a cleaning procedure to rejuvenate permselective ion exchange electromembranes *in situ* in electrochemical cells after the electromembrane has become at least partly fouled by insoluble compounds of multivalent cations from the brine anolyte. The patent relates to the electrolysis of aqueous alkali metal halide solutions to a halogen at the anode. The brine is specified to contain no more than 5 mg/l hardness (expressed as Ca) and no more than 70 mg/l carbon oxide (expressed as carbon dioxide). The electromembrane is regenerated preferably by contacting both sides, but by contacting at least one side, of the fouled electromembrane with solutions maintained below the pH of the electrolyte which is in contact with the electromembrane during normal operation. Contact is carried out for a time sufficient to dissolve most of the compounds of polyvalent cations plugging and/or fouling the electromembrane. Regeneration may be carried out at substantially reduced or zero current density. The cathode is protected from corrosion during regeneration by the use of either inhibitors or by operation of the cell at potentials enabling cathodic protection. It is claimed that drying of the electromembrane after removal of the contaminants further enhances regeneration.

Neytzell-de Wilde (1985) examined the fouling of electromembranes used in electrodialysis applications by organic and inorganic contaminants present in various industrial effluents. He distinguished fouling from poisoning by stating that poisoning results in irreversible bulk penetration of the electromembrane, whereas fouling gives rise to surface layers which may be removed by washing or chemical treatment.

According to Austin (1985), plants using Nafion® 300 series electromembranes performed acceptably with only primary pretreatment of brine to remove hardness ions, whereas high performance bimembranes (900 series) require secondary brine treatment. Process control (of hardness ions) is more critical with high current densities, since the electromembrane is working harder and becomes more susceptible to brine impurities. Furthermore, at low anolyte concentrations, where the water transport number is high, water may be accumulated between layers of polymers, causing blistering. Blistering may result in voltage escalation, but not necessarily in lower current efficiencies.

Water Transport

A phenomenon which has practical implications is the transport of water molecules through the electromembrane (see Section 5.4.4.3). Depending on the type of electromembrane used, and the electrolyte concentrations, 3 to 9 moles of water/mole of sodium ions are

transported to the cathode compartment in conventional membrane cell electrolysis (Buckley, 1984). A large part, and in some cases, all of the water required in the cathode compartment comes from the anolyte compartment in this way, resulting in volume loss of the anolyte.

Gas Blinding

A further phenomenon which effects the operation of the cell is gas blinding. This is the adhesion of gas bubbles to the electromembrane. It occurs less with sulphononic-based electromembranes than with carboxylic-based electromembranes.

5.4.4.9. Cell Design

The design of an electrochemical cell for waste water treatment must take into consideration a number of constraints that are evident from the preceding discussion. There are various designs of reactors specifically tailored to the requirements of waste water treatment, all aiming to overcome the problem of competing electrode reactions or transfer processes at low reactant concentrations by maximising mass transfer efficiency and minimising unproductive energy losses (Eilbeck and Mattock, 1987). Fleet (1989) has carried out a useful review of the development of electrochemical reactor systems for waste water applications. Cell configurations are based on different electrode forms, but they may be broadly classified as either two-dimensional arrangements, where the electrode is in sheet form; or three-dimensional arrangements, where the electrode is constructed so as to provide opportunity for electrochemical reaction from three axial sources. Particular cell designs include parallel plate systems, spiral wound configurations, rotating electrodes, packed bed electrodes, tumbled-bed reactors, and fluidised bed systems (Eilbeck and Mattock, 1987).

Two-dimensional cells are most common commercially and are of interest in this dissertation. They use parallel plate electrodes, in which anodes and cathodes are stacked alternatively to give a total working surface which will provide a suitable current density. Mass transfer is usually maximised by providing electrolyte flow between the electrodes by a recirculation system. The systems are either monopolar or bipolar, the difference lying in the electrical interconnections of the individual cells. If the cells are connected in parallel, the system is monopolar, and the electrolyser current is the sum of the individual currents, and the voltage on the electrolyser is the same as across a single cell. If the cell is connected in series, the system is bipolar, and the electrolyser voltage is the sum of the cell voltages, while the total current is equal to that flowing through a single cell (Peters and Pulver, 1977).

An increasingly popular design is the *zero gap* cell (Eilbeck and Mattock, 1987). In cases where the electrolyte concentrations are low, large voltage drops occur across the solutions,

with increased energy requirements. One way to minimise the drop is to reduce the electrode-to-electromembrane distance. In a typical design, the perforated electrode is pressed against the electromembrane, having a space behind it for gas to escape and electrolyte to circulate. Disadvantages include the occurrence of regions of high current density where the electrode contacts the electromembrane, which may result in electromembrane damage. Furthermore, gas may not escape quickly enough, causing increased cell resistance. The movement of electrolyte over the face of the electromembrane may be obstructed by the presence of the cathode, causing polarisation.

5.5. Chemical Recovery Potential of the Process Sequence

The proportion of sodium which is recovered from the effluent and recycled to the scouring process is a function of various parameters, as described below.

- 1) The amount of liquid remaining on the fabric after rinsing. As a fraction of the sodium mass on the cloth entering the rinse range, the proportion lost on the fabric after rinsing in a four-bowl counter-current range (Figure 4.10, Section 4) is given by the equation:

$$loss = \frac{m_0 C_0}{m_4 C_4} \quad (5.51)$$

- 2) The water recovery achieved during cross-flow microfiltration and nanofiltration. As a fraction of the sodium mass in the feed entering the units ($C_f Q_f$), the proportion lost in the concentrates is given by the equation:

$$loss\ in\ concentrate = \frac{C_c Q_c}{C_f Q_f} \quad (5.52)$$

- 3) The concentration of salt in the depleted anolyte during electrolysis. This will vary according to the acceptable background concentration in the wash water. The volume flow (Q), sodium mass flow (N) and concentration (C) characteristics of the depleted brine and recovered sodium hydroxide streams are given by the following series of equations. For the sodium hydroxide stream:

$$N_{NaOH} = N_{mi} - N_{mo} - N_{cc} - N_{nc} - N_{brine} \quad (5.53)$$

$$Q_{NaOH} = N_{NaOH} \cdot n_w \cdot \rho \quad (5.54)$$

$$C_{NaOH} = \frac{N_{NaOH}}{Q_{NaOH}} \quad (5.55)$$

For the depleted brine solution:

$$Q_{brine} = Q_a - Q_{NaOH} \quad (5.56)$$

$$C_{brine} = \frac{Q_a C_a - N_{NaOH}}{Q_{brine}} \quad (5.57)$$

$$N_{brine} = C_{brine} \cdot F_{brine} \quad (5.58)$$

where N = sodium mass flow from anolyte to catholyte in kg/h
 Q = volume flow in m³/h
 C = concentration in kg/m³
 $NaOH$ = recovered sodium hydroxide stream
 mi = moisture on cloth into rinse range
 mo = moisture of cloth out of rinse range
 cc = cross-flow microfiltration concentrate
 nc = nanofiltration concentrate
 $brine$ = depleted brine stream
 a = anolyte (feed) stream
 ρ = density of water in kg/m³

SECTION 6

EXPERIMENTAL PROCEDURES

This section describes experimental techniques, and is subdivided into four subsections. Section 6.1 examines the design of the pilot-plant equipment, while Section 6.2 describes experimental procedure and pilot-plant trials. Section 6.3 describes supplementary studies of nanofiltration, including laboratory techniques, chemical speciation and transport modelling. Section 6.4 describes supplementary studies of electrolysis, including the use of other anodes, electromembrane fouling and electromembrane cleaning.

6.1. Pilot-Plant Design

The pilot plant was designed at a capacity sufficient to provide meaningful data for the design of a full-scale plant. It consisted of an absorption column, a cross-flow microfiltration unit, a nanofilter and an electrochemical recovery unit. Details of these individual units are summarised in Table 6.1.

6.1.1. Neutralisation Unit

The neutralisation unit consisted of three main components: a feed tank; a pump for recirculating the effluent through the column; and a packed bed absorber. Figure 6.1 is a schematic diagram of this unit. The effluent was transferred manually to the 60 litre-capacity, polyethylene, feed tank (T1) from the scouring rinse range. The effluent was then pumped (P1) to a distributor at the top of the absorption column, from where it flowed downward through the packing at a rate of approximately 10 l/min. The feed flowrate was controlled using a valve (V3). The acid gas vented from the anolyte compartment of the electrochemical cell entered the column at the base; the carbon dioxide was absorbed into the effluent and the oxygen passed upwards through the column to the top, where it was vented to the atmosphere. A suitable liquid level was maintained in the column by means of a U-bend below the outlet.

6.1.2. Cross-Flow Microfiltration Unit

The cross-flow microfiltration unit consisted of four components: a feed tank; a pump for maintaining pressure and flow through the system; a microfilter tube; and a product tank. Figure 6.2 is a schematic diagram of the unit. The neutralised effluent was transferred manually from the neutralisation feed tank, to the microfilter feed tank, T2, which had a capacity of 80 litres. A pump, P2, was used to circulate the feed through the woven polyester

filter tube, and was connected to a level controller, LP1, in the feed tank. The feed flowrate was controlled by valves V5 and V9.

Table 6.1
Summary of Pilot Plant Specifications

Unit	Parameter	Specifications
Absorption column	height diameter material of construction packing material pH of treated effluent effluent flow pump	1 000 mm 150 mm Perspex polyethylene saddles (25 mm length) 8,5 10 l/min magnetic coupled centrifugal
Cross-flow microfilter	tube diameter filtration area tube material tube velocity pump operating pressure	12 mm 1,13 m ² woven polyester 2 to 3 m/s low pressure, high-flow positive displacement 200 to 300 kPa
Nanofilter	membrane type membrane area cartridge prefilter pump operating pressure	spiral wrap NF40 (FilmTec) 0,37 and 0,56 m ² 5 µm string wound polyester positive displacement 1,6 MPa
Electrochemical cell	cell pairs electrode size anode material cathode material material of frame construction electrochemical membrane pumps electrolyte flow volt requirements current density	2 4 each of 0,05 m ² DSA mild steel PVC Nafion 324 (Du Pont) magnetic coupled centrifugal 10 to 15 l/min 4 to 10 V/cell pair 300 to 3 000 A/m ²
Pilot plant	daily capacity	150 l effluent used to produce: 3 kg NaOH (at 50 to 200 g/l) 135 l low quality water 75 g (850 l) H ₂ gas 600 g (420 l) O ₂ gas 15 l concentrated impurities

The cross-flow microfiltration tube was 12 mm in diameter and 30 m in length, although this was reduced to 20 m, and then further to 12 m during the trials. The cloth area for the 30 m length was 1,13 m², for the 20 m length was 0,75 m², and for the 12 m length was 0,45 m². The tube was wound in a spiral of 1 m diameter and was supported in a horizontal, circular tray. The inlet pressure on the unit was maintained between 200 and 300 kPa by adjusting the valve V8 on the retentate line, while the pressure drop down the tube was 100 kPa. Retentate flow rate was maintained at approximately 2 to 3 m/s. Diatomaceous earth and limestone were used as filter aids.

Figure 6.1
Schematic Diagram of Neutralisation Unit

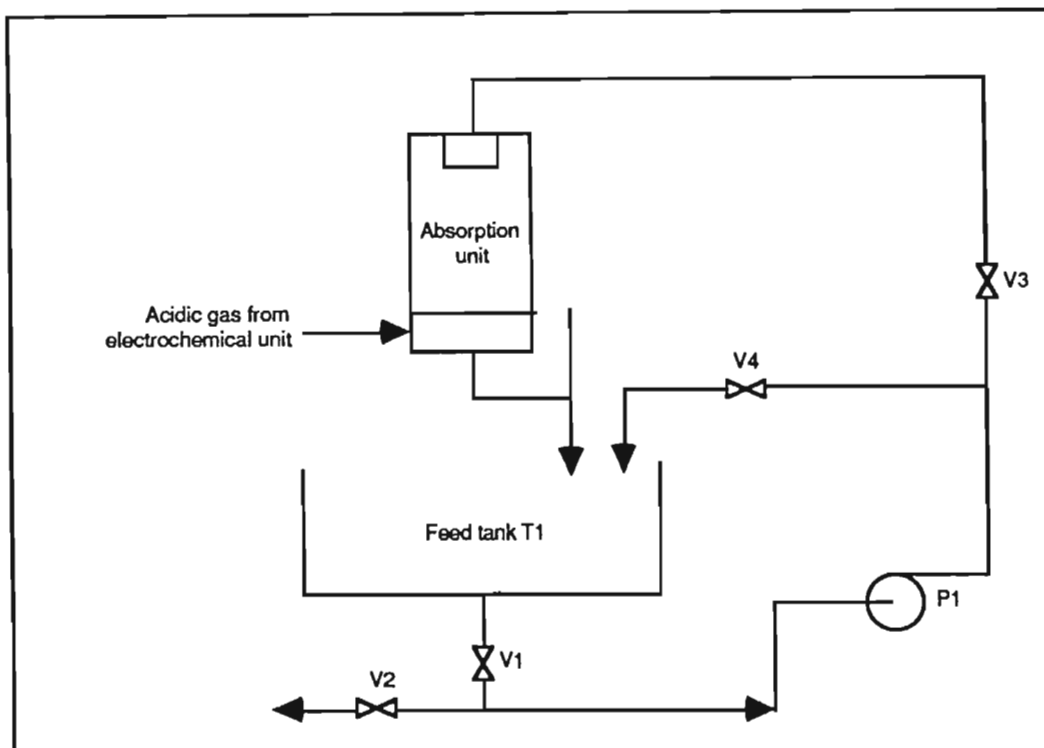
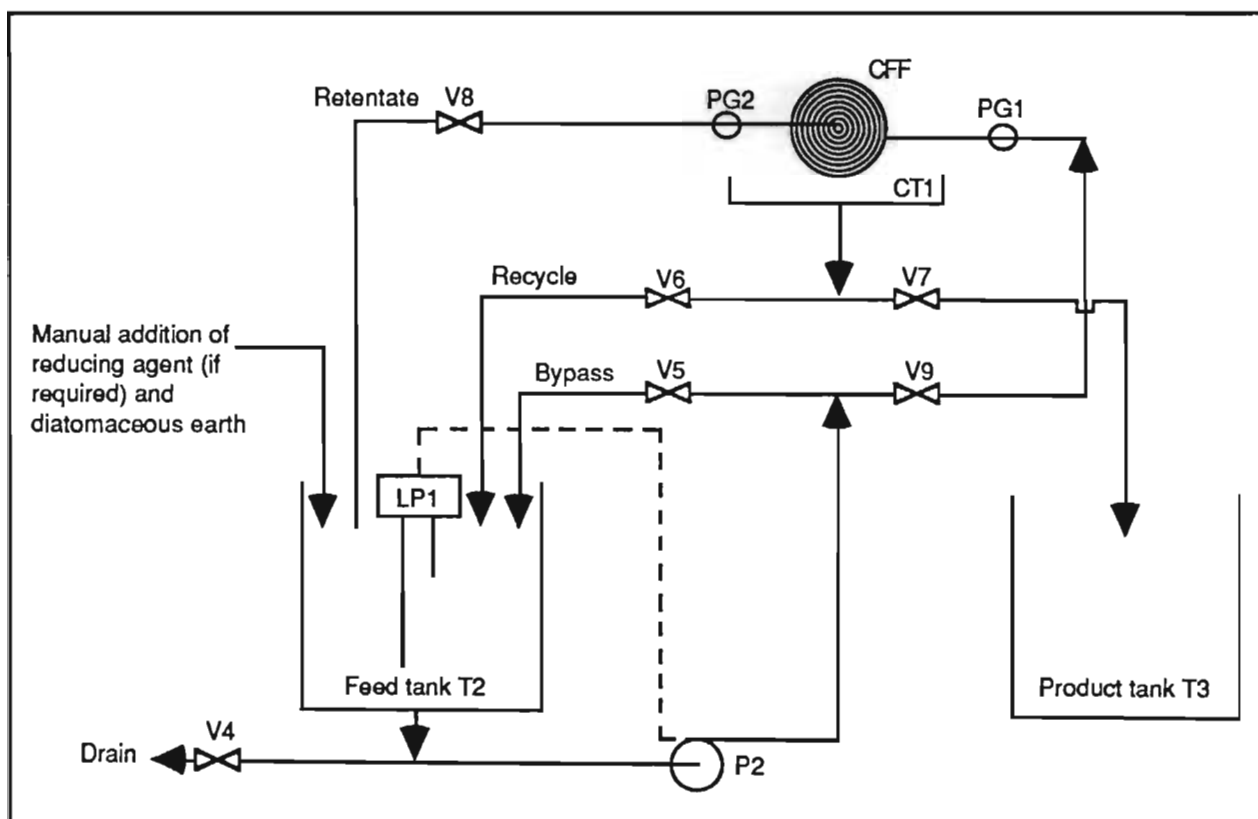


Figure 6.2
Schematic Diagram of Cross-Flow Microfiltration Unit



6.1.3. Nanofiltration Unit

The nanofiltration unit consisted of five components: a feed tank; a prefilter, installed as a precautionary measure; a pump for maintaining pressure and flow through the system; a nanofiltration module; and a product tank. Figure 6.3 is a schematic diagram of the unit. The cross-flow microfiltrate was transferred manually from the cross-flow product tank, T3 to the nanofiltration feed tank, T4, which had a capacity of 50 litres. The prefilter was a wound nylon cartridge with a porosity of 5 μm . Effluent was circulated through the unit using the high pressure pump, P3, which was fitted with a high pressure cut-out switch to safeguard the membrane in the event of a blockage.

The membranes were spiral wrap FilmTec NF40. Two different membrane models were used, which differed in area. The manufacturer's specifications of these membranes are summarised in Table 6.2. Initially, model NF40-2512 HP, with an area of 0,56 m², and mounted in a stainless steel module holder, was used. For this model, inlet pressures of 1,6 MPa were applied. A smaller module, NF40-1812, with an area of 0,37 m², and mounted in a PVC/fibreglass module holder, was used towards the end of the trials. For this module, inlet pressures were maintained at 1 MPa (although the membrane could withstand higher pressures, the holder could not). Pressure and flow through the module were controlled by valves V12 and V13 on the feed and retentate lines respectively. Because the pump delivery was constant, the product flow rate was controlled by fixing the retentate flow rate at approximately 20 to 30 l/min, and using valve V11 to control the flow rate to the module. No cooling system was fitted, although the temperatures were maintained below 45°C to prevent degradation of the membrane.

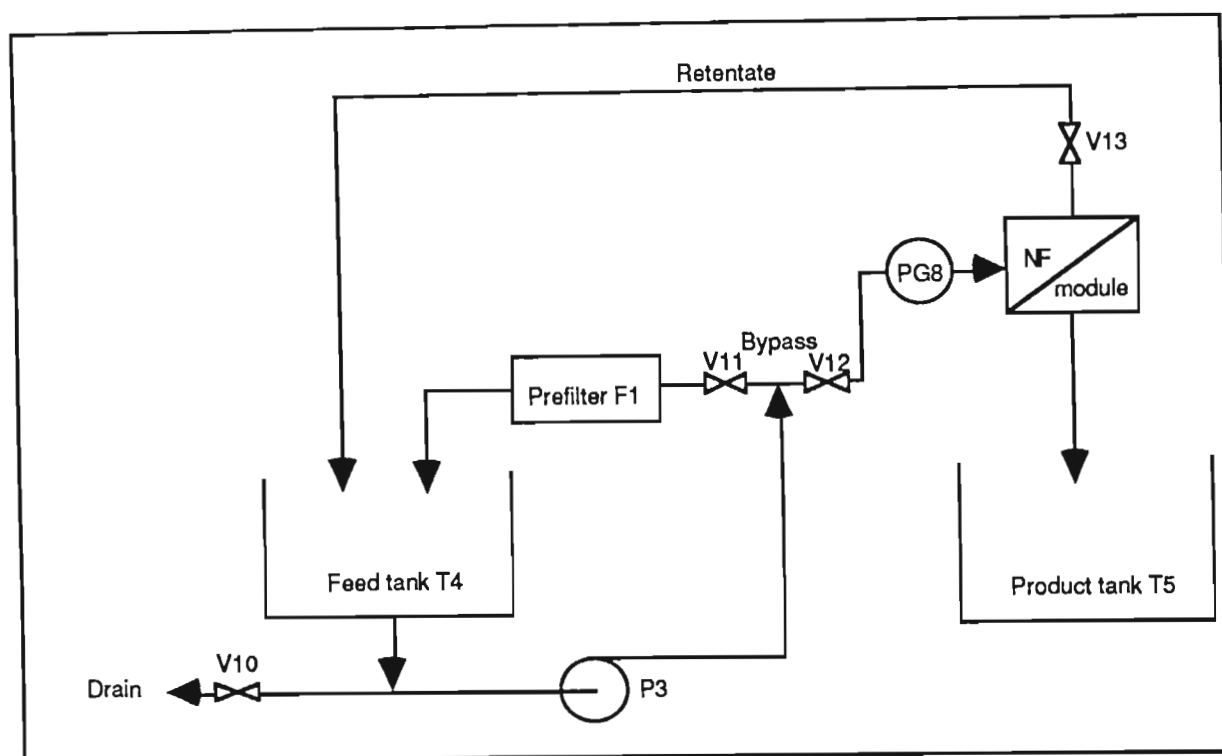
Table 6.2
Nanofiltration Membranes: Manufacturer's Specifications

Parameter	Model NF40-1812	Model NF40-2512
membrane area	0,37 m ²	0,56 m ²
permeate flow ¹	0,097 m ³ /h	0,146 m ³ /h
retention ² :		
NaCl (58 g/mol)	45 %	45 %
CaCl ₂ (111 g/mol)	70 %	70 %
MgSO ₄ (120 g/mol)	93 %	93 %
glucose (180 g/mol)	90 %	90 %
sucrose (342 g/mol)	98 %	98 %
raffinose (504 g/mol)	99 %	99 %
operating pressure	1,0 MPa	1,6 MPa
maximum pressure	4,1 MPa	4,1 MPa
maximum feed temperature	45 °C	45 °C
maximum free chlorine in feed	0,5 mg/l	0,5 mg/l
recommended feed pH	2 to 11	2 to 11

Note: ¹ 2 g/l MgSO₄ at 25°C and 1,6 MPa

² 2 g/l solute at 25 °C and 1,6 MPa

Figure 6.3
Schematic Diagram of Nanofiltration Unit



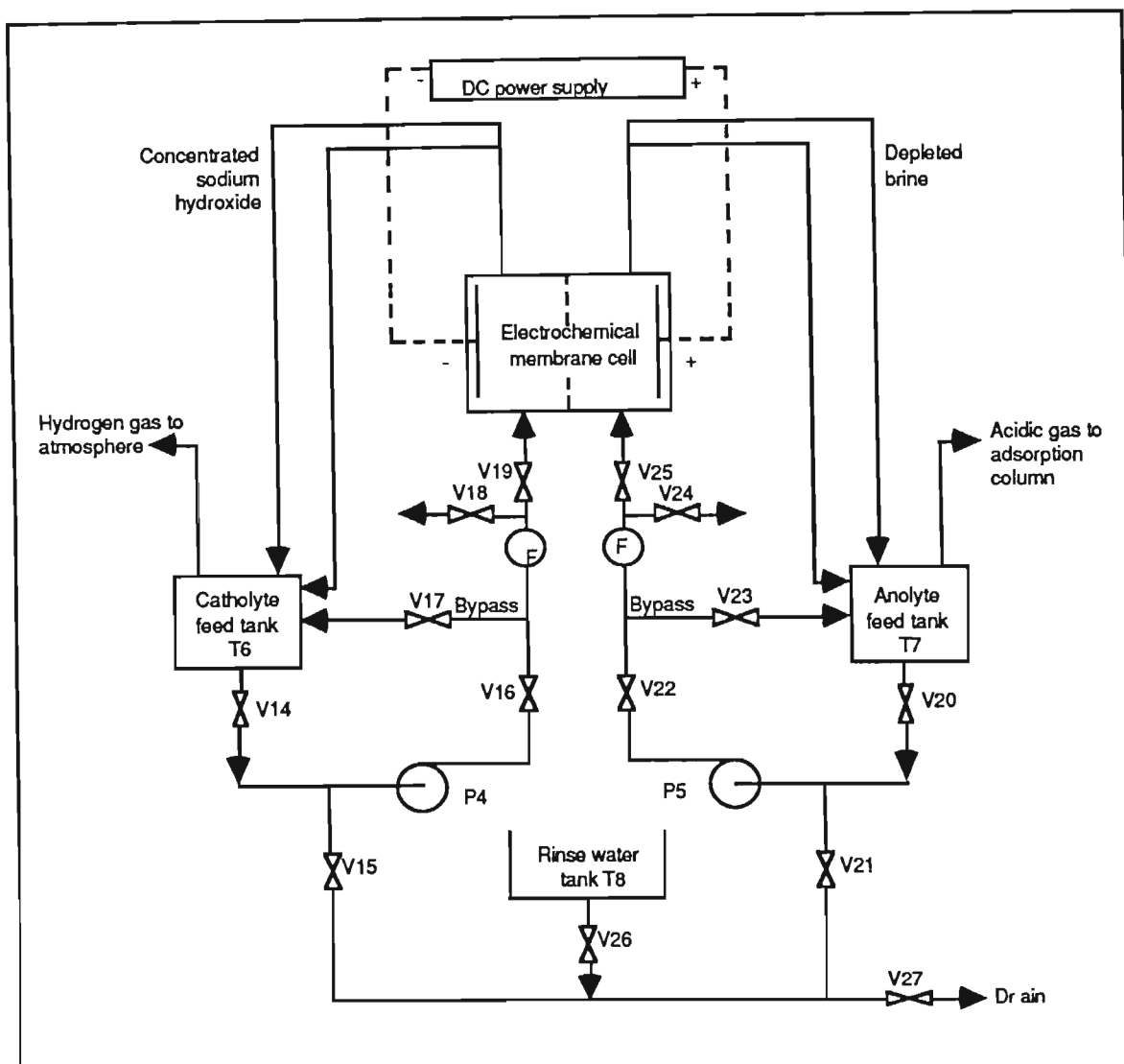
6.1.4. Electrochemical Recovery Unit

The electrochemical recovery unit comprised six components: anolyte feed tank; catholyte feed tank; two pumps for circulating the anolyte and catholyte; electrochemical cell containing a cation-exchange membrane; rinse water tank for cell flushing; and a regulated DC power supply. Figure 6.4 is a schematic diagram of this unit.

The feed tanks, T6 and T7, each 60 litres capacity, were filled manually and the electrolytes were circulated through the system using pumps P4 and P5. The electrochemical cell was constructed from PVC and contained two cells of a bipolar stack, purchased from Steetley Engineering Ltd, in the UK. Each cell was fitted with a hydrogen generating dished steel cathode and a titanium anode which was coated with precious metal oxides that are specific to the application of oxygen generation. The anolyte compartment was sealed from the atmosphere, and the acid gases were piped to the absorption column. The hydrogen gas evolved from the catholyte was vented to the atmosphere. The electrochemical membrane was supplied by Du Pont, under the brand name Nafion. The Nafion 324 electromembrane type, a reinforced composite of two sulphonic acid films, was used, and the exposed electromembrane area was 0,05 m² per cell. The electromembrane specifications are

summarised in Table 5.1. To minimise ohmic losses, the cell was operated with minimal gap between the electromembrane and electrodes, with the electromembrane-electrode distance being less than 5 mm.

Figure 6.4
Schematic Diagram of Electrochemical Unit



The flows of catholyte (sodium hydroxide) and anolyte (brine) through the cell were controlled by valves V16, V17 and V19, and V22, V23 and V25 respectively. Valves V18 and V24 allowed samples of catholyte and anolyte respectively to be collected for laboratory analysis. The flow of electrolytes through the two cells was either in series or was divided to give parallel feed to each cell. Typically, the total flow to the unit was 800 l/h of anolyte and 900 l/h of catholyte (in series configuration, flow through each cell was equivalent to total flow, whereas in parallel configuration, flow to each cell was halved).

Electrolysis was conducted under conditions of constant current, maintained by a direct current (DC) power supply with a maximum capacity to provide 500 A and 25 V. The positive and negative terminals of the supply were connected to the anode and cathodes respectively. A digital readout voltmeter, together with platinum wires inserted on either side of the electromembrane, was used to measure accurately the potential differences between the electrodes; between the electromembrane and each electrode; and across the electromembrane. In order to prevent the heating of the electrolytes to temperatures in excess of 60 °C, the voltage drop across both cells was maintained below 15 V, and the total power input was maintained below 1 100 W. A 10 mm change of liquid level in the electrolyte feed tanks was equivalent to a volume change of 0,73 litres.

6.2. Experimental Procedures and Trials

The trials were designed to:

- 1) Determine the technical feasibility of the treatment sequence;
- 2) Evaluate the potential for the reuse of the products in the scouring operation;
- 3) Provide data for the design of a commercial unit;
- 4) Develop estimates for the cost effectiveness of the treatment sequence.

All pilot-plant trials were conducted batchwise, as a series of individual experiments. Each individual experiment consisted of carbonation, cross-flow microfiltration, nanofiltration and electrolysis. The scouring effluent was neutralised to pH 8,5 with carbon dioxide gas. Thereafter it was treated by cross-flow microfiltration. The microfiltrate, clear and free of suspended matter, was transferred to the nanofiltration unit where the sodium salt was separated from the other constituents. The nanofiltrate was divided into two or three batches, and each batch was electrolysed in the anolyte compartment of the electrochemical unit until the desired degree of depletion had been achieved. Where additional carbon dioxide was required, this was produced by operating the electrochemical unit using a prepared solution of sodium carbonate or sodium bicarbonate.

Table 6.3 summarises typical characteristics of the scouring effluent which was used in the trials. The concentration of the effluent varied with the type of fabric being processed, the level of control of operating parameters, and the rinse water flow.

In total, 21 individual experiments were conducted (although five were carried out using other anode materials and are described in Section 6.4.3 below). Appendix 5 contains a detailed

description of operational procedures for each experiment, modifications carried out to the procedures and equipment during the trial period, mechanical problems encountered, and analytical methods for the determination of chemical parameters. During the three pretreatment stages, and as considered appropriate, samples of effluent, feed and permeate were taken and fluxes, pressures and temperatures were recorded. The pretreatment stages are conventional and proven techniques for applications similar to those for which they were being used in the current investigation. Furthermore, the principal advantage of the process lies in the ability to recover reusable chemicals and water.

Table 6.3
Characterisation of Scouring Effluent

Determinand	Units	Range
pH	-	13 to 14
conductivity	S/m	3 to 9
total carbon	g/l	2,0 to 4,0
inorganic carbon	g/l	0,1 to 0,4
organic carbon	g/l	1,9 to 3,6
chemical oxygen demand	g/l	4 to 14
sodium	g/l	4 to 12
calcium	mg/l	10 to 50
magnesium	mg/l	1 to 10
carbonate	g/l	1 to 3
hydroxide	g/l	2 to 8
total solids	g/l	15 to 36

Therefore, although the performances of the pretreatment stages were monitored, the operation of these stages was not considered to be as critical as the operation of the electrochemical recovery stage, the success of which was imperative to the success of the whole process. The experiments aimed to:

- 1) Investigate the performance of the cross-flow microfiltration and nanofiltration processes for the pretreatment of carbonated effluent (experiments 1 to 21);
- 2) Examine the long term effects of the process on the electrodes and electromembrane by repetitive operation of the electrochemical unit (experiments 1 to 17);
- 3) Investigate the effect of catholyte and anolyte concentrations and current densities on current efficiencies and cell voltages (experiments 1 to 21);
- 4) Investigate the effect of electrolyte flow rate and flow configuration on cell voltages and gas blinding (experiment 12);
- 5) Determine the effects of a background salt concentration on the operation of the system (experiments 18 and 19);
- 6) Determine the dependence of operational current densities and voltages on temperature and anolyte concentrations (experiments 1 to 21);

- 7) Determine the relationship between limiting current density and anolyte sodium concentration (experiment 18);
- 8) Monitor changes in cell performance over time by repetitive operation using prepared solutions of sodium carbonate and/or sodium bicarbonate as a basis for comparison (experiments 1 to 18);
- 9) Investigate the suitability of other anode materials (experiments 17, 19, 20 and 21 - see Section 6.4.3).

The results of the pilot-plant trials are presented in Section 7.

6.3. Supplementary Investigations of Nanofiltration

To supplement the main pilot-plant trials, laboratory investigations were carried out to examine certain practical aspects of nanofiltration under controlled conditions and assist in selecting the most suitable conditions for pilot-plant operation. In addition, theoretical chemical speciation and membrane transport modelling was carried out to describe and predict the observed performance characteristics of the membrane. The procedures for each of these investigations are described below.

6.3.1. Effect of Electrolyte Characteristics on Nanofilter Performance

To assist in identifying the preferred conditions for operating the pilot-plant nanofiltration unit, the retention and flux characteristics of the nanofiltration membrane on aqueous solutions of sodium carbonate were examined using laboratory apparatus.

Apparatus

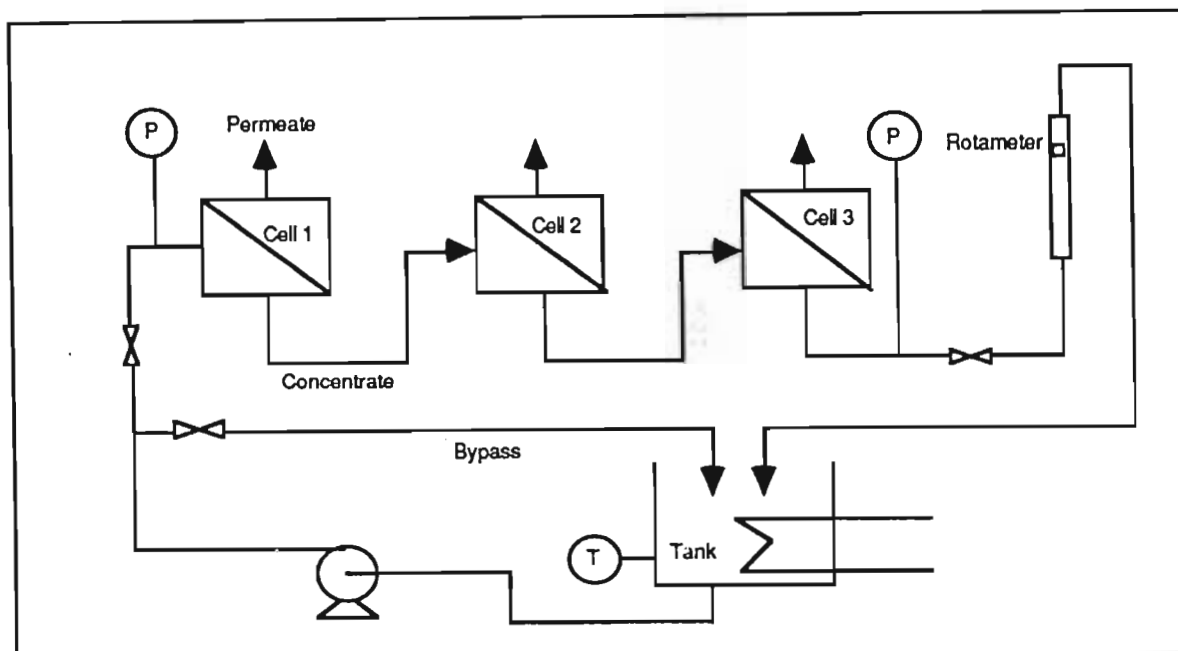
A schematic of the three-cell laboratory rig, designed to hold three flat sheets (30 mm diameter) of FilmTec NF40 membrane, is shown in Figure 6.5 (Gutman, 1987). The effective membrane area of each cell was 0,0011 m². The rig was designed to operate at an inlet pressure of 1,3 MPa, while a cooling system allowed the temperature of the circulating effluent to be maintained at 26 °C. Unless otherwise specified, the flow rate was 1 l/min, and the linear velocity was 2 m/s.

Procedure

Prior to installation in the apparatus, the membranes were conditioned by soaking in deionised water for 24 hours. Test solutions were prepared using analytical grade chemicals. During the trials, the pH of the solutions was adjusted with nitric acid as appropriate and the system was allowed to equilibrate for 0,5 hours prior to sampling. The rig was cleaned with

deionised water between each series of tests. During the runs, temperatures, pressures and flowrates were kept constant at 26 °C, 1,3 MPa and 1,010 l/min respectively, unless otherwise stated.

Figure 6.5
Schematic of Laboratory Nanofiltration Rig



Three relationships were investigated as follows.

- 1) Effect of pH and concentration on retention performance. Sodium carbonate solutions containing 1, 10 and 30 g/l Na were tested in three separate experiments over a pH range of 11,2 to 6,3 (where carbonate and bicarbonate anions co-exist). Feed and permeate samples were analysed in order to characterise the inorganic carbon species present over the range of pH, and determine membrane retention variation as a function of solution pH.
- 2) Effect of pH and concentration on flux performance. Examination of fluxes was carried out during the evaluation described in 1) above.
- 3) Effect of pH on calcium and magnesium retention. In a fourth experiment, sodium carbonate solution, containing 10 g/l Na, 10 mg/l Ca (as CaCl_2) and 10 mg/l Mg (as $\text{Mg}(\text{OH})_2$) was tested over a pH range of 11,0 to 7,0. Feed and permeate samples were analysed to determine the dependence of the retention of divalent ions on pH.

The results of the laboratory tests are presented in Section 8.1.

6.3.2. Effect of Chelating Agents on Nanofilter Performance

Using the equipment described in Section 6.3.1 above, the effect of chelating agents on the retention of calcium and magnesium in carbonate solutions was determined at a range of pH values. The test solution contained 10 g/l Na, 10 mg/l Ca (as CaCl_2) and 10 mg/l Mg (as $\text{Mg}(\text{OH})_2$), to which was added 0,1 g/l of EDTA (as tetra-sodium salt). EDTA was selected following an investigation of five chelating agents to determine the most effective one (Pollution Research Group, 1989) . The retentions of divalent ions over the pH range 11,0 to 7,0 were determined by the analysis of feed and permeate samples.

The results of the trials are presented in Section 8.2.

6.3.3 Chemical Speciation Modelling of Nanofiltration

Whereas analytical methods were used in Section 6.3.1 and 6.3.2 to determine the main components in solution during nanofiltration, it was not feasible to use these methods for determining accurately the distribution of these components among all species which exist at equilibrium. The availability of data precisely characterising and quantifying these chemical species was considered to be an invaluable input for modelling the transport of ions through the nanofiltration membrane (see Section 6.3.4) and for providing a qualitative explanation of observed membrane performance. As a result, chemical speciation modelling was carried out to precisely define the water chemistry of carbonate solutions by describing the distribution of the various physico-chemical forms of ions, or species, present in the feed and permeate streams, and predicting precisely the number, type and concentration of these species. The modelling procedures combined analytical data of the main components in solution during nanofiltration with equilibrium chemical calculations to determine the distribution of these components among species.

Speciation Program

While a number of general speciation programs are available in the field of physical chemistry, the program MINTEQA2 (Allison, Brown and Novo-Gradac, 1990), distributed by the United States Environmental Protection Agency was selected for use because of its user-friendliness. MINTEQA2 is a versatile geochemical equilibrium speciation model for predicting the behaviour of components in dilute aqueous solutions, equilibrium compositions, and mass distribution of dissolved, adsorbed and multiple solid phases under a variety of conditions. It is used primarily as an environmental tool for predicting the behaviour of pollutants in surface and ground waters.

MINTEQA2 has an extensive thermodynamic database containing over 1 500 neutral and charged chemical species. It is designed to formulate and solve multiple-component chemical equilibrium problems by simultaneous solution of nonlinear mass action expressions and linear mass balance relationships. A detailed explanation of the chemical and mathematical concepts embodied in the model and the procedures for running it are given elsewhere (Allison, Brown and Novo-Gradac, 1990). For practical purposes, MINTEQA2 is complemented by PRODEFA2, an interactive preprocessing program used for creating input files. Chemical analysis data for the components of interest are used to predict the equilibrium composition. Other relevant invariant measurements, such as pH or pe, are also input.

Procedure

Speciation modelling was based on analytical results of hypothetical solutions containing sodium carbonate. The precise nature of the species present in solutions of different strength and pH was predicted by speciation modelling. Specifically, sodium carbonate solutions containing 1, 10 and 30 g/l Na at pH values ranging from the maximum natural pH (determined by experimentation as 11,2; 11,3 and 11,5 respectively) to around 7,0, adjusted by addition of nitric acid, were speciated. In addition, hypothetical carbonate solutions (10 g/l Na) spiked with calcium, magnesium and EDTA, were speciated to predict the effect of chelation on the distribution of hardness ions in solution.

The speciation model was run using the following procedure:

- 1) Primary information was conveyed through the input file using PRODEFA2. This information included the total dissolved concentration of each original component of the system (reaction products are not input), which were selected from a predetermined set. System parameters, including the temperature and pH of the solution, were imposed and inorganic carbon was defined as total carbonate concentration. From the input data, PRODEFA2 automatically guessed activities for each component which were then input into MINTEQA2.
- 2) MINTEQA2 solved the equilibrium problem at fixed pH iteratively by computing mole balances from estimates of component activities. Specifically, it interpreted the input files; listed species together with log K values, enthalpy, molar mass, charge, and Debye-Huckel constants; listed calculated concentration, activities and adjusted log K values for each species; provided percentage distribution of components among each species; provided values for mass distribution, ionic strength, and pH etc at equilibrium; and listed saturation indices of all database solids with respect to the solution.

- 3) From the output of 2) above, the concentrations of hydrogen ions present at equilibrium were determined and PRODEFA2 was then rerun by allowing the pH to be computed from hydrogen ion concentrations. The concentration of nitrate ions (added to the carbonate solution as nitric acid during pH adjustment) were also specified at this stage.
- 4) The PRODEFA2 file output from 3) above was input to MINTEQA2 for recalculation of the variables described in 2) above.
- 5) For the modelling of experiments 4 and 5, where the saturation indices in the MINTEQA2 output from stage 4) above indicated that precipitation of calcium- and magnesium-containing minerals was thermodynamically possible, PRODEFA2 and MINTEQA2 were rerun by allowing precipitation to occur.

The concentrations, activities and activity coefficients for each of the components and species present in solution at equilibrium were extracted and tabulated for each of the 29 feed samples for the five experiments, to be used as input information in mass transport modelling (see Section 6.3.4).

In addition, the effect was evaluated of changing solution concentration and pH on:

- 1) The concentration of individual species, and the mass distribution of components between individual species.
- 2) Total species present, and their distribution between neutral, anionic and cationic species, as well as between monovalent and divalent ions.

Finally, the effect was determined of complexing agents on the speciation of calcium and magnesium components in a sodium carbonate solution (10 g/l Na) at varying pH, and the precipitation potential of various calcium and magnesium species.

The results of the chemical speciation study are presented in Section 8.3.

6.3.4 Transport Modelling of Nanofiltration

The purpose of this part of the study was to theoretically predict the separation ability of the nanofiltration membrane for the carbonate/bicarbonate system, over a range of different pH, concentration and operating conditions, and to compare the predicted results with experimental results from the investigations described in Section 6.3.5.

Membrane Transport Program

A membrane separation process modelling program, PREMSEP, written in Borland C++ to run under MS-Windows, was developed during the course of the current investigation (Brouckaert, Baddock and Wadley, 1994), and used interactively to interpret the speciation data. The program provides a framework in which a variety of membrane transport models could be set. It was implemented as a set of *objects* which interact with each other in a similar way to their physical counterparts (at least in the context of a membrane separation plant). These objects are primarily chemical *components*, *membranes*, *modules*, and *streams*, although these may have sub-objects which handle various aspects of their behaviour. For instance, a stream has an *intensive thermodynamic state* object and one or more *experimental data set* objects associated with it. The idea is that, when considering membrane transport modelling code, one should be able to focus on how the membrane interacts with a stream and its components, without being concerned with other aspects such as the module geometry or how to obtain model parameters from experimental data by regression.

The membrane transport model is based on the extended Nernst-Planck diffusion equation, which calculates an electrical potential gradient that imposes electro-neutrality on the fluxes of the diffusing species. Charged membranes are modelled by including the concentration of fixed ionic groups in the electroneutrality condition. Neutral species are accommodated in the same framework.

Procedure

The PREMSEP model was developed by Brouckaert in conjunction with the nanofiltration experimentation. Specific experimental and chemical speciation data was determined as required for the program development. The program was used to extend the quantitative understanding of the nanofiltration process.

The experimentally determined feed and permeate compositions were speciated using MINTQA2 (Section 6.3.3). This data, together with the experimentally determined permeate flux, operating pressure, flowrates and temperatures (Section 6.3.5,) was used to regress for the membrane transport parameters. Water flux and gross permeate composition were predicted as a function of feed pressure. Also, water and solute fluxes (individual species) were predicted as a function of pH. This data was used to calculate concentrations of individual permeate species, which were then summed to give total component concentrations. Note that the reported permeate composition is not at equilibrium, and the permeate will respeciate.

The results of the transport modelling are presented in Section 8.5.

6.3.5 Supplementary Experimentation for Quantitative Explanation of Membrane Performance and PREMSEP Development

While the experiments described in Section 6.3.1 and 6.3.2 provided practical information on general retention and flux performance characteristics of the nanofiltration membranes, a further series of experiments (nanofiltration experiments 6 to 9) was considered necessary to obtain detailed experimental results, against which the speciation and the mass transport model (PREMSEP) could be verified and for which qualitative explanations of membrane performance, based on mass transport theory, could be provided. Four separate experiments were carried out using the flat sheet rig in accordance with the procedures described in Section 6.3.1. The initial solution in each case was prepared from analytical grade anhydrous sodium carbonate, and nitric acid was used for pH adjustment. The experiments were run at 26 °C. The conditions are summarised in Table 6.4, and are the same as those specified for the hypothetical solutions for which speciation and mass transport models were developed (as described in Sections 6.3.3 and 6.3.4 above).

Table 6.4
Summary of Experimental Conditions for Nanofiltration Modelling Experiments

Experiment No	Feed Concentration (g/l Na as Na ₂ CO ₃)	pH Range	Pressure (MPa)	Flow (ml/min)
6	1	11,0 to 6,9	1,3	1 010
7	10	11,2 to 7,2	1,3	1 010
8	30	11,5 to 7,9	1,3	1 010
9	10	9,6	variable at 0,4; 0,85 and 1,5	variable at 445; 1 010 and 1 610

While the first three experiments were used to provide data for speciation modelling, the fourth experiment provided data for evaluating the effect of pressure and flow on membrane performance and predicting the occurrence of concentration polarisation.

During each experiment, samples of the feed and permeate were collected and analysed for pH, conductivity, osmotic pressure, sodium ions, total inorganic carbon, hydroxide ions, carbonate ions and bicarbonate ions. Temperatures, flows, pressures and fluxes were also recorded.

Various correlations were developed between the experimentally observed water and solute fluxes and the operating conditions, particularly applied pressure, cross-flow velocity and

solution pH, and these were explained using a combination of transport theory and predictions of speciation.

Predicted concentrations of individual species were used to determine the osmotic pressure of the solutions by a computer model based on the method described in Section 5.4.3.3. These were compared to experimentally determined results and used to explain observed flux and retention variations under conditions of constant and changing applied pressure.

Finally, the experimental results were used to test the predictions of the transport model PERMSEP at different stages during its development (Section 8.5). They provided a full set of target data towards which the model could be iteratively modified to produce predictions that would more closely predict the practical situation.

The results of nanofiltration experiments 6 to 9 are discussed in Section 8.4.

6.4 Supplementary Investigations of Electrolysis

To supplement the main pilot-plant trials, certain laboratory investigations were carried out to examine selected practical aspects of electrolysis under controlled conditions, specifically the fouling and cleaning of the electromembrane, and the use of other electrode materials. The results of these investigations were used to assist in selecting the most suitable conditions for pilot-plant operation, explaining observations made during pilot-plant operation and selecting the design criteria for the full-scale plant. The procedures for each of these investigations are described below.

6.4.1. Electromembrane Fouling

In order to evaluate the life of the ion-selective, cation permeable electromembrane, a fouling test was undertaken under controlled conditions in the laboratory.

Apparatus

The equipment used was a small-scale replica of the electrochemical cell used in the pilot-plant trials, as illustrated in Figure 6.6 (Schoeman, 1986). It consisted of a two-cell flow-through apparatus, feed tanks, power supply and electrical instrumentation. Pumps delivered a flow of 2 l/min through each cell. The flow-through apparatus comprised two Perspex cells, fitted with neoprene gaskets, between which the electromembrane was clamped. The electromembrane used in the test was a Nafion 324 cation exchange electromembrane, conditioned before use by soaking in 10 % NaOH for 24 hours. The exposed area of the

electromembrane and the two platinum electrodes, positioned on either side of the electromembrane, was 0.001 m^2 .

Platinum probes extended into each cell, at a distance of 9,5 mm on either side of the electromembrane (Figure 6.7) and were connected to a potentiometric high impedance input chart recorder and a digital readout voltmeter, in order to measure the volt drop across the electromembrane. A DC power supply, equipped with constant current control, was used to maintain the required conditions of current density.

Figure 6.6
Schematic Diagram of Fouling Apparatus

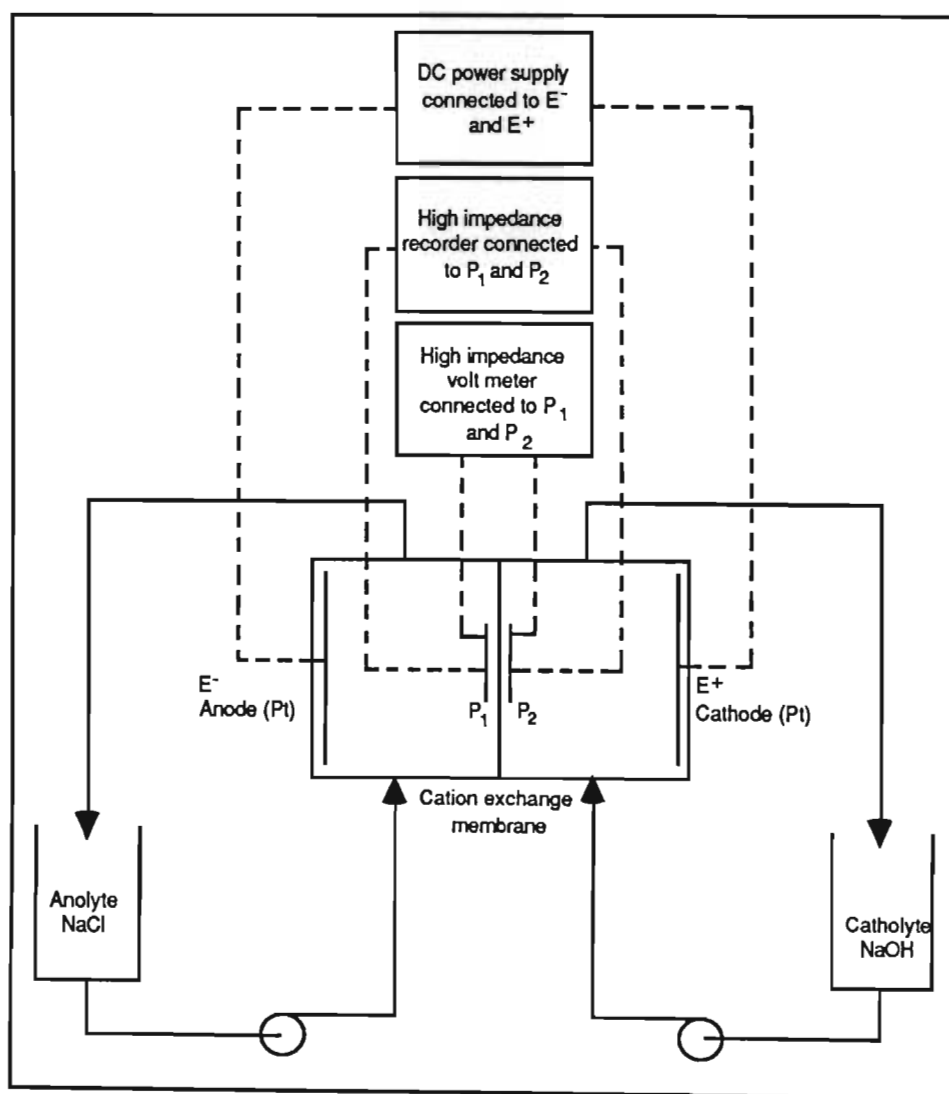
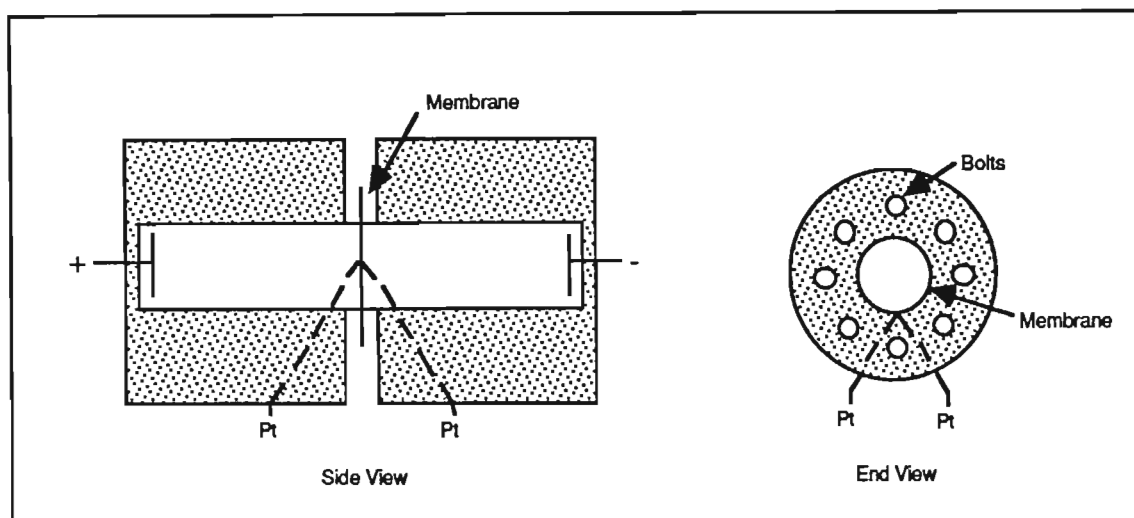


Figure 6.7
End and Side View of Flow-Through Cell Showing Position of Platinum Probes



Procedure

The experiment ran continuously over a 4 month period, during which time 160 l of pretreated effluent, divided into four 40 l batches, was electrolysed. The pretreated effluent constituted the anolyte, while the catholyte was 40 l of 10 % NaOH. The electrolytes were pumped through the respective chambers of the test cell. At the beginning of each batch run, a constant current density of 1 200 A/m² was applied, but as the electromembrane voltages increased, the current density was reduced progressively to 500 A/m². When the electromembrane volt drop at this current density became unacceptably high, the anolyte was replaced. The potential difference between the two platinum probes was monitored on both the chart recorder and the digital voltmeter. The chemical compositions and temperatures of the electrolytes were monitored throughout each experiment.

Between batches 3 and 4, the electromembrane was subjected to acid treatment to remove visible insoluble material from its surface. The cleaning electrolytes complied with the specifications given by Burney and Gantt (1983) (see Section 5.4.4.8), that the pH must be maintained below that of the electrolyte that was in contact with each side of the electromembrane during normal operation. Approximately 500 ml of 6 N nitric acid was diluted to 20 l giving an acid wash solution of pH 1.8. This constituted the anolyte. The catholyte was 5 l of deionised water. The apparatus was operated for a period of 48 hours, with samples of cleaning solutions taken after 24 and 48 hours.

The results of the fouling trials are presented in Section 9.1.

6.4.2. Electromembrane Cleaning

Laboratory tests were carried out to investigate the possibility of using nitric acid to rejuvenate the heavily-scaled electromembrane removed from the pilot-plant unit. Three cleaning techniques were examined:

- 1) Acid soaking in a stirred container;
- 2) Electrolysis using acidic electrolytes;
- 3) A combination of acid soaking followed by electrolysis.

The development of an effective and efficient method for restoring electromembrane performance is critical in ensuring long electromembrane life, a necessary criteria for the economic viability of the process.

Apparatus

The tests were conducted batchwise in a small electrochemical cell (Figure 6.8), consisting of two compartments, each capable of holding 860 ml, separated by a sheet of fouled Nafion 324 electromembrane with an exposed area of 0,0081 m². The electrodes, positioned 23 mm apart on either side of the electromembrane, were constructed from expanded platinised titanium mesh. Overhead stirrers were used to agitate the electrolytes. A DC power supply, delivering a maximum of 3 A and 60 V, and connected to a digital read out voltmeter, was used to provide the desired current.

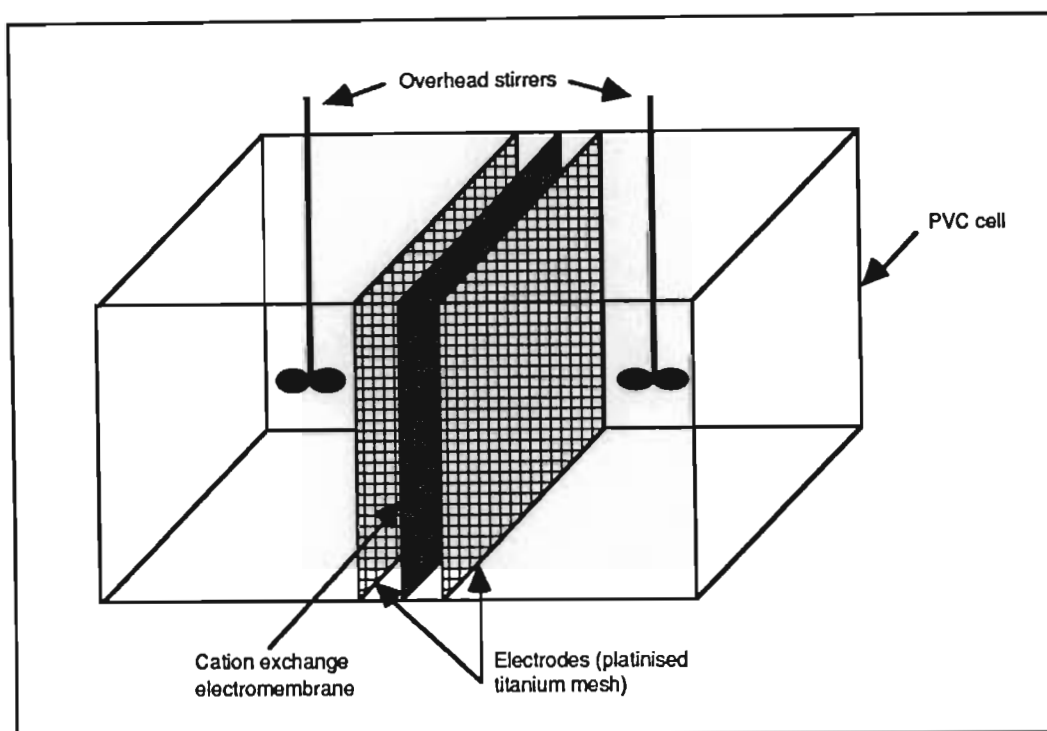
Procedure

The tests were preceded by the qualitative identification of the visible white crust, which formed on the electromembrane surface during the pilot-plant trials as a result of water polarisation and back migration of carbonate, bicarbonate and hydroxide ions. Portions of the electromembrane were cut to fit the laboratory apparatus. The success of the cleaning procedure was evaluated by monitoring the performance of the electromembrane during electrolysis of sodium bicarbonate and sodium hydroxide solutions, both before and after cleaning.

During descaling by the acid-soaking procedure, the electromembrane was immersed in a beaker containing a solution of nitric acid, which was agitated by means of a magnetic stirrer. Aliquots of nitric acid were removed from the beaker for analysis of calcium and magnesium. During electrolytic descaling, the electromembrane portion was mounted in the laboratory cell, and the two electrolyte compartments were charged with nitric acid. A constant current

was then passed between the electrodes for a certain period of time, during which aliquots of the electrolytes were removed and analysed to determine the concentration of calcium and magnesium.

Figure 6.8
Schematic of Laboratory Apparatus for Electromembrane Cleaning



In order to evaluate the performance of the electromembrane, it was mounted in the cell, and the compartments were each charged with 800 ml of electrolyte. The anolyte was a solution of sodium bicarbonate (50 g/l) and the catholyte was sodium hydroxide (100 g/l). The cell was operated at a constant current density of 310 A/m^2 for five to eight hours, during which time aliquots were removed and analysed for sodium, bicarbonate, carbonate and hydroxide ions. The volt drop between the electrodes, system temperatures and volumes of the electrolytes were also monitored.

The experimental parameters for four sets of experiments is summarised in Table 6.5. The results of the cleaning tests are presented in Section 9.2.

Table 6.5
Summary of Experimental Procedure for Electromembrane Cleaning

Experiment	Description	Electrolyte/Solution	Current Density (A/m ²)	Duration (h-min)	Faradays (F)
1.1*	reference run - scaled membrane	anolyte 50 g/l NaHCO ₃ catholyte 100 g/l NaOH	310	5-15	0,49
1.2	reference run - virgin membrane	anolyte 60 g/l Na ₂ CO ₃ catholyte 100 g/l NaOH	390	9-45	0,92
2.1	acid electrolysis	anolyte HNO ₃ pH 1,5 (2 batches) catholyte HNO ₃ pH 1,5	62 240	21-00 20-00	0,39 1,49
2.2	performance test	anolyte 50 g/l NaHCO ₃ catholyte 100 g/l NaOH	310	5-40	0,53
2.3*	acid electrolysis	anolyte HNO ₃ pH 1,8 catholyte HNO ₃ pH 1,8	50	8-35	0,13
2.4	performance test	anolyte 50 g/l NaHCO ₃ catholyte 100 g/l NaOH	285	6-00	0,51
3.1*	acid soak	2 000 ml HNO ₃ pH 1,5	-	72-00	-
3.2	performance test	anolyte 50 g/l NaHCO ₃ catholyte 100 g/l NaOH	310	6-20	0,62
3.3*	acid soak	HNO ₃ pH 0,5	-	72-00	-
3.4	performance test	anolyte 50 g/l NaHCO ₃ catholyte 100 g/l NaOH	310	5-35	0,52
3.5*	acid soak	600 ml HNO ₃ pH 1,3	-	47-05	-
4.1	acid electrolysis on acid-soaked electromembrane	anolyte HNO ₃ pH 2 catholyte HNO ₃ pH 2	62	16-00	0,30
4.2	performance test	anolyte 50 g/l NaHCO ₃ catholyte 100 g/l NaOH	310	7-45	0,54
4.3	acid electrolysis	anolyte HNO ₃ pH 1 catholyte HNO ₃ pH 1	62	6-45	0,13
4.4	performance test	anolyte 50 g/l NaHCO ₃ catholyte 100 g/l NaOH	310	6-00	0,56

Note that * denotes each case in which a 'new' section of scaled electromembrane was used.

6.4.3. Other Electrodes

Under normal circumstances, dissolution of the precious metal oxide, with the accumulation of nonconducting oxides in the interfacial layer between the titanium base metal and the coating, was found to be minimal for the dimensionally stable anodes (DSA), and a long anode life was predicted. However, the costs of recoating, even infrequently, are high and it was considered appropriate to evaluate possible other anode materials.

During the pilot-plant trials, the substitution of coated anodes by stainless steel was investigated (experiment 17). In addition, nickel anodes were evaluated both on pilot-plant scale (experiments 19, 20 and 21) and in the laboratory. The laboratory experiments were specifically designed to allow the corrosion rate of the nickel anode to be correlated with the anolyte pH.

Pilot-Plant Procedure

At the end of experiment 17, the manifold system of the cell was rearranged to allow use of one cell only. This cell was fitted with two stainless steel electrodes. Electrolysis was carried out using a solution of sodium bicarbonate (50 g/l) as anolyte, while physical and analytical measurements were taken in a manner similar to those described for the other pilot-plant trials. The experiment was discontinued after 1,75 hours because of visible corrosion of the anode.

For the latter part of experiment 19, and for experiments 20 and 21, electrolysis was carried out using a nickel anode. In total, the cell was operated for over 30 hours before tests were discontinued because of anode corrosion. The pH of the anolyte was observed to range from approximately 9 to 6.

Laboratory Apparatus

The two-cell flow-through apparatus described in Section 6.4.1 and shown in Figures 6.6 and 6.7 was used. The platinum anode was replaced by a nickel anode, while the cathode material was platinum.

Laboratory Procedure

The anolyte constituted 5 l of a solution of sodium bicarbonate (50 g/l) and sodium carbonate (20 g/l), while an equivalent volume of sodium hydroxide (100 g/l) was used as the catholyte. A constant current, ranging from 1 000 to 2 000 A/m² was applied for a period of almost 100 hours, during which time intermittent measurements were taken for temperature, electromembrane volt drop, cell volt drop, anode mass, and pH. In addition, aliquots of samples were collected for analysis and the anode was visually inspected. From the experimental data, it was possible to correlate the loss in the mass of the anode with the pH of the solution to determine whether there was a potential-pH zone of operation in which the nickel would exhibit immunity to corrosion.

The results of the evaluation of other electrode materials are presented in Section 9.3.

SECTION 7

RESULTS AND DISCUSSION OF PILOT PLANT TRIALS

This section presents and discusses the results of the pilot plant investigations aimed at evaluating the technical and economic performance of the treatment sequence and examining the inter-dependence of the most important process variables. The apparatus and procedures relating to these investigations are presented in Sections 6.1 and 6.2, while the theory is discussed in Section 5.

Appendix 6 is a record of all results, data manipulations and calculations for the pilot plant trials, and includes:

- 1) 92 tables of analytical and physical data relating to each of the four stages of the treatment sequence for each of experiments 1 to 19;
- 2) 56 tables of calculations of current efficiencies for changes in concentration of sodium in the catholyte and anolyte, hydroxide in the catholyte, inorganic carbon in the anolyte, and inorganic carbon and hydroxides in the absorption column feed for all electrolysis stages of experiments 1 to 19;
- 3) Polarisation data for experiment 18B;
- 4) Data relating to monitoring of the condition of the anode (DSA).

The discussion below does not relate to experiments 17B, 19B, 20 or 21, which aimed to evaluate the performance of other anode materials. The results of these evaluations are discussed in Section 9.3.

The current discussion is subdivided as follows. Section 7.1 examines, in general terms, the effect of each stage of the treatment sequence on the characteristics of scouring effluent. Sections 7.2, 7.3 and 7.4 examine the performance of the neutralisation, cross-flow microfiltration and nanofiltration pretreatment operations separately and respectively. The discussion on the performance of the electrochemical recovery unit is presented in Section 7.5 and examines current efficiencies, power consumption, interdependence of operational variables (such as temperature, flow, electrolyte concentrations, current density and applied potential), anode and electromembrane performance, recovery of sodium salts, water transport, and background concentration closed-loop rinse recycle.

7.1. Effect of Treatment Sequence on Scouring Effluent

The intermediate and final characteristics of the treated effluent and the recovered sodium hydroxide are presented in Table 7.1. The scouring effluent contained 8 g/l of sodium, present mainly as sodium hydroxide and carbonate and was contaminated by organic compounds (8 g/l COD) and calcium and magnesium compounds (10 to 60 mg/l in total). The treatment sequence was designed to remove colour and impurities and to recover sodium hydroxide from the effluent. The pretreatment stages neutralised the effluent and removed approximately 95 % of the COD, all the colour, 80 % of the organic impurities (as TOC), 90 % of the calcium compounds, and 85 % of the magnesium compounds.

In the final stage, the sodium hydroxide was recovered as a pure solution at a concentration between 100 and 200 g/l. This stream was suitable for reuse in the scouring saturator. The depleted effluent contained low concentrations of dissolved solids, and was suitable for reuse in the scouring rinse range.

The cross-flow microfiltration and nanofiltration stages produced two retentates, each containing 50 to 60 g/l total solids, and together comprising 10 to 20 % of the volume of the total effluent treated.

Table 7.1
Average Composition of Scouring Effluent After Each Stage of the Treatment Sequence

Determinand	Units	Scouring Effluent	Effluent After Neutralisation	Effluent After Cross-Flow Microfiltration	Effluent After Nanofiltration	Brine After Electrolysis	Recovered NaOH
pH		13,5	8,6	8,4	9,0	5,2	14,0
Conductivity	mS/cm	6 400	2 400	2 500	2 300	200	
TS	g/l	22,0	22,0	20,0	-	0,5	
TC	g/l	4,0	7,9	7,6	5,9	0,4	
TIC	g/l	0,3	4,3	4,6	5,2	0	
TOC	g/l	3,7	3,6	3,0	0,7	0,4	
COD	g/l	8,3	8,3	5,3	0,5	0,5	
NaOH	g/l	10,0	0	0	0	0	170,0
CO ₃	g/l	2,6	1,9	2,0	3,4	0	1,5
HCO ₃	g/l	0	16,1	16,5	11,5	0	0
Na	g/l	8,4	8,2	8,8	7,2	0,3	97,0
Ca	mg/l	45,0	45,0	3	2	2	
Mg	mg/l	7,0	5,0	2	1	1	

TS total solids; TC total carbon; TIC total inorganic carbon; TOC total organic carbon; COD chemical oxygen demand

7.2. Neutralisation

The inorganic carbon balance across the system (between the electrochemical cell and the absorption column, obtained from the raw data in Appendix 6) indicated that carbon dioxide absorption was complete, with no gas loss in the absorbant pH range 8,0 to 14,0. Most efficient recovery of sodium salts in the nanofiltration stage was achieved when the pH of the

effluent was lowered to between 8,0 and 8,5 during neutralisation (see Appendix 6). In this pH range, the predominant inorganic carbon species was the bicarbonate ion (see Figure 5.3). The neutralisation process also resulted in the formation of a fine suspension of insoluble organic compounds, believed to be waxes, pectins and other similar cotton extracts (See Section 2.5.2).

7.3. Cross-Flow Microfiltration

Cross-flow microfiltration removed the suspended, particulate and colloidal matter from the neutralised effluent, producing a clear, but coloured, product. This matter included saponified waxes and pectins, lint and other insoluble contaminants. Point retentions are summarised in Table 7.2. Variable results are explained by changes in effluent compositions and microfiltration feed, varying operation of the microfilter unit which affected retention and sampling analytical error. During the pilot-plant study, the total reduction in contamination averaged 40 % for COD, 10 % for total solids and over 50 % for calcium compounds. Although performance varied with operating conditions and procedure, optimum performance was obtained when the cross-flow microfiltration unit was operated at an inlet pressure of 300 kPa, with a feed velocity of 3,0 to 3,5 m/s, and using a limestone (15 µm) precoat, applied before exposure of the tube surface to the effluent at a coverage of 100 g/m². Under these conditions, calcium retentions were above 90 %, while fluxes averaged 50 l/m²h at 20 °C. Flux and retention performances were poor under non-ideal conditions. For example, at feed velocities below 2 m/s and pressures below 150 kPa, fluxes dropped to 5 l/m²h; while with a poorly applied precoat, retentions of calcium and magnesium averaged 35 to 55 %.

The most effective cleaning solution for the removal of waxy deposits on the surface of the cross-flow microfiltration fabric was a solution containing 20 g/l sodium hydroxide and 1 g/l scouring detergent, which was recirculated through the tube for 2 to 3 hours.

Up to 90 % of the initial feed volume was recovered as filtrate. It was not possible to achieve higher recoveries because the pipework of the system limited retentate volumes to a minimum of 10 litres. Because of outdoor operation and prevailing climatic conditions, up to 25 % of the volume of the permeate was lost during each run as a result of evaporation as it passed through the tubes.

Table 7.2
Point Retentions for Cross-Flow Microfiltration (%)

Experiment	TOC	TIC	COD	Na	Ca	Mg	Total CO ₂	TS
1	72	0	35	3	48	0	10	35
2	33	14	39	0	12	0	2	13
3	25	25	36	2	28	0	25	7
4	100	0	91	0	0	-	15	62
5	67	0	90	0	54	0	16	14
6	-	-	-	-	-	-	-	45
7	25	30	70	2	26	62	3	15
8	28	25	65	4	64	38	15	27
9	65	28	58	15	77	50	17	28
10	50	4	-	1	54	40	5	-
11	20	20	35	12	50	15	18	18
12	12	10	63	0	65	29	5	17
13	71	31	-	6	86	78	21	26
14	83	3	-	25	81	63	34	32
15	78	2	-	5	68	52	5	28
16	67	25	95	26	62	50	30	40
17	78	2	-	0	70	82	13	30
18	-	-	-	7	70	10	0	4
19	-	-	-	7	50	20	15	10
Average	55	14	61	6	54	35	15	25

TIC total inorganic carbon; TOC total organic carbon; COD chemical oxygen demand; TS total solids

7.4. Nanofiltration

Appendix 6 contains the experimental data. Control of the pH of the feed to the nanofilter was important to ensure that the sodium present was predominantly associated with the monovalent bicarbonate species. In the form of sodium bicarbonate, the sodium could permeate the membrane and be separated from the effluent contaminants. Since, in the pH range 8 to 8,5, a significant portion of the ions in the feed were monovalent, and readily permeated through the membrane, there was a minimal osmotic pressure differential across the membrane and consequently a high flux could be obtained at a low pressure. Because of the pH dependence of the bicarbonate/carbonate ion equilibrium, feed pH was the most important factor affecting flux through the membrane. For example, at ambient temperature (25 °C) and at an inlet pressure of 1 MPa, average fluxes varied from 5 l/m²h at pH 9,7 to 30 l/m²h at pH 8,0. Marginal flux decline occurred during each individual experiment at high permeate recoveries. Membrane fluxes dropped after experiment 4, in which the retentate at 93 % permeate recovery contained particulate matter, causing irreversible physical blockage of the flow passages in the membrane structure.

Nitric acid was used to control the pH of the feed within the range of 8 to 8,5. This was necessary, since the disproportionate removal of bicarbonate ions from the feed, relative to carbonate ions, caused an increase in the ratio of carbonate and bicarbonate ions remaining, and thereby a progressive increase in feed pH.

Point retentions during nanofiltration are summarised in Table 7.3 for experiments 1 to 19. The total reduction in effluent contaminants during nanofiltration averaged 90 % for COD and 50 to 70 % for calcium and magnesium compounds. Sodium point retentions were 20 to 30 %, although it was possible to recover up to 90 % of the sodium in the feed. In addition, all residual colour was removed. Supplementary investigations (see Section 8.1) indicate that retentions of free ionic species decrease with increasing concentration as a result of increased charge shielding of the membrane surface by counter-ions. During the pilot-plant trials, retentions of sodium and inorganic carbon species followed this trend. However, retentions of organic compounds, calcium and magnesium increased at high permeate recoveries. This phenomena is expected for organic compounds, which are retained on a size exclusion basis, since concentration increases the portion of non-permeable species in the feed. The fact that calcium and magnesium followed the same trend as the organic compounds suggests that they are present mostly in a chelated form.

Table 7.3
Point Retentions for Nanofiltration (%)

Experiment	TOC	TIC	COD	Na	Ca	Mg	Total CO ₂	TS
1	85	-	96	60	92	95	55	68
2	0	65	91	32	75	44	20	40
3	70	72	91	42	91	72	25	53
4	-	33	77	24	64	42	18	31
5	85	25	83	25	72	48	30	44
6	74	45	85	39	55	58	29	49
7	67	18	90	29	72	63	24	41
8	70	30	87	35	63	70	32	50
9	70	47	82	20	61	46	20	29
10	98	0	99	11	80	85	7	40
11	48	23	85	30	-	64	35	45
12	50	40	72	42	-	60	40	44
13	92	15	-	23	78	68	25	38
14	15	61	-	23	42	48	15	32
15	40	10	-	26	60	53	23	31
16	73	42	91	40	74	53	43	30
17	-	-	-	-	-	-	-	-
18	-	-	-	12	40	32	28	4
19	-	-	-	13	66	68	6	15
Average	62	35	94	29	70	61	28	38

TIC total inorganic carbon; TOC total organic carbon; COD chemical oxygen demand; TS total solids

Nanofiltration was carried out to permeate recoveries in excess of 90 %. Recovery was limited by the requirements of a minimum liquid level in the feed tank. If it had been physically possible to achieve higher permeate recoveries, a greater portion of the sodium would have been recovered.

Membrane cleaning was most effectively achieved using scouring detergent (Kieralon) and circulating this through the module for 2 to 3 hours.

The nanofiltration component of the pilot trials achieved three purposes:

- 1) It provided a mechanism to pretreat and soften the scour effluent to a quality suitable for subsequent trials to evaluate the recovery of sodium hydroxide by electrolysis.
- 2) It allowed the practical aspects of the technology to be assessed for the purpose of removing organic and inorganic impurities from sodium carbonate/bicarbonate solutions.
- 3) It provided technical information which could be used in the design and operation of a full-scale treatment and recovery plant.

However, the pilot nanofiltration trials were not designed to provide information on the detailed mechanism of the chemical transport process and the precise effects of operating variables on membrane performance. Thus, the results of these trials should be viewed in combination with those from the supplementary investigations relating to the nanofiltration of sodium carbonate solutions (Section 8), in which controlled laboratory experiments aimed to examine the precise effects of solution chemistry and operating parameters on membrane performance.

7.5. Electrochemical Recovery

The pilot-plant electrochemical recovery stage, being the heart of the process, was designed specifically to provide a detailed analysis of all variables affecting the operation and performance of the cell and to define the dependencies of membrane and electrode performance on these variables. Because of the original nature of the work on the electrolysis of pretreated scouring effluents and low concentration carbonate solutions in the presence of high levels of impurities, this information could not be deduced from outside sources, but was considered critical to the evaluation of the technical and economic viability of the overall process. As with nanofiltration, some aspects of the evaluation, including electromembrane fouling, were considered more appropriately carried out under controlled laboratory conditions. Thus, the results of the pilot-scale tests should be viewed in combination with the results of the laboratory experiments discussed in Section 9.

7.5.1. Current Efficiency

The current efficiency (η) for sodium hydroxide recovery determines the plant size and operational costs. The current efficiencies for all the experiments are summarised in Table 7.4.

Table 7.4
Summary of Electrolysis Results

Experiment	Anolyte	Initial Anolyte g/l Na	Final Anolyte g/l Na	Initial Catholyte g/l NaOH	Final Catholyte g/l NaOH	Initial CD at 9V A/m ²	Initial Temp. °C	Total Faradays	η % for Na	η % for OH	η % for CO ₂
1 carb.	Na ₂ CO ₃	31	2	85	130	1 680	28	16	80	80	77
1A	nanofiltrate	2	0,3	118	113	300	21	1,0	80	0	80
1B	nanofiltrate	2	0,3	122	113	300	26	1,3	65	100	63
2 carb.	Na ₂ CO ₃	45	3	55	113	1 380	18	51	90	50	84
2A	nanofiltrate	6	0,7	85	103	-	-	3,8	64	76	80
2B	nanofiltrate	6	0,7	92	103	-	-	3,0	55	100	63
3 carb.	Na ₂ CO ₃	45	6	85	240	-	-	50	86	80	60
3A	nanofiltrate	12	0,6	121	136	680	24	7,2	90	65	85
3B	nanofiltrate	12	2	131	139	650	15	6,6	88	65	96
4 carb.	Na ₂ CO ₃ +NaHCO ₃	30	5	122	188	1 220	18	36	78	63	68
4A	nanofiltrate	7	0,3	89	124	695	15	7,8	58	55	56
4B	nanofiltrate	7	0,3	108	129	418	20	8,1	53	40	51
4C	nanofiltrate	7	0,3	107	120	440	22	6,5	68	20	68
5 carb.	Na ₂ CO ₃ +NaHCO ₃	32	11	92	148	870	16	36	65	50	55
5A	nanofiltrate	5	0,3	99	120	616	19	4,6	69	60	57
5B	nanofiltrate	4	0,3	90	110	488	16	3,8	50	100	61
5C	nanofiltrate	6	0,3	87	98	474	21	2,8	82	50	52
6 carb.	Na ₂ CO ₃ +NaHCO ₃	29	13	106	137	1 400	22	32	58	60	84
7 carb.	Na ₂ CO ₃ +NaHCO ₃	29	5	50	153	1 168	26	41	66	53	58
7A	nanofiltrate	5	0,4	162	181	854	23	5,3	51	60	49
7B	nanofiltrate	6	0,5	151	166	655	23	4,6	68	68	61
7C	nanofiltrate	7	1	111	109	657	23	4,9	67	-	58
8 carb.	Na ₂ CO ₃	27	16	94	122	1 100	22	23	64	60	36
8A	nanofiltrate	8	3	160	177	920	22	8,1	52	-	50
8B	nanofiltrate	5	0,2	148	155	652	19	5,1	51	-	44
8C	nanofiltrate	5	0,4	110	124	620	18	6,9	50	-	47
9 carb.	Na ₂ CO ₃	28	18	104	137	925	22	25	50	42	40
9A	nanofiltrate	8	0,5	172	177	720	25	8,3	53	25	50
9B	nanofiltrate	6	0,3	126	141	662	18	7,4	41	50	41
10 carb.	Na ₂ CO ₃	28	9	87	143	-	-	34	66	41	-
10A	nanofiltrate	8	0,2	167	184	795	26	8,9	43	72	45
10B	nanofiltrate	8	0,3	143	148	670	21	8,0	50	42	50
11 carb.	Na ₂ CO ₃	30	7	104	165	1 000	20	45	62	40	50
11A	nanofiltrate	7	0,3	148	169	620	16	10	58	80	50
11B	nanofiltrate	7	1	153	161	620	19	11	42	48	42
11C	nanofiltrate	7	0,1	111	131	620	19	9,4	59	20	49
12A	nanofiltrate	7	1	113	123	600	20	12	40	40	38
12B	nanofiltrate	6	2	113	113	600	19	9,1	43	-	50
13 carb.	Na ₂ CO ₃ +NaHCO ₃	31	13	104	132	900	18	33	75	50	75
13A	nanofiltrate	5	0,4	111	118	-	20	7,0	46	55	40
13B	nanofiltrate	8	0,4	98	106	620	23	9,7	48	-	50
13C	nanofiltrate	8	0,7	100	105	750	22	11	55	-	42
14A	nanofiltrate	4	0,7	108	111	520	24	6,9	55	-	40
14B	nanofiltrate	5	0,4	96	103	620	26	7,0	43	-	34
14C	nanofiltrate	6	1	87	102	555	22	7,6	55	60	45
15 carb.	Na ₂ CO ₃	18	0,4	88	117	1 000	23	23	48	44	47
15A	nanofiltrate	5	0,8	87	103	-	25	5,8	63	62	50
15B	nanofiltrate	5	0,8	70	78	420	25	5,5	53	70	51
15C	nanofiltrate	5	0,7	78	97	-	22	4,3	54	-	43
16A	nanofiltrate	4	0,9	90	95	260	24	4,1	50	57	55
16B	nanofiltrate	5	1	65	84	-	23	4,4	53	80	58
17 carb.	Na ₂ CO ₃	21	2	91	112	780	21	17	50	43	48
18 carb.	Na ₂ CO ₃	25	0,6	69	80	720	26	37	50	50	50
18A	nanofiltrate	41	26	62	leak	1 045	23	46	55	-	60
18B	nanofiltrate	48	9	94	98	900	19	41	70	50	70
19A	nanofiltrate	39	19	56	40	600	25	30	66	45	77

Current efficiencies may be calculated from changes in the concentration of cations and anions in the anolyte, catholyte and absorption column during electrolysis (see Section 5.4.4.6). In theory, current efficiencies calculated by each method should be equivalent, although they vary in practice as a result of sampling and analytical error. For example, changes of sodium content of the anolyte (as opposed to sodium content of catholyte) has been selected as a more accurate indication of sodium transport current efficiencies, since range limitations of atomic absorption required that catholyte samples be

diluted up to 1 000 times prior to analysis. In such cases, small inaccuracies are magnified and yield analytical deviations greater than the actual change in concentration being observed.

Current efficiencies ranged from approximately 40 to 90 % and averaged 60 %. Since the trials were of an investigative nature, the electrochemical cell was frequently operated under non-ideal conditions. Operated under carefully selected and controlled conditions, it is suggested that, as a conservative estimate, current efficiencies would be 70 to 80 %. Current efficiency is closely related to specific power consumption (see Section 7.5.2).

Section 5.4.4.6 examines the theoretical aspects of current efficiencies and inefficiencies. Inefficiencies result primarily from the passage of current through the electromembrane by cations other than sodium (mostly hydrogen) and from the migration of anions, in particular hydroxide ions, through the electromembrane from an area of high concentration to one of low concentration. The operating parameters affecting cell performance, including current efficiencies, are discussed in the Sections below with reference to the pilot-plant results.

7.5.2. Power Consumption and Cost

Table 7.5 summarises the power consumption and costs (1988) for the production of sodium hydroxide for each experiment. The specific power consumption varied from below 4 000 to above 10 000 kWh/tonne of 100 % NaOH, and averaged 6 897 kWh/tonne. In five of the 56 electrolysis experiments, specific power consumption exceeded 10 000 kWh/tonne. Since many of the trials were conducted under non-ideal conditions (with phenomena such as concentration polarisation, and nonuniform flow and current distribution being a common occurrence), it is anticipated that, under controlled operation, average specific power consumption may be reduced to as low as 3 500 to 4 000 kWh/tonne of 100 % NaOH.

The power costs were calculated assuming an electrical energy cost of R0,05/kWh and averaged R345/tonne of 100 % NaOH for the cell stack. Power costs are proportional to voltages, which were up to 60 % lower in the first cell than in the second cell as a result of insufficient anolyte flow (see Section 7.5.3). If it is assumed that sodium hydroxide production was similar for both cells, then the average power costs were R230 and R460 per tonne of 100 % NaOH for the first and second cells respectively.

In order to minimise power consumption in commercial plants, the following recommendations are made:

Table 7.5
Summary of Power Consumptions and Costs for Sodium Hydroxide Recovery

Experiment	Amp-h	Average Voltage ¹ V	Total Power Consumption kWh	Recovered NaOH moles	Recovered NaOH kg	Specific Power Consumption kWh/tonne 100 % NaOH	Power Cost R/tonne 100 % NaOH ²
1 carb.	421	9,7	4,08	25,5	1,02	4 000	200
1A	27	18,0	0,49	1,7	0,07	7 000	350
1B	35	16,0	0,56	2,0	0,08	7 000	350
2 carb.	1 378	10,1	13,90	93,3	3,73	3 727	186
2A	102	12,7	1,30	4,9	0,20	6 500	325
2B	80	13,0	1,04	4,4	0,18	5 778	289
3 carb.	1 343	10,0	13,40	87,4	3,50	3 829	191
3A	193	13,0	2,51	12,9	0,52	4 827	241
3B	177	13,0	2,30	11,6	0,46	5 000	250
4 carb.	957	10,7	10,20	55,4	2,22	4 595	230
4A	209	12,9	2,70	9,0	0,36	7 500	375
4B	225	12,3	2,77	9,0	0,36	7 694	385
4C	174	12,6	2,19	8,8	0,35	6 257	313
5 carb.	973	11,6	11,30	47,5	1,90	5 947	297
5A	123	13,9	1,71	6,3	0,25	6 840	342
5B	102	12,5	1,28	3,6	0,14	9 143	457
5C	78	12,0	0,94	4,8	0,19	4 947	247
6 carb.	852	11,0	9,37	29,3	1,17	8 009	400
7 carb.	1 085	11,5	12,50	53,8	2,15	5 814	291
7A	142	13,9	1,97	5,4	0,22	8 955	448
7B	123	14,0	1,72	6,2	0,25	6 615	331
7C	131	13,7	1,79	6,5	0,26	6 885	344
8 carb.	619	11,1	6,87	29,4	1,18	5 822	291
8A	217	13,3	2,89	9,3	0,37	7 811	391
8B	137	13,7	1,88	5,6	0,22	8 545	427
8C	185	13,9	2,57	6,9	0,28	9 179	459
9 carb.	673	12,6	8,55	26,0	1,04	8 221	411
9A	222	13,9	3,09	9,6	0,38	8 132	407
9B	198	14,5	2,87	9,3	0,37	7 757	389
10 carb.	900	14,4	13,00	44,1	1,76	7 386	369
10A	239	13,5	3,22	14,1	0,56	5 750	289
10B	214	14,7	3,15	8,1	0,32	9 844	492
11 carb.	1 198	12,1	14,50	55,8	2,23	6 502	325
11A	271	13,4	3,63	10,6	0,42	8 642	432
11B	289	13,5	3,90	9,0	0,36	10 833	542
11C	252	13,6	3,43	11,1	0,44	7 795	390
12A	308	13,6	4,19	10,7	0,43	9 744	487
12B	244	13,7	3,34	7,8	0,31	10 774	539
13 carb.	874	12,4	10,80	43,6	1,74	6 207	310
13A	188	13,6	2,56	6,4	0,26	9 846	492
13B	260	13,5	3,51	9,3	0,37	9 486	474
13C	281	12,1	3,40	9,4	0,38	8 947	447
14A	185	13,0	2,41	9,6	0,38	6 342	317
14B	188	14,1	2,65	6,0	0,24	11 042	552
14C	204	13,7	2,79	9,4	0,38	7 342	367
15 carb.	608	17,0	10,30	23,4	0,94	10 957	548
15A	155	14,2	2,20	6,1	0,24	9 167	458
15B	147	13,2	1,94	5,8	0,23	8 435	422
15C	107	12,0	1,28	4,1	0,16	8 000	400
16A	110	13,8	1,52	4,2	0,17	8 941	447
16B	118	13,6	1,60	4,7	0,19	8 421	421
17 carb.	442	15,4	6,81	17,1	0,68	10 015	500
18 carb.	981	12,0	11,80	37,7	1,51	7 814	391
18A	1 225	8,7	10,70	42,0	1,68	6 369	318
18B	1 088	11,4	12,40	52,4	2,10	5 905	295
19A	793	12,9	10,20	40,0	1,60	6 375	319

Note 1 obtained by averaging the overall cell stack voltage
2 based on an electrical power cost of R0,05/kWh

- 1) The electrochemical unit should operate at higher temperatures. In the pilot-plant trials, initial electrolyte temperatures were 15 to 25 °C, and these were allowed to increase to a maximum of 60 °C during electrolysis. A commercial plant, constructed from suitable materials, would incorporate heat exchangers which would supplement heat generated during electrolysis to facilitate operation at 80 to 90 °C. It is anticipated that total power consumption for sodium hydroxide production would be decreased by up to 35 % if the

average operating temperature was increased from 40 to 80 °C (see Section 7.5.6). It is estimated this would equate to a power consumption as low as 2 600 kWh/tonne of 100 % NaOH (R150) for the first cell.

- 2) Flow and current should be uniformly distributed and maintained at levels which minimise concentration polarisation (see Sections 7.5.3 and 7.5.4).

7.5.3. Flow Distribution

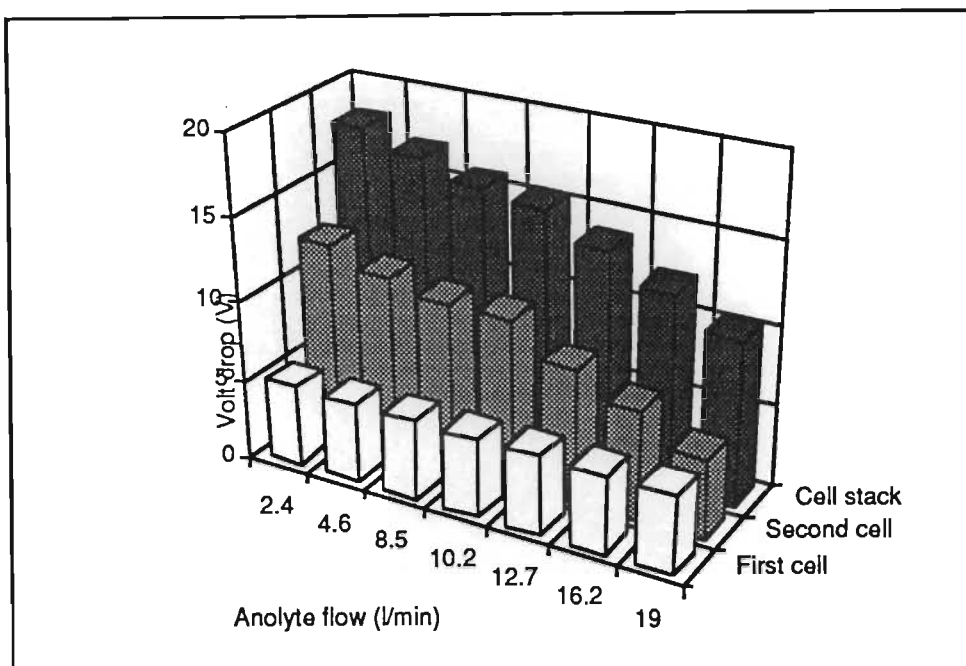
Sufficient and uniform flow inhibits gas blinding and increases the supply of sodium ions to the electromembrane surface, thereby minimising concentration polarisation. Both gas blinding and concentration polarisation reduce current efficiencies (and increase power requirements), and the occurrence of these phenomena may be inferred from voltage measurements. During experiment 12A, the variations in voltage with increasing anolyte and catholyte flows were monitored at current densities of both 600 and 1 000 A/m². The main observations are as follows:

- 1) The flow of anolyte was the principal factor affecting volt drop. Figure 7.1 shows the experimentally determined relationship between anolyte flow (at constant catholyte flow of 15 l/min) and volt drop across each cell, assembled in a series flow configuration, and the cell stack for measurements at 1 000 A/m². Data at 600 A/m² produced parallel plots, but at lower volt drops. The increase in observed volt drop across the cell stack at low anolyte flows was almost entirely a result of an equivalent increase across the second cell. The volt drop across the first cell remained constant throughout the entire flow range. For the pilot plant, anolyte flow had to be maintained above 20 l/min to minimise the volt drop in the second cell, thereby increasing current efficiencies and reducing specific power consumption.
- 2) Variation in catholyte flow (at constant anolyte flow of 2 l/min) had minimal effect on cell or cell stack voltage.

During pilot plant trials where both cells were used and assembled in series flow configuration (experiments 1 to 16), anolyte and catholyte flows were, for the most, maintained at 13,5 and 15,3 l/min respectively. Data in Figure 7.1 suggests that, at these flows, volt drops across the second cell were significantly higher than the possible minimum value, resulting in comparatively high observed power consumption and low current efficiencies.

Figure 7.1
Relationship Between Anolyte Flow Rate and Volt Drop

Conditions: catholyte flow constant at 15 l/min, CD 1 000 A/m², temperature 35 °C



7.5.4. Limiting Current Densities

The combination of the limiting current density and current efficiency determines the electromembrane area requirements for a particular duty. Current density determines the rate at which ions are transported through the electromembrane. Below the limiting value for a given combination of operating conditions, current is carried almost exclusively by sodium ions, with correspondingly high current efficiencies of sodium hydroxide production. If the limiting value is exceeded, the deficiency in the supply of cations at the electromembrane surface is supplemented by a supply of hydrogen ions, generated by the process of concentration polarisation. This phenomenon manifests itself through pH disturbances in the diffusion layer, increased voltages and reduced current efficiencies.

Using polarisation data for experiment 18B, the limiting current density was determined for pretreated scouring effluents containing 46 to 9 g/l Na by noting the points at which the rate of increase in voltage was disproportionately higher than the rate of increase in the applied current density (Pollution Research Group, 1989). The ratio of the limiting current density and the conductivity of the anolyte was determined to be $2,6 \times 10^{-3} \text{ A/m}^2 \text{ per mS/cm}$. Therefore, using this ratio, and knowing the anolyte conductivity, the limiting current density can be predicted at any temperature by the equation:

$$\text{limiting } CD = 2,6 \times 10^{-3} \times L$$

(7.1)

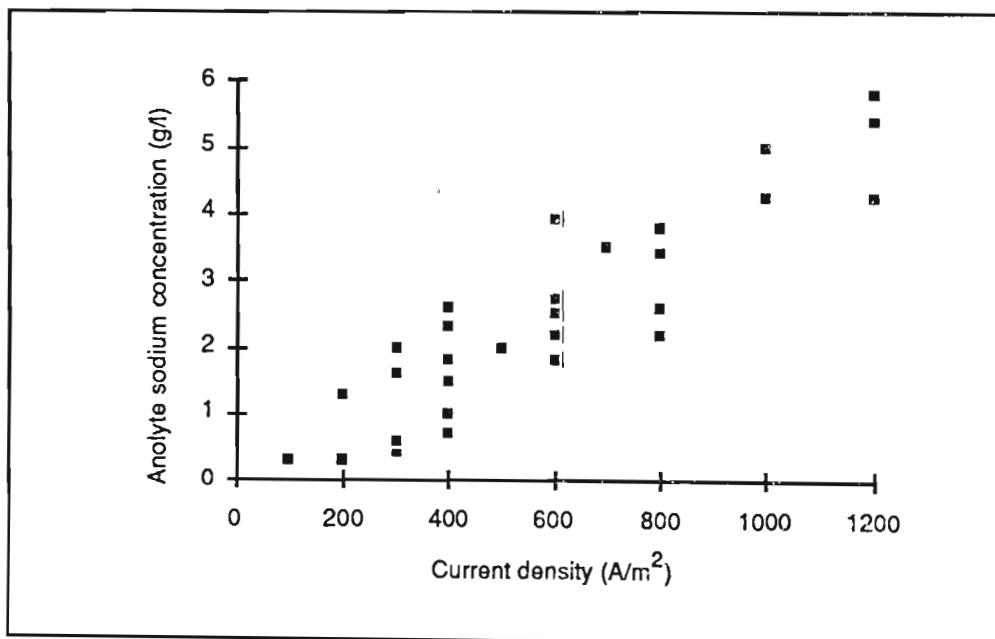
where L = length in m

7.5.5. Effects of Anolyte Concentration

The influence of anolyte concentration on current densities (for a fixed applied potential) was determined by examining, for a series of experiments, the current densities which could be achieved at a constant overall cell stack voltage of 15 V for anolyte concentrations ranging up to 6 g/l (Figure 7.2). Below the limiting value, achievable current densities were observed to decrease at a rate of approximately 250 A/m² for every 1 g/l decrease in anolyte sodium concentration.

Figure 7.2
Experimentally Observed Relationship Between Achievable
Current Density and Anolyte Concentration

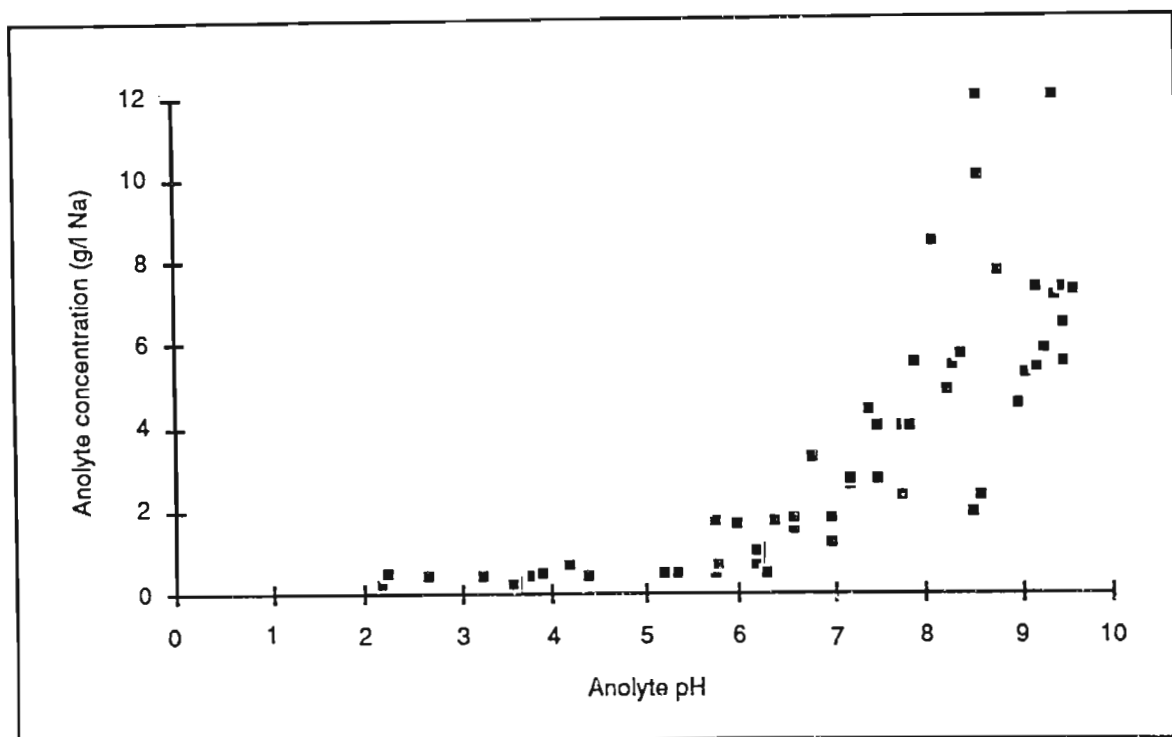
Conditions: constant overall cell stack volt drop 15 V, temperatures 40 to 50 °C



The pH of the final brine is a function of the degree of depletion of the pretreated effluent stream. Figure 7.3 has been plotted from experimental data. At brine concentrations above 3 g/l Na, the evolution of carbon dioxide from the anolyte during electrolysis buffers the pH, maintaining the value around 8 to 9. At low sodium concentrations, the buffer capacity is reduced and the pH decreases sharply. At low anolyte concentration and pH, the gradients

across the electromembrane are increased, encouraging migration of hydroxide ions from the catholyte towards the anolyte.

Figure 7.3
Relationship Between the Anolyte Concentration and pH



7.5.6. Temperature Effects

The pilot plant trials were conducted at temperatures between ambient and 60 °C. The construction of sections of the equipment from PVC prevented the use of higher temperatures. Temperature has a significant effect on cell volt drop, in particular the volt drop through the electrolytes, thereby indirectly influencing limiting current densities, power requirements and current efficiencies.

The total cell volt drop is the sum of the drops through the individual cell components (or the decomposition voltage) and the electromembrane and electrolytes. The experimentally determined decomposition voltage for the system was 2,7 V. This is the potential which must be applied before any current flows. The average membrane volt drop was 0,3 V.

Using equation 5.19 to predict the volt drop through the electrolytes, the overall operating potential for the system can be determined for any temperature from the equation:

$$E = E_a + E_{ca} + 2,7 + 0,3 \quad (7.2)$$

The influence of temperature on electrolyte conductivity is an important aspect when considering that, during the electrolysis experiments, the volt drop between the anode and the electromembrane consistently accounted for over 70 % of the total observed volt drop. The relationships between temperature and electrolyte conductivities are illustrated in Figures 5.6 and 5.7. Figure 5.6 illustrates that, as an approximation, the conductivity of the anolyte is halved with an increase in temperature from 40 to 80 °C. Since volt drop is proportional to conductivity (equation 5.19), doubling the average operational temperature to 80 °C may lower cell stack voltage (and thus power consumption) by as much as 35 %.

7.5.7. Dimensionally Stable Anode Performance

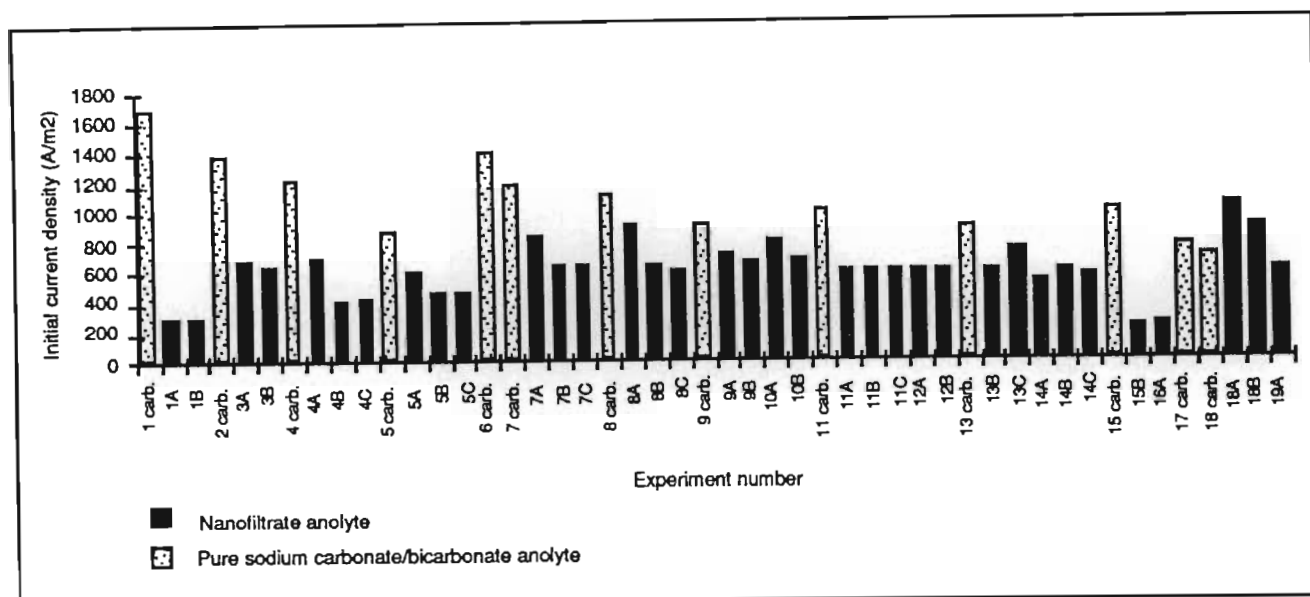
These precious metal coated titanium anodes are specifically formulated for low overpotential oxygen generation, but prolonged use causes gradual dissolution of the coating, with concomitant accumulation of non-conducting oxides in the interfacial layer between the titanium substrate and the coating and increased volt drop for a given passage of current. Since recoating is costly (£2 500/m² in 1987) as is increased power consumption, it is important to understand the potential degradation of the coating under the applied conditions of operation.

Any deterioration in the performance of the coated anode would be apparent from long term observation of cell volt drops at constant applied current. Figure 7.4 shows the initial current densities for all experiments at 9,0 V. Note that, in presenting this data, neither the variation of initial temperature from 15 to 25 °C nor the sodium concentrations have been considered. There is no noticeable downward trend in initial current densities, and it is suggested that deterioration of the anode coating is negligible. This observation was verified by physical examination of the electrode surface; after experiment 17, the anode from the first cell was analysed by back scattering techniques to determine the thickness of the coating. This analysis was carried out on behalf of Steetley Engineering by the Electricity Generating Research Council in the UK.

Results of this examination indicated that, in most places, little or no degradation of the anode surface had occurred. However, loss of precious metal oxides had occurred as a result of mechanical abrasion in areas where the anode had been in direct contact with the electromembrane. In these areas, the anode was imprinted with the grid appearance of the electromembrane. The Electricity Generating Research Council predicted that an anode coating life in excess of four years could be achieved if mechanical abrasion is prevented.

Figure 7.4
Initial Current Density for Each Experiment

Conditions: overall cell stack voltage 9 V



During electrolysis, a white precipitate was progressively deposited on the surface of the coated anode, cathode and conducting plate. After experiment 17, the cell was operated using the scaled electrode and a sodium bicarbonate solution at 1 400 A/m². The electrodes and conducting plates were then sanded and the experiment repeated under identical conditions. No obvious differences were observed. It was concluded that the effect of this deposit on electrode resistance and volt drop was minimal.

7.5.8. Electromembrane Performance

Electromembrane life expectancy is decreased by the aggregation of insoluble salts within the structure; the formation of blisters between the two polymeric layers; and high operational temperatures.

Aggregation of Insoluble Salts

In the pilot-plant trials, calcium and magnesium levels (approximately 20 and 3 mg/l respectively) were far in excess of those recommended by the electromembrane manufacturers for non-fouling performance (0,5 and 0,1 mg/l respectively). No change in the resistance of the electromembrane was observed, despite monitoring to an accuracy of 0,01 V at intervals throughout each experiment for the duration of the study. However, a mass balance of calcium and magnesium across the system indicated that the total amount of these ions present in the electrolytes before each experiment was higher than that present at the end of each experiment. Furthermore, a white precipitate, which was identified by X-ray

diffraction as the aragonite polymorph of calcium carbonate, formed on the anode surface of the electromembrane. This precipitate was most heavily deposited in areas which had not been in contact with the anode surface, and as a result of non-uniform flow and current distribution. It is likely that these areas would have been subjected to high current densities, with localised polarisation resulting in zones of high pH at the surface of the electromembrane. This effective decrease in available electromembrane area would adversely affect current efficiencies, while the zones of high pH would facilitate the precipitation of calcium carbonate.

The electromembrane was descaled (see Section 9.2) by contact with nitric acid, and current efficiencies were restored to 100 %.

Experience from the pilot plant suggests that the design of a commercial plant should give appropriate consideration to the control of flow patterns and pressure differentials to prevent electromembrane bulging and subsequent contact with electrodes, as well as to the development of a programme of regular and effective membrane cleaning cycles.

Blister Formation

Blistering is caused by increased internal forces in the electromembrane beyond the strength of the interlayer bond. This occurs because the highly selective, low-conducting, polymer on the cathode side transports water at a lower rate than the conducting polymer on the anode side. The accumulation of water within the electromembrane is dependent on the concentration gradient across the electromembrane. At constant catholyte concentration, the amount of water transported through the electromembrane, the so-called water transport number, increases with decreasing anolyte concentration (see section 7.10). The manufacturers recommend operation of the electromembrane at anolyte concentrations above 170 g/l NaCl (or equivalent concentration of other soluble salts) to prevent blistering. Although anolyte concentrations in the current application are far lower, applied current densities are also lower, possibly preventing serious water transport differentials between the different polymers of the electromembrane.

Excessive Temperatures

During the pilot-plant investigation, temperatures were maintained below 60 °C. This is below the maximum level (80 °C) specified for safe operation by the manufacturers of the electromembrane.

7.5.9. Recovery of Sodium Salts

Depending on the degree of anolyte depletion, up to 99 % of the sodium ions and inorganic carbon species were recovered as sodium hydroxide and carbon dioxide gas. Table 7.6 summarises the data for each experiment. The calculations have taken into account changes in anolyte volume.

Table 7.6
Recovery of Sodium and Inorganic Carbon Species from Anolyte

Experiment	Initial Mass of Na g	Final Mass of Na g	Recovery of Na %	Initial Mass of Inorganic Carbon g CO ₂	Final Mass of Inorganic Carbon g CO ₂	Recovery of CO ₂ %
1 carb.	620	33	95	566	66	88
1A	45	7	84	75	10	87
1B	58	13	78	102	16	84
2 carb.	2 250	104	95	1 980	184	91
2A	120	8	94	176	10	94
2B	144	13	89	166	31	82
3 carb.	2 250	239	89	1 725	393	77
3A	310	14	95	400	9	98
3B	305	38	88	400	54	86
4 carb.	1 500	225	85	1 675	337	80
4A	216	8	96	312	8	98
4B	216	8	96	312	19	94
4C	216	14	94	312	8	98
5 carb.	1 575	483	69	1 900	907	52
5A	153	8	95	204	34	83
5B	90	8	91	159	20	87
5C	116	6	95	106	8	92
6 carb.	1 425	572	60	1 215	718	41
7 carb.	1 440	202	86	1 675	293	83
7A	130	5	96	173	5	97
7B	148	5	97	195	12	94
7C	168	18	89	188	19	90
8 carb.	1 365	689	50	1 325	1 173	13
8A	205	77	63	275	124	55
8B	233	5	96	155	7	95
8C	286	27	85	228	13	93
9 carb.	1 390	791	43	1 310	1 063	18
9A	234	14	94	342	19	94
9B	148	7	95	195	9	95
10 carb.	1 410	396	72	1 180	626	47
10A	190	4	98	273	0	100
10B	193	6	97	273	6	98
11 carb.	1 500	282	81	1 850	424	78
11A	252	9	96	378	0	100
11B	252	44	83	378	59	84
11C	259	3	99	350	0	100
12A	245	34	84	319	31	90
12B	252	73	71	352	81	77
13 carb.	1 540	537	65	2 320	799	66
13A	159	11	93	201	19	90
13B	225	10	96	357	18	95
13C	234	18	92	288	34	88
14A	154	22	86	182	27	85
14B	150	11	93	162	42	74
14C	200	32	84	224	72	68
15 carb.	549	10	98	696	36	95
15A	162	22	86	219	25	89
15B	156	22	86	216	16	93
15C	108	14	83	122	24	80
16A	120	24	80	138	32	77
16B	135	27	80	177	32	82
17 carb.	420	26	94	758	60	92
18 carb.	876	8	99	1 768	18	99
18A	1 652	702	58	2 168	834	62
18B	2 068	47	98	2 563	255	90
19A	1 158	112	90	1 575	30	98

7.5.10. Water Transport

The transport of water from the anolyte to the catholyte during electrolysis dilutes the sodium hydroxide and reduces the volume of the anolyte. The water transport number, n_w , is a function the concentration gradient across the electromembrane, and should be minimised, especially at high current densities, to prevent accumulation of water between the polymeric layers of the electromembrane. Experimental data from selected experiments have been used to calculate the water transport numbers at various stages of electrolysis, which are summarised in Table 7.7. Figure 7.5 illustrates that there is an exponential relationship between the anolyte sodium concentration and the water transport number, with n_w ranging from 2 to 35 moles water per mole of sodium. Regression of this curve gives the following relationship:

$$n_w = 6,5 \times 10^{-6} C^5 + 6,6 \times 10^{-4} C^4 - 2,5 \times 10^{-2} C^3 + 0,4 C^2 - 3,5 C + 17,8 \quad (7.3)$$

where C is the anolyte sodium concentration (g/l)

n_w is in g water/g sodium

Examination of the sodium ratios in Table 7.7 indicates that n_w ranges from 3 to 8 moles water per mole for sodium ratios above 0,2 (ie, where the sodium concentration in the catholyte is less than five times the concentration of sodium in the anolyte). Below sodium ratios of 0,2 (ie, where the sodium concentration in the catholyte is more than five times the concentration of sodium in the anolyte) the water transport number increases rapidly from 8 to 35 moles water per mole sodium.

7.5.11. Background Concentration Closed-Loop Recycle

The anolyte concentration is one of the most important factors affecting the operation and performance of the electrochemical unit, including current density, current efficiency, water transport and power consumption. In all cases, performance is adversely effected by low sodium concentrations. To improve performance, a system involving the closed-loop recycle of rinse water with a background concentration (Figure 7.6) has been considered. In this system, a sodium bicarbonate solution is used to rinse cotton fibre after scouring, in place of mains water. Only pick-up sodium, say 10 g/l, is recovered in the treatment process. Experimentally determined results have indicated that the limiting current density can be increased substantially, with a corresponding decrease in required electromembrane area for a given application. This system is considered in detail in Section 10.

Table 7.7
Water Transport Numbers

Experiment	Faradays	Anolyte Concentration g/l Na	Catholyte Concentration g/l Na	Na Ratio anolyte Na catholyte Na	Volume Change l	Water Change moles	Sodium Change moles	nw mol water mol Na
1 carb.	4,0	24,0	58	0,410	0,6	33	6,9	4,8
	9,6	14,0	66	0,210	1,2	67	8,9	7,5
	12,6	80,0	68	0,120	0,6	33	4,7	7,1
	15,7	20,0	74	0,030	1,1	61	5,0	12,2
2 carb.	2,8	39,0	33	1,200	0,6	33	13,2	2,5
	10,1	33,0	41	9,800	1,3	72	15,2	4,7
	18,0	29,0	52	0,560	0,9	50	9,9	5,1
	29,1	19,0	62	0,310	2,3	128	21,8	5,9
	35,4	18,0	65	0,280	1,6	89	3,5	25,4
	39,4	13,0	76	0,170	0,5	28	9,7	2,9
	40,7	13,0	69	0,190	0,2	11	0,0	-
	43,5	10,0	67	0,150	1,1	61	6,8	9,0
	51,4	3,0	67	0,040	1,6	89	13,5	6,6
2A	1,7	5,0	53	0,090	2,8	156	1,8	87,0
	3,5	1,0	56	0,020	0,7	39	2,7	14,4
	3,8	0,5	59	0,010	0,2	11	0,4	27,5
3 carb.	11,2	38,0	48	0,790	1,7	94	18,0	5,2
	38,5	16,0	59	0,270	5,4	300	50,0	6,0
	50,1	6,0	70	0,090	2,4	133	19,4	6,9
3A	2,3	8,0	73	0,110	0,3	17	5,2	3,3
	6,8	3,0	78	0,040	1,1	61	5,4	11,3
	7,2	0,6	78	0,010	0,2	11	2,3	4,8
4 carb.	8,5	25,0	80	0,310	0,6	33	11,5	2,9
	10,9	20,0	93	0,220	1,9	106	13,8	7,7
	27,9	11,0	104	0,110	2,5	139	17,8	7,8
	35,7	5,0	109	0,050	1,8	100	12,3	8,1
4B	5,1	4,0	71	0,060	1,4	78	5,0	15,6
	8,1	0,6	75	0,010	0,8	45	3,7	12,2
	8,6	0,3	74	0,004	0,6	33	0,3	110,0
5 carb.	20,5	21,0	75	0,280	2,8	156	25,0	6,2
	26,7	16,0	77	0,210	1,7	94	12,2	7,7
	36,3	11,0	85	0,130	0,8	45	10,3	4,4
6 carb.	17,1	21,0	76	0,280	2,8	156	19,5	8,0
	21,9	20,0	77	0,260	0,5	28	1,8	15,8
	27,7	18,0	79	0,230	11,1	616	13,6	45,3
	31,8	13,0	79	0,160	8,9	494	2,2	225,0
7 carb.	11,2	23,0	46	0,500	1,2	67	13,6	4,9
	21,7	17,0	62	0,270	2,7	150	12,5	12,0
	25,7	14,0	70	0,200	1,1	61	6,7	9,1
	40,5	5,0	88	0,060	3,8	211	18,0	11,7
7B	3,5	3,0	85	0,040	9,9	550	4,6	120,0
	4,6	0,5	95	0,005	14,7	817	1,6	511,0
8 carb.	13,4	21,0	67	0,310	4,8	266	17,7	15,0
	23,1	16,0	71	0,230	1,6	89	11,7	7,6
8B	4,4	2,0	87	0,020	1,3	72	4,1	17,6
	5,1	0,2	88	0,002	0,6	33	1,5	22,0
9 carb.	8,5	25,0	61	0,410	2,2	122	8,0	15,3
	25,1	18,0	76	0,240	3,6	200	18,0	11,0
10 carb.	13,9	13,0	60	0,220	3,1	172	35,4	4,9
	33,6	9,0	82	0,110	4,3	239	11,3	21,2
11 carb.	14,6	18,0	67	0,270	1,1	61	27,8	2,2
	28,5	16,0	81	0,200	4,5	250	6,9	36,2
	44,7	7,0	95	0,070	3,6	200	21,1	9,5
11A	7,9	3,0	98	0,030	4,0	222	10,3	21,6
	10,1	0,3	97	0,003	2,0	111	0,3	370,0
11B	8,3	4,0	91	0,040	3,8	211	5,1	41,4
	10,8	1,4	93	0,020	0,9	50	3,9	12,8

Table 7.7 continued
Water Transport Numbers

Experiment	Faradays	Anolyte Concentration g/l Na	Catholyte Concentration g/l Na	Na Ratio anolyte Na catholyte Na	Volume Change l	Water Change moles	Sodium Change moles	nw mol water mol Na
12A	9,3	3,0	69	0,040	2,5	139	6,8	20,4
	11,5	1,0	71	0,010	1,3	72	2,4	30,0
12B	6,9	3,0	62	0,050	0,9	50	5,5	9,1
	9,1	2,0	65	0,030	0,6	33	2,3	14,3
13A	4,6	2,0	68	0,030	1,8	100	4,3	23,3
	7,0	0,4	68	0,006	0,5	28	2,1	13,3
13B	6,9	3,0	58	0,050	2,1	117	6,0	19,5
	9,7	0,4	61	0,007	1,8	100	3,3	30,3
14A	2,3	3,0	63	0,050	0,7	39	2,1	18,6
	6,9	0,7	64	0,010	3,1	172	7,5	22,9
14C	2,3	4,0	52	0,080	1,1	61	2,8	21,8
	7,6	1,0	59	0,020	2,4	133	4,5	29,6
15 carb.	1,8	4,0	55	0,070	0,7	39	2,7	14,4
	5,8	0,8	59	0,010	2,0	111	3,4	32,6
15A	9,5	13,0	61	0,210	1,7	94	8,1	11,6
	16,5	2,0	65	0,030	2,2	122	9,0	13,6
17 carb.	20,1	28,0	62	0,450	8,4	467	33,1	14,1
	26,4	25,0	84	0,300	0,1	6	3,7	1,6
	39,3	25,0			4,4	244	5,2	46,9
18A	11,3	31,0	72	0,430	1,3	72	18,6	3,9
	20,1	33,0	48	0,670	6,0	330	6,1	54,1
19A	29,6	19,0	40	0,480	11,9	661	20,8	31,8

Figure 7.5
Effect of Anolyte Sodium Concentration on Water Transport Numbers, n_w

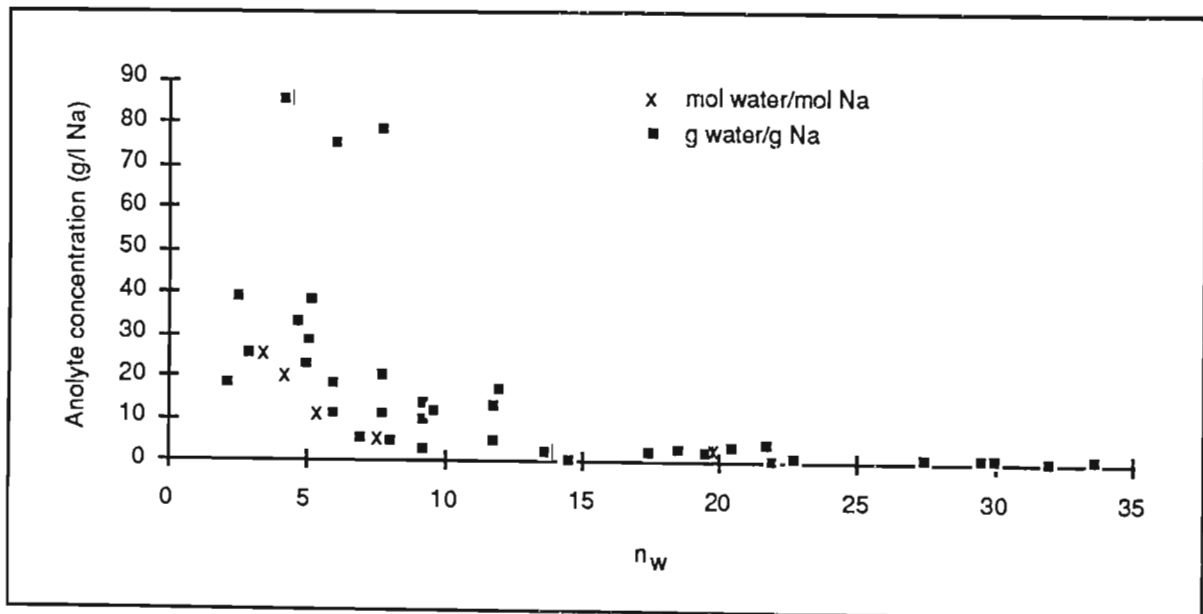
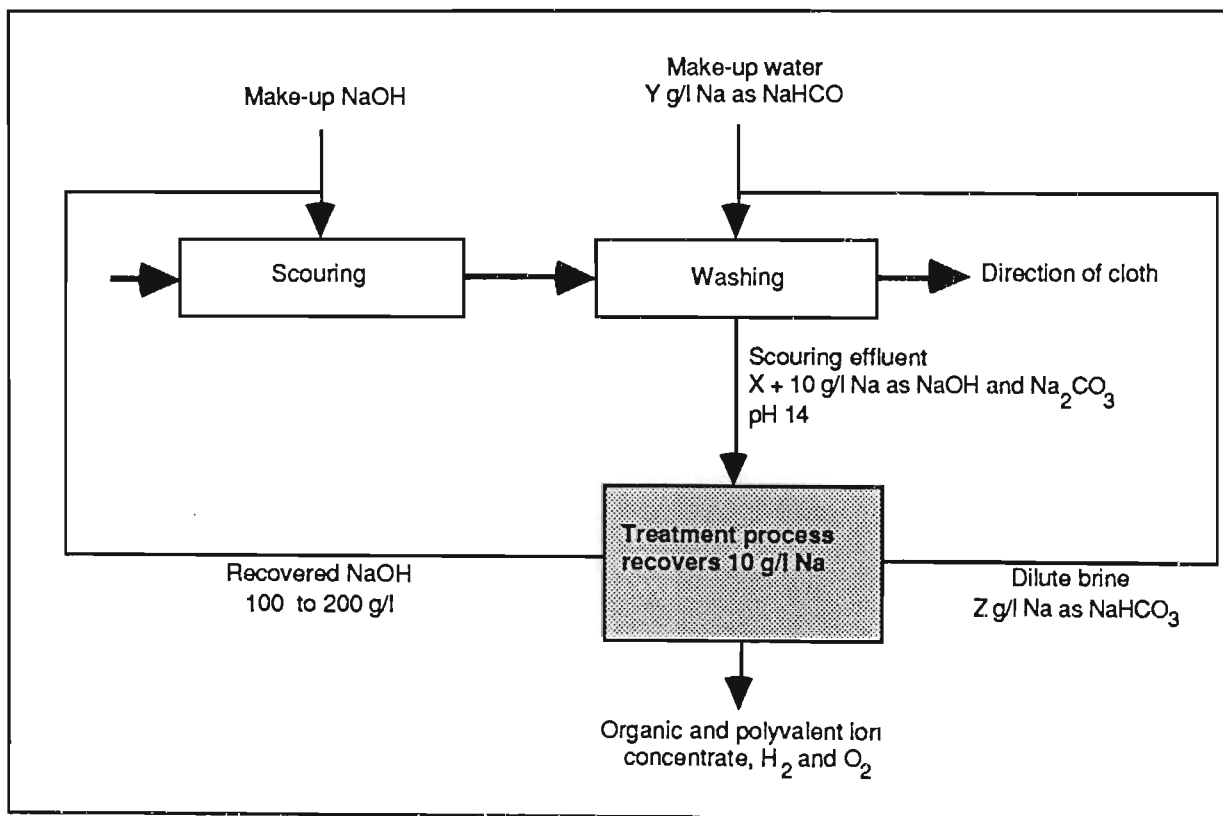


Figure 7.6
Closed-Loop Recycle of Rinse Water with a Background Concentration



SECTION 8

RESULTS AND DISCUSSION OF SUPPLEMENTARY INVESTIGATIONS OF NANOFILTRATION

This section presents and discusses the results of the supplementary investigations aimed at examining more closely, either practically, under controlled laboratory condition, or theoretically, certain aspects of nanofiltration. The procedures relating to these investigations are presented in Section 6.3.

The effect on nanofiltration performance of electrolyte characteristics is given in Section 8.1, while that of chelating agents is given in Section 8.2. Chemical speciation modelling of nanofiltration is given in Section 8.3. A semi-quantitative explanation of nanofiltration performance is given in Section 8.4, and Section 8.5 describes the results of transport modelling of nanofiltration.

8.1. Effect of Electrolyte Characteristics on Nanofilter Performance

These investigations aimed to determine the effect of pH and concentration of sodium carbonate/bicarbonate solutions on the nanofiltration membrane flux and retention performance in three separate experiments. A fourth experiment allowed the retention of calcium and magnesium salts to be determined in a sodium carbonate solution at varying pH. The procedures and apparatus used for these investigations are described in Sections 6.3.1 and 6.3.2. Results were used to select the most beneficial conditions under which to operate the pilot-plant nanofiltration unit, thereby obtaining maximum sodium and inorganic carbon recovery, at elevated fluxes and with high retentions of divalent cations.

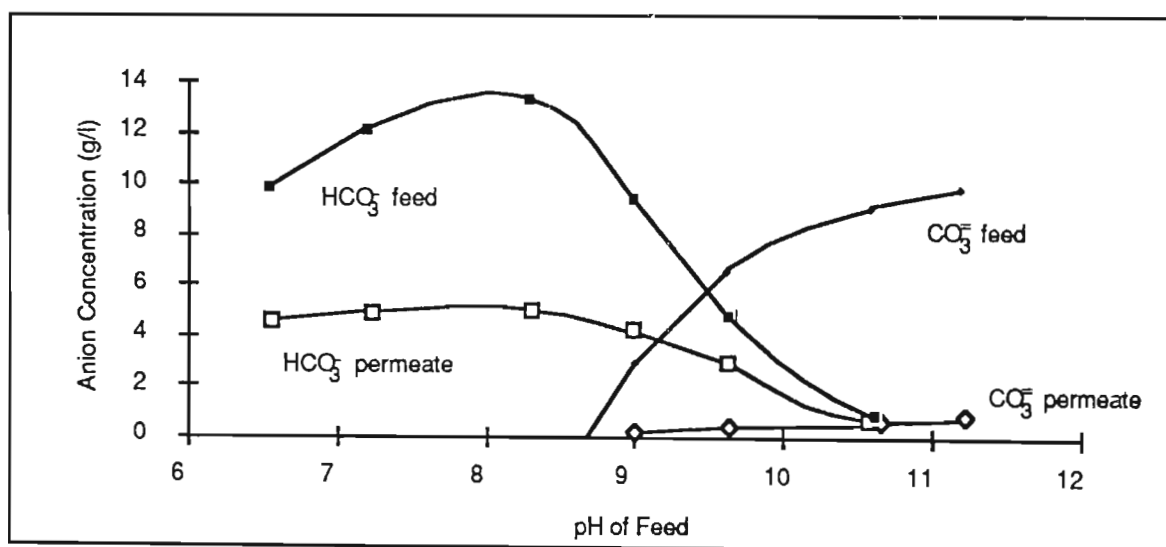
The experimental and analytical results are presented in Appendix 7. Specifically, Tables A7-1 to A7-3 in this Appendix give data for experiments 1, 2 and 3 (corresponding to 1, 10 and 30 g/l Na as sodium carbonate), while Table A7-4 gives data for experiment 4 (10 g/l Na as sodium carbonate spiked with 10 mg/l each of Ca and Mg).

The results of these experiments were the first ever published on the nanofiltration of the carbonate system in solution (Simpson *et al*, 1987). After publishing these results, further studies were undertaken on the same system to provide detailed experimental data to supplement speciation modelling and to verify mass transport modelling predictions. The results of these further studies are presented in Sections 8.3 and 8.4).

8.1.1. Effect of pH and Concentration of Sodium Salts on Membrane Retention

As described in Section 5.3, the pH of a solution containing inorganic carbon is critical in determining the nature of the components present, and therefore the retention performance of the nanofiltration membrane. Figure 8.1 shows the experimentally determined distribution of inorganic carbon components between the retentate and permeate for the range of pH values examined. Although these results relate specifically to a solution containing 10 g/l Na, the distribution followed a similar pattern for both the 1 and 30 g/l Na solutions. Figure 8.1 illustrates both the change in predominating component (from carbonate ions to bicarbonate ions) as the solution pH is lowered, as well as the relative degree of retention of the two carbon components by the membrane; the retention of the carbonate ion by a nanofiltration membrane is obviously higher than that of the bicarbonate ion.

Figure 8.1
Distribution of Inorganic Carbon Components Between Nanofiltrate
Permeate and Feed Over a Range of pH Values

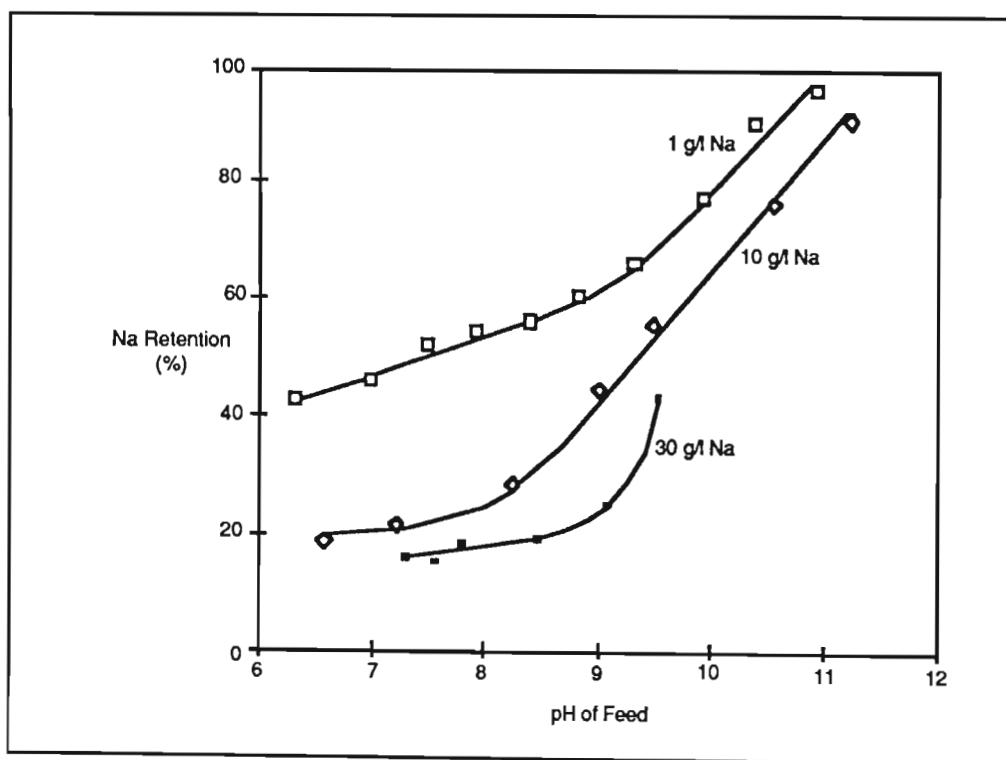


Using the analytical results, Figures 8.2 and 8.3 have been plotted to illustrate the influence of the pH on membrane retention of sodium ions and inorganic carbon components respectively in solutions containing 1, 10 and 30 g/l Na. The inorganic carbon components have been represented in Figure 8.3 as total inorganic carbon (expressed as total CO₂), carbonate ions and bicarbonate ions.

Two trends are apparent:

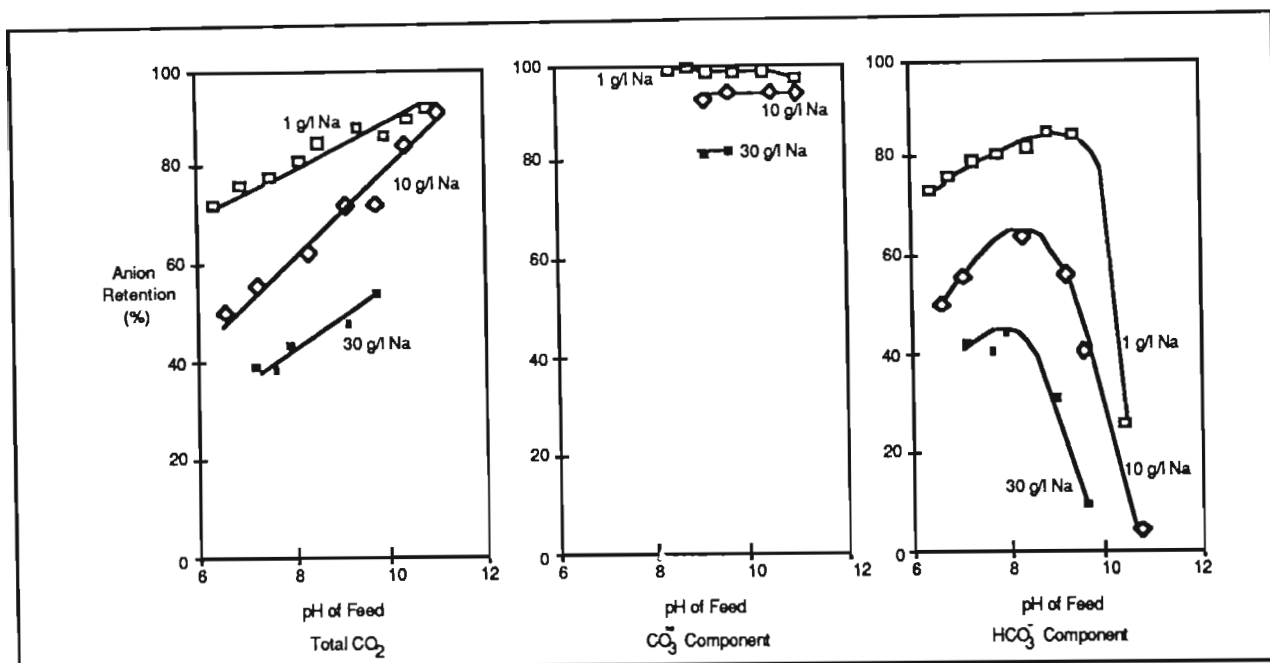
- 1) The membrane retention of anionic and cationic species at any fixed pH increases with decreasing feed concentration. This is because of the increased shielding of negatively charged groups on the membrane surface at high cation concentrations, thereby decreasing the membrane selectivity and surface-co-ion repelling forces.
- 2) At any fixed feed concentration, the membrane retention for total CO_2 and carbonate species increases with increasing pH. This results from the equilibrium shift of inorganic carbon, from monovalent bicarbonate ions of low charge density at low pH values, to divalent carbonate ions of high charge density at high pH values. When carbonate ions predominate, there is an increase in surface-co-ion repelling forces, retention of anions, and retention of cations, as a result of the requirements of electroneutrality.

Figure 8.2
Dependence of Membrane Na Retention on Feed pH and Salt Concentration



The practical implications of these relationships are that the nanofiltration membrane may be operated as a reverse osmosis membrane or as an ultrafiltration membrane, depending on the pH of the sodium carbonate solution. Careful pH control enables retention characteristics and permeate characteristics to be selected. At elevated pH values, where the carbonate is the predominant anionic component, sodium retentions exceed 90 %. Retentions are more than halved at neutral pH values, where the predominant anionic component is bicarbonate.

Figure 8.3
Dependence of Membrane Anion Retentions on Feed pH and Salt Concentration
 (Note anion components presented as total CO_2 ; carbonate ions and bicarbonate ions)



Clearly, in the application of nanofiltration which is currently being considered, maximum separation of sodium and inorganic carbon species from impurities is achieved at pH values below 8.0, where these ions are separated from the impurities and pass through the membrane into the permeate. The pilot-plant trials were carried out in this pH vicinity to maximise the desired separation.

8.1.2. Effect of pH and Concentration of Sodium Salts on Membrane Flux

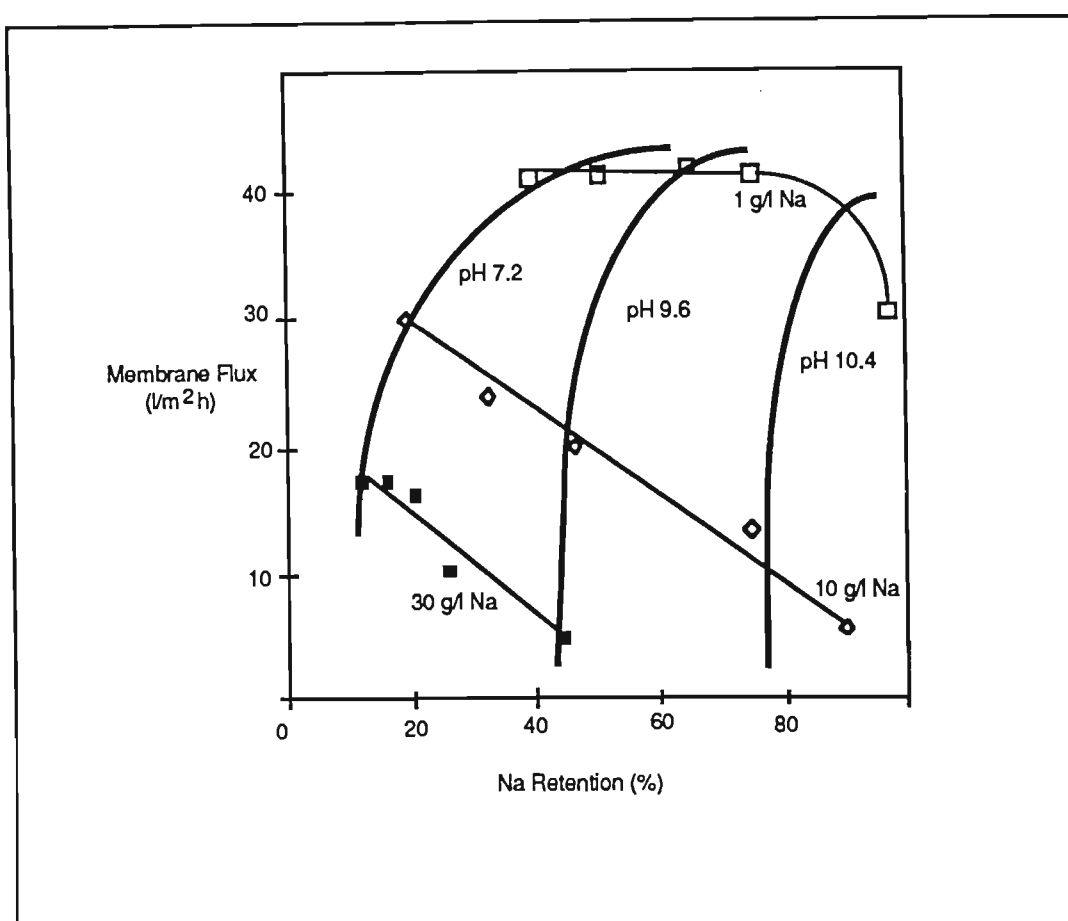
Figure 8.4 has been plotted from analytical data and flux measurements. It illustrates the relationship between flux and sodium retention (which is pH dependent) for three concentrations of sodium carbonate solution (1, 10 and 30 g/l Na). At high pH values, where the membrane characteristics approached those of reverse osmosis, the high osmotic pressure differential created across the membrane caused membrane fluxes to be greatly reduced. As the pH was lowered, with a change in the predominant anionic component, fluxes increased with a simultaneous loss of retention. A comparison of the curves for the three different concentrations indicates that flux decreases with increasing concentration, again a result of increased osmotic pressure differential across the membrane. Thus, at high ionic strength and high pH values, osmotic pressure differentials become the limiting factor in membrane performance.

In the application currently under consideration, maximum benefit in terms of flux performance can be achieved by operating the nanofiltration stage at minimum acceptable pH values.

8.1.3. Effect of pH on Membrane Retention of Divalent Ions

The retentions of divalent cations in a solution of sodium carbonate/bicarbonate were determined to be pH dependent, as illustrated in Figure 8.5. The retentions of calcium and magnesium parallel those of sodium in solutions of varying pH value. Retentions exceed 90 % above pH 11, but decrease to below 60 % at pH 7,2.

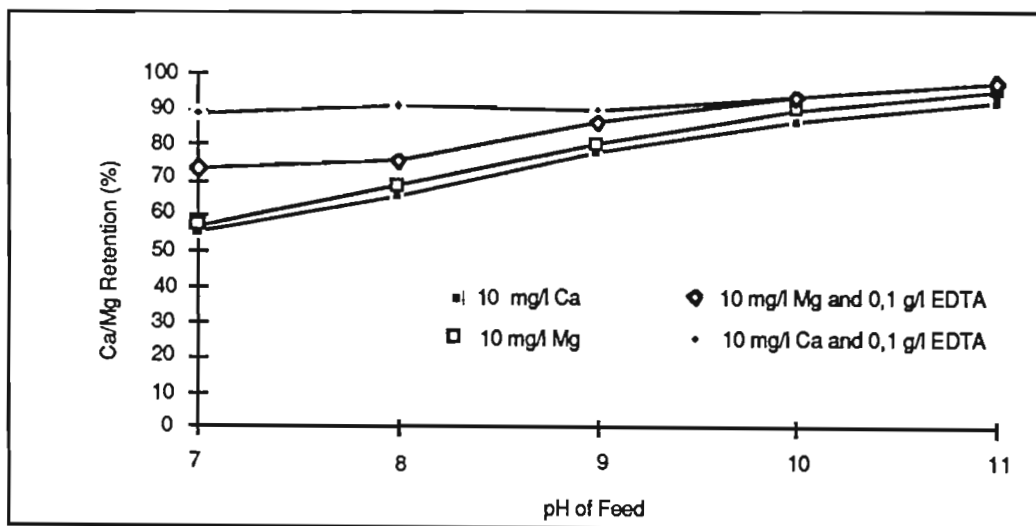
Figure 8.4
Dependence of Membrane Flux on Feed pH and Salt Concentration



The ability of nanofiltration to separate sodium salts from potential scale forming cations, even at relatively low pH values, has obvious benefits to the current study; calcium and magnesium ions may be removed (and concentrated) from solution prior to electrolysis, thereby reducing the possibility and/or severity of electromembrane fouling. Although a low pH value is most beneficial in terms of increased potential sodium salt recovery and improved membrane fluxes, it is least desirable when retention of divalent cations is considered. Therefore, in commercial installations, the most cost-effective operating regime will need to be determined.

It is appropriate, at this stage, to examine the comparative rates at which membrane retention for sodium and divalent cations falls as the pH of the solution is decreased. Figure 8.6 indicates the ratio of retention of sodium to calcium and magnesium in the sodium carbonate/bicarbonate solution containing 10 g/l Na over the pH range 7,3 to 11,2. At pH values near the lower end of the range, the relative permeability of sodium increases at a greater rate than that of calcium or magnesium. In the application currently under consideration, maximum benefit in terms of separation of calcium and magnesium can be achieved by operating at low pH values.

Figure 8.5
Dependence of Membrane Retention of Divalent Cations on pH of Sodium Carbonate/Bicarbonate Solution (10 g/l Na)



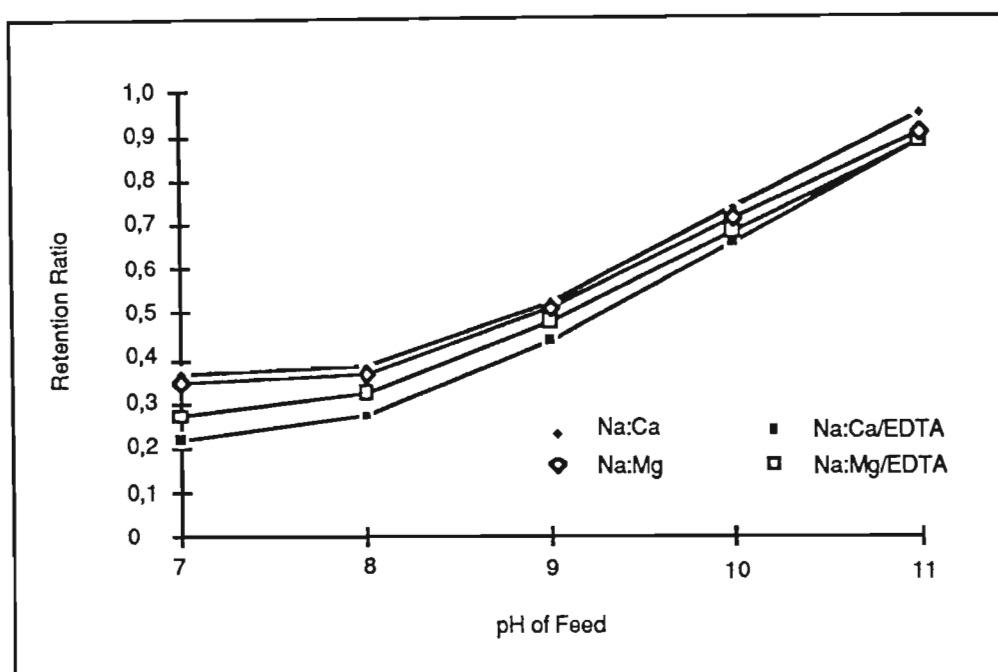
8.2. Effect of Chelating Agents on Nanofilter Performance

The experimental and analytical results of the effect of EDTA on the retention of calcium and magnesium ions in a sodium carbonate solution containing 10 g/l Na are presented in as experiment 5 in Table A7-5 of Appendix 7.

The pronounced effects of the addition of a chelating agent (100 mg/l EDTA as tetra-sodium salt) on the retentions of divalent cations, particularly at lower pH values, is illustrated in Figure 8.5. At the lower end of the pH range evaluated, retentions of calcium and magnesium increased from 56 and 57 % to 89 and 74 % respectively. The greater improvements in calcium retention in the presence of EDTA is explained by considering the stability constants of the complexes which form. At 20 °C, Ca-EDTA has a stability constant of 5×10^{10} , while that of Mg-EDTA is two orders of magnitude lower (5×10^8) (Flaschka, 1964). Since the calcium complex is more stable, the calcium is preferentially complexed in solutions containing both

calcium and magnesium in similar concentrations. Complexing in such a way improves membrane retention performance. Also, comparisons have been done on a mass basis and not on a molar basis.

Figure 8.6
pH Effect of a Sodium Carbonate/Bicarbonate Solution (10 g/l Na) on Na:Ca and Na:Mg Retention Ratios



8.3 Chemical Speciation Modelling of Nanofiltration

While the series of experiments discussed above aimed to provide practical information on the most beneficial operating conditions for separation of solution components by nanofiltration, this phase of the investigation aimed to determine, from the overall chemical analysis of carbonate solutions, the equilibrium distribution of all dissolved and precipitated chemical species present during nanofiltration. This enhanced understanding of the solution chemistry allowed predictions to be made of ion behaviour in the nanofiltrate feed and permeate under changing circumstances of concentration, pH and impurity levels, providing invaluable information on the bulk chemistry of the system for input into the transport modelling exercise (see Section 8.4). Section 6.3.3 describes the methodology and approach to chemical speciation modelling.

Appendix 7 contains detailed results. These include a summary of the concentrations, activities and activity coefficients in Tables A7-10 to A7-14 for each species present at a range of pH values in sodium carbonate solutions containing concentrations of 1, 10 and 30

g/l Na; and a condensed version of the MINTEQA2 output files from which Tables A7-10 to A7-14 were derived, giving percent distribution of components among species and other information.

A limitation of the procedure used is that MINTEQA2 is most applicable to solutions with ionic strengths below 0.7 m. In the current study, the most concentrated solution used (30 g/l Na) has an ionic strength of approximately 1 m. At this concentration the activity constant correlation is not valid and inaccuracies may occur.

8.3.1 Pure Sodium Carbonate Solutions

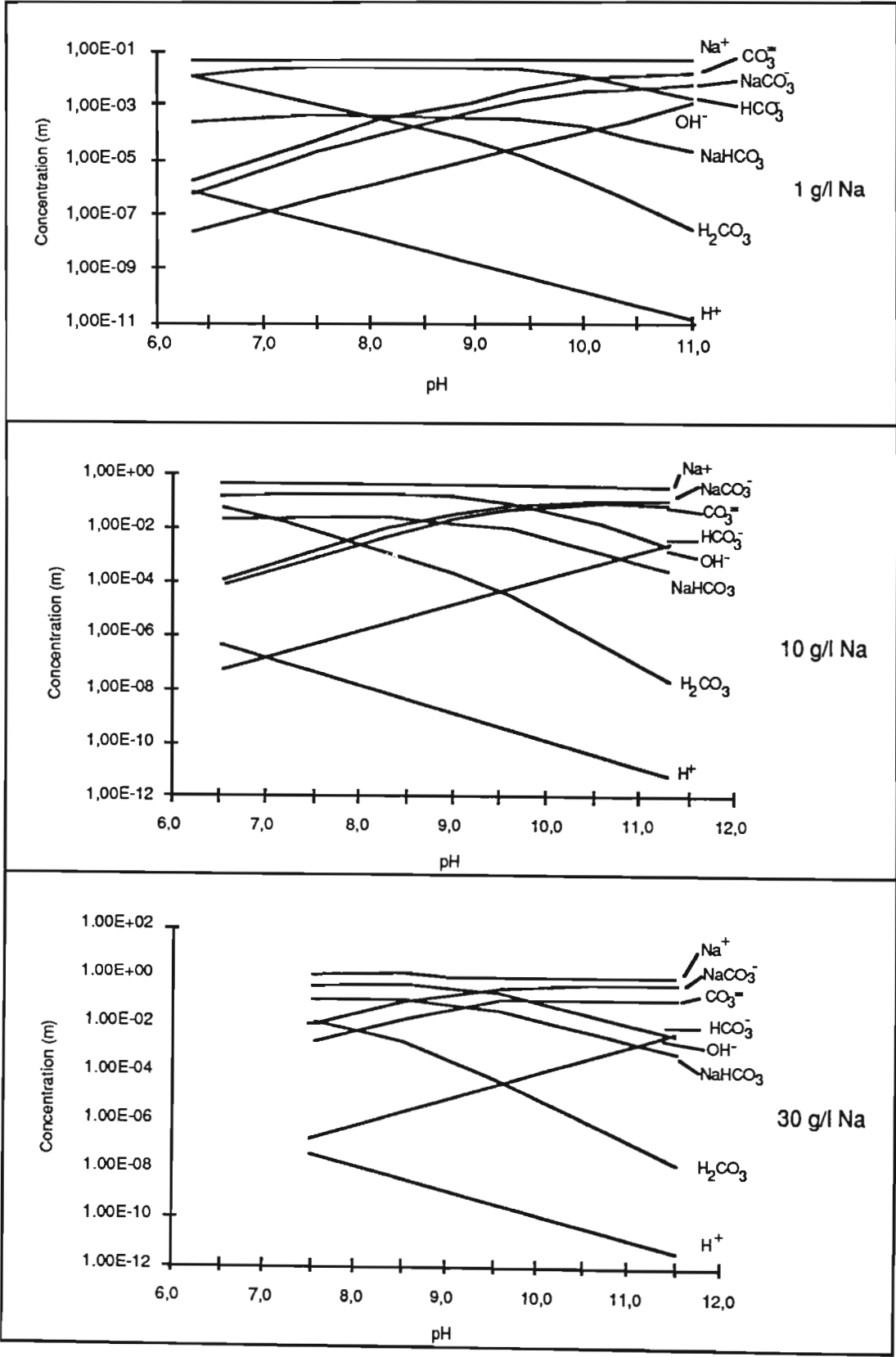
8.3.1.1 Equilibrium Speciation Concentrations

The principal determinands, or components, present in a pure sodium carbonate solution are total sodium and total inorganic carbon (expressed analytically as carbonate and bicarbonate ions). In actual solutions, these components speciate into eight individual forms of free ions, ion pairs or complex ions, as described in Section 5.3. Figure 8.7 is plotted from speciation results and illustrates how the equilibrium concentrations of these eight species in pure sodium carbonate solutions containing 1, 10 and 30 g/l Na vary with pH. Nitrate ions, present as a result of nitric acid addition during pH adjustment, affect the ionic strength, hence activity coefficient but do not affect the distribution of the other species in solution, and have been excluded from consideration.

The trends observed are similar for solutions of all concentrations. While the total concentrations of the determinands (sodium and inorganic carbon) remain constant at all pH values, the distribution pattern of the individual species varies with pH, and all species are present throughout the entire pH range. The following complementary relationships exist:

- 1) The concentration of sodium existing as free Na^+ ions and in the ion pair NaHCO_3 , decreases with increasing pH, as the NaCO_3^- complex ion becomes the dominant species. As the solution concentration increases, the proportion of Na bound in the monovalent complex ion NaCO_3^- and the neutral ion pair NaHCO_3 increases, with a corresponding decrease in the proportion existing as free Na^+ ions.

Figure 8.7
Equilibrium Concentrations of Dominant Species Present In Sodium Carbonate
Solutions of Varying Strength and pH



- 2) Inorganic carbon, existing primarily in the form of the ion pairs H_2CO_3 and NaHCO_3 , and the ion HCO_3^- at low pH values, is present dominantly as the ions HCO_3^- and $\text{CO}_3^{=}$ and the ion pair NaCO_3^- at higher pH values. The change in the distribution of the $\text{CO}_3^{=}$ component between the $\text{CO}_3^{=}$ ion and the NaCO_3^- complex ion as the concentration of the solution increases is interesting. While in the 1 and 10 g/l Na solutions, the concentration of divalent $\text{CO}_3^{=}$ ion is higher than that of the NaCO_3^- complex ion almost throughout the pH range, in the 30 g/l Na solution, the monovalent complex ion NaCO_3^- is present in higher concentrations than the divalent $\text{CO}_3^{=}$ ion.
- 3) The concentrations of H^+ and OH^- ions vary symmetrically in opposite directions and cross-over at pH 7 and concentrations of 10^{-7} .

Clearly, because of the importance of electrostatic interactions between the membrane and the charged species in solution in determining membrane performance during nanofiltration, the effect that changing pH has on the charge and nature of the dominant species is of considerable interest in this work. At this stage, it is suggested that membrane performance may be correlated to the charge on the dominant species, and that discontinuities in membrane performance will be observed at those pH values where there is a change in the charge of these dominant species. For example, at the pH values at the points of intersection of the H_2CO_3 curve and the curves of either $\text{CO}_3^{=}$ or NaCO_3^- (around 7,5 to 8,5 depending on concentration), or the point of intersection of the HCO_3^- curve with the $\text{CO}_3^{=}$ curve (around 9,0 to 10,0 depending on concentration), changes in membrane performance trends may be predicted.

8.3.1.2 Mass Distribution of System Components

The output file from MINTEQA2 also provides information on the mass distribution of each system component between dissolved species at equilibrium. Figure 8.8 is the equilibrium composition, showing the mass distribution of inorganic carbon between the dissolved species in solutions containing 1, 10 and 30 g/l total sodium. At all concentrations, the HCO_3^- ion is the dominant species in the *low* pH range and in low concentration solutions, while the $\text{CO}_3^{=}$ ion, and then the NaCO_3^- ion complex, dominate at 'high' pH values and in concentrated solutions. The pH value at which each species becomes dominant varies with concentration, the transition from HCO_3^- to $\text{CO}_3^{=}$ to NaCO_3^- occurring at higher pH values for more concentrated solutions. For example, 59 % of the inorganic carbon in a 30 g/l Na solution is present as NaCO_3^- at pH 9,6; at the same pH in a 10 g/l Na solution, the HCO_3^- ion and NaCO_3^- ions account for 40 and 36 % respectively of the inorganic carbon; while in a 1 g/l Na solution at pH 9,6, 70 % of the inorganic carbon present is in the form of HCO_3^- .

Figure 8.8
Equilibrium Composition Showing Mass Distribution Between Dissolved Species of Inorganic Carbon Present in Sodium Carbonate Solutions of Varying Strength and pH

Note: Only species comprising more than 1 % of total species are represented

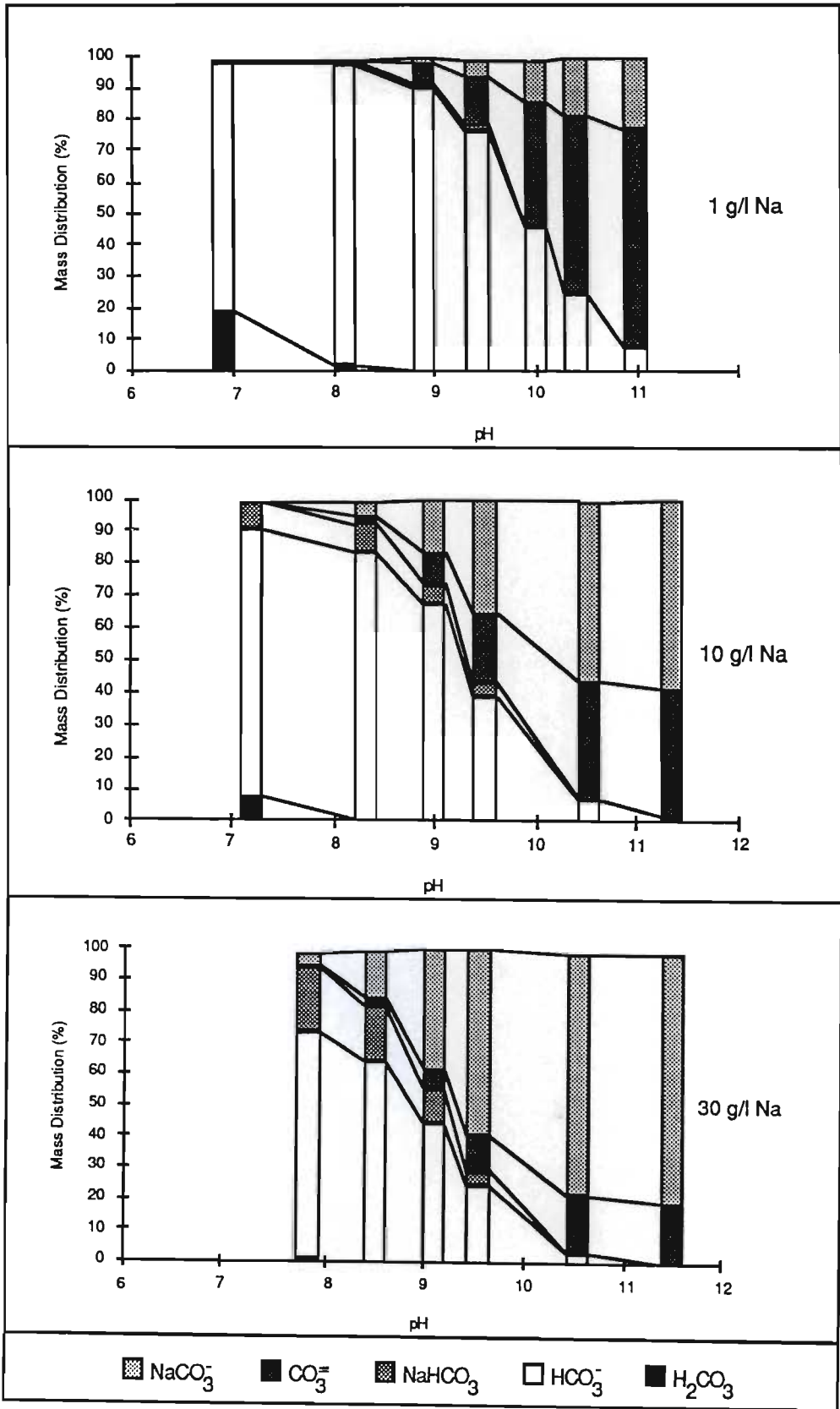


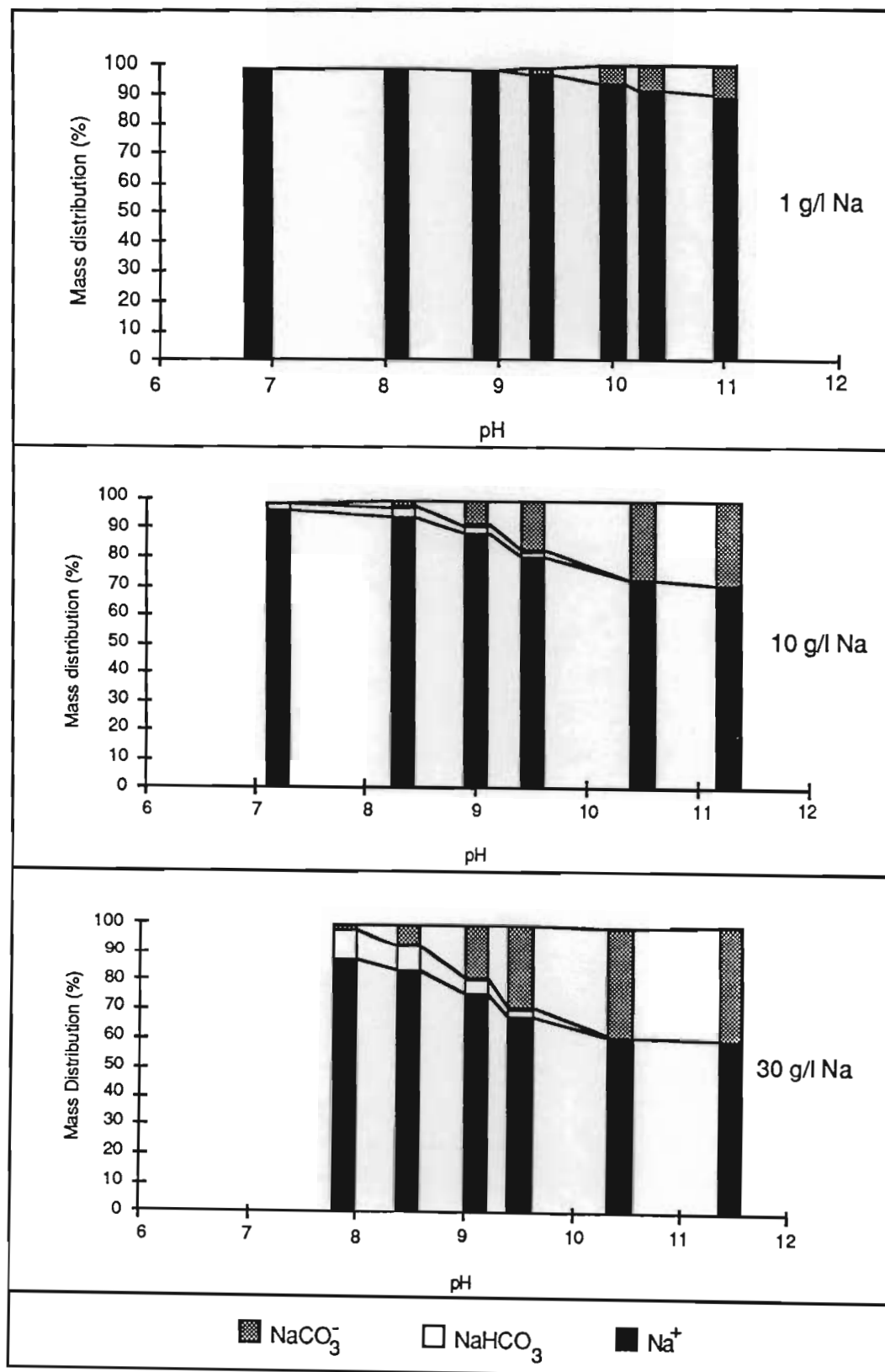
Figure 8.9 provides the analogous mass distribution data for sodium species in sodium carbonate solutions containing 1, 10 and 30 g/l total sodium.

Speciation is apparently, then, an important tool for identifying the practical implications of solution chemistry on nanofiltration. A knowledge of the precise nature of the species present and the distribution of solution components between these species can assist in the understanding of the observed mass transport properties of the membrane. The passage of ionic species relies on the interaction of the charged groups on the membrane surface with aqueous ionic species, and depends on the charge density of the species, their size, concentration and their ability to either repel or shield charges on the membrane. Clearly, speciation indicates that:

- 1) Although predominantly present as the positively-charged free ion, sodium may be present bound into neutral or negatively charged species. The free ion, Na^+ , is a counter-ion, which shields the charges on the membrane, decreasing its selectivity. Present as the ion pair NaHCO_3 , sodium is present as a neutral species and does not interact electrostatically with the membrane surface. Finally, if sodium is present as the NaCO_3^- ion complex, it will exhibit properties of a co-ion, and will be repelled by the membrane. This form of sodium may be significant, for example, it accounts for 40 % of total sodium in a sodium carbonate solution containing 30 g/l Na^+ at pH 11,5.
- 2) The bicarbonate component may be bound in neutral species, as in the ion pairs H_2CO_3 and NaHCO_3 ; or negatively charged, as in the free ion HCO_3^- . As with sodium, the species present influence the ability of the bicarbonate component to interact electrostatically with the membrane surface.
- 3) The carbonate component may exhibit a single negative charge, as in the ion complex NaCO_3^- ; or it may exhibit a double negative charge, as in the species CO_3^{2-} . Since these two ions have different size and charge densities, the membrane will exhibit different abilities to repel them. Clearly, the free ion species will be retained more effectively by the membrane, while the mass transport of the carbonate component in the membrane will increase as the proportion of ion complex increases. The proportion of monovalent NaCO_3^- is particularly significant at high pH values in concentrated solutions, for example, it accounts for over 80 % of the carbonate component at pH 11,5 in a 30 g/l Na solution.

Figure 8.9
Equilibrium Composition Showing Mass Distribution Between Dissolved Species of Sodium Present in Sodium Carbonate Solutions of Varying Strength and pH

Note: Only species comprising more than 1 % of total species are represented



Since the overall proportion of divalent anions increases with pH and decreases with concentration, it is predicted that, because of electroneutrality requirements, and because of the tendency of the nanofiltration membrane to retain divalent anions, the retention of the solute should increase with increasing pH and decreasing concentration.

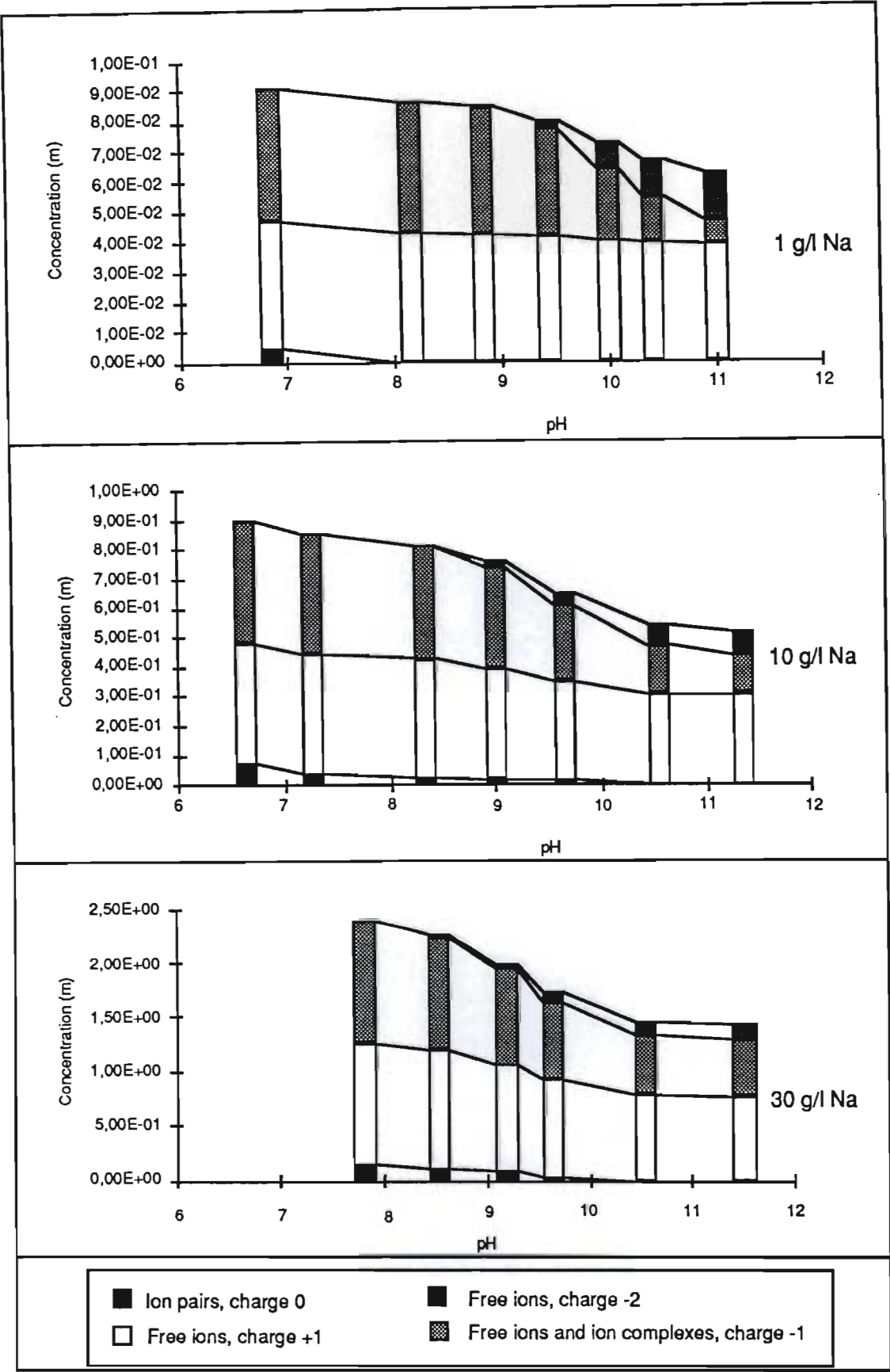
A comparison between Figures 8.8 and 5.3 (Section 5.3) suggests that, while the simple and commonly-used analysis of carbonate solutions presented in Figure 5.3 gives the distribution of inorganic carbon between carbonate and bicarbonate components, it does not adequately describe the nature, charge or concentration of actual species present. For example, Figure 5.3 suggests that up to 100 % of inorganic carbon in alkaline solutions may be present as the divalent CO_3^{2-} species. Speciation modelling suggests that, in practice, concentrations of the free divalent CO_3^{2-} anion may be far lower because of its association with sodium ions in the monovalent ion complex NaCO_3^- . This effect is attenuated at high concentrations. Because the transport properties of the nanofiltration membrane depend on the charge densities of the anions and cations present in solution, it is important that, for modelling purposes, particularly of concentrated solutions, the distinction be made accurately between monovalent and divalent species of the carbonate component.

8.3.1.3 Charge Distribution of Equilibrium Species

Figure 8.10 has been plotted to illustrate the distribution of charge between neutral, anionic and cationic species in the three sodium carbonate solutions at varying pH. Knowledge of such a distribution is important in understanding the function of nanofiltration systems, since the membrane interacts differently, and therefore performance alters, with species of different charge and charge density. As predicted from a knowledge of carbonate chemistry, while the concentration of monovalent cations remains relatively constant at all pH values in all solutions, the concentration of monovalent anions decreases with increasing pH, while the concentration of divalent anions increases. Figure 8.10 also clearly shows that the proportion of species present both as monovalent cations and as divalent anions decreases in solutions of high concentrations and pH relative to monovalent anions.

The transfer of negative charge from monovalent species to divalent species at increasing pH values is primarily responsible for the observed decrease in the total concentration of all species present. This decrease in total species is reflected in the colligative properties of the solution. For example, the osmotic pressure of the solution increases as the pH value is decreased, and this has practical implications in pressure-driven membrane processing. These implications are discussed in Section 8.5.

Figure 8.10
Distribution of Total Charge In Sodium Carbonate Solutions of Varying Strength and pH



8.3.2 Impure Sodium Carbonate Solutions

The presence of the free ions Ca^{++} and Mg^{++} in the nanofiltration permeate cause severe scaling of the electromembrane in the subsequent electrolysis stage and shorten its useful life. Therefore, maximum removal of these divalent cations is essential during nanofiltration. The removal efficiency depends on a number of factors, including the concentration and pH of the solution, as well as on the presence of organic complexing agents. To assist in understanding the performance of the nanofiltration membrane in impure solutions, speciation modelling was used to predict: the characteristics of calcium and magnesium species in a sodium carbonate solution containing 10 g/l Na, and varying in pH; and the effect of low concentrations of EDTA on the distribution of the calcium and magnesium components between free ions and other species. While the behaviour of EDTA resembles that of complexing agents used in the scouring process, these investigations provide a qualitative indication only of the behaviour of complexing agents in scouring effluent, since this effluent comprises an array of synthetic and natural organic materials which have varying degrees of influence on the solution chemistry with respect to free calcium and magnesium ions.

To simulate pretreated scouring effluent, speciation was carried out on a hypothetical sodium carbonate solution containing 10 g/l Na and 10 mg/l each of calcium and magnesium. The effect of complexing agents on the concentration of the free ions Ca^{++} and Mg^{++} was then investigated by the addition of 100 mg/l of EDTA (tetra-sodium salt) to the speciation model. The bulk chemistry of the system, as determined by speciation, resembles that of the pure sodium carbonate solution containing 10 g/l and discussed in Section 8.3.1. The analysis in this Section concentrates on the species containing calcium, magnesium and EDTA, which together account for less than 0,2 % of all species present, but which determine the fouling potential of the solution to electromembranes.

8.3.2.1 Equilibrium Species Concentration

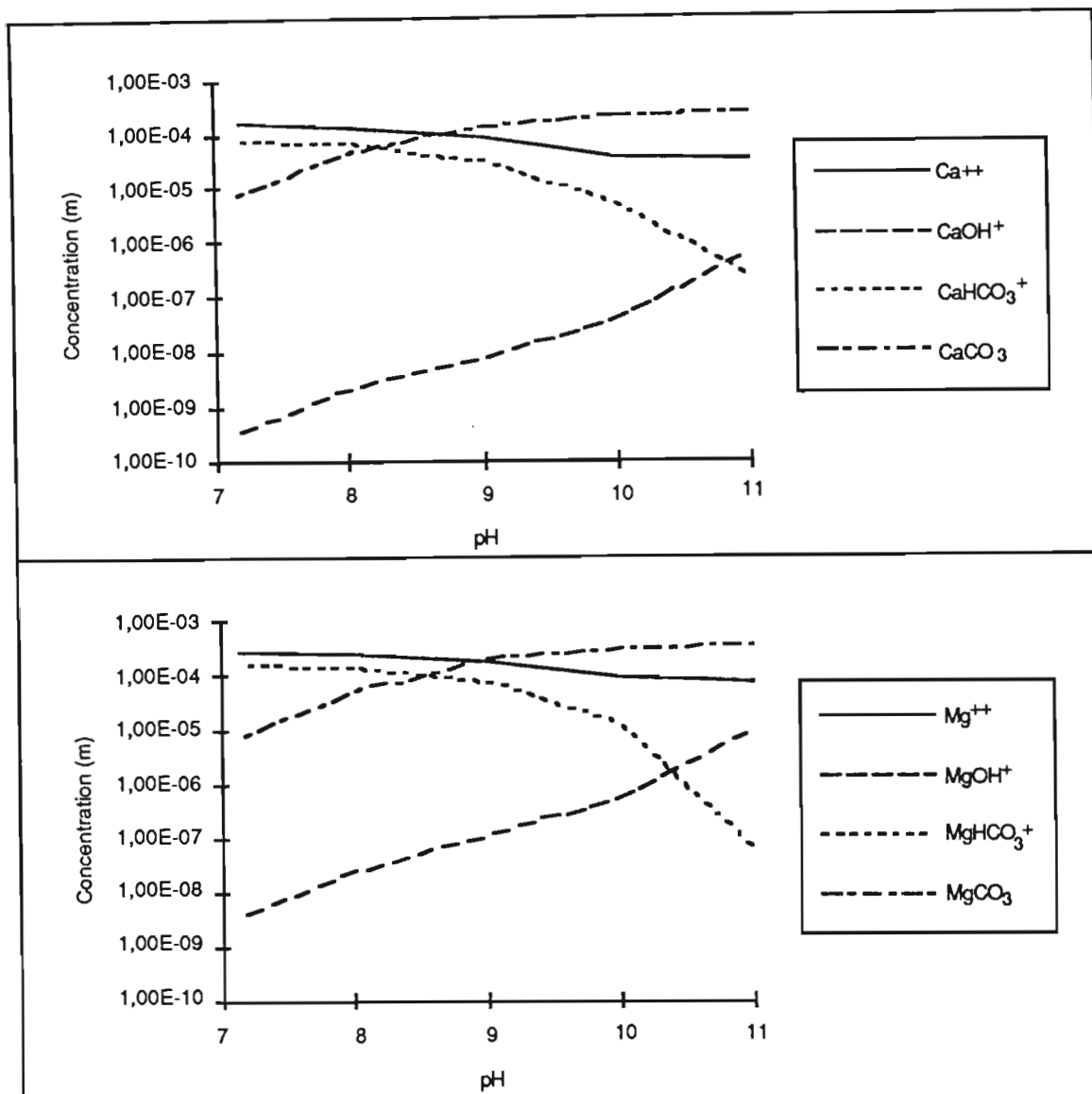
MINTEQA2 was initially applied to the case where precipitation was not allowed to occur. Tables A7-13 and A7-14 in Appendix 7 summarise the concentrations, activities and activity coefficients for the solutions with calcium and magnesium, and with calcium, magnesium and EDTA respectively.

In the absence of EDTA, the speciation model predicts the presence of eight Ca- and Mg-containing dissolved species at equilibrium. This is in addition to the eight species present in a pure sodium carbonate solution, the nitrates present as a result of pH adjustment with nitric acid, and the chlorides present as a result of the addition of calcium chloride. Figure 8.11 gives the equilibrium concentration of each of the Ca- and Mg-containing species throughout the pH range 7.2 to 11.0.

Similar trends are observed for both calcium and magnesium. All species are either neutral or positively charged. Free ionic species and the monovalent bicarbonate ion complex predominate at low pH values, but the neutral carbonate ion pair predominates at high pH values. These trends parallel those of the inorganic carbon species in a pure sodium carbonate solution.

In the presence of EDTA, the speciation model predicts the occurrence of 11 EDTA-containing species at equilibrium. These species occur in addition to the 18 species described above in the sodium carbonate solution containing only calcium and magnesium, and include six EDTA species in different valence states, one Na-containing complex, two Ca-containing complexes and two Mg-containing complexes. Figure 8.12 is analogous to Figure 8.11, but accounts for EDTA.

Figure 8.11
Equilibrium Concentration of Ca- and Mg-Containing Species In a Sodium Carbonate Solution Containing 10 g/l Na, and at Different pH Values



Speciation modelling of the EDTA solution indicates that:

- 1) While Mg and Ca complex with EDTA in two forms (with EDTA and with HEDTA), the Ca-EDTA and Mg-EDTA complexes are the dominant species over the entire pH range. Thermodynamic considerations indicate that Ca-HEDTA and Mg-HEDTA are most concentrated in low pH solutions, where HCO₃⁻ is the dominant inorganic carbon component. However, even at these low pH values, the concentration of Ca and Mg bound in the HEDTA complex is only 0,1 % of that bound in the EDTA complex.

- 2) The concentrations of Ca-EDTA and Mg-EDTA are almost constant throughout the entire pH range, while the concentrations of Ca-HEDTA, Mg-HEDTA, CaHCO_3 and MgHCO_3 decrease significantly at high pH values.
- 3) Speciation predicts Ca-EDTA to be the predominant Ca-containing species throughout the pH range, whereas, for Mg, MgCO_3 predominates at pH values above 9, while the free ion Mg^{++} predominates at pH values below 9. It is suggested that this tendency for non-complexed Mg to predominate at all pH values can be used to explain the lower retentions observed for Mg than for Ca in EDTA solutions at all pH levels in Figure 8.5. This phenomenon is discussed further in Section 8.4.
- 4) The strong complexing tendency of EDTA is illustrated. EDTA exists predominantly as Ca-EDTA and Mg-EDTA complexes throughout the pH range. The higher concentrations of Ca-EDTA are explained by the higher stability of the Ca-EDTA complex. Concentrations of other EDTA species are almost insignificant, accounting for, at most, 0,1 % (pH 7,2) of total EDTA present.
- 5) All Ca and Mg species in the EDTA solution are either bound in neutral species, or in mono- and divalent cations.

8.3.2.2 Equilibrium Mass Distribution

In the absence of EDTA, Ca and Mg each exist at equilibrium as the free divalent ions, Ca^{++} or Mg^{++} , or are bound into one neutral ion pair, CaCO_3 or MgCO_3 , or two single-charged positive ion complexes, CaHCO_3^+ and CaOH^+ , or MgHCO_3^+ and MgOH^+ . The mass distribution of each of these species over the pH range is shown in Figure 8.13. The species CaOH^+ and MgOH^+ do not comprise more than 1 % of the total species present and are not represented on Figure 8.13. The trends observed for Ca and Mg are similar except that the proportion of Ca bound up in the neutral species CaCO_3 is greater than the proportion of Mg bound up as MgCO_3 throughout the pH range. Similarly, the proportions of Mg bound up as MgHCO_3^+ and Mg^{++} are greater than those of Ca bound up as CaHCO_3^+ and Ca^{++} .

Figure 8.12
Equilibrium Concentration of Ca- and Mg-Containing Species In a Sodium Carbonate Solution Containing 10 g/l Na and 100 mg/l EDTA, and at Different pH Values

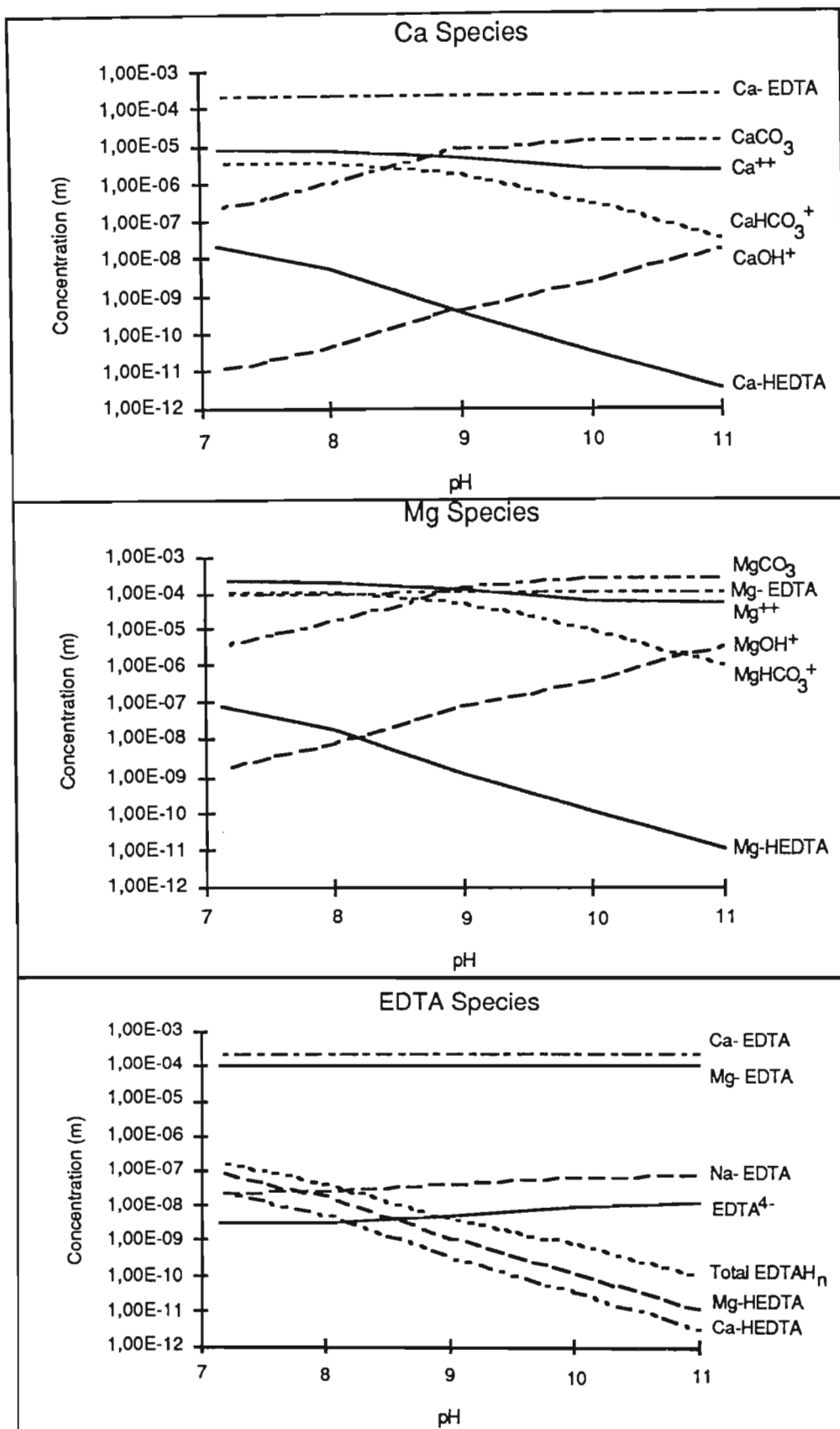


Figure 8.13
Mass Distribution of Ca and Mg Between the Species at Equilibrium In a Sodium Carbonate Solution Containing 10 g/l Na

Note: Only species comprising more than 1 % of total species are represented

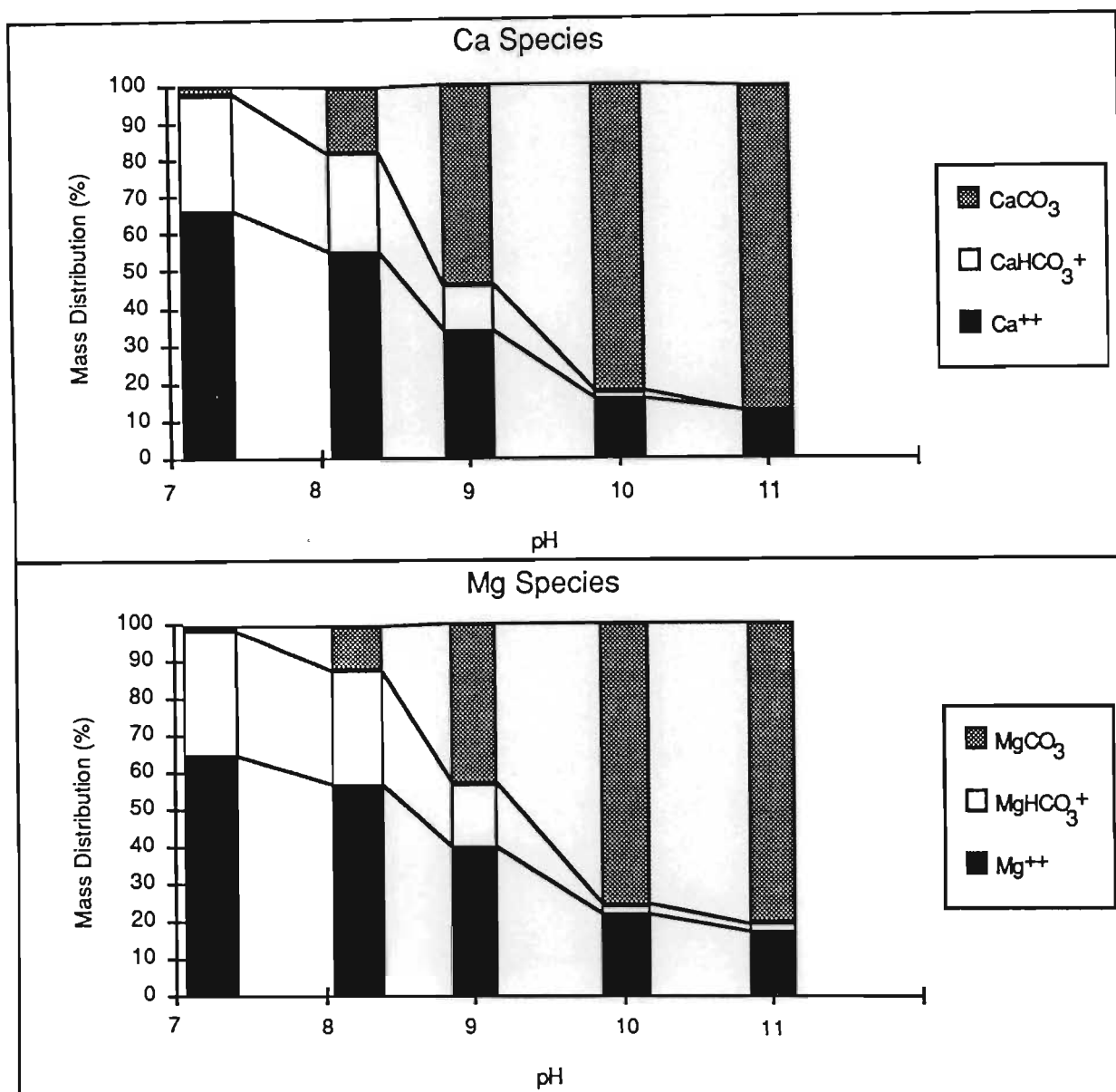
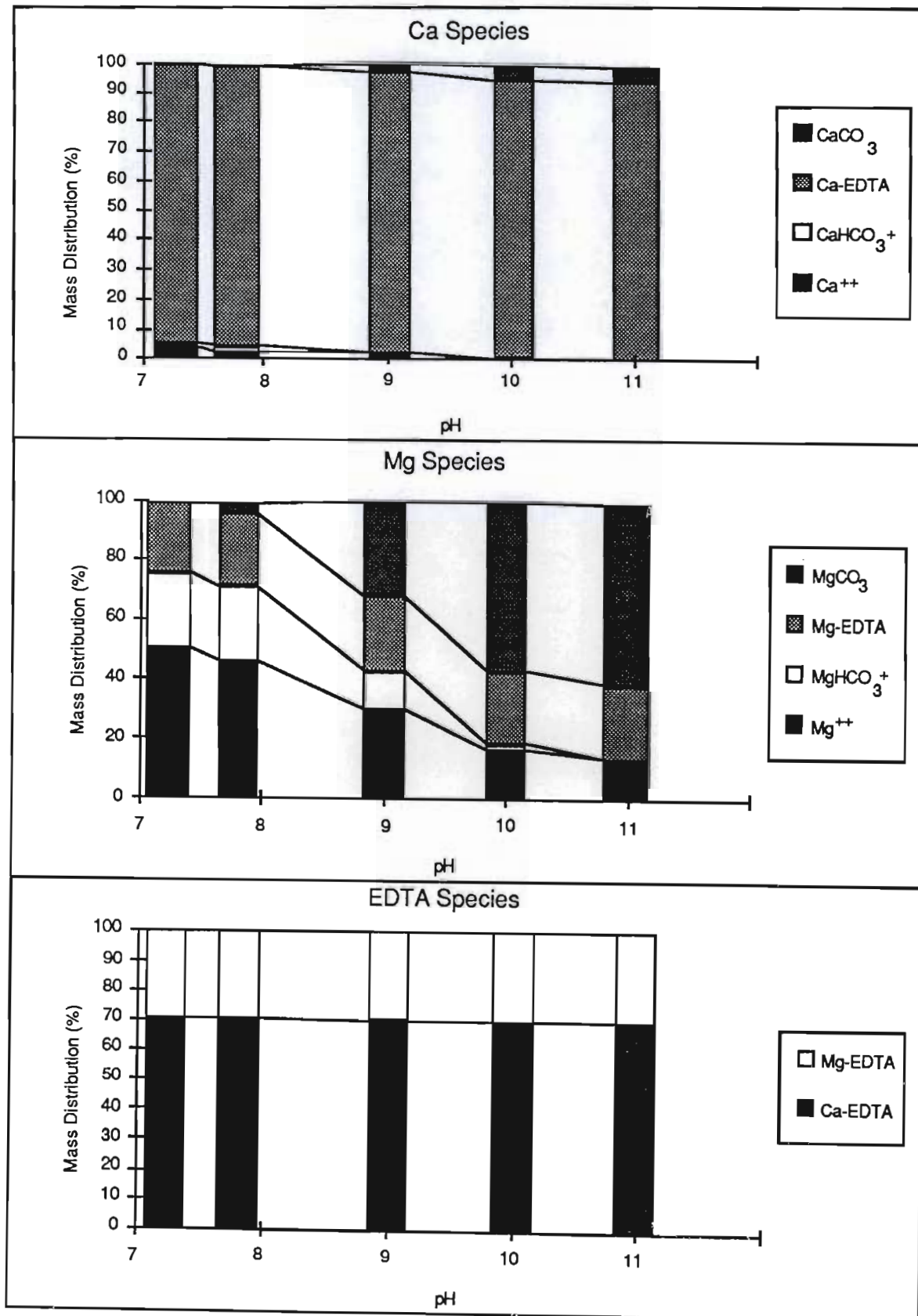


Figure 8.14 is the analogous diagram for the system containing EDTA. It illustrates the predicted mass distribution of EDTA between the EDTA-containing species at equilibrium, as well as the distribution of Ca and Mg. The difference in the affinities of Ca and Mg to complexation with EDTA is striking:

Figure 8.14
Mass Distribution of EDTA, Ca and Mg Between the Species at Equilibrium in a Sodium Carbonate Solution Containing 10 g/l Na

Note: Only species comprising more than 1 % of total species are represented



- 1) Whereas the proportion of Ca complexed as Ca-EDTA is above 93 % over the entire pH range, increasing slightly at lower pH values, the proportion of Mg complexed as Mg-EDTA increases slightly with pH to reach a maximum of 25 %.
- 2) The proportion of free Mg^{++} ions is significantly higher than the proportion of free Ca^{++} ions at all pH values, being highest (50 % of total Mg) at pH 7.2.
- 3) While the Ca-EDTA is the dominant Ca species throughout the pH range, Mg^{++} (at low pH values) and $MgCO_3$ (at high pH values) are the predominant Mg species.
- 4) At any pH, the amount of EDTA bound with Ca is more than double that bound with Mg. This results from the greater thermodynamic stability of the Ca-EDTA complex.

Whether the dominant mechanism for membrane transport relies on electrostatic forces or size exclusion factors, the predicted differences in the behaviour of Ca and Mg in EDTA solutions should manifest itself in observed differences in the transport of these components through nanofiltration membranes. Correlations between theoretical and experimental observations are discussed further in Section 8.4.

8.3.2.3 Saturated Solids and Precipitation

The discussion above relates to the speciation modelling case in which precipitation is not allowed to occur. However, the output data from MINTEQA2 suggests that it is thermodynamically possible for precipitation of selected Ca- and Mg-containing minerals to occur. These minerals are those for which the saturation index is exceeded. The condensed versions of MINTEQA2 output for experiments 4 and 5 in Appendix 7 list these minerals for each given pH. For example, minerals such as brucite and dolomite are predicted to precipitate at low pH values from sodium carbonate solutions not containing EDTA, while at high pH values it is thermodynamically possible for minerals such as aragonite, artinite, brucite, calcite, dolomite, huntite, hydromagnesite and magnesite to precipitate from the same solution.

The presence of EDTA is predicted to influence precipitation. For example, in the EDTA-containing solution, it is not thermodynamically possible for any minerals to precipitate at low pH values, whereas at higher pH values the saturation indices for possible precipitation are less positive.

Because the precipitation of minerals can change the concentration of dissolved species in solution, and because the precipitation of one mineral can alter the saturation indices of other minerals, MINTEQA2 was rerun for the case where precipitation was allowed to occur. Condensed versions of the output from experiments 4 and 5, where precipitation is allowed to occur, are included in Appendix 7.

Where the sodium carbonate solution contains no EDTA, thermodynamic data suggests that dolomite will precipitate at low pH values, and dolomite and magnesite will precipitate at high pH values. Furthermore, it suggests that at pH 7,2, 45 % of the Ca component and 27 % of the Mg component will be present as dolomite (not dissolved) and that at pH 11,3, over 98 % of both Ca and Mg will be precipitated.

Again, the presence of EDTA is predicted to influence saturation indices. No precipitation of Ca- and Mg containing minerals is thermodynamically possible in solutions containing EDTA and at pH 7,2. In the same solution at pH 11,3, only magnesite is predicted to precipitate, and 76 % of Mg is bound in this mineral.

These predictions correlate well with those of Butler (1982), who studies carbon dioxide equilibria. He predicts that qualitatively, solutions with a high Na:hardness cation ratio will tend to produce carbonate minerals with only Na, or a high ratio of Na:hardness cation. But he acknowledges that equilibria are not always reached and quantitative predictions are not easily made.

For further correlation of theoretical speciation results with experimental derived nanofiltration results, the possible precipitation of minerals from the nanofiltration solutions has been ignored. This was considered appropriate since:

- 1) MINTEQA2 is based on thermodynamic data, and does not consider kinetic probability in predicting precipitation. While it is kinetically feasible for some minerals to precipitate, other minerals will not precipitate. This complicates the practical situation.
- 2) During experiments 4 and 5, 10 mg/l each of Ca and Mg components were added to the nanofiltration feed. No precipitation or solution turbidity was observed during the trials, and analytical results indicated that the total dissolved components in the nanofiltrate feed over the entire pH range was constant, and equal to the initial concentration added. Experimental results suggest, therefore, that kinetic and thermodynamic equilibrium were not reached before the nanofiltration experiments were completed.

8.4. Semi-Quantitative Explanation of Nanofiltration Performance

Although the experimental method used in experiments 6 to 8 resembled that used in experiments 1 to 3 (discussed in Section 8.1), experiments 6 to 8 aimed to provide detailed experimental results from which correlations could be developed and explained by chemical speciation or mass transport theory. Therefore, experiments 6, 7 and 8 involved the nanofiltration of sodium carbonate solutions containing 1, 10 and 30 g/l Na respectively and at pH values corresponding to the pH values at which speciation modelling had been undertaken. These experiments were supplemented by experiment 9 (10 g/l Na as sodium carbonate at pH 9.6), which aimed to deduce the dependence of membrane performance on feed velocities and applied pressure. The experimental results are summarised in Tables A7-6 to A7-9 for experiments 6 to 9 respectively; Table A7-15 summarises predicted and experimentally observed osmotic pressures.

While the basic relationships between retention, flux, concentration and pH observed and discussed in Section 8.1 are equally applicable here to experiments 6 to 8, the discussion below presents a more theoretical analysis of the experimental results. It attempts to explain trends in water and solute fluxes against the operating conditions of pressure and flow, and by consideration of the predicted chemical species at equilibrium. For experiments 6 to 8 respectively, Tables A7-16 to A7-18 (Appendix 7) present calculated values of various parameters which have been used in the current analysis. Table 8.1 summarises this data, listing the water and solute fluxes (for Na and inorganic carbon components) at each pH, feed and permeate pH value and effective driving force (pressure).

Table 8.1
Summary of Calculated Flux, pH and Effective Pressure Values
For Experiments 6, 7 and 8

Experiment	pH		Effective Driving Force (kPa)	J_W (l/m ² h)	J_{Na} (mol/m ² h)	J_{IC} (mol/m ² h)
	Feed	Perm				
No. 6 1 g/l Na	11,0	10,9	1 184	55,6	0,02	0,07
	10,4	10,1	1 191	58,4	0,39	0,12
	10,0	9,7	1 212	69,8	0,89	0,23
	9,4	9,2	1 216	70,9	1,44	0,32
	8,9	8,8	1 227	70,9	1,68	0,38
	8,1	8,2	1 243	62,2	1,73	0,43
	6,9	7,1	1 239	49,1	1,41	0,31
No. 7 10 g/l Na	11,3	11,5	476	17,3	1,54	0,74
	10,6	10,0	569	25,5	3,10	1,07
	9,6	9,0	787	34,9	7,74	2,52
	9,0	8,5	889	40,9	12,98	3,92
	8,3	8,1	939	41,1	14,56	4,66
	7,2	7,4	946	41,4	13,67	4,57
No. 8 30 g/l Na	11,5	-	-	-	-	-
	10,6	10,4	211	3,4	2,79	1,26
	9,6	9,2	293	9,0	7,61	3,19
	9,1	8,6	572	16,7	15,92	6,26
	8,5	8,2	517	25,5	25,36	8,55
	7,9	7,9	485	27,8	29,31	9,32

8.4.1. Osmotic Pressure Variations

Since the osmotic pressure of a solution, or more precisely the osmotic pressure difference of a solution across a membrane, is a key variable in the consideration of its treatment using membrane separation processes, and for explaining membrane performance, this parameter has been predicted (Table A7-15, Appendix 7) from equilibrium speciation data using the method described by Brouckaert *et al* (1994) (see Section 5.4.3.3). Figure 8.15 indicates the good correlation between experimental and predicted trends osmotic pressures at each feed sample pH for each of the three sodium carbonate solutions.

For all concentrations of carbonate solutions, osmotic pressures are observed to decrease with increasing pH. This is in accordance with the predicted decrease in the concentration of total species at high pH (see Figure 8.10), which in turn manifests itself by a change in the colligative properties of the solutions.

The experimentally determined osmotic pressures for the feed and permeate samples has been used to calculate effective pressures, presented in Table 8.1, using the equation:

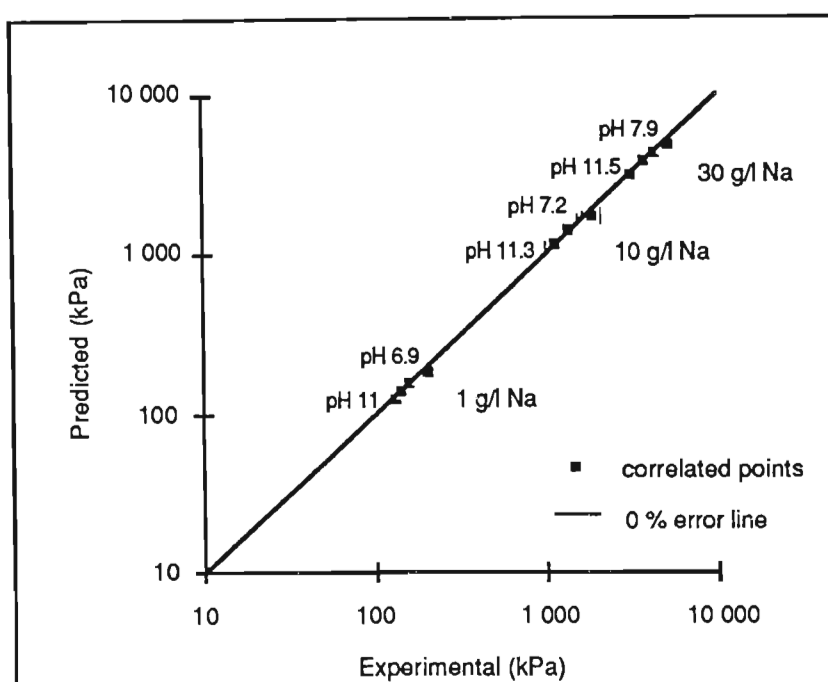
$$\text{Effective membrane pressure (kPa)} = \Delta P - \Delta \pi \quad (8.1)$$

where ΔP = transmembrane (or applied) pressure in kPa

$\Delta\pi$ = osmotic pressure difference across membrane (kPa)

Effective pressure is the driving force for water flux across the membrane and is a function of solute flux.

Figure 8.15
Correlation Between Predicted and Experimental Osmotic Pressures
In Sodium Carbonate Solutions of Varying Strength and pH

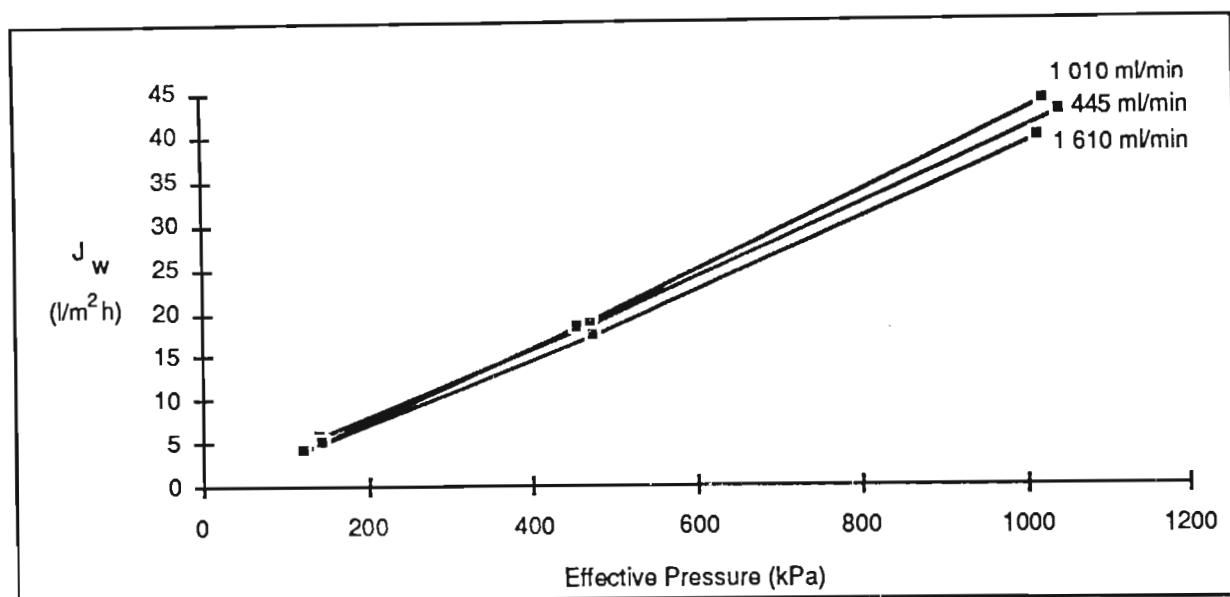


8.4.2. Concentration Polarisation

The flux/pressure measurements taken in experiment 9 aimed to indicate whether the effects of concentration polarisation, or the concentration gradient of solute near the membrane surface, were significant.

The results shown in Figure 8.16 indicate that for a feed concentration of 10 g/l Na, and for the three feed velocities investigated, the water flux through the membrane is proportional to the effective pressure. This indicates that it is likely that concentration polarisation is of minor importance under the experimental conditions employed. Note that experiments 6, 7 and 8 were operated within the range presented in Figure 8.16, using constant applied pressures and velocities of 1 300 kPa and 1 010 ml/min respectively.

Figure 8.16
Water Flux as a Function of Effective Pressure for Three Different Feed Velocities



Because the results suggest that concentration polarisation is small, it has been assumed in the subsequent qualitative analysis of the system, that the concentration of any solute in the bulk feed (C_{f-sol}) is equal to the concentration of that solute at the membrane-feed interface (C_{i-sol}). This allows mass transport across the membrane to be described for any solute, provided that the concentrations of the solute are known in the feed and permeate.

Typically, increasing cross-flow velocities past the membrane, and decreasing operating pressures, reduce concentration polarisation and result in higher separation and higher solute flux.

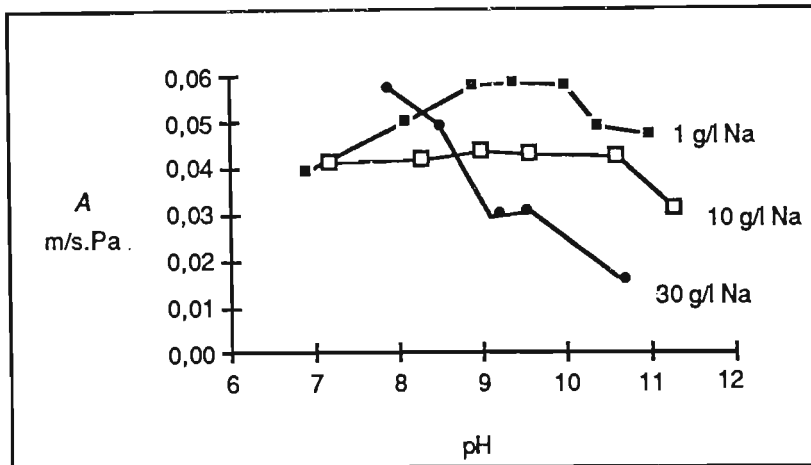
8.4.3. Determination of Water Permeability Constant, A

The water permeability parameter, A , has been calculated from experimental data using equation 5.28 and plotted in Figure 8.17 against solution pH for the three sodium carbonate solutions at different concentration.

Under ideal conditions, A is a constant for any one membrane system at constant temperature and independent of solution concentration and speciation. Figure 8.17 suggests that, in the present case, A is dependent both on solution pH and solution concentration. Typically, any changes in A are indicative of the occurrence of fouling, compaction or concentration polarisation. Clearly, fouling or compaction is not occurring, since water permeability does not follow a consistent downward trend throughout each experiment (from high pH to low pH) and from experiment to experiment (from low concentration to high concentration). It is possible

that concentration polarisation is occurring, but this phenomenon has not been predicted to occur under the prevailing conditions of feed velocity and pressure (see Section 8.4.2). Furthermore, the trends in A follow the J_W trends (Figure 8.18) rather closely, except that J_W decreases steadily with increasing concentration, while A apparently does not.

Figure 8.17
Variability of Water Permeability Parameter, A , with pH and Concentration of Sodium Carbonate Solutions Containing 1, 10 and 30 g/l Na



Given the properties of the nanofiltration membrane and the nature of the feed solution, it is postulated that the non-uniformity of A with pH results from the occurrence of one or both of the following phenomena:

- 1) Changes in the membrane chemistry, and therefore charge, with pH. Discussions with Dr Peter Sehn, of the Dow Membrane Technical Engineering Division in Germany (1994) confirm that the carboxylic acid groups on the membrane surface function as a weak cation exchange resin, the degree of negative charge, and therefore transport characteristics and permeability, being dependent on pH.
- 2) A secondary effect is the influence of pH on the geometry of the polymer comprising the membrane surface, which undergoes coiling or elongation under different conditions of pH. These physical or structural changes in turn alter the repulsion forces within the polymeric structure causing changes in the water permeability of the membrane.

The observed disparity in the trends of A and J_W at increasing solution concentration suggests that concentration polarisation may be having an effect in high concentration solutions. If this is the case then the osmotic pressure difference used in calculating A is too small (since it was based on feed concentration, which exceeds the concentration at the membrane surface), and the difference depends on the speciation at a given salt

concentration. However, the major effect between the different feed concentrations is feed osmotic pressure. In other words, the correction based on feed osmotic pressure is adequate to compensate for the differences in salt concentration, but not for the difference in speciation at a given salt concentration.

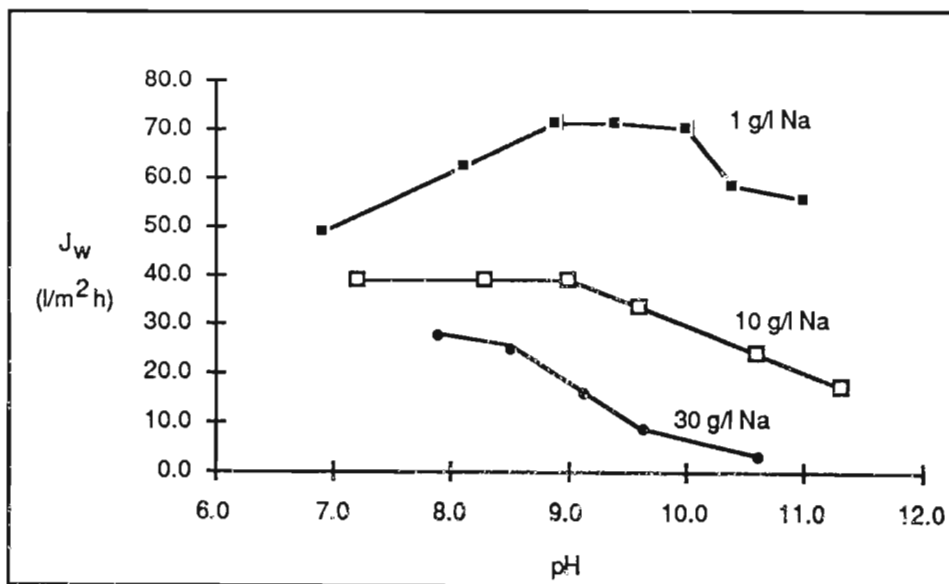
It is proposed therefore, that the apparent variations in A result from a complex arrangement of speciation, concentration polarisation, osmotic pressure and membrane polymer structure.

8.4.4. Water Flux Dependence on Solution Characteristics

Figure 8.18 indicates the observed variation of water fluxes with solution pH and concentration. As noted above in Section 8.4.3, trends in J_W parallel those of A , except in solutions of high concentrations and low pH. Obvious discontinuities in the observed trends occur at two pH values in the 1 and 30 g/l Na solutions and at one pH value in the 10 g/l Na solution. The pH values at which these discontinuities occur are listed in Table 8.2.

If the predominant influence on J_W was the osmotic pressure difference across the membrane, then, at constant applied pressure, it would be expected that J_W would increase proportionally with $\Delta\pi$ over the entire pH range from acidic to basic. However, trends in J_W are not consistent with $\Delta\pi$, and do not increase with decreasing pH over the whole pH range. It is proposed, therefore, that the effects of solution chemistry and speciation are the most important factors in determining the water flux for a particular solution concentration and pH.

Figure 8.18
Variation of Water Fluxes with pH in Sodium Carbonate Solutions
Containing 1, 10 and 30 g/l Na



In order to test this proposal, the observed discontinuities in J_W have been considered in the light of speciation theory. In this respect, Table 8.2 also lists observations regarding speciation at each of the pH values where discontinuities in J_W occur (these observations are based on Figure 8.7).

Table 8.2
Water Fluxes: Correlation of Discontinuities in Water Flux with Speciation Trends

Concentration (g/l Na)	Discontinuity in J_W	Speciation Trends
1 g/l Na	pH 10 to 10,4 pH 8,8	point of cross-over of HCO_3^- and $\text{CO}_3^{=}$ point of cross-over of NaHCO_3 and NaCO_3^-
10 g/l Na	pH 9	point of cross-over of NaHCO_3 and NaCO_3^-
30 g/l Na	pH 9,6 pH 8,5	point of cross-over of HCO_3^- and $\text{CO}_3^{=}$ point of cross-over of NaHCO_3 and NaCO_3^-

Analysis of Table 8.2 shows a clear correlation between observed discontinuities in J_W and speciation trends, and this correlation is consistent for all concentrations. Discontinuities in J_W occur at the cross-over point where two curves intersect (Figure 8.7), and when the species represented by these two curves have different charges. For example, in the solution containing 1 g/l Na, a sharp discontinuity in water flux is observed at around pH 10, where the divalent anion $\text{CO}_3^{=}$ replaces the monovalent anion as the dominant anionic species (or vice versa). Furthermore, as the divalent (monovalent) anion becomes the dominant species, that is at pH values higher (lower) than the pH of intersection, the water flux decreases (increases). This is consistent with membrane-solute interaction theory - retention of anions (and therefore cations) by the membrane increases with charge on the anions, resulting in increased osmotic pressure differences across the membrane, lower driving forces and lower water fluxes.

A similar discontinuity in J_W is observed at pH 9,6 in the solution containing 30 g/l Na. Again it is proposed that this results from the increasing importance of divalent $\text{CO}_3^{=}$ in the system, compared to monovalent HCO_3^- . Although no corresponding discontinuity was observed in the 10 g/l Na solution, it is proposed that J_W should have increased more rapidly below pH 9,6, and that the fact that this increase was not observed was a result of inaccuracies in the physical measurement of fluxes.

Speciation data for each solution, also strongly suggests that the discontinuity in J_W at pH 8,8; 9; and 8,5 for the 1; 10 and 30 g/l Na solutions respectively can be related to the points at which the concentrations of the neutral species NaHCO_3 equals that of the monovalent anion pair, NaCO_3^- . Flux trends are consistent with the theory that, while neutral species pass freely through the membrane, there is a tendency for negative species to be retained, and this in

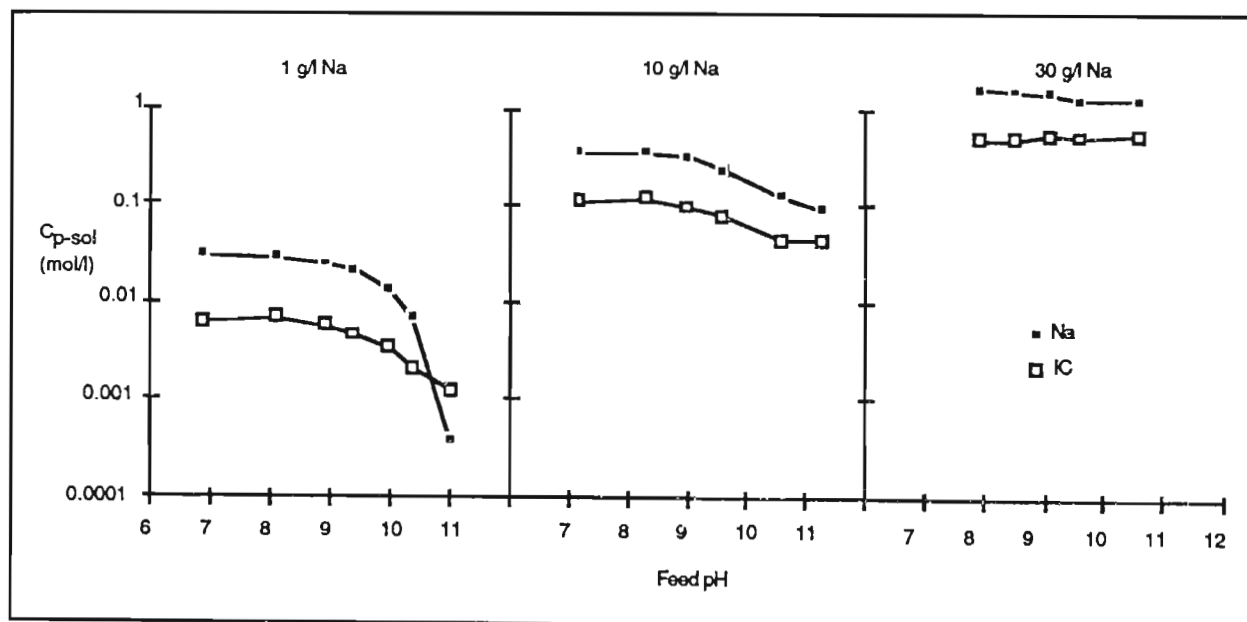
turn leads to higher osmotic pressure differences and lower water fluxes at pH values below the point of cross-over of the NaCO_3^- and NaHCO_3 curves.

8.4.5. Solute Flux Dependence on Solution Characteristics

The retention level of a solute expresses the solute flux, and can vary widely depending on the operational parameters and the chemical interactions or surface forces that occur between the solvent, solute and membrane. The retention and solute flux should be considered in the context of the chemistry and the test conditions for nanofiltration.

Figure 8.19 indicates the observed trends in permeate concentration (Na and inorganic carbon components) with pH and solution concentration. While permeate concentration increases with decreasing pH for both components in all solutions, the relative increase is highest in low concentration solutions. Considering speciation data, and specifically total charge in sodium carbonate solutions at varying pH and concentration (Figure 8.10), it is suggested that the relatively sharp decrease in permeate concentration at elevated pH values in low concentration solutions (1 g/l Na) results from the larger portion of species existing as divalent anions in these solutions, than in more concentrated solutions at equivalent pH values. This relatively high proportion of divalent anions increases retention and osmotic pressure gradient, resulting in reduced flux of solute (and water, although water flux decreases at a slower rate).

Figure 8.19
Variation In Permeate Na and IC Concentrations with pH and Concentration of Sodium Carbonate Solutions



Although the trends in permeate concentration are interesting, a more appropriate method of examining solute transfer is to consider normalised solute flux variations with pH and solution concentration. In a single salt solution, in the absence of concentration polarisation (where the concentration in the bulk feed equals the concentration at the membrane interface), the solute fluxes are expected to be directly dependent on the concentration gradient across the membrane (see equation 5.29). Figure 8.20 indicates the relationship between normalised solute fluxes and solution pH and concentration. (Because of the analytical limitations in measuring actual species, this evaluation focuses rather on the two principal solution components.) Again inconsistent trends are observed. Particularly the peak in the Na fluxes is dramatic for the 1 and 10 g/l Na solutions. The pH values at which discontinuities occur in J_{Na} are listed in Table 8.3.

Figure 8.20
Variation In Solute Fluxes with pH and Concentration of Sodium Carbonate Solutions

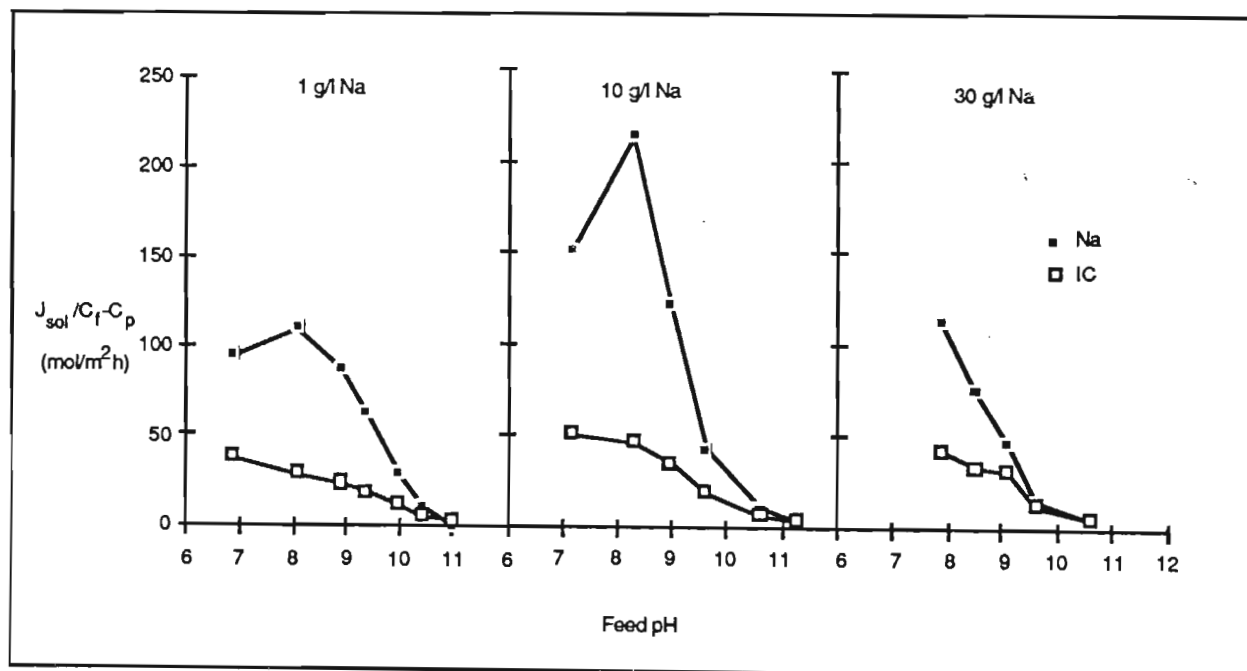


Table 8.3
Solute Fluxes: Correlation of Discontinuities In Water Flux with Speciation Trends

Concentration (g/l Na)	Discontinuity in J_{Na}	Speciation Trends
1 g/l Na	pH 10 to 10,4 pH 8,2	point of cross-over of HCO_3^- and $NaCO_3^-$ point of cross-over of H_2CO_3 and $NaCO_3^-$
10 g/l Na	pH 9,6 pH 8,3	point of cross-over of HCO_3^- and $NaCO_3^-$ point of cross-over of H_2CO_3 and $NaCO_3^-$
30 g/l Na	pH 9,5	point of cross-over of HCO_3^- and $NaCO_3^-$

Table 8.3 also lists points of cross-over which occur at pH values corresponding to discontinuities in J_{Na} . It is proposed that the discontinuities observed at higher pH values result from a change in the predominant monovalent anion, from HCO_3^- at pH values below the point of cross-over to $NaCO_3^-$ at pH values above this point. This is consistent with the observation that at pH values above this point of cross-over, the rate of decrease in the ratio $J_{Na}/C_f - C_p$ falls off, implying that J_{Na} is increasing at a faster rate than the concentration gradient. This can be explained by assuming that negative charge is transported across the membrane predominantly by the $NaCO_3^-$ ion complex at higher pH values, and by HCO_3^- ions at lower pH values.

The discontinuities of J_{Na} at pH values of 8,2 and 8,3 in the 1 and 10 g/l Na solutions respectively, correspond to the points:

- 1) Of cross-over of H_2CO_3 and $NaCO_3^-$
- 2) Near which the curves of $NaHCO_3$ and $NaCO_3^-$ intersect
- 3) At which the concentration of the predominant monovalent anionic species, HCO_3^- starts to decline - and is replaced in solution by the $NaCO_3^-$ ion complex.

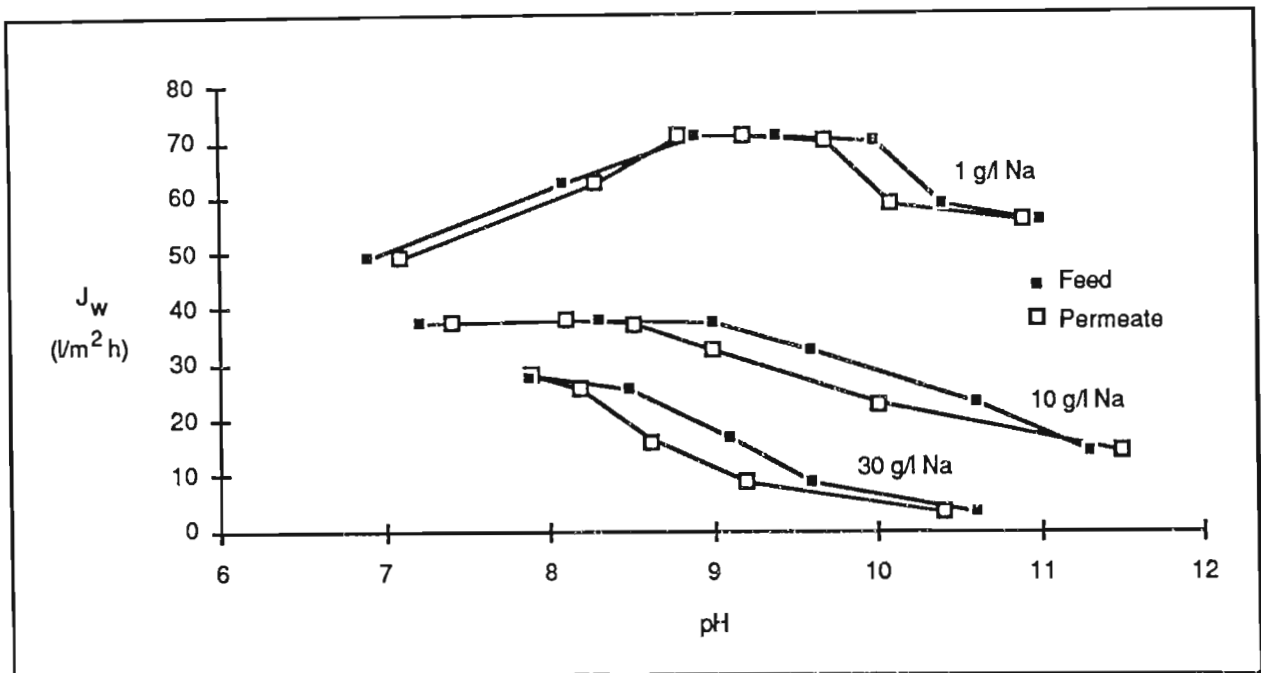
At pH values below these points of cross-over, where $NaHCO_3$ and H_2CO_3 predominate over $NaCO_3^-$, the ratio of $J_{Na}/C_f - C_p$ falls off steeply, implying that J_{Na} is decreasing fast relative to the concentration gradient. Based on these observations, it is predicted that an analogous peak in the ratio will occur at in the 30 g/l Na solution at pH 7,5 - which is outside the range of pH in the current experimental investigation.

Note that throughout the pH and concentration ranges under consideration, the dominant Na species is the Na^+ ion. However, the concentration of this ion in solution remains relatively constant throughout the pH excursion, and does not influence the membrane performance; instead performance is determined by variations in the less concentrated species.

8.4.6. pH Variation Across the Membrane

Figure 8.21 has been plotted to show the trends in feed and permeate pH for different water fluxes. The observed variation in the pH values of the feed and permeate is consistent for solutions of all concentrations investigated:

Figure 8.21
Relationship Between Feed and Permeate pH Values for Different Water Fluxes In Sodium Carbonate Solutions of Varying Concentration



- 1) At high feed pH values, the difference in the pH of the feed and permeate is small, and in the case of the 10 g/l Na solution, is actually negative ie the permeate pH is higher than the feed pH.
- 2) The pH of the permeate is significantly lower than that of the feed for mid-range pH values.
- 3) The gap between permeate pH and feed pH closes again at lower pH values, and in the 1 g/l Na solution shows a reverse trend ie the permeate pH is higher than that of the feed.

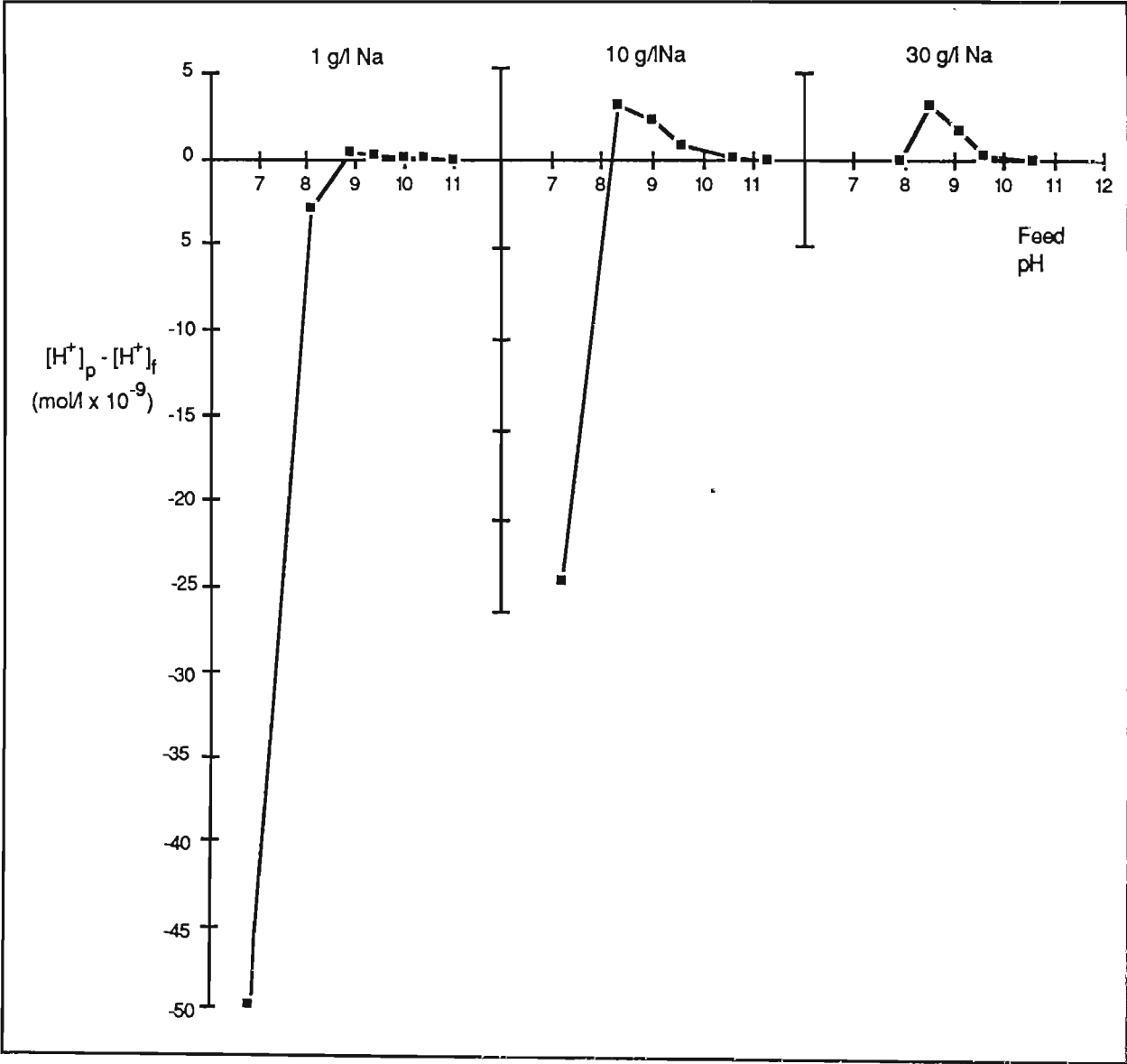
In all cases, the observed difference in pH between the feed and the permeate results primarily from preferential transport of certain species through the membrane, and the redistribution of these species in the permeate to attain equilibrium. The direction and magnitude of redistribution determines the direction and magnitude of pH changes.

To examine, in more detail, the variation of acidity between the feed and the permeate, the difference in hydrogen ion concentrations in the two streams has been compared for each sample set in each of the three experiments. Table 8.4 summarises these results, while Figure 8.22 illustrates the dramatic effect of feed pH on the hydrogen ion concentration gradient across the membrane, irrespective of concentration, and particularly in solutions of low pH.

Table 8.4
Gradient in Hydrogen Ion Concentration Across the Membrane During Nanofiltration of Sodium Carbonate Solutions at Varying pH and Concentration

Experiment 6 1 g/l Na		Experiment 7 10 g/l Na		Experiment 8 30 g/l Na	
Feed pH	$[H^+]_p - [H^+]_f$	Feed pH	$[H^+]_p - [H^+]_f$	Feed pH	$[H^+]_p - [H^+]_f$
11,0	2,6E-12	11,3	-2,0E-12	10,6	1,5E-11
10,4	4,0E-11	10,6	7,5E-11	9,6	3,8E-10
10,0	1,0E-10	9,6	7,5E-10	9,1	1,7E-09
9,4	2,3E-10	9,0	2,2E-09	8,5	3,2E-09
8,9	3,3E-10	8,3	2,9E-09	7,9	0
8,1	-2,0E-09	7,2	-6,0E-07		
6,9	-5,0E-08				

Figure 8.22
Gradient in Hydrogen Ion Concentration Across the Membrane During Nanofiltration of Sodium Carbonate Solutions at Varying pH and Concentration



An examination of the trends predicted by speciation modelling has been undertaken to understand the influence of solution chemistry on the pH profiles of the feed and permeate streams.

On decreasing the pH of the feed solutions from their maximum value, there is a consistent upward trend in the magnitude of the hydrogen ion gradient across the membrane, and furthermore, this gradient is positive initially (permeate $\{H^+\} > \text{feed } \{H^+\}$). The positive gradient results because of the retention of divalent CO_3^{2-} anions by the membrane and the preferential passage of monovalent $NaCO_3^-$ and HCO_3^- anions through the membrane. To address the imbalance in the permeate, these anions redistribute themselves, with the formation of CO_3^{2-} anions and the release of hydrogen ions. The slope (rate of increase in the magnitude of the gradient) changes slightly at pH values of approximately 10,0; 9,7 and 9,6 for the 1; 10 and 30 g/l Na solutions respectively. Using Figure 8.7, these pH values may be correlated with the intersection of the HCO_3^- and CO_3^{2-} equilibrium curves. At pH values above the point of cross-over, CO_3^{2-} anions predominate, and solute fluxes are low; although redistribution of species occurs in the permeate, overall concentrations of species are low, as are effects of redistribution on the hydrogen ion concentration. As the relative concentration of HCO_3^- anions increase, solute fluxes increase and redistribution of species within the permeate results in the release of increasing amounts of hydrogen ions.

The dramatic change in the magnitude and direction of the hydrogen ion concentration gradient at pH values of approximately 8,6; 8,3 and 8,5 for the 1; 10 and 30 g/l Na solutions respectively may be correlated to points of cross-over of the $NaCO_3^-$ anion and the $NaHCO_3$ ion pair in an environment where the HCO_3^- anion predominates. It is proposed that the magnitude of the change results mainly from the high solute fluxes at lower pH values; and the fact that redistribution in a relatively concentrated solution has a more pronounced effect on hydrogen ion concentrations. The direction of the change is such that the hydrogen ion concentration in the permeate is lower than that in the feed; this implies that the shift in the equilibrium of the transported species is in a direction which consumes hydrogen ions. In turn, this would indicate that, at low concentrations, the transport of monovalent species predominates over the transport of neutral ion pairs ($NaHCO_3$ and H_2CO_3), and that the rebalance of equilibrium involves the formation of these neutral species in the permeate.

8.4.7. Impure Sodium Carbonate Solutions

Speciation theory has been used to examine, in a qualitative way, the observed performance of the nanofiltration membrane during experiments 4 and 5, in which sodium carbonate

solutions (10 g/l Na), contaminated with magnesium and calcium salts (10 mg/l Ca and 10 mg/l Mg), were nanofiltered and the effect of the complexing agent EDTA (100 mg/l as tetra-sodium salt) on hardness ion retentions was evaluated.

The empirical results are discussed in Sections 8.1.3 and 8.2 and summarised in Figure 8.5. The retention of hardness ions was observed to be pH dependent, varying from below 60 % at neutral pH to 90 % at pH 11. In the absence of EDTA, Ca retentions were marginally lower than magnesium retentions throughout the pH range. The addition of EDTA had a dramatic effect in Ca retention, increasing it above Mg retention to around 90 % throughout the pH range. Mg retentions also improved throughout the pH range, but to a lesser degree (ranging from 74 % at neutral pH to above 90 % at pH 11).

Section 8.3.2 describes the results of chemical speciation modelling of Ca, Mg and EDTA species in a sodium carbonate solution (10 g/l Na).

8.4.7.1 Solutions Without EDTA Complexation

In the absence of EDTA, all Ca and Mg species are neutral or positively charged. Therefore, they either do not interact significantly with the nanofiltration membrane, or they interact positively with it, that is, they are adsorbed by the membrane. Because the principal objective of using this technique is to separate the hardness ions from the solution, this feature (tendency of the species to be pass freely through, or be adsorbed by, the membrane) is counterproductive, since it reduces the ability of the membrane to retain species containing hardness ions.

The nature of the Ca and Mg species present at different pH values, parallels that of the inorganic carbon species, as illustrated in Figure 8.11. That is to say, at high pH values, the neutral species CaCO_3 and MgCO_3 predominate, while at lower pH values (say below 9), the divalent Ca^{++} and Mg^{++} species predominate, together with high concentrations of CaHCO_3^- and MgHCO_3^- . Thus, the observed trend of decreasing retention with decreasing pH can be explained by consideration of the solution chemistry. Figure 8.13 illustrates the distribution of Ca and Mg between various species at equilibrium over the pH range under consideration. At lower pH values, there is a prevalence of divalent cations, which are adsorbed by the membrane. In addition, at lower pH values, the predominant species are smaller than at high pH values. These two aspects (membrane adsorption and size) account for the reduced retention at lower pH values. At increasing pH values, the predominant species become larger and neutral, and their passage through the membrane is not facilitated by positive membrane-

solute interactions and, in fact, may be further hindered by size exclusion. Therefore, solute flux is reduced and retentions are increased.

Speciation modelling can be used to explain the fact that, in the absence of EDTA, observed Ca retentions are slightly lower than observed Mg retentions throughout the pH range. If it is assumed that ion permeability is mainly a function of size and charge on the species, speciation modelling projects that Ca retentions will be lower than Mg retentions throughout the pH range, since the proportion of Mg existing as cationic species is higher throughout this range than the proportion of Ca existing as cationic species (Figure 8.13).

8.4.7.2 Solutions With EDTA Complexation

In the presence of EDTA, speciation modelling predicts a difference in the relative distribution of Ca and Mg between species in solution over the pH range under consideration. This difference can explain the observed disparity between the performance of the nanofiltration membrane towards Ca and Mg species in solutions which contain EDTA, as well as the inconsistency between the trends in retention of each component with pH.

Figure 8.12 and especially Figure 8.14 illustrate the strong complexing tendency of Ca and EDTA to form the very stable Ca-EDTA complex, which predominates at all pH values, and which accounts for over 95 % of the Ca present in solution. By contrast the Mg-EDTA complex is less stable, and does not predominate at any pH. Instead, Mg^{++} ions predominate at low pH values and $MgCO_3$ predominates at high pH levels. Throughout the pH range, the proportion of Ca bound up in EDTA complexes is more than double that of Mg bound up in analogous complexes. Since EDTA complexes are excluded from permeating the membrane because of size and steric considerations, Ca species will exhibit a far greater tendency to be retained than will Mg species.

While Ca retention in the presence of EDTA does not show much variation with pH, Mg retention is pH dependent. This is explained by the fact that the distribution of Ca between species remains relatively constant throughout the pH range (and is almost exclusively Ca-EDTA), while Mg is distributed between at least four Mg-containing species over this range (see Figure 8.14). These species are either divalent cations, monovalent cations or neutral species, and their equilibrium distribution at any one pH determines the permeability of Mg through the membrane. For example, at low pH values, where Mg^{++} predominates, retention is lowest, while retention is highest where the neutral species $MgCO_3$ and Mg-EDTA predominate.

8.5. Transport Modelling of Nanofiltration

The membrane transport model, PERMSEP, was run for sodium carbonate solutions containing 1; 10 and 30 g/l Na. The complete results are presented in a separate publication (Brouckaert, in press), and the input and output data is in Appendix 7. The graphical results for the 10 g/l Na solution are presented in Figures 8.23 to 8.30.

The major observations are as follows:

- 1) For experiment 9 (10 g/l Na; pH 9,6; variable feed pressures and flow rates), very good correlations were obtained for the effects of feed pressure on permeate flux (Figure 8.23), total carbonate concentration (Figure 8.24) and total hydrogen ion concentration (Figure 2.25). However, for the relationship between sodium concentration and pressure, the model predicted a monotonic decrease of sodium concentration with pressure, whereas the experimental results showed a minimum concentration (Figure 8.26).
- 2) For experiment 7 (10 g/l Na; variable pH; constant feed pressure and flow), predicted permeate fluxes were in good agreement with experimental data (Figure 8.27), as are the predicted concentrations of total carbonates, hydrogen ions and sodium (Figures 8.28, 8.29 and 8.30).
- 3) For experiment 7, the initial feed was 10 g/l sodium carbonate at a pH of 11,2, and the pH was reduced by the addition of nitric acid. Similar trends are predicted of nitrate concentration, bicarbonate concentration and Na^+ ion and the total sodium concentration as a function of pH (Figures 8.28, 8.29 and 8.30). The nitrate component does not speciate significantly into any species other than nitrate ions, and at lower pH values is the major anion. Furthermore, of common anions, nitrate ions are least retained by a nanofiltration membrane (Section 5.3.4.2). The passage of a cation is enhanced by the presence of permeable (small size and charge density) anions. In order to maintain electroneutrality, the passage of nitrate ions enhances the permeation of sodium ions. On the other hand, if the solution were acidified with sulphuric acid, it is predicted that sodium permeation would have been reduced. The greater influence of nitrate ions than bicarbonate ions on sodium transport at lower pH values, was not predicted in the semi-quantitative work discussed in Section 8.4, since for this work, the nitrate component, being non-speciating, was excluded from consideration. However, PERMSEP modelling data indicates that the nitrate ion has major influence on sodium permeation and cannot be excluded if accurate predictions are to be made.

Figure 8.23
Predicted Permeate Flux as a function of Feed Pressure and Flow Rate
(Nanofiltration Experiment 9)

Note: The continuous line represents the PERMSEP prediction, whereas the points are the measurements

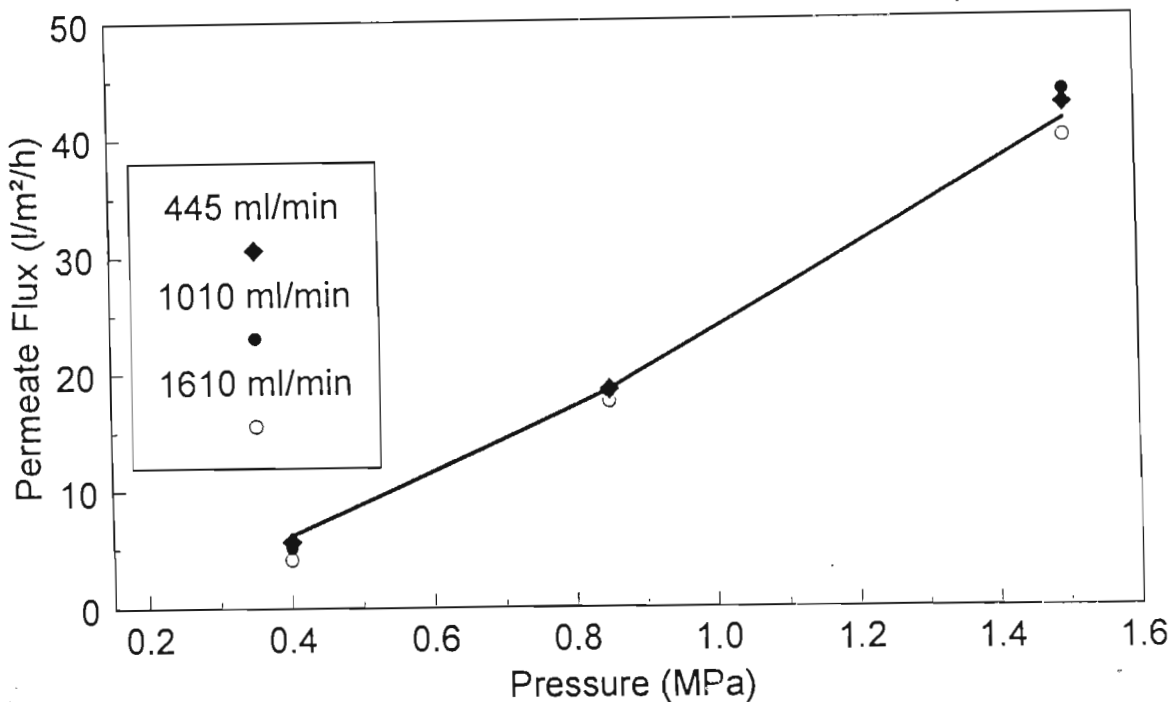


Figure 8.24
Predicted Permeate Total Carbonate Concentration as a Function of Feed Pressure
and Flow Rate (Nanofiltration Experiment 9)

Note: The continuous line represents the PERMSEP prediction, whereas the points are the measurements

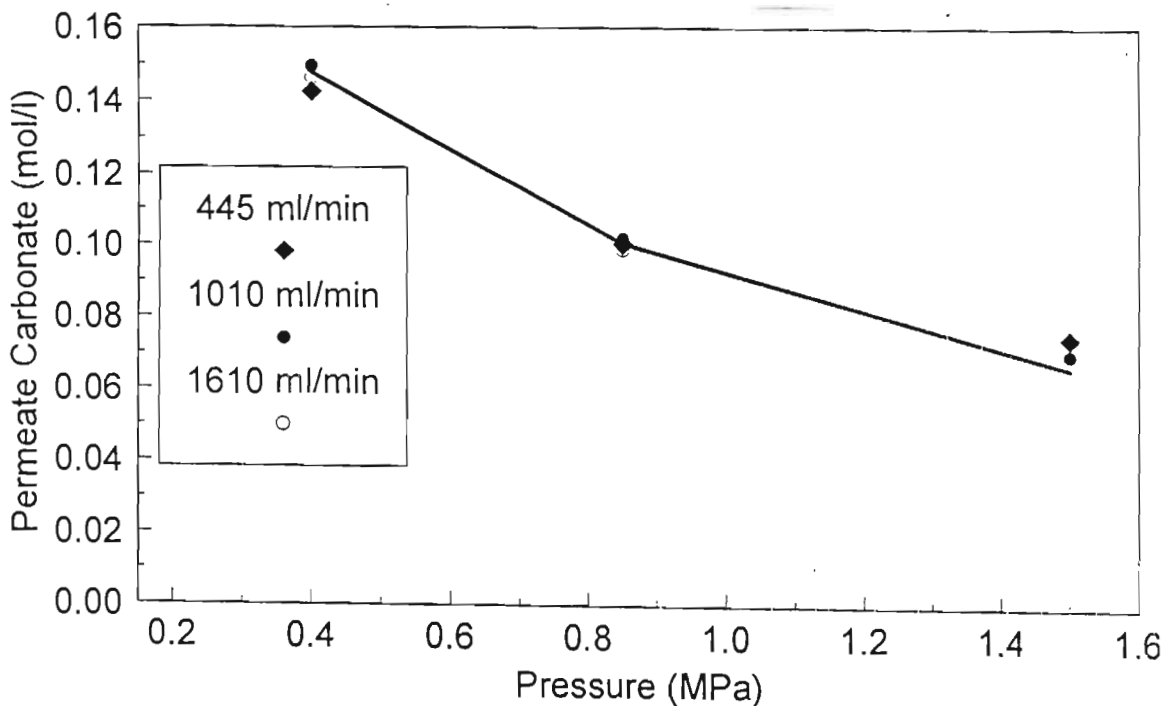


Figure 8.25
Predicted Permeate Total Hydrogen Ion Concentration as a Function of Feed Pressure and Flow Rate (Nanofiltration Experiment 9)

Note: The continuous line represents the PERMSEP prediction, whereas the points are the measurements

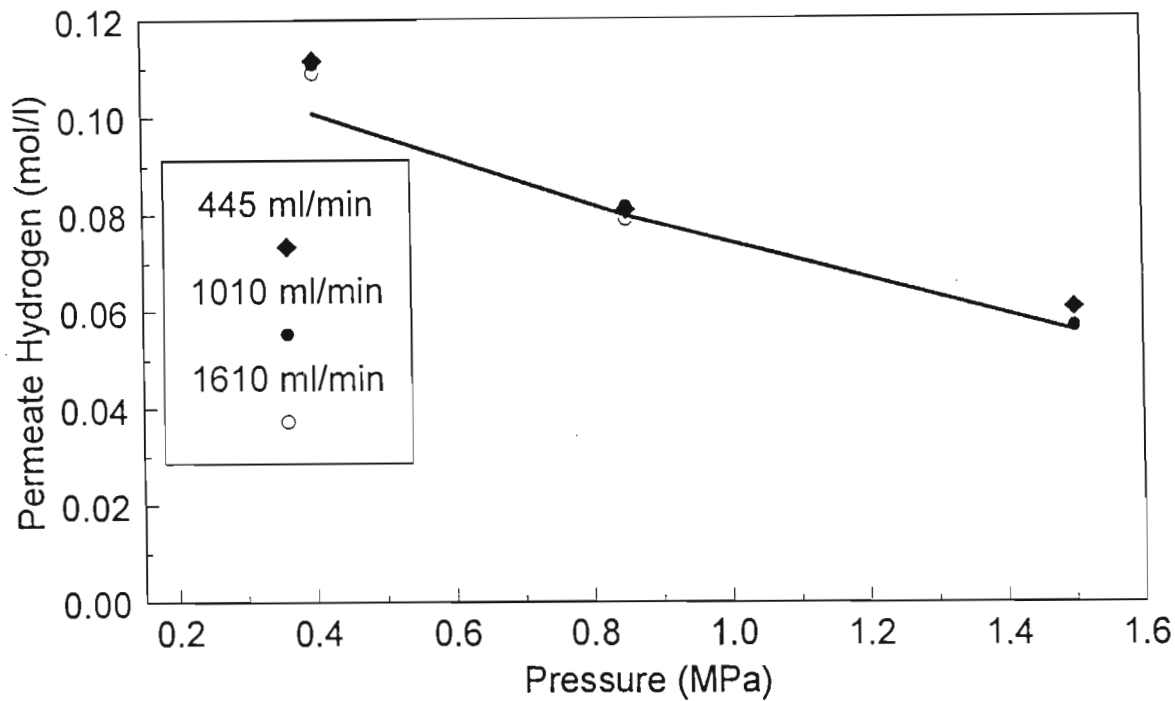


Figure 8.26
Predicted Permeate Total Sodium Concentration as a Function of Feed Pressure and Flow Rate (Nanofiltration Experiment 9)

Note: The continuous line represents the PERMSEP prediction, whereas the points are the measurements

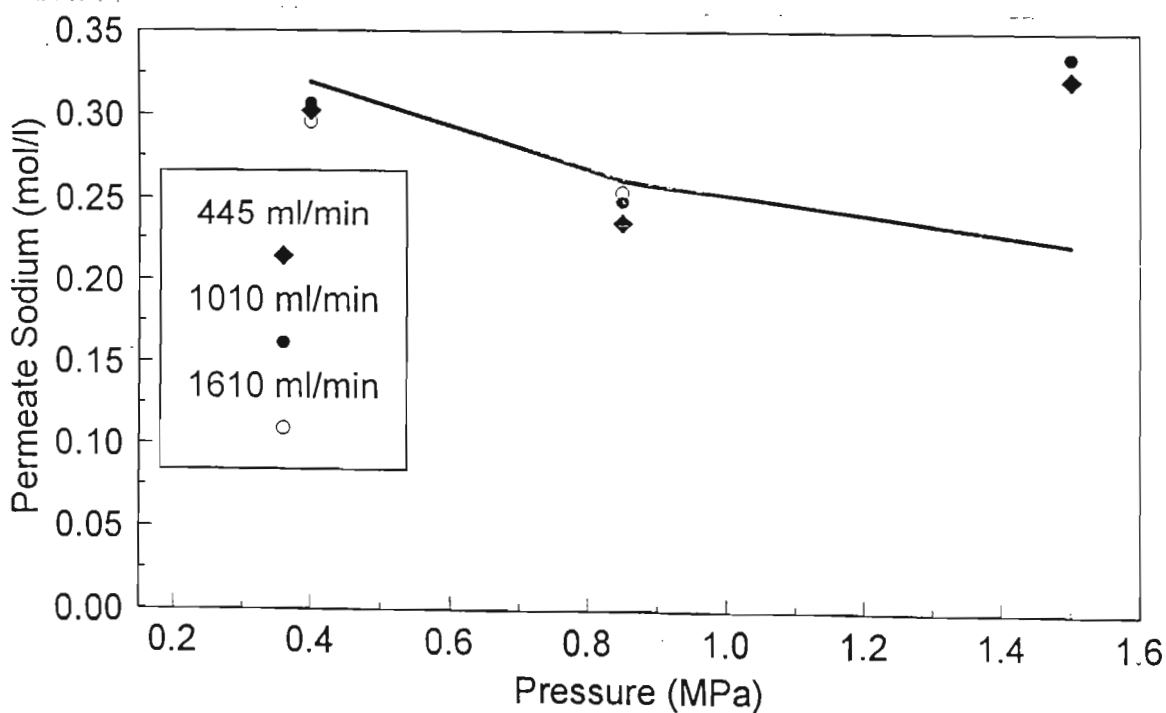


Figure 8.27
Predicted Permeate Flux as a Function of Feed pH (Nanofiltration Experiment 7)

Note: The continuous line represents the PERMSEP prediction, whereas the points are the measurements

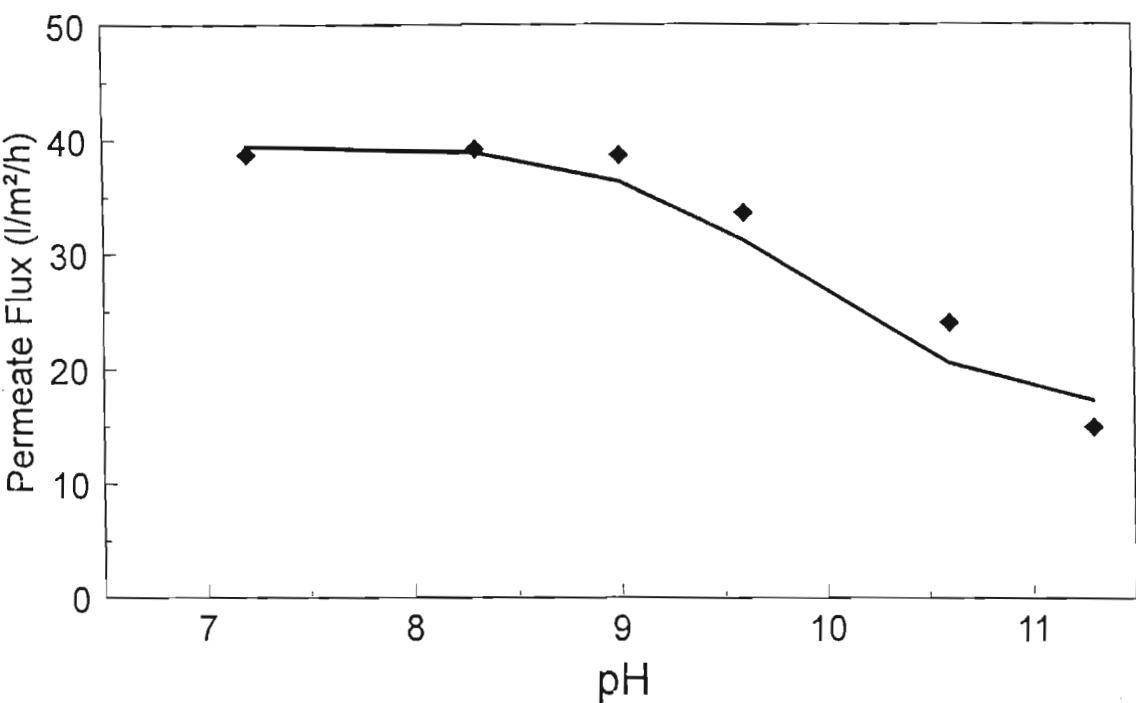


Figure 8.28
Predicted Permeating Concentrations of Total and Individual Carbonate Species as a Function of Feed pH (Nanofiltration Experiment 7)

Note: The continuous line represents the PERMSEP prediction, whereas the points are the measurements

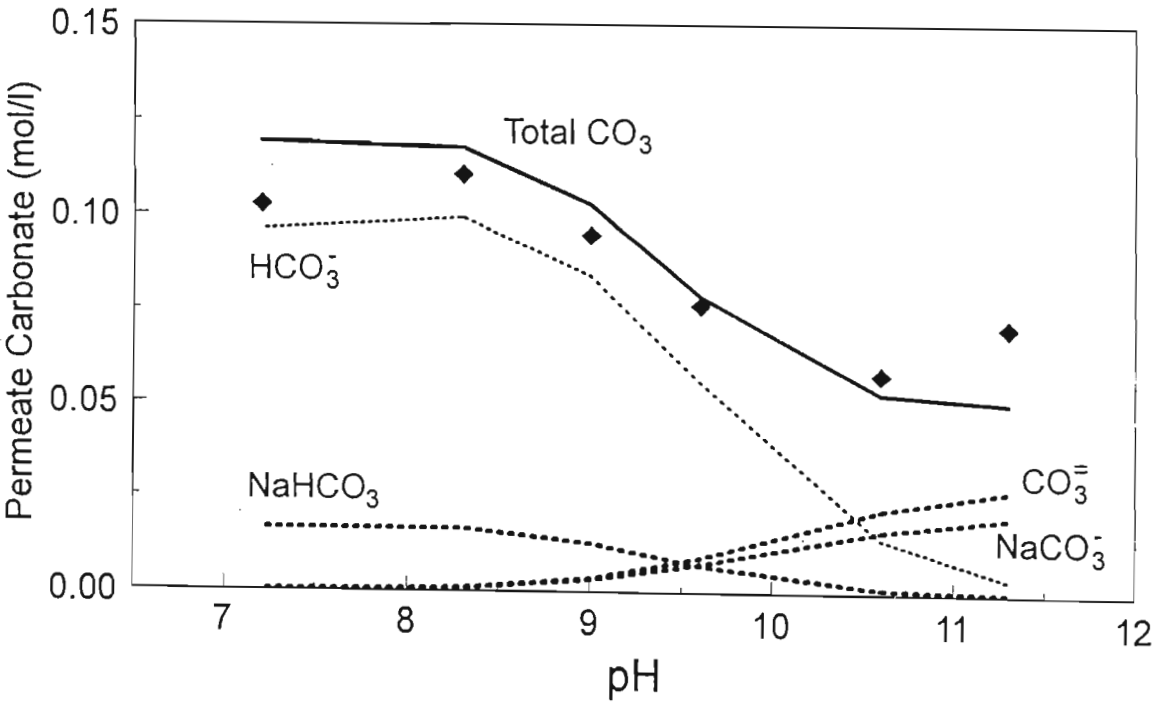


Figure 8.29
Predicted Permeating Concentrations of Total and Individual Hydrogen Ion Species
as a Function of Feed pH (Nanofiltration Experiment 7)

Note: The continuous line represents the PERMSEP prediction, whereas the points are the measurements

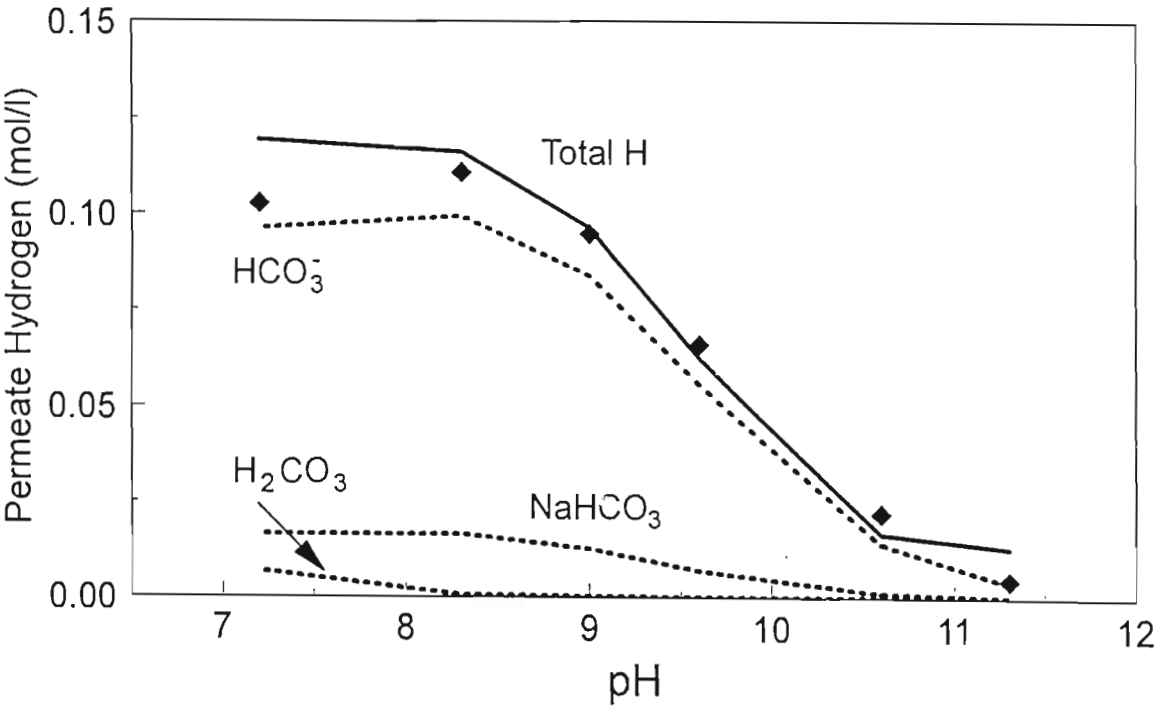
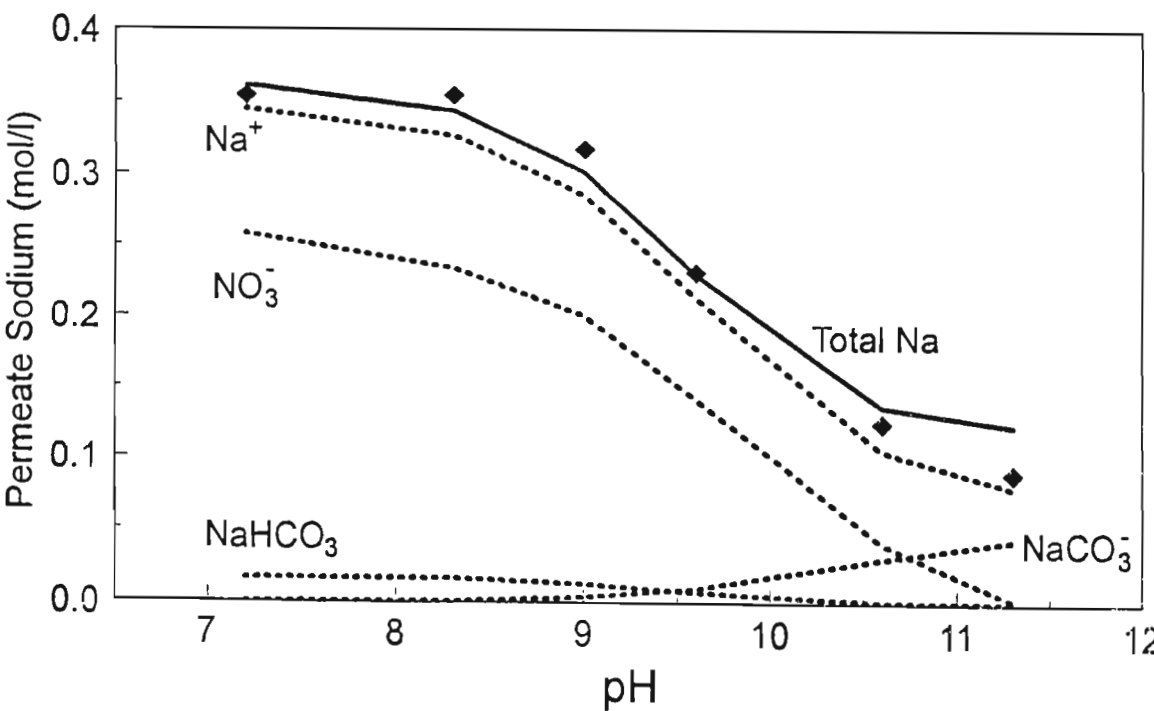


Figure 8.30
Predicted Permeating Concentrations of Nitrate, and Total and Individual Sodium
Species as a Function of Feed pH (Nanofiltration Experiment 7)

Note: The continuous line represents the PERMSEP prediction, whereas the points are the measurements



SECTION 9

RESULTS AND DISCUSSION OF SUPPLEMENTARY INVESTIGATIONS OF ELECTROLYSIS

This section presents and discusses the results of the supplementary investigations aimed at examining more closely, either practically under controlled laboratory conditions or theoretically, certain aspects of electrochemical recovery.

Electromembrane fouling is covered in Section 9.1, electromembrane cleaning in Section 9.2 and other electrode materials in Section 9.3. The procedures relating to these investigations are presented in Section 6.4.

9.1. Electromembrane Fouling

These laboratory experiments aimed to examine, under controlled conditions, the potential for divalent cations present in the pretreated effluent to foul the electromembrane, causing temporary or permanent loss of performance, and to understand the mechanism whereby insoluble compounds of these cations are deposited on the electromembrane surface. The experimental apparatus and procedures are detailed in Section 6.4.1. The experimental and analytical results are presented in Appendix 8 (Tables A8-1 to A8-4) for the four batches of pretreated scouring effluent which were electrolysed during the laboratory trials. The first three batches were electrolysed consecutively. The fourth batch was electrolysed after the electromembrane had been examined and treated to remove fouling agents, thereby restoring performance. The current discussion of the results examines the effects of long term exposure of the electromembrane on its area-resistance; the relationship between the area-resistance and concentration of hardness ions in the anolyte; current efficiencies; scale characteristics and restoration of electromembrane performance.

9.1.1. Electromembrane Area-Resistance

An increase in the electromembrane area-resistance, R_{mem} , may be an indication that fouling or scaling of the electromembrane has occurred. R_{mem} is calculated from the equation:

$$R_{mem} = \frac{E_{mem}}{CD} \quad (9.1)$$

where E_{mem} is the volt drop across the electromembrane, which is calculated from equations derived in Appendix 8 using experimentally determined volt drops between the platinum

probes positioned on either side of the electromembrane. In carrying out these calculations, the effect of variations in electrolyte concentration and temperature were considered, since both these parameters influence conductivity and resistance. Conductivity corrections are presented in Appendix 8, together with the derivation of equations used to calculate electromembrane area-resistance.

Tables A8-5 to A8-8 in Appendix 8 give the calculated figures for R_{mem} for batches 1 to 4 respectively. These results are summarised in Figure 9.1, which illustrates the relationship between the electromembrane area-resistance and the total current passed during each batch. For each batch of effluent, there is an increase in electromembrane area-resistance with increasing passage of current. Such an increase could be indicative of electromembrane fouling, or could result from decreasing anolyte concentration. Figure 9.2 shows such an effect, with R_{mem} increasing with decreasing sodium concentration in the anolyte. Although some increase will result from lower anolyte concentrations, progressive fouling is indicated by the fact that the electromembrane area-resistance did not return to its initial level when a new batch of effluent was introduced. In fact, the electromembrane area-resistance at the start of batches 1, 2 and 3 increased from 1,7 to 3,0 to 5,9 ohms/1 000 m² respectively. The effects of cleaning the electromembrane between batches 3 and 4, which gave rise to significant improvement in performance, are discussed in a later section.

9.1.2. Effect of Hardness-Ion Concentration on Area-Resistance

In considering the economic viability of the treatment sequence, one of the criteria for success is a long electromembrane life, with minimal, or at least controlled and reversible, fouling and scaling. The manufacturers of Nafion 324 electromembrane recommend upper limit concentrations of 0,1 mg/l Mg and 0,5 mg/l Ca for non-fouling performance (based mainly on the assumption that the precipitation of hydroxides of divalent cations is the primary area of concern). The magnesium and calcium concentrations of the pretreated effluent significantly exceed these recommended values. In fact, the average concentrations of magnesium and calcium present were 6 and 13 mg/l respectively. The fate of these divalent cations during electrolysis has been examined; using recorded electrolyte concentration and volume data, the total amount of calcium and magnesium present in the anolyte during each batch has been calculated and monitored over the course of electrolysis. These calculations are detailed in Table A8-9 in Appendix 8 and plotted in Figures 9.3 and 9.4 for magnesium and calcium respectively. The relatively small decrease in the total amounts of magnesium in the anolyte during batch 1 (and particularly during the initial stages) would suggest that magnesium loss was not the main cause of increased electromembrane area-resistance. Likewise, the total amount of calcium stayed relatively constant for the first four days. As the

experiment progressed, total amounts of magnesium and calcium present in the anolyte decreased substantially, by 15 and 50 % respectively with a total passage of 16,4 F. However, there was no parallel increase in calcium and magnesium in the catholyte, indicating presumably that these cations are leaving the anolyte and entering the electromembrane structure. Therefore, it is suggested that the increase in area-resistance during the initial stage of batch 1 was mainly a result of the decrease in the conductivity of the anolyte as the sodium concentration fell from 9,06 g/l to 5,7 g/l, and that the increase from day 4 resulted from a combination of both electromembrane fouling and decreasing anolyte concentration. This suggestion is confirmed in Figure 9.5, where for a period of four days current efficiencies for sodium transport were 100 %. Further substantiating evidence for this suggestion is obtained from similar studies carried out using sodium chloride anolytes (Pollution Research Group, 1989).

These studies showed that, at low anolyte concentrations (6 to 12 g/l Na), fouling by precipitation of divalent metal hydroxides is accelerated and pronounced, compared to that observed in solutions of higher electrolyte concentration. Examination of Figures 9.3 and 9.4 indicates that, compared to batch 1, the loss of magnesium and calcium from the anolyte in batches 2, 3 and 4 was accelerated. Over the course of batch 2 (33,5 F), total calcium and magnesium loss was 67 and 69 % respectively, while during batch 3 (49 F) total loss was 74 % for each cation. During electrolysis of the second batch, a white crust became visible on the cathode side of the electromembrane, which also developed a bulge towards the cathode, reducing the distance between the cathode and electromembrane. This reduced distance has been considered in all calculations. The formation of this crust and the concurrent loss of calcium, and to a lesser extent, magnesium from the electrolytes suggested that the precipitation of insoluble salts was the most likely cause of the observed loss in electromembrane performance (see Section 9.1.3). Total loss of calcium and magnesium during batch 4, after the electromembrane had been treated, was 52 and 59 % respectively for a passage of 35 F of current. During electrolysis of this batch, visible growth of the white crust continued, this time on the anode side of the electromembrane. The formation of this crust is discussed in more detail in Section 9.1.5.

Figure 9.1
Dependence of Membrane Area-Resistance on Current Passed

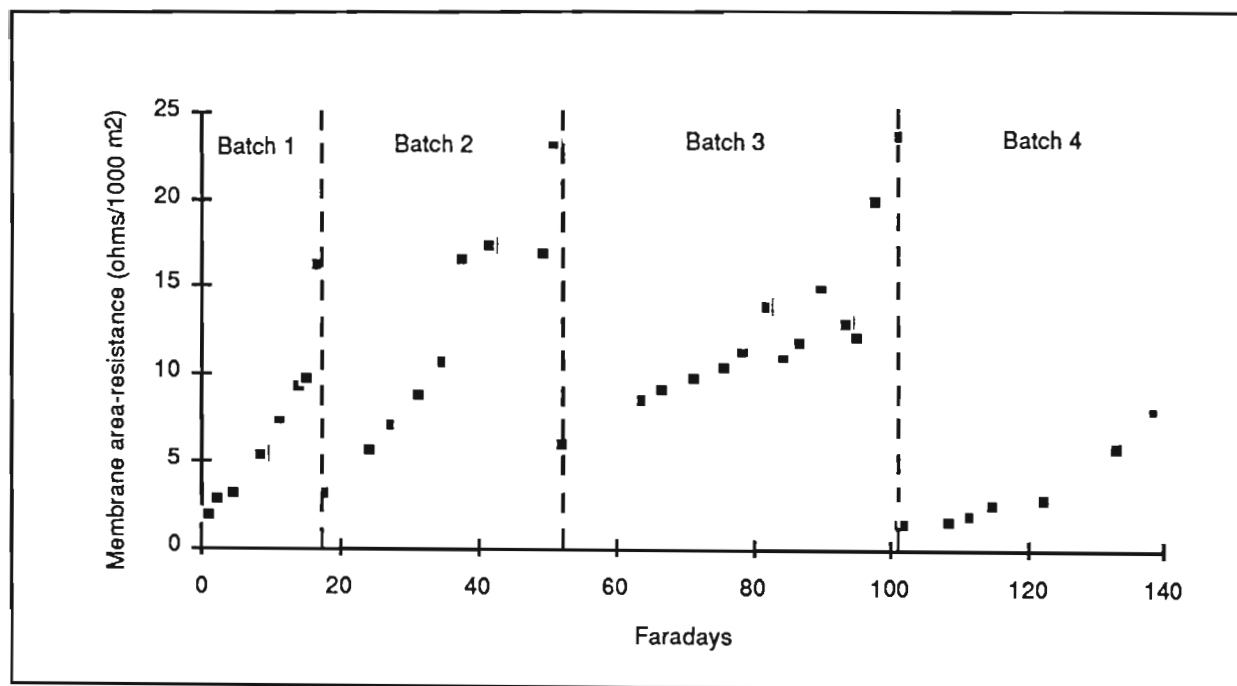


Figure 9.2
Dependence of Membrane Area-Resistance on Anolyte Sodium Concentration

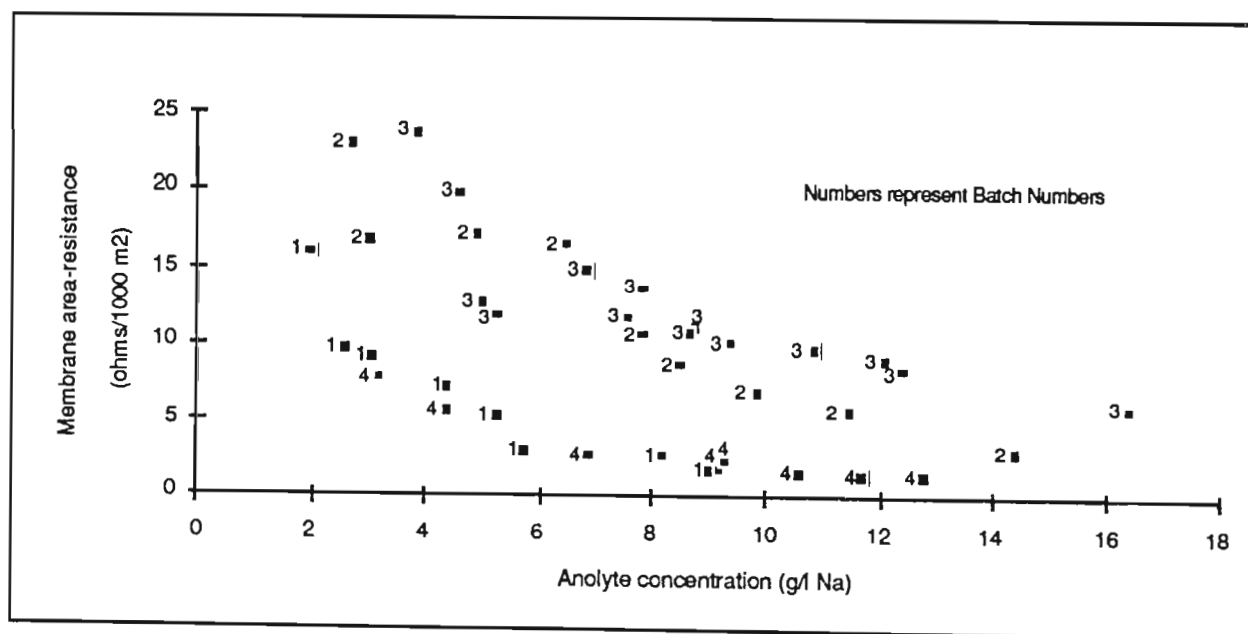


Figure 9.3
Relationship Between Membrane Area-Resistance and Total Magnesium

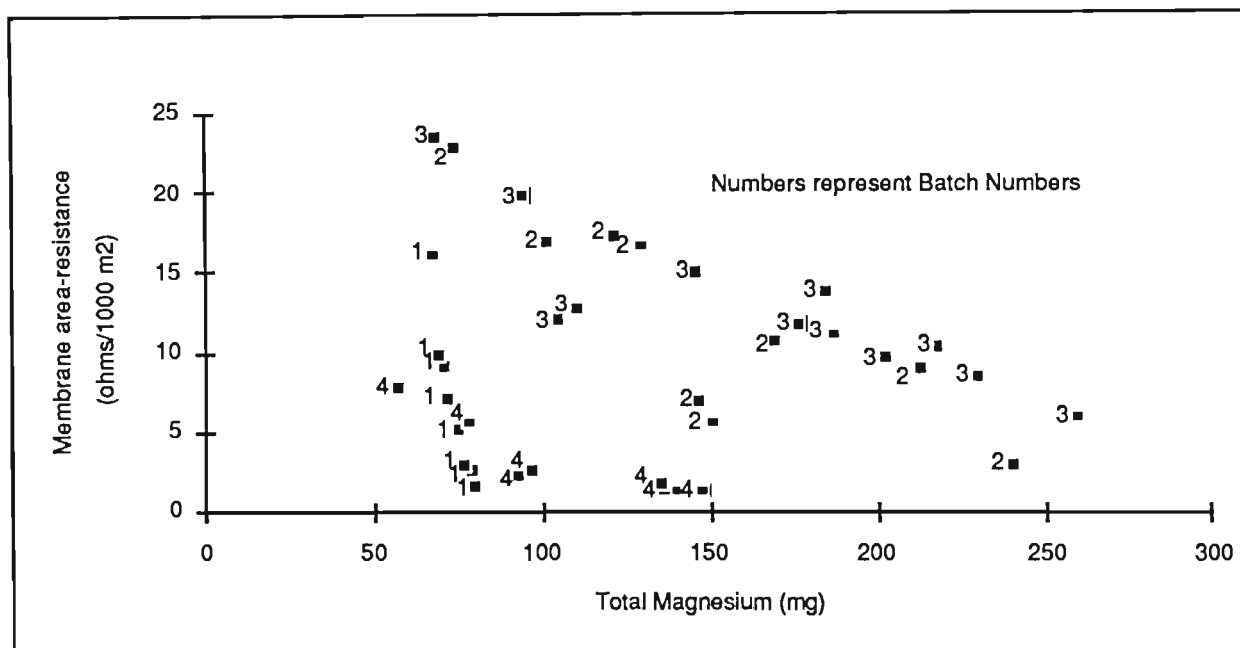


Figure 9.4
Relationship Between Membrane Area-Resistance and Total Calcium

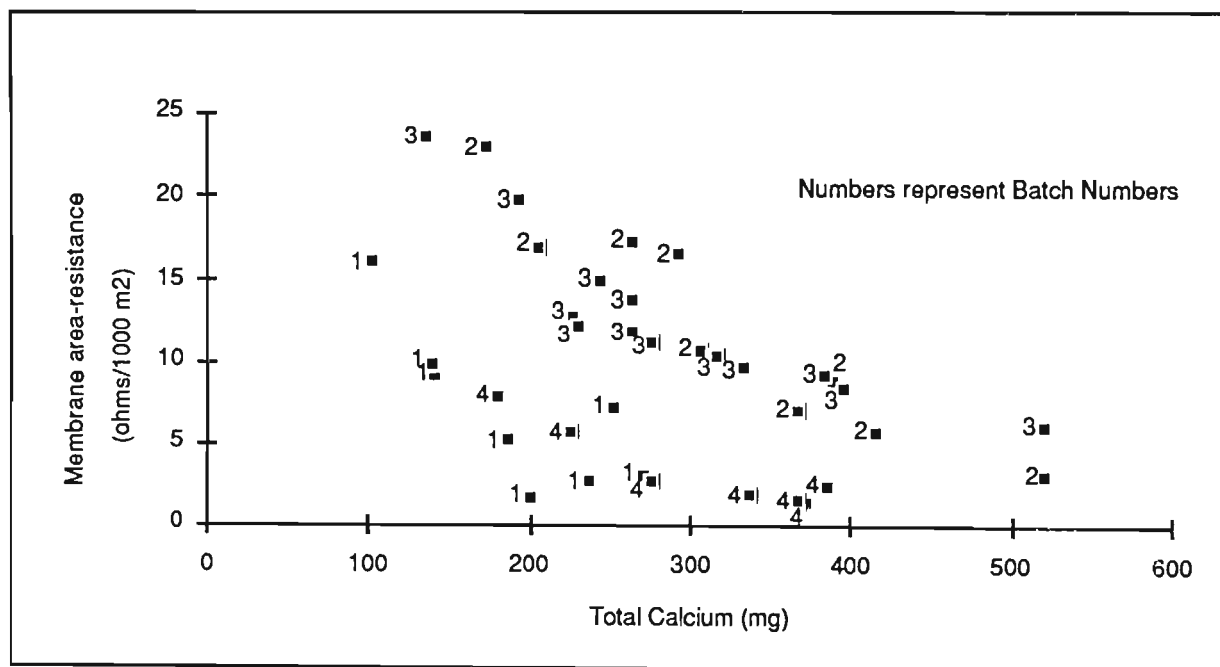


Table 9.1 presents a mass balance for calcium and magnesium cations for the four batches. In each case there was a loss of calcium and magnesium from the anolyte, which was not balanced by an equivalent gain in the catholyte. For the first three batches, 0,8 g of calcium and 0,3 g of magnesium were lost from the electrolytes, presumably accumulating in the electromembrane structure or on the electromembrane surface.

Table 9.1
Mass Balance For Divalent Cations

Batch	Anolyte Volume (l)	Total Calcium (mg)			Total Magnesium (mg)		
		initial	final	lost	initial	final	lost
1	40 initially 34 finally	200	88	112	80	68	12
2	40 initially 24,7 finally	520	173	347	240	74	146
3	40 initially 17,3 finally	520	137	383	260	69	191
4	40 initially 28,5 finally	372	180	172	140	57	83

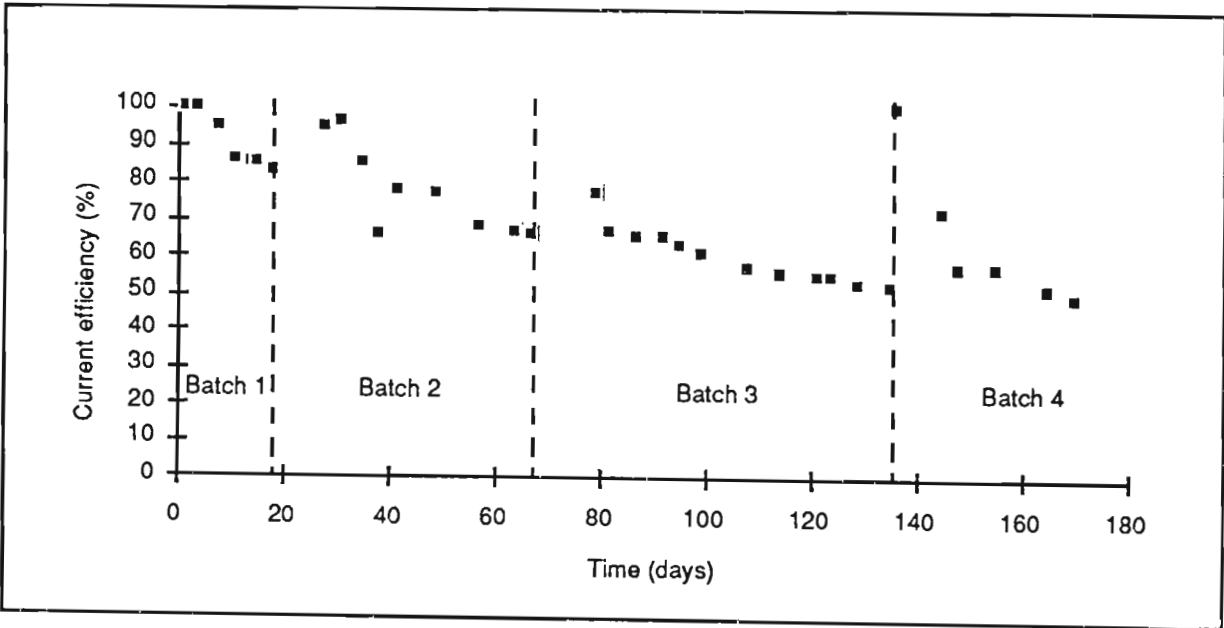
It is appropriate at this stage to refer again to the similar study carried out on sodium chloride anolytes, both pure solutions, as well as scouring effluent which had been neutralised with chlorine gas (in place of carbon dioxide) and pretreated by both microfiltration and nanofiltration (Pollution Research Group, 1989). The results of this study indicated that fouling by calcium and magnesium cations present in pure sodium chloride solutions was severe: electromembrane area-resistance increased by 300 % (from 2×10^{-3} to $5 \times 10^{-3} \Omega m^2$) during the passage of only 3 F of electricity when 15 mg/l of calcium and 5 mg/l of magnesium were added to an anolyte containing 13 g/l Na. It is assumed that the fouling resulted from the precipitation of insoluble hydroxides on or within the electromembrane structure. Fouling could not be controlled by the addition of chelating agents, including EDTA, borax and citric acid, to either the anolyte or the catholyte. By comparison, however, pretreated scouring effluent containing 17 g/l Na (as NaCl), 6 mg/l Ca and 8 mg/l Mg showed no tendency to foul, even at depletion to below 5 g/l Na after the passage of 7 F of electricity. Electromembrane area-resistances remained below $2,5 \times 10^{-3} \Omega m^2$, loss of divalent cations from the anolyte was negligible, and no visible deposit formed on the electromembrane surface. It was suggested that the divalent cations present during scouring were incorporated into strongly bonded organo-metallic complexes that are not destroyed during pH adjustment or pretreatment, and these species prevent migration and precipitation of these cations in the electromembrane structure during electrolysis.

A comparison of the results of electrolysis of chlorinated and carbonated scouring effluent indicates that divalent cations present in carbonated effluent have greater tendency to increase electromembrane area-resistance than those in chlorinated scouring effluent. The difference clearly relates to the nature of the anion in the anolyte, and the difference in solubilities of the carbonate and hydroxide salts. For example, calcium hydroxide is between 30 and 100 times more soluble in hot and cold water respectively than calcite or aragonite polymorphs of calcium carbonate (Weast, 1987), and therefore less likely to precipitate in solutions of low calcium concentration. By contrast, the reverse is true for magnesium, although interestingly enough magnesium hydroxides were not identified as contributing significantly, if at all, to the scale. Section 9.1.5 examines divalent ion deposition more closely.

9.1.3. Current Efficiencies

The efficiency of electrolysis was measured by comparing the observed change in the number of moles of sodium ions in the anolyte, with the theoretical change that should occur if all the current was used to transport sodium ions. Current efficiency data for the four batches is calculated in Table A8-10 in Appendix 8, and summarised in Figure 9.5.

Figure 9.5
Incremental Change In Current Efficiencies



Clearly electromembrane performance deteriorates during each batch and from one batch to the next. Incremental current efficiencies during batch 1 drop from 100 % at the start to 83 % after the passage of 16,4 F of current. For batches 2 and 3, current efficiencies range from 95

and 77 % respectively to 66 and 52 % after the passage of 33 and 49 F of electricity. The overall trend is a decrease in current efficiencies. Treatment of the electromembrane after batch 3 (see Section 9.1.4) to remove visible scale restored current efficiencies to 100 %, although continued electrolysis caused a further decline in current efficiencies to the levels observed before treatment. The phenomena responsible for reduced current efficiencies are discussed in Section 5.4.4.6, and include the passage of current by cations other than sodium; back-migration of hydroxide ions from the catholyte; and concentration polarisation (water splitting) at the electromembrane surface. Furthermore, in areas of the electromembrane where precipitants build up, shielding occurs with consequent loss of electromembrane area available for sodium migration.

If water polarisation or back-migration are wholly responsible for decreased current efficiencies, then renewal of the anolyte should result in restoration of electromembrane performance. This effect is seen only partially in Figure 9.5, where current efficiencies improved from 83 to 95 % between batches 1 and 2, and 66 to 77 % between batches 2 and 3. Furthermore, if water polarisation is responsible for reduced current efficiencies, reducing current densities to levels below the limiting value should result in improved current efficiencies. This was the case during batch 2 (after 38 days). However, during batch 3, reduction of current density had no effect on current efficiency. This, together with the overall decrease of current efficiencies from batch 1 to 3, suggests that electromembrane fouling was becoming increasingly the major controlling factor in cell performance.

9.1.4. Restoration of Cell Performance

After 135 days of almost continuous operation, and electrolysis of 120 l of pretreated scouring effluent, the current efficiency was 52 % and the experiment was stopped. As a result of loss in current efficiency; an imbalance in the total calcium and magnesium distributed between the electrolytes; and a bulging and encrusted electromembrane surface on the cathode side, it was concluded that considerable fouling or scaling of the electromembrane had occurred. An attempt was made to restore the performance of the electromembrane by removing the crust by circulating deionised water through the cell.

Analytical data of the deionised water circulating through the catholyte compartment indicated that there was an increase in sodium concentration from 2 to over 700 mg/l, probably as a result of contamination by sodium hydroxide remaining in the equipment. Results for hardness ions were inconclusive: calcium and magnesium each increased from zero to 2 mg/l, a total increase of 10 mg for each cation (far lower than the amount which was lost from the anolyte without trace to the catholyte). The grey-white crust on the cathode side of the

electromembrane fell away during cleaning and was collected and analysed by X-ray diffraction (see Section 9.1.5).

Subsequent to electromembrane treatment, and to evaluate the effectiveness of the cleaning procedure, the fourth batch of effluent was electrolysed. The analytical results and calculations of electromembrane area-resistance, divalent cation loss and current efficiencies have already been referred to in Appendix 8. Figures 9.1 to 9.4 illustrate that the relationship between electromembrane area-resistance and cation concentrations for the duration of batch 4 parallels those for batches 1, 2 and 3. A mass balance calculation (Table 9.1) indicates that the discrepancy between anolyte loss of divalent cations and catholyte gain was approximately 0,2 g of calcium and 0,08 g of magnesium. This is less than that lost for batch 2, where the total amount of electricity passed was similar.

At the start of the batch, immediately following electromembrane treatment, current efficiencies were measured to be 100 %. However, subsequent decline was more rapid than any decline encountered during the electrolysis of preceding batches for equivalent passage of current. After day 10 of batch 4, a white crust became visible on the electromembrane, this time on the anolyte surface. The formation of this crust coincided with a sharp decline in the current efficiencies, from 72 % on day 10 to 57 % on day 13 (Figure 9.5). It is possible that:

- 1) Partial damage occurred to the electromembrane structure, either by the acid wash, or the growth of calcite within the polymer;
- 2) Seed nuclei of calcium carbonate may have remained within the electromembrane structure after cleaning, facilitating rapid regrowth of crystals;
- 3) Ineffective or partial cleaning could initially restore current efficiencies to 100 %, as long as the limiting current density was not exceeded in any part of the electromembrane. It is also conceivable that migrating sodium ions pass through the areas of electromembrane which exhibit least resistance. As the limiting current density is approached, scale formation on the electromembrane surface is accelerated, and current efficiencies decline.

Even in the fouled state, the electromembrane continues, at least in the short term, to exhibit the ability to recover sodium hydroxide from pretreated scouring effluent, *albeit* at current efficiencies as low as 50 %.

9.1.5. Scale Characterisation and Mechanism of Deposition

The X-ray diffractograms of the scales formed, first on the catholyte surface of the electromembrane and subsequently on the anolyte surface, showed 20 major peaks indicating a crystalline structure which was identified as calcite (calcium carbonate).

The formation of calcite on the catholyte surface of the electromembrane suggests that calcium ions passed through the electromembrane structure before precipitating as carbonate. The presence of carbonate ions in the catholyte is explained by one of two mechanisms: migration of carbonate (or bicarbonate) ions from the anolyte under a concentration gradient (but against the direction of the current flow and through a cation-selective barrier); or, more likely, absorption of carbon dioxide into the catholyte from the atmosphere during circulation. The electromembrane surface would provide a high energy interface where nucleation could occur easily, with subsequent growth being controlled by the diffusion of calcium ions through the electromembrane. The highly alkaline nature of the catholyte would ensure that the calcite remained as a solid which accumulated on the cathode surface.

The formation of calcite on the anolyte side of the electromembrane is only likely to occur when the pH of the anolyte in the diffusion layer is alkaline. High pH values in this layer are only possible if concentration polarisation gives rise to water splitting at the electromembrane surface, or if hydroxide ions migrate from the catholyte to the anolyte under a high concentration gradient (because of interruption of power supply). In this case, since the diffusion of carbonate and calcium ions through the electromembrane are not the rate-limiting step, the growth of calcium carbonate would be expected to be more rapid than in the case where conditions are such that the growth of the precipitate occurs on the catholyte surface of the electromembrane.

The ability of calcite to form on either side of the electromembrane suggests that its formation is controlled by the interaction of a number of variables such as current density, and the tendency for concentration polarisation or back-migration of carbonate or hydroxide ions.

It is suggested that scaling, in the form of surface, and partly-reversible, precipitation of carbonates, rather than fouling, in the form of the irreversible internal precipitation of hydroxides, is the predominant phenomenon. Hydroxide fouling is the primary, and most widely investigated, factor of concern in conventional chlor-alkali processes. The laboratory results indicate that carbonate scaling is accelerated during electrolysis with anolytes of low

concentrations, and when concentration polarisation occurs at the electromembrane surface, causing localised areas of high pH. Bicarbonate ions in the vicinity of the electromembrane are transformed into carbonate ions, which have the ability to precipitate with divalent cations on the electromembrane surface.

The results of a more thorough investigation into electromembrane cleaning techniques are presented in the following Section.

9.2. Electromembrane Cleaning

This investigation aimed specifically to evaluate a range of nitric acid treatment cleaning techniques for their ability to rejuvenate the electromembrane removed from the pilot-plant electrochemical unit. A description of the procedures and apparatus used is given in Section 6.4.2. The first experiment involved electrolysis to obtain reference performance data for virgin electromembrane and scaled electromembrane. The subsequent three experiments examined the effectiveness of acid soaking, acid electrolysis, and a combination of the two techniques respectively. These experiments consisted of a series of stages in which the electromembrane was first treated, followed by performance testing.

Appendix 9 presents the experimental data and calculations as follows:

- 1) Tables A9-1 to A9-7 give the physical and analytical data for all cleaning stages;
- 2) Tables A9-8 to A9-14 give the physical and analytical data for the reference runs and performance tests;
- 3) Tables A9-15 to A9-22 give the calculations for the current efficiencies for the reference runs and performance tests. Volume changes resulting for evaporative losses, electrolytic water transport, and sampling have been taken into account for these calculations.

Table 9.2 summarises the results for each experiment, presenting data for both the total amounts of calcium and magnesium removed from the electromembrane by the three techniques of cleaning, and current efficiencies for the change in ionic concentrations in the anolyte (Na and total CO₂) and the catholyte (Na and OH) during performance testing.

Table 9.2
Summary of Cleaning and Performance Results

Experiment	Cleaning Technique		Divalent Ion Removal (mg/cm ²)		Current Efficiencies (%)			
	acid soak	acid electrolysis	Ca	Mg	anolyte Na	anolyte CO ₂	catholyte Na	catholyte OH
1,1-scaled 1,2-virgin	- -	- -	- -	- -	0 76	4 -	0 76	0 -
2.1	-	pH 1,5 62 A/m ² -20 h 240 A/m ² -21 h	3,5	0,3	-	-	-	-
2.2	-	-	-	-	45	50	65	70
2.3	-	pH 1,8 50 A/m ² -8,6 h	6,0	1,8	-	-	-	-
2.4	-	-	-	-	72	65	51	39
3.1	pH 1,5-72 h	-	5,3	1,7	-	-	-	-
3.2	-	-	-	-	65	60	70	60
3.3	pH 0,5-72 h	-	6,3	2,1	-	-	-	-
3.4	-	-	-	-	95	98	85	80
3.5	pH 1,3-47 h	-	8,2	1,5	-	-	-	-
4.1	pH 1,5-72 h (from 3.1)	pH 2 62 A/m ² -16 h	5,8	1,71	-	-	-	-
4.2	-	-	-	-	40	40	33	45
4.3	pH 0,5-72 h (from 3,3)	pH 1,3 62 A/m ² -6,7 h	7,0	2,15	-	-	-	-
4.4	pH 1,3-16 h -	-	-	-	73	65	60	77

9.2.1. Scale Characterisation

During the pilot-plant trials, no obvious increase in electromembrane resistance was observed. However, current efficiencies for sodium hydroxide production decreased progressively, while a balance over the process indicated that the amount of divalent cations lost from the anolyte was considerably higher than that gained by the catholyte, indicating their accumulation either in the electromembrane structure or on its surface. Furthermore, a visible white scale had formed on the anode surface of the electromembrane. Using X-ray diffraction techniques, this scale was identified as aragonite, a polymorph of calcium carbonate. Aragonite has a crystalline structure different from that of calcite, which was formed in the fouling tests discussed in Section 9.1.

Current efficiency data reported in Table 9.2 indicate that, under the test conditions, performance of the electromembrane was almost wholly impaired (to below 4 %) by the presence of the aragonite scale (Experiment 1.1). Under similar conditions, virgin electromembrane exhibits current efficiencies for sodium hydroxide production of 76 %. The severe effect that scale deposition has on cell performance emphasises the need to develop

a rapid and effective technique for controlling scale accumulation during electrolysis, if the process is to be economically viable.

9.2.2. Comparison of Effectiveness of Cleaning Techniques

The effectiveness of each cleaning technique is measured by the degree to which cell performance is restored after cleaning, as well as the rate and extent to which scale is chemically removed from the electromembrane structure by the cleaning procedure.

Restoration of Performance

Current efficiency data in Table 9.2 indicates that, in terms of restoration of performance:

- 1) Acid soaking produced the best results. Data suggests that the degree of rejuvenation depends on the acid strength. For equal time periods, soaking at pH 0,5 restored sodium current efficiencies to approximately 90 %, while at pH 1,5 they were restored to approximately 68 %.
- 2) Acid electrolysis at pH 1,5 and 1,9 was only partially effective in restoring performance. Current efficiencies for sodium transfer after electrolytic cleaning were 55 to 60 %.
- 3) Acid electrolysis, subsequent to acid soaking, served only to lower performance restoration by as much as 25 to 30 % below that obtained by acid soaking alone.

Results suggest that partial damage may occur to the electromembrane structure if relatively harsh (electrolysis) cleaning procedures are applied. This suggestion is supported by the fact that restoration of performance appears to be inversely proportional to the period of electrolysis.

Extent of Removal of Scale

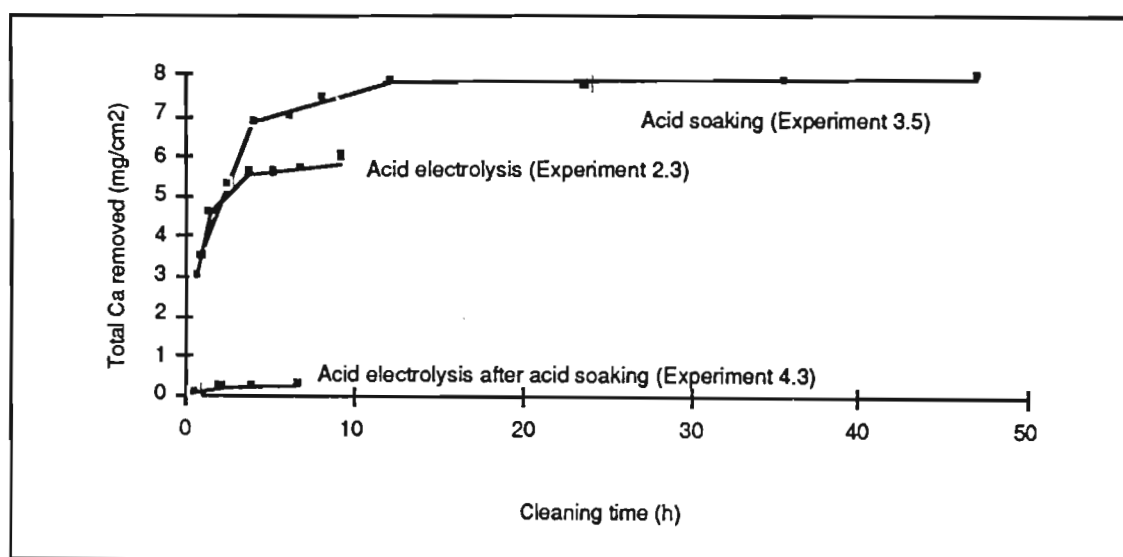
Table 9.2 presents, for each cleaning technique, data for the approximate mass of calcium and magnesium removed per unit area (cm^2) of electromembrane. Although the scale deposition on the original section of electromembrane was not wholly uniform, it is assumed that this nonuniformity would present only minor variations in the total amount of scale present at the start of any cleaning experiment. The average loading of removable scale on the electromembrane surface varied between 4 to 8 mg/cm^2 for calcium and 1 to 2 mg/cm^2 for magnesium. Using measurements of electromembrane mass loss resulting from cleaning, as well as analytical results indicating divalent ion removal, the total loading of the electromembrane was approximately equivalent to half the mass of the electromembrane itself.

Data suggest that, on average, acid soaking removes more scale from the electromembrane than electrolysis. Furthermore, in cases where the electromembrane was cleaned by a combination of soaking and electrolysis, up to 99,6 % of the scale removed was removed during acid cleaning, while up to 4 % was removed during electrolysis.

Rate of Scale Removal

The rate of scale removal has been calculated during experiments 2.3 (acid electrolysis); 3.5 (acid soaking); and 4.3 (acid soaking and acid electrolysis) in Tables A9-23 to A9-25 in Appendix 9, and illustrated in Figures 9.6 and 9.7.

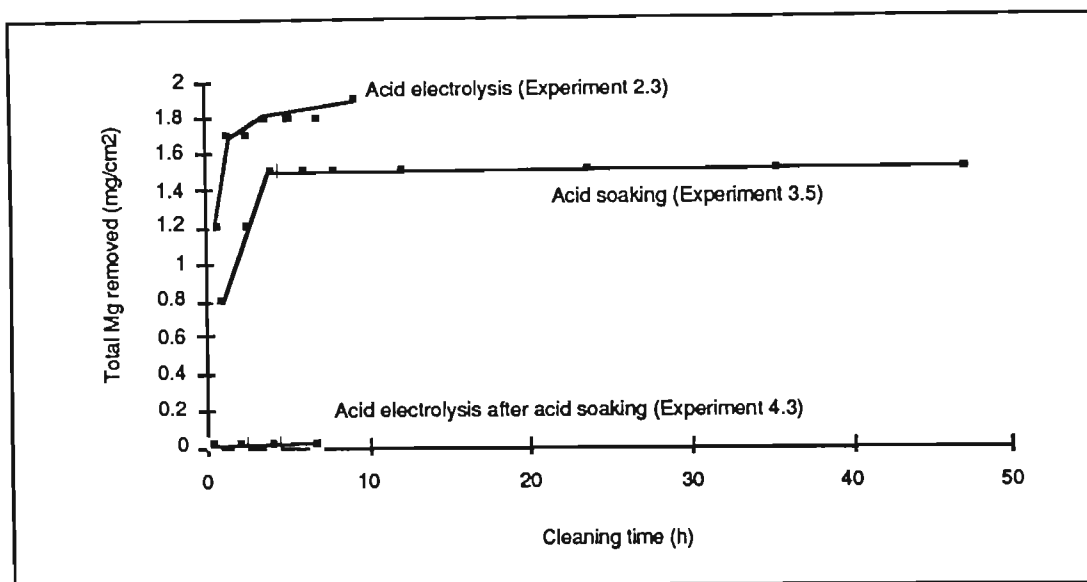
Figure 9.6
Rate of Calcium Removal For Three Acid Cleaning Techniques



The following observations can be made.

- 1) The major portion of the removable scale is released into the acid cleaning solution during the first 3 to 5 h of treatment, regardless of the technique used.
- 2) Acid electrolysis appears to remove scale at a greater rate initially than acid soaking. If the mechanism of acid cleaning involves a reduction of the pH inside the electromembrane structure, thereby dissolving foreign salts impregnated therein, then it is suggested that acid electrolysis produces an acid environment within the electromembrane at a faster rate than acid soaking.

Figure 9.7
Rate of Magnesium Removal For Three Cleaning Techniques



9.2.3. Selection of a Suitable Scale Control Technique

Obviously the preferred option for scale control is to eliminate the cause, rather than to treat the result. Prevention of scale formation during normal cell operation has been discussed in other sections of this report, and is examined briefly below.

Control By Prevention

Since the aragonite deposit occurred on the anolyte surface of the electromembrane during pilot-plant trials, and since aragonite is a salt containing the anion predominant in the anolyte (carbonate) and not that predominant in the catholyte (hydroxide), it is concluded that precipitation of calcium (and to a lesser extent magnesium) was induced in the anolyte, in the vicinity of the electromembrane, and not as a result of conditions encountered by migrating calcium ions during or after transportation through the electromembrane towards the catholyte. This deposition in the anolyte is only possible where the diffusion layer in the vicinity of the anolyte surface of the electromembrane is alkaline, as a result of either back-migration of hydroxide ions from the catholyte or polarisation of water in the vicinity of the electromembrane.

The electromembrane has been shown to be non-fouling and non-scaling during long-term fouling tests for scouring effluent which has been pretreated by chlorination and not carbonation (see Section 9.1.2). Therefore, it is suggested that, if carbonate species are

eliminated in the vicinity of the electromembrane surface, then a non-fouling performance, or at least a situation of slow and controllable scale growth, may be approached. In practice, three principal mechanisms exist for preventing the presence of carbonate ions in the vicinity of the electromembrane.

- 1) Maintaining operational current densities below the limiting value minimises concentration polarisation at the electromembrane surface, thereby preventing the formation of hydroxide ions in the diffusion layer.
- 2) Careful selection of electrolyte flow and cell design characteristics promotes turbulence at the electromembrane surface, thereby ensuring an adequate supply of sodium ions to the diffusion layer.
- 3) Operation of the process at lowest acceptable sodium hydroxide concentrations, reduces the pH gradient across the electromembrane, thereby minimising back diffusion of hydroxide ions.

Note that manufacturer information on Nafion 324 suggests that, in conventional chlor-alkali cells, where the pH values on either side of the electromembrane are 2 and 14, hydroxide back-migration is minimal if the sodium hydroxide concentration is maintained below 20 %. In the present application, the pH values on either side of the electromembrane are 8 and 14, while a sodium hydroxide concentration of 10 to 15 % is acceptable for reuse in scouring. Therefore, it is unlikely that back-migration is the predominant source of alkalinity in the vicinity of the anolyte surface of the electromembrane. This fact is substantiated by the results of the fouling tests on prechlorinated effluent referred to above, in which, had back-migration been a prevalent phenomenon, it is likely that insoluble hydroxide precipitates would have accumulated on the surface, or within, the electromembrane. Membrane area-resistance data suggested that no such accumulation occurred. It is suggested, therefore, that concentration polarisation is the main cause of scale deposition, and that careful selection of operating variables and cell design will significantly limit scale deposition.

Control By Routine Cleaning

In the practical situation it is unlikely that scale growth can be prevented altogether. Furthermore, the electrolyte characteristics (carbonate/bicarbonate anolyte and hydroxide catholyte) will promote scale deposition and not removal. Therefore, consistent performance and prolonged electromembrane life can be achieved only by the implementation of a regular and effective cleaning cycle, in which the electromembrane is contacted with a solution of sufficiently low pH to dissolve insoluble divalent species. In the absence of regular cleaning

cycles, it is suggested that scale formation will continue until the electromembrane surface is physically blocked and current efficiencies are reduced to virtually zero.

Although acid soaking is a more time-consuming technique than acid electrolysis, it is the preferred and recommended descaling method for electromembrane rejuvenation. The conditions and frequency of routine cleaning will need to be determined empirically for each individual situation. Conditions should be selected which ensure both uniformity and completeness of scale removal over the electromembrane surface. Rapid regrowth of scale will be facilitated if seed nuclei of calcium carbonate remain within the electromembrane structure. The time and acidity requirements for effective scale removal in the current investigations are considered to be an extreme example of cleaning conditions, since the electromembrane used had not been cleaned during its use, was heavily scaled and its performance had been severely inhibited.

9.3. Other Electrodes

Pilot-plant and laboratory tests aimed to determine the suitability of stainless steel and nickel metal, in place of coated titanium (DSA), for anode applications in the electrochemical cell. Although coated titanium is an ideal electrode material, its life is limited by passivation preceded by a gradual dissolution of the precious metal oxide coating. Recoating costs are in excess of £2 500/m² (1987). DSA electrodes were originally developed to withstand the extreme oxidising and corroding conditions of chloride ions and chlorine gas in chlor-alkali applications. Newer variations are specifically formulated for low overpotential oxygen generation. However, for the current oxy-alkali application, it would be cost-effective if other materials were found to be suitable for performing the function of water oxidation at low overpotential. Since the most significant volt drop in the system occurs across the anolyte, because of its low conductivity, small increases in anode overpotential could be tolerated without significantly influencing power requirement. The other materials should also exhibit resistance to corrosion, because if the depleted brine solution is contaminated with heavy metals it would not be suitable for reuse in rinsing. Furthermore, there should be no formation of non-conducting oxide layers; the metal should be available at lower costs; and it should have a similar life expectancy as coated anodes, without the necessity for recoating.

9.3.1. Stainless Steel Anodes

Data for the operation of the pilot-plant cell using stainless steel anodes is presented in Table A8-1. The experiment was discontinued after 1,75 hours (4,5 F) because corrosion of the anode had resulted in discoloration of the anolyte. However, results indicate that sodium

current efficiencies were 65 %, and comparable with those obtained using coated anodes. Furthermore, the total operating voltages were 0,3 V lower for the stainless steel electrode under comparable conditions of temperature, current and electrolyte concentration.

It is possible to predict the ohmic losses in the stainless steel anode as follows. The overall volt drop in the system was 5,5 V for a current density of 1 400 A/m², and an anolyte containing 9 to 13 g/l of Na at 50 °C and pH 8,5. The volt drop measured between the anode and electromembrane was 2,3 V. Using equation 5.18, the volt drop through the anolyte is calculated to be 2,0 V, indicating that the anode volt drop is 0,3 V. Using this voltage, and knowing the pH of the anolyte, predictions of metal stability may be made from phase-equilibrium diagrams (Pourbaix, 1966).

Figure 9.8 is the potential-pH diagram for iron in water at 25 °C (Pourbaix, 1966). The electrode potentials given are relative to the standard calomel electrode ($E = +0,25$ V). The diagram shows that oxidation of iron metal may give rise to a variety of different products. The exact nature of the products depends on the pH and electrode potential, but they include soluble products (Fe^{2+} ; Fe^{3+} ; HFeO_2^-) and insoluble products ($\text{Fe}(\text{OH})_2$; Fe_3O_4 ; Fe_2O_3). There are two areas on the diagrams where corrosion is possible, an area where it is impossible, and an area where passivation may occur. Figure 9.9 shows the theoretical conditions of pH and potential which may result in corrosion, immunity or passivation.

Under the experimental potential-pH conditions (pH 8,5 and 0,3 V), theory predicts that iron is passivated if the solution is at 25 °C. However, in practice, temperatures were 50 °C and electrolysis resulted in anode corrosion with the formation of a brown precipitate. The potential-pH diagrams suggest that if the pH could be increased and the cell operated at higher voltages (current densities) iron would not corrode.

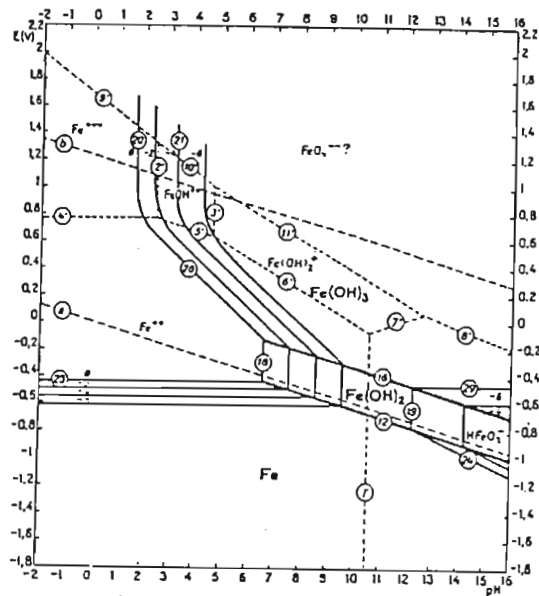
Therefore, although iron exhibits low oxygen overpotentials, it is unsuitable as a coated titanium substitute under the required electrolysis conditions because of its tendency to corrode.

9.3.2. Nickel Anodes

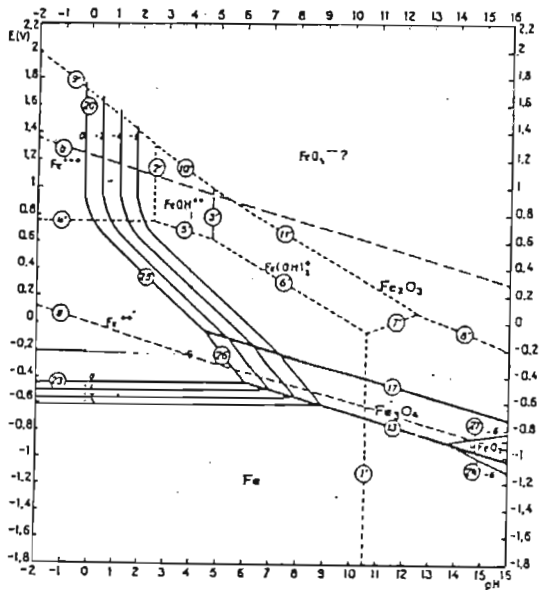
Data for the operation of the pilot-plant cell using nickel anodes is presented in Appendix 10, Tables A10-2 to A10-8. Tables A10-9 and A10-10 present data for the laboratory experiments. Tables 9.3 and 9.4 summarise the current efficiencies achieved for the pilot-plant and laboratory tests respectively.

Figure 9.8
Potential-pH Equilibrium Diagram for the System Iron-Water, at 25 °C

Considering as solid substances only Fe, Fe(OH)₂ and Fe(OH)₃



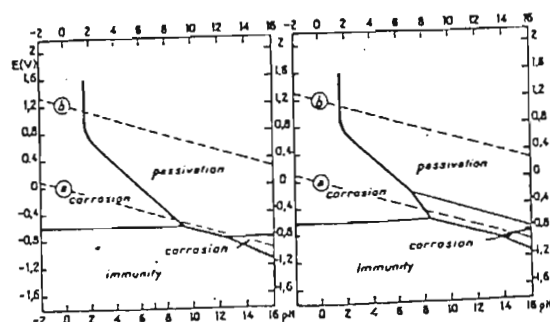
Considering as solid substances only Fe, Fe₃O₄ and Fe₂O₃



Source: Pourbaix, 1966

Figure 9.9
Theoretical Conditions for Corrosion, Immunity and Passivation of Iron

Considering passivation by Fe_2O_3
 Considering passivation by Fe_3O_4 and Fe_2O_3



Source: Pourbaix, 1966

Table 9.3
Summary of Results of Pilot-Plant Tests Using Nickel Anodes

Experiment	Initial Anolyte g/l Na	Final Anolyte g/l Na	Initial Catholyte g/l Na	Initial Voltage V	Initial CD A/m ²	Current Efficiency % Na	Current Efficiency % OH	Comment ¹
19B	37	19	85	4,3	2 000	70	-	pale green ppt formed at pH 6,9 black ppt formed at pH 6,2 pale green ppt formed at pH 8 black ppt formed at pH 7,3
20A	26	19	107	4,6	2 000	96	74	
20B	26	12	172	5,7	2 000	79	75	
21A	16	9	110	7,1	2 000	38	58	pale green ppt formed at pH 7,8 black ppt formed at pH 7,6
21B	21	10	136	12,3	800	49	51	
21C	15	9	160	15,8	600	31	65	

Table 9.4
Summary of Results of Laboratory Tests Using Nickel Anodes

Time h	Faraday	Anode Mass Loss mg	Anolyte pH	Anolyte Ni gain mg	Current Efficiency % Na	Current Efficiency (% OH)	Comment ¹
0,0	0,0	-	9,6	-	-	--	black ppt formed in the in anolyte
22,3	1,4	170	9,1	75	60	90	
44,3	2,3	509	8,6	318	76	100	
68,8	3,7	963	8,6	369	70	82	
98,8	5,3	2636	8,7	672	52	62	

Note that the nickel precipitate settled in the anolyte tank, inhibiting homogeneous sampling. This explains the discrepancy between anode mass loss and anolyte nickel gain.

¹ ppt indicates precipitate

During the pilot-plant trials it is apparent that current efficiencies for sodium hydroxide production decreased from experiment 19B through to experiment 21C, concomitant with the progressive solution of the nickel anode and the deposition of nickel carbonate and nickel oxide on the electromembrane surface. Similarly in the laboratory trials, current efficiencies for sodium hydroxide production decreased progressively to 52 % during the final stages of the experiment. Furthermore, in the pilot-plant trials, the initial current density which could be

achieved with applied voltage decreased steadily, indicating increased resistance in the system. In fact, the resistance was observed to increase more than ten-fold, from 43 m Ω (4,3 V/100 A) at the start of experiment 19B to 527 m Ω (15,8 V/30 A) at the start of experiment 21C. This increased resistance was attributed to the accumulation of non-conducting deposits on the nickel anode surface and high resistance deposits on the electromembrane. Finally, the severity of the effects of corrosion on the cost of sodium hydroxide recovery are seen by comparing the specific power consumption of experiment 19B with that of experiment 21C.

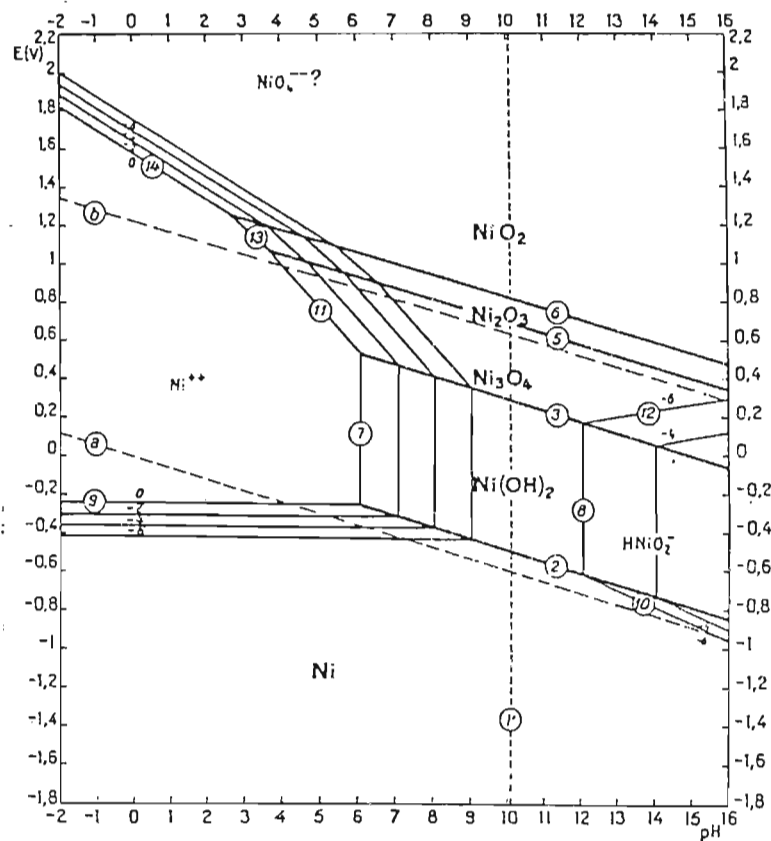
Assuming average operating conditions, the specific power consumption increased from 4 861 kWh/tonne 100 % NaOH in experiment 19B to 16 217 kWh/tonne 100 % NaOH in experiment 21C. At a cost of R0,05/kWh, this equates to an increase in power costs from R243 to R811 for each tonne of sodium hydroxide recovered.

Figure 9.10 is the theoretical potential-pH equilibrium diagram for the nickel-water system (Pourbaix, 1966). Nickel may be considered to be slightly noble, in that its domain of thermodynamic stability has a small zone in common with that of water. The corrosion resistance of nickel depends on the combination of oxidising conditions and pH to which it is subjected. The conditions of corrosion, passivation and immunity of nickel are shown in Figure 9.11. Nickel is not expected to corrode in neutral or alkaline solutions free from air, nor in alkaline conditions in the presence of air. However, corrosion is possible in neutral and acid conditions in the presence of air.

In the pilot-plant trials, the anolyte pH value decreased in the range 9 to about 6, with corrosion being observed to accelerate at pH values below 8. The pale green deposit formed initially was identified as nickel carbonate, while the black precipitate was identified as a combination of nickel metal powder and nickel oxide. The formation of these deposits suggests that the potential-pH combination to which the anode was exposed during the trials fell into the corrosion zone. The laboratory trials were carried out to evaluate the relationship between the rate of corrosion and the pH of the anolyte for a given range of potential. Figure 9.12 shows this relationship. As electrolysis proceeded, and pH of the anolyte decreased, the rate of corrosion increased to 0,9 g Ni per Faraday of electricity passed at pH 8,6. The black nickel oxide precipitated at higher pH values during the laboratory trials than during the pilot-plant trials. This results from the differences in applied potential during the two studies. Figure 9.11 suggests that if electrolysis was carried out at higher oxidising potentials, conditions of passivation may be observed in which corrosion is prevented or controlled. In practice, however, to maintain the current density below the limiting value, the maximum potential which can be applied is restricted and falls within the corrosion zone.

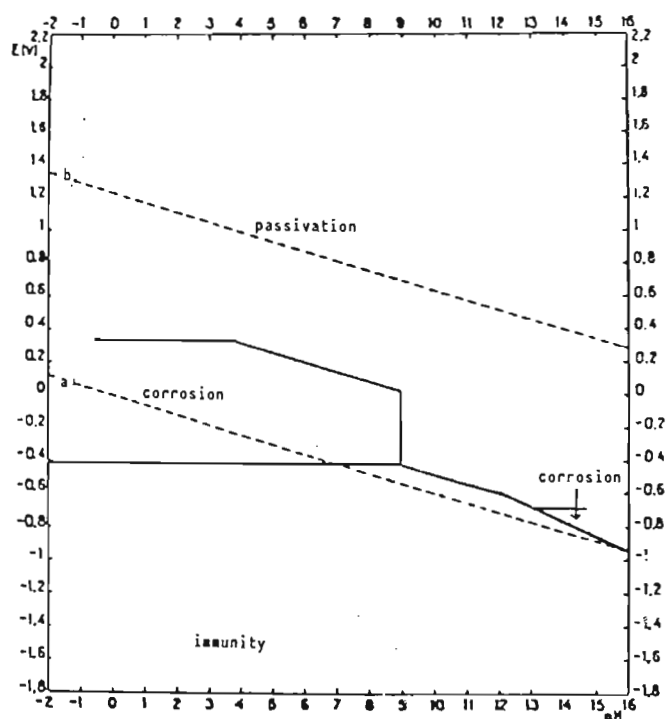
The pilot and laboratory trials indicate that, although nickel metal may be stable in sodium carbonate/bicarbonate solutions under certain conditions of pH and applied potential, under those conditions observed experimentally, rapid dissolution occurs, followed by precipitation and deposition. The effect of this deposition on cell performance and power consumption is so severe that nickel must be considered an unsuitable material for the present application.

Figure 9.10
Potential-pH Equilibrium Diagram for the System Nickel-Water, at 25 °C



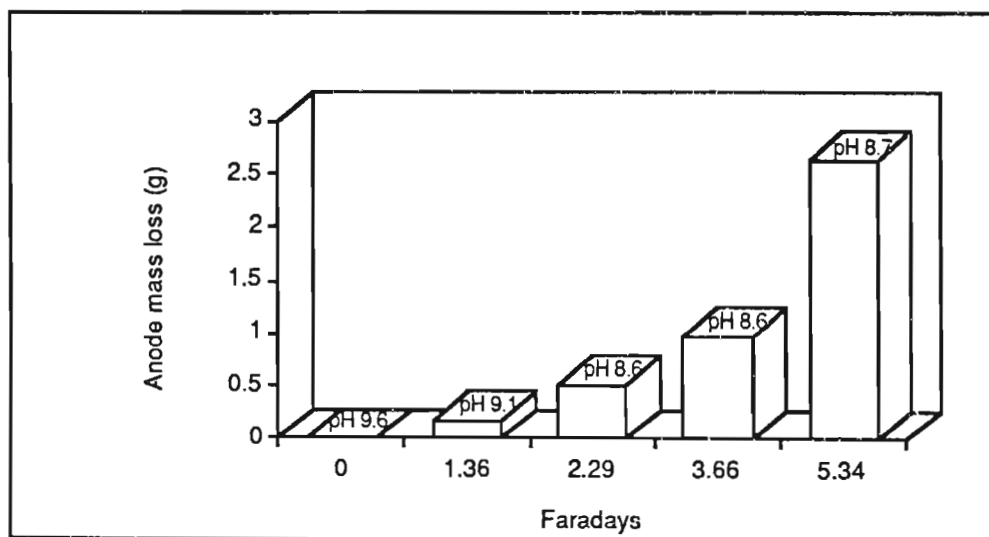
Source: Pourbaix, 1966

Figure 9.11
Theoretical Conditions for Corrosion, Immunity and Passivation of Nickel
in Chloride-Free Solutions



Source: Pourbaix, 1966

Figure 9.12
Dependence of Anode Mass Loss on Electricity Passed and Anolyte pH



SECTION 10

DESIGN OF A PLANT FOR THE ELECTROCHEMICAL RECOVERY OF STRONG SCOURING EFFLUENTS

The pilot-plant and supplementary investigations have demonstrated the technical feasibility of the four stage treatment sequence of neutralisation, cross-flow microfiltration, nanofiltration and electrochemical recovery to produce reusable water and sodium hydroxide from scouring effluent. The current section examines the technical and economical aspects of one specific design example. Since the treatment sequence under consideration is a closed-loop recycle system, it must be integrated into the factory operations. Thus a factory considering the implementation of such a programme must first develop an overall chemical, water and effluent management strategy as outlined in Section 3, specifically Section 3.1.2.

The design example is outlined in Section 10.1, general design considerations are outlined in Section 10.2, the design basis is defined in Section 10.3. The specifications of the batch neutralisation, cross-flow microfiltration, nanofiltration, and electrochemical recovery units in Sections 10.4 to 10.7. The synopsis of the design is in Section 10.8 and is followed by the economic evaluation in Section 10.9.

10.1. Design Example

A mill processing 30 to 40 million metres per annum of woven cotton and polyester/cotton is considered. The scouring operation is described in Section 4.3.1. Scouring is achieved continuously in an open-width Vaporloc machine, using an impregnation solution containing 50 g/l sodium hydroxide and a sodium hydroxide reinforcement factor of four. The cloth speed is 50 m/min and the average cloth mass is assumed to be 260 g/linear m. The four-bowl counter-current rinsing range produces an effluent at 100 °C. One high-expression roller (0,5 l/kg cloth) is installed after the final rinsing bowl, while the moisture content after the other nip rollers averages 0,8 l/kg cloth. Following analysis of the rinsing range variables using washing theory, recommendations were made (Section 4.3.6) to improve the performance of the rinsing process. The recommended modifications amount to savings of 77 % of water intake to this machine, reducing the annual consumption from 38 000 m³ to approximately 8 000 m³. They also result in an annual savings of approximately 80 tonnes of 100 % sodium hydroxide, as well as savings in heat energy. Table 10.1 compares the washing variables of the existing process, the existing process at reduced water flow, and the recommended process. At the expense of a small loss in washing efficiency, the effluent loading may be significantly decreased.

The design example assumes the operation of the rinsing range under the recommended conditions.

Table 10.1
Comparison of Rinsing Processes

Rinsing Variable	Units	Existing Process	Existing Process Reduced Flow	Recommended Process
specific water consumption	l/kg cloth	6,5	1,5	1,5
number of high-expression nips		1	1	2
rinsing efficiency	%	99,8	96,7	95,7
effluent concentration	g/l Na	3,4	12,4	9,2
cloth chemical loading	g Na/kg cloth	0,1	0,8	0,6
effluent chemical loading	g Na/kg cloth	22,9	22,2	13,8

10.2. General Considerations

The design details of a treatment plant are specific to each factory and depend on the following factors:

- 1) Characteristics of the scouring process and the cloth;
- 2) Rinsing efficiency and water use;
- 3) Purity of the rinse water;
- 4) Efficacy of the individual stages of the treatment sequence.

The electromembrane area requirement of the electrochemical unit depends on the concentration of the anolyte, which may be increased by changing the process configurations. Although configurations using evaporation and reverse osmosis have been considered (Pollution Research Group, 1990), this dissertation examines the closed-loop recycle of rinse water with a background concentration (Figure 7.6). Where a background concentration is employed, two options for making up the sodium short-fall exist: sodium may be added to the washing section as sodium bicarbonate; or to the scouring section as sodium hydroxide. The selected option will be dependent on the relative economics of each, and will in turn determine the degree of depletion of the effluent in the electrochemical unit. The design example assumes the case where sodium hydroxide is added to scouring, and electrochemical depletion is achieved to the extent where the final effluent stream contains an equivalent amount of sodium to yield a rinse water of the selected background concentration after additional make-up of water. Such a system would result in increased loss of sodium salts by drag-out on the cloth after rinsing. The implications of producing a washed cloth with a high sodium loading must be assessed on the basis that the effluent from subsequent wet processes would contain proportionately higher amounts of sodium. The

chemical nature of any effluents produced elsewhere in the factory should not be altered to such an extent that their present manner of discharge becomes unacceptable.

The design factors requiring consideration relate to textile processing, pretreatment requirements, scaling prevention, membrane selection and module arrangement. These are discussed below.

10.2.1. Textile Processing Considerations

Consideration should be given to the compatibility of the materials of construction of the plant, particularly the valves, seals and pump components, with the nature of the effluent. Furthermore, all nanofiltration and electrochemical membranes have pH and temperature limits, operation outside of which may permanently damage the membranes. Generally, chemicals such as solvents, chlorine and other oxidising agents, which may cause membrane damage, are not used in the scouring process under consideration. However, particular attention should be paid to the presence the following materials:

- 1) Polymeric substances;
- 2) Textile auxiliaries and detergents, especially cationic and non-ionic types which may cause membrane fouling;
- 3) Sizing chemicals which, if not properly removed before scouring, will result in the formation of a viscous scouring effluent, resistant to pumping and prone to cause blockages of equipment.

10.2.2. Pretreatment Requirements

To facilitate the smooth operation of the treatment plant, certain aspects require consideration.

- 1) Screening is essential to remove fibre and gross solids to avoid pumping problems and blockage of the neutralisation unit.
- 2) Flow-balancing is required to avoid wide fluctuations in the flow, temperature and concentration of scouring effluent entering the treatment plant. Storage requirements depend on the production of scoured fabric, and generally two to six hours is adequate, although additional facility may be required during periods of plant maintenance.

- 3) The characteristics of the effluent must be controlled in compliance with membrane specifications. It is recommended that the following chemical analysis be carried out to characterise the scouring effluent: temperature; total dissolved solids; suspended solids ($>0,45\text{ }\mu\text{m}$); sodium; calcium; magnesium; iron; detergent; pH; chlorides; sulphate; silica; carbonate; hydroxide; solvents; and organic materials which may be incompatible with selected membranes.
- 4) Colloidal and suspended solids should be removed prior to treatment by nanofiltration. The degree of pretreatment depends on the type of nanofiltration module being used. For example, hollow fine fibre modules require extensive filtration to remove all solids greater than 1 to 2 μm . Spiral modules require filtration to between 5 and 10 μm , whereas plate and frame or tubular modules require minimal filtration to 100 and 500 μm respectively.

10.2.3. Scaling Prevention

Sparingly soluble compounds, such as carbonates, hydroxides and sulphates of calcium, magnesium, iron and aluminium, in the absence of chelation, will form scale on the nanofiltration and electrochemical membranes. The precipitation of these species is a complex function of composition, pH, temperature and the nature of chelating agents which may be present. It is recommended that computer and laboratory techniques, such as speciation and X-ray diffraction be undertaken to assess the different pretreatment methods (Buckley et al, 1987).

10.2.4. Membrane Selection and Module Arrangement

The basis on which the cross-flow microfiltration precoat, the nanofiltration membrane and the electromembrane are chosen depends on various factors including:

- 1) Rejection and flux characteristics;
- 2) Robustness;
- 3) Compatibility with scouring chemicals and textile auxiliaries;
- 4) Temperature;
- 5) Water recovery;
- 6) Fouling and cleaning;
- 7) Concentration of electrolytes (electromembrane only).

10.3. Design Basis

The overall design basis is summarised in Table 10.2, with special reference to Figure 10.1. Standard membranes are available and have been assumed in the design where necessary. The standard sizes chosen are as follows:

- 1) Cross-flow microfiltration tubes, each 25 mm in diameter and assembled in a curtain arrangement containing 31 tubes in parallel (surface area = 2,43 m²/linear m).
- 2) Spiral nanofiltration elements, each 100 mm in diameter and 1 000 mm in length (approximate membrane area = 6,5 m²). Elements of 62 mm; 150 mm and 200 mm diameter are also available (approximate membrane areas are 2; 13 and 26 m² respectively).
- 3) Electrochemical stack of individual cells in a plate and frame arrangement, each cell containing 1 m² of membrane area.

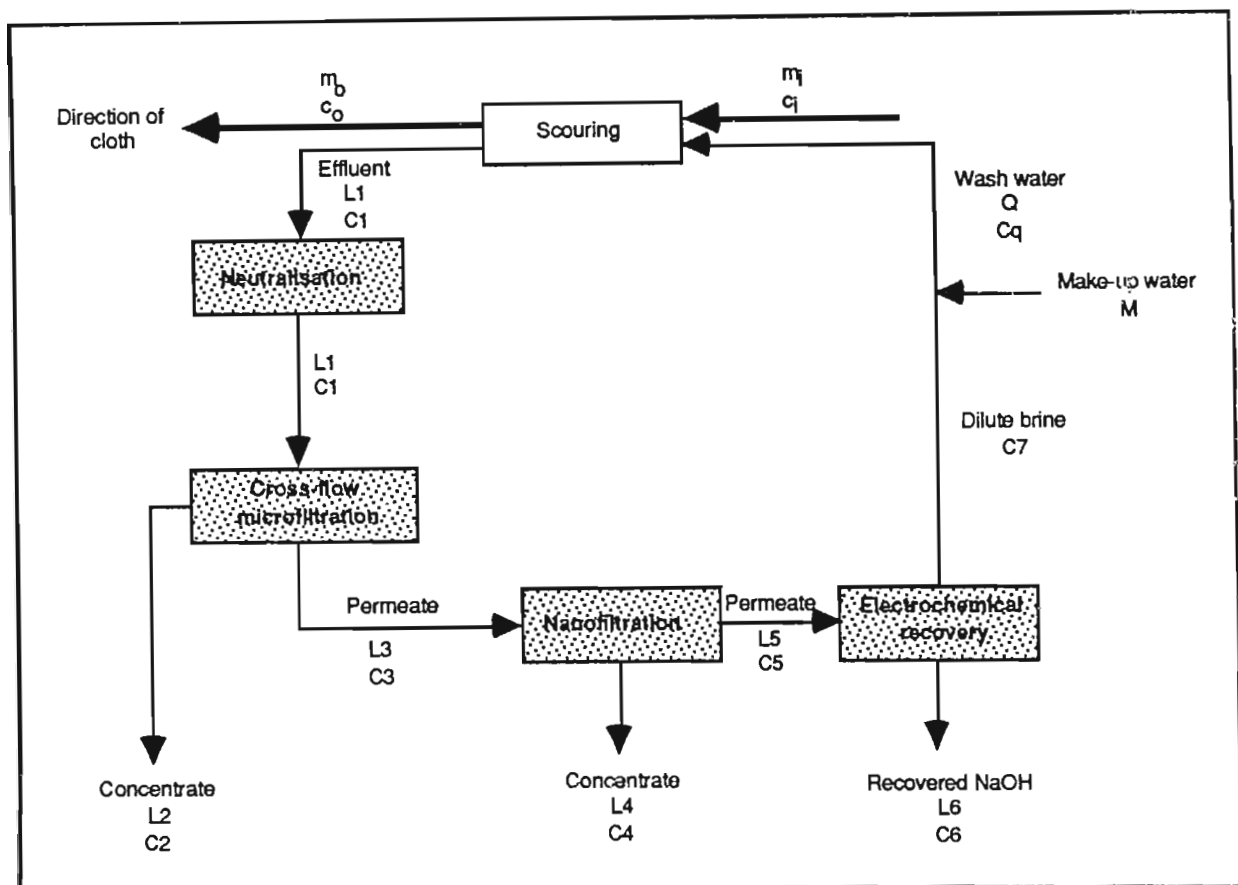
Table 10.2
Design Data for Treatment Sequence

Determinand	Units	Design Value
<u>Scouring variables</u>		
average cloth mass	g/linear m	260
cloth speed	m/min	50
	kg/h	780
production time	h/d	20
	d/a	340
moisture content of cloth into rinsing range	l/kg cloth	0,5
moisture content of rinsed cloth	l/kg cloth	0,5
saturation concentration	g/l NaOH	50
rinsing parameter		0,15
specific water use	l/kg cloth	1,5
total rinse water flow	m ³ /h	1,17
	m ³ /d	24
background rinse water concentration	g/l Na	5
washing efficiency	%	79
<u>Effluent variables</u>		
total dissolved solids	g/l	25
chemical oxygen demand	g/l	12
calcium	mg/l	45
magnesium	mg/l	8
sodium	g/l	12,6
sodium mass loading	g/kg cloth	18,9

Auxiliary requirements for the treatment plant would include:

- 1) A pump sump within the factory;
- 2) Pipeline and valves for transfer from the factory;
- 3) Coarse screening to remove dirt, lint and gross suspended solids;
- 4) Steam, electrical and water supplies;
- 5) Suitable housing facilities;
- 6) Emergency effluent handling facilities in case of breakdown;
- 7) Drains.

Figure 10.1
Mass Balance Basis for Recovery Process Using Background Sodium Concentration



10.4. Specification of Batch Neutralisation Unit

10.4.1. Equipment

Table 10.3 provides a detailed list of equipment and Figure 10.2 is a schematic of the neutralisation unit. The residence time is controlled by a flow control valve. A pH controller on the return line controls the bleed from the system to the cross-flow microfilter and prevents

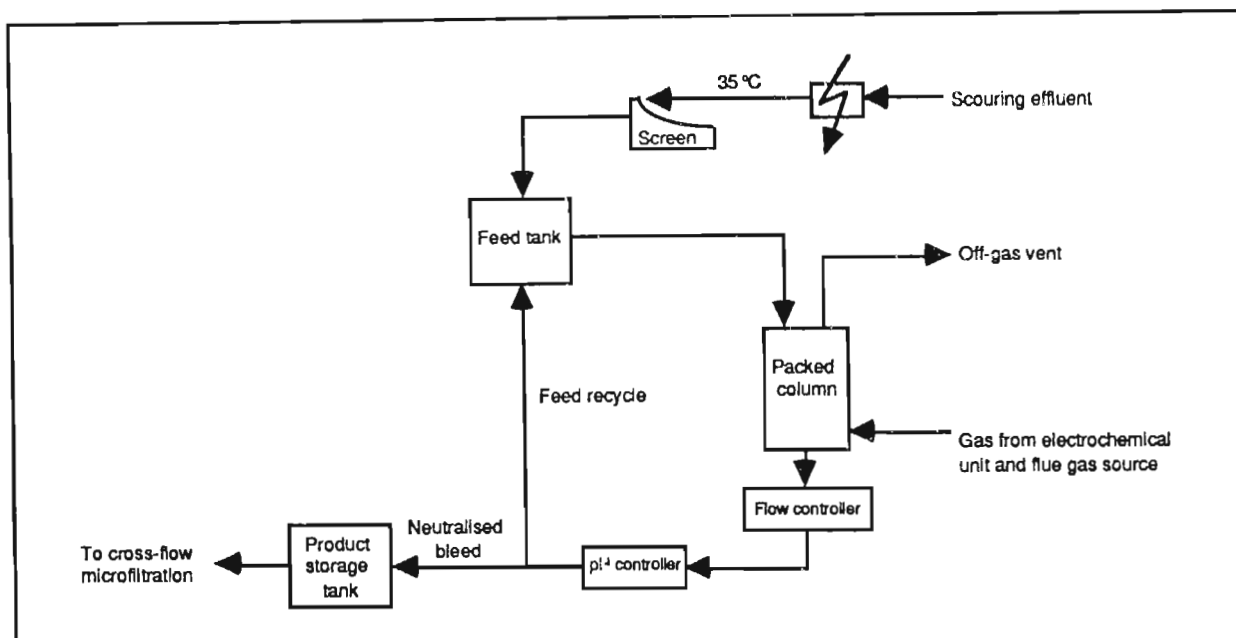
over-neutralisation, at which stage carbon dioxide is no longer absorbed. Control instrumentation for temperatures and tank levels are required. In addition, sampling ports should be provided.

The carbon dioxide for neutralisation is evolved in the electrochemical unit, which operates in a batch mode and hence the rate of neutralisation depends on the operation of the electrochemical unit. The effluent storage and sump facilities should provide approximately 6 to 12 h storage to provide for minor breakdowns and maintenance. The feed tank to the absorption column must accommodate the batch requirements of the treatment system.

Table 10.3
Batch Neutralisation Equipment Requirements

<p><u>Effluent transfer and storage</u></p> <p> piping and valves for transfer to absorption tank feed tank product storage tank transfer piping and valves from reticulation tank to column transfer piping for oxygen and carbon dioxide from electrochemical unit to packed bed transfer piping for make-up gases from waste flue gas emissions transfer piping to cross-flow microfiltration unit </p> <p><u>Packed bed absorber</u></p> <p> packed column dispersed liquid inlet facilities and off-gas vent at the top gas inlet facilities at the base </p> <p><u>Pumps</u></p> <p> pump for effluent transfer from the factory low-pressure pump for reticulation through packed bed low-pressure pump for transfer to cross-flow microfiltration unit </p> <p><u>Controls</u></p> <p> flow and pressure measurement pH control during batch carbonation pump motors, starters and interlocks level sensors and low-level alarm malfunction control interlocks interlock with electrochemical unit </p> <p><u>Ancillaries</u></p> <p> heat exchanger on effluent feed line to cool effluent to 35 °C suitable break tank between electrochemical cell and absorption tank </p>
--

Figure 10.2
Schematic of Batch Neutralisation Unit



10.4.2. Sizing

Carbon dioxide undergoes hydrolysis in sodium hydroxide to form various soluble ions. Because efficient transfer occurs, specially designed gas transfer facilities and off-gas systems are not necessary. With proper mixing and adequate dispersion, complete absorption is achieved and minimum retention time within the vessel is required. The oxygen associated with the carbon dioxide is vented.

The pressure drop in the absorber should be taken into account in the sizing of the unit to avoid excessive pressure in the electrochemical cell.

For the design basis in Table 10.2, approximately 19 kg of sodium hydroxide (474 mol) must be neutralised per hour in 1,17 m³ of effluent. An equivalent amount of 474 mol/h of carbon dioxide is required to transform the sodium hydroxide into sodium bicarbonate. For start-up purposes, and to compensate for losses in inorganic carbon from the system, supplementary carbon dioxide must be provided. The flue gas from liquid petroleum gas-fired equipment is a clean and convenient source of carbon dioxide.

10.5. Specification of Batch Cross-Flow Microfiltration Unit

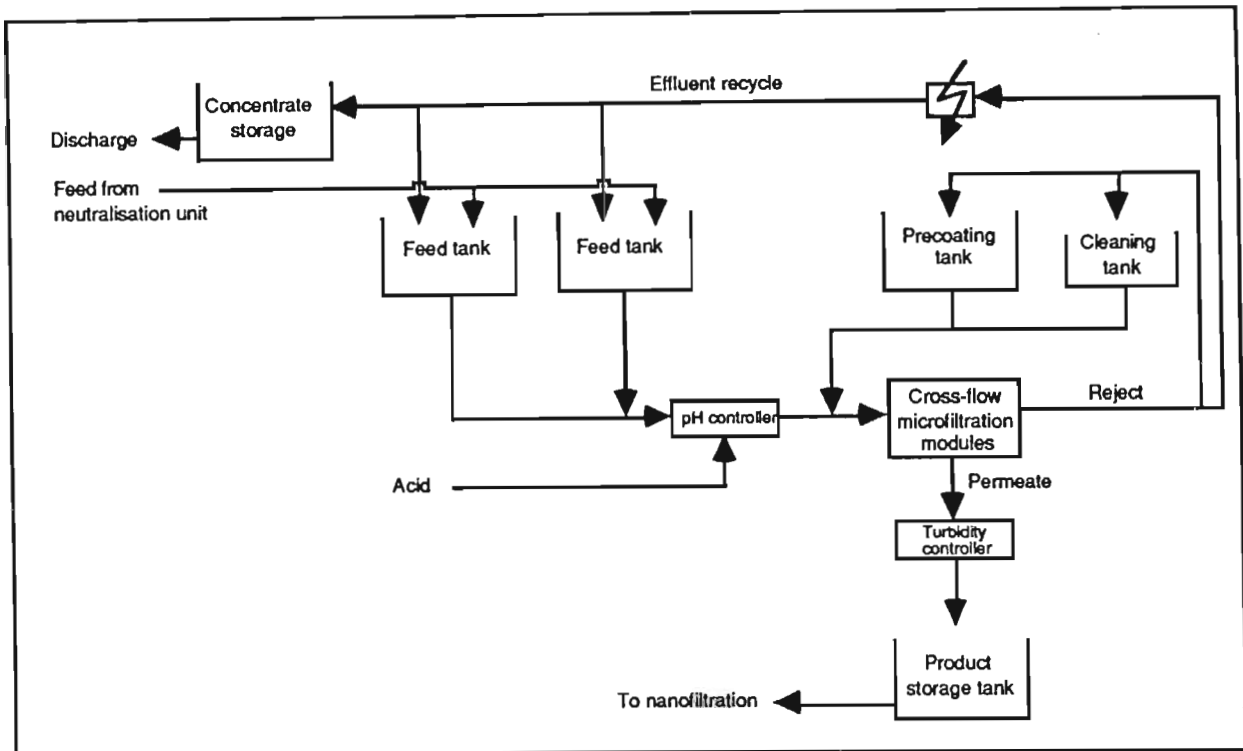
10.5.1. Equipment

Table 10.4 provides a detailed list of equipment and Figure 10.3 is a diagram of the cross-flow microfiltration unit. The neutralised effluent is not corrosive to most materials of construction, but should be in the temperature range of 30 to 40 °C.

Table 10.4
Batch Cross-Flow Microfiltration Equipment Requirements

<u>Effluent transfer and storage</u> two feed tanks retentate storage tank product storage tank precoat slurry and cleaning chemicals recirculation and storage tanks transfer piping and valves for effluent transfer from neutralisation transfer piping and valves for feed reticulation in cross-flow microfilter transfer piping and valves for final retentate storage and disposal transfer piping and valves for product to nanofiltration unit transfer piping for flue gas addition to the system
<u>Cross-flow microfiltration modules</u> tubular curtains and assemblies module racks/hangers piping and valves for feed, final retentate and permeate collection tray for permeate
<u>Pumps</u> high-pressure pump for reticulation through modules, precoating and cleaning pump for transfer of retentate and product flow and pressure measurement, indication and control of all streams
<u>Controls</u> permeate flow measurement feed recycle flow controller pH control of feed to ensure maintenance of desired equilibrium pump motors, starters and interlocks high- and low-pressure alarms low-flow alarm permeate turbidity measurement and high alarm malfunction and alarm control interlocks control panel
<u>Ancillaries</u> sampling ports on-line cooling of recycled streams to maintain feed temperatures of 35 °C

Figure 10.3
Schematic of Batch Cross-Flow Microfiltration Unit



Pumping duties for the tubular membranes are 500 to 600 kPa. Detrimental effects of pump vibration on the system must be considered. The process control system is dependent on the module type and pump. In general, the process is required to produce a predetermined water recovery in a batch mode. The pump may be:

- 1) Multi-stage or high-speed centrifugal, for which the normal control arrangement is a flow valve or a back pressure valve on the reject line;
- 2) Positive displacement, for which the discharge flow is not a function of the discharge pressure, and the control system is a flow controller on the reject line (to alter the system pressure to compensate for changes in flux) and a high-pressure alarm or a pressure relief valve on the pump discharge (to protect the cross-flow microfiltration module).

Effluent, product and retentate storage of the duration of a batch is necessary to provide for microfilter cleaning, minor breakdowns and maintenance.

10.5.2. Sizing

Although several types of microfilter are available, good results were obtained during the pilot-plant investigation using a woven tubular polyester unit. These are considered in this design. The pressure limitation of the tubular system is 600 kPa and a design pressure drop of 400 kPa has been used. During pilot-plant investigation, tube velocities in the range 2,5 to 3 m/s gave good fluxes on a limestone (15 μ m) precoated tube. Fouling by solids on the tube was minimal.

Table 10.5 gives the specifications for the current design, as well as a summary of the design calculations and performance. The pressure drop/velocity correlation for water, assuming an absolute roughness factor of 0,5 mm and 25 mm diameter tubes is:

$$DP = 0,93 V^2 L \quad (10.1)$$

where DP = pressure drop measured in kPa at ambient temperature

L = length in m

V = velocity in m/s

For a limestone precoat, experimental results (Pollution Research Group, 1989) suggest that at constant velocity, the flux is independent of pressure above values of 250 kPa, while at constant pressure, flux is proportional to velocity.

The membrane area of a 25 mm diameter tube is 0,0785 m² per m of linear length. The allowable length per parallel pass, is calculated from pressure drop considerations, for a velocity of 2,5 m/s, as:

$$L = \frac{400 \text{ kPa}}{(0,93 \text{ kPa} \cdot \text{s}^2/\text{m}^3) (2,5 \text{ m/s})^2} = 69 \text{ m} \quad (10.2)$$

and for 3,0 m/s, as:

$$L = \frac{400 \text{ kPa}}{(0,93 \text{ kPa} \cdot \text{s}^2/\text{m}^3) (3,0 \text{ m/s})^2} = 48 \text{ m} \quad (10.3)$$

The velocity will drop down the length of the tube because of permeation of liquid through the tube.

The pressure drop depends on various factors including temperature and solids concentration. For the design example, a linear length of tube is assumed to be 60 m, which will provide for an exit velocity of 2,5 m/s. Table 10.5 summarises the design calculations. Since the water recovery of each length is a function of inlet velocity and the production rate, the water recovery will increase at higher production rate and lower inlet velocity.

10.5.3. Design Configuration

Possible design configurations include batch concentration, continuous feed and bleed, and series taper. For the present application, the batch concentration configuration is described (Figure 10.3). This is the simplest configuration, but requires at least two batch storage tanks. The number of parallel tubes, at 60 m per pass, required for a total tube length of 331 m is six. The pump flow for an inlet tube velocity of 3 m/s and for 6 passes is 32 m³/h. The water recovery is set by the difference in tank levels at the start and end of each batch. The retentate is discharged on completion of the batch.

10.5.4. Overall Performance

The overall performance of the cross-flow microfiltration unit is presented in Table 10.5.

10.6. Specification of Batch Nanofiltration Unit

10.6.1. Equipment

Table 10.6 provides a detailed list of equipment and Figure 10.4 is a diagram of the nanofiltration unit. The feed to the nanofilter is neither abrasive nor corrosive to most materials of construction. The comments made in Section 10.5.1 regarding pumps, control systems and storage for cross-flow microfiltration apply also to nanofiltration. Pressure pumping duties are approximately 1,6 MPa for nanofiltration membranes. The temperature of the effluent will be maintained at 35 °C by a cooling system on the recycle line. During the course of the concentration process, the pH of the feed will increase, necessitating acid addition (flue gas or nitric acid).

Table 10.5
Cross-Flow Microfiltration: Design Specifications, Calculations and Performance

Parameter	Units	Calculation Basis	Value		
Design Specifications					
Feed flow	m ³ /day m ³ /h l/kg cloth		24 1,17 1,5		
Feed Na concentration	g/l		12,6		
Tube diameter	mm		25		
Tube velocity	m/s		2,5 - 3,0		
Design flux	l/m ² h		45		
Temperature	°C		35		
Feed COD	g/l		12		
Feed Ca	mg/l		45		
Feed Mg	mg/l		8		
COD rejection	%		40		
Ca rejection	%		90		
Mg rejection	%		40		
Na rejection	%		0		
Design Calculations					
Membrane area	m ²	flow x flux	26		
Total tube length	m	membrane area x 0,0785 m ² /m	331		
Tube length/pass	m	calculated in text	60		
Production rate/pass	l/h	length/pass x flux x 0,0785 m ² /m	212		
Flow in/pass	m ³ /h	given	5,3		
Flow out/pass	m ³ /h	flow in - production rate	5,1		
Water recovery/pass	%	100 x (production rate - flow in)/flow in	4		
Performance					
Water recovery	%		90	95	98
Product flow	m ³ /day		21,06	22,23	22,93
Product COD	g/l		8,1	10,0	10,6
Product Ca	mg/l		10,0	12,0	15,0
Product Mg	mg/l		5,4	6,3	7,1
Product Na	g/l		12,6	12,6	12,6
Reject flow	m ³ /day		2,34	1,17	0,47
Reject COD	g/l		47	50	78
Reject Ca	mg/l		360	610	1445
Reject Mg	mg/l		31	40	50
Reject Na	g/l		12,6	12,6	12,6

Table 10.6
Batch Nanofiltration Equipment Requirements

Effluent transfer and storage

feed tank
retentate storage tank
product storage tank
cleaning chemicals recirculation and storage tank
transfer piping and valves for effluent transfer from cross-flow microfiltration
transfer piping and valves for feed reticulation in nanofilter
transfer piping and valves for final retentate storage and disposal
transfer piping and valves for product to electrochemical unit
transfer piping for flue gas addition to the system

Nanofiltration modules

cartridge filters and associated pressure controller and control interlock
membrane elements and assemblies
module housings and racks
piping and valves for feed, final retentate and permeate

Pumps

high-pressure pump for reticulation of feed and cleaning solution through modules
pump for transfer of retentate and product
flow and pressure measurement, indication and control of all streams

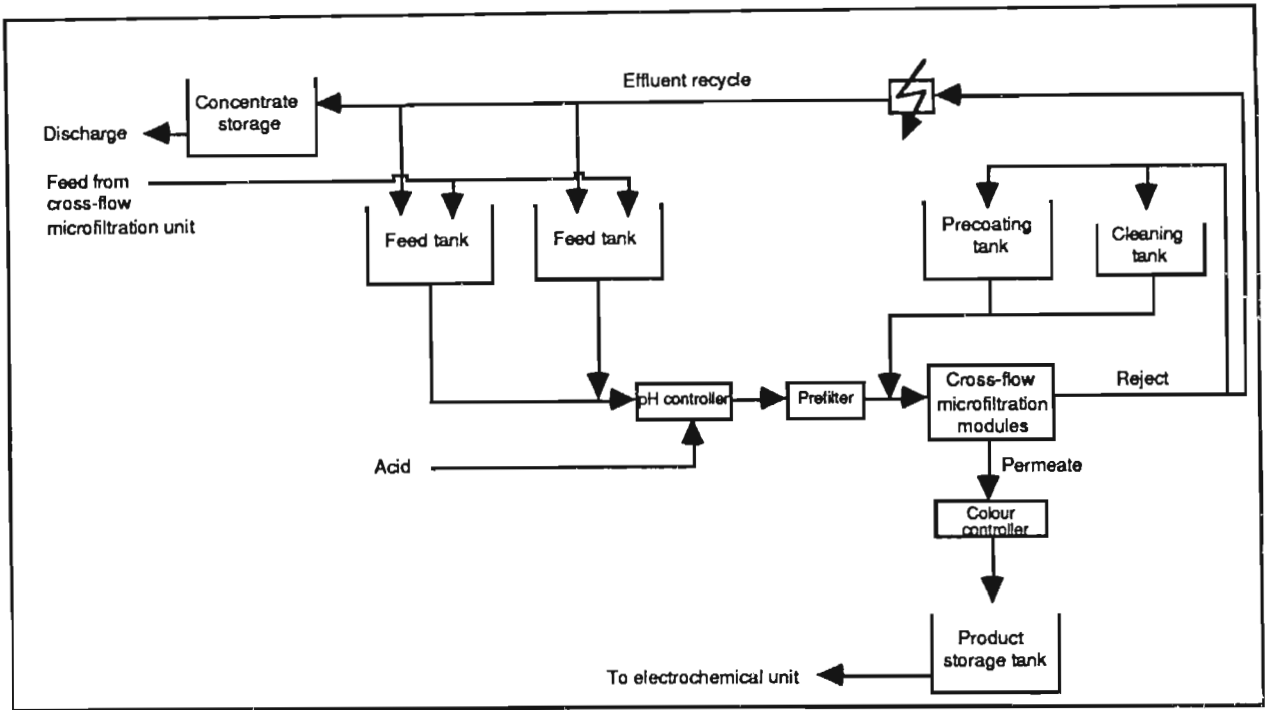
Controls

permeate flow measurement
feed recycle flow controller
pH control of feed to ensure maintenance of desired equilibrium
pump motors, starters and interlocks
high- and low-pressure alarms
low-flux alarm
permeate colour measurement and high alarm
malfunction and alarm control interlocks
control panel

Ancillaries

sampling ports
on-line cooling of recycled streams to maintain feed temperatures of 35 °C

Figure 10.4
Schematic of Batch Nanofiltration Unit



10.6.2. Sizing

Although various membrane configurations are available, the design method for the nanofiltration unit is outlined using spiral-wrap membranes as the module type. The design specification is given in Table 10.7, together with data on predicted performance. A cross-flow microfiltration water recovery of 95 % is assumed for the calculations.

The relationship between membrane flux, J , and the major operating variables is:

$$J = A (P - \Delta\pi) \quad (10.4)$$

where A = the membrane permeability and is a product of the design membrane permeability ($\text{l/m}^2\text{h.MPa}$) and the temperature correction factor ($1.03^{(T-25^\circ\text{C})}$)

P = the pressure differential across the membrane in MPa

$\Delta\pi$ = the osmotic pressure differential across the membrane in MPa

If the pressure of the permeate is assumed to be zero, then P equals the average of the inlet and outlet pressures of each element.

Table 10.7
Nanofiltration: Design Specifications, Calculations and Performance

Parameter	Units	Value		
<u>Design Specifications</u>				
Feed flow	m ³ /day	22,2		
	m ³ /h	1,11		
	l/kg cloth	1,43		
Feed Na concentration	g/l	12,6		
Feed pH		8		
Membrane element area	m ²	6,5		
Design flux	l/m ² h	43		
Pressure	MPa	1,6		
Temperature	°C	35		
Feed COD	g/l	10,0		
Feed Ca	mg/l	12,0		
Feed Mg	mg/l	6,3		
Feed Na	g/l	12,6		
COD rejection	%	97		
Ca rejection	%	80		
Mg rejection	%	70		
Na rejection	%	15		
<u>Design Calculations</u>				
Membrane area	m ²	26		
<u>Performance</u>				
Water recovery	%	90	95	98
Product flow	m ³ /day	20,00	21,12	21,79
Product COD	g/l	0,6	0,8	0,1
Product Ca	mg/l	9,7	11,0	11,9
Product Mg	mg/l	4,0	5,1	6,4
Product Na	g/l	2,8	3,5	4,3
Reject flow	m ³ /day	2,23	1,11	0,44
Reject COD	g/l	94	185	500
Reject Ca	mg/l	39	43	44
Reject Mg	mg/l	83	143	288
Reject Na	g/l	38	60	105

The concentration of ionised species in the feed is an important flux design parameter in any membrane process because of its relationship with osmotic pressure. The major ions present during nanofiltration will be sodium and bicarbonate which are not rejected by the nanofiltration membrane. The osmotic pressure differential across the membrane will be a function of the osmotic pressure of the rejected organic ions and the divalent ions. This will be minimal and flux decline as a result of increased osmotic pressure differentials will be significant.

The maximum achievable water recovery is a function of the applied pressure and the osmotic pressure differential across the membrane, which is in turn a function of the rejection characteristics of the membrane for the ionised species. Since most of the ionised species permeate the nanofiltration membrane in the present application, high water recoveries can be achieved.

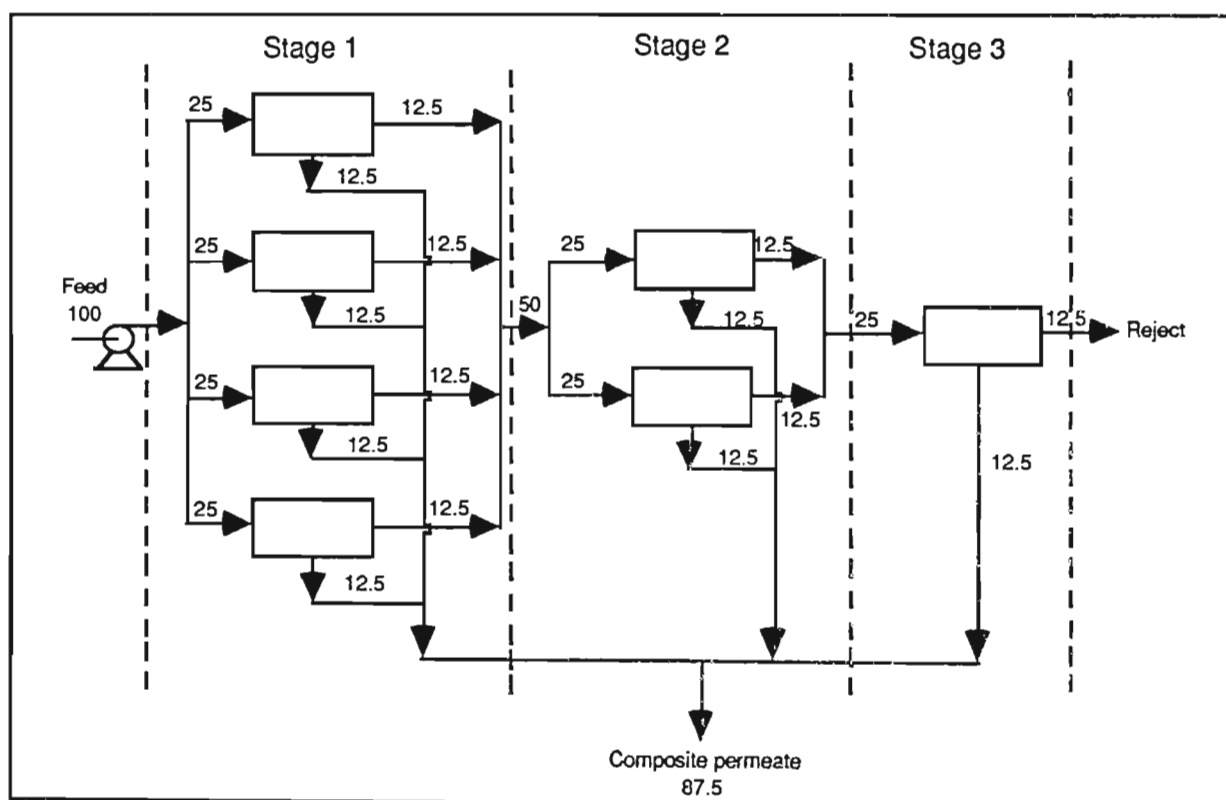
For the design example, the inlet pressure is below the maximum pressure of the membrane to accommodate flux decline during the life-time of the membrane. In the pilot-plant investigation, the membrane permeability of the nanofilter feed at pH 8 was 20 l/m²h.MPa at 25 °C. These values are specific to the membrane used and to the feed pH. Other membranes and different feed pH values will result in different permeability characteristics.

The membrane area requirements are calculated to be 26 m² in Table 10.7. The 100 mm diameter and 1 000 mm long spiral wrap elements have approximately 6,5 m² of membrane area each. Thus four membrane elements of these dimensions are required.

10.6.3. Design Configuration

Spiral modules are normally configured as a staged series-taper plant, as illustrated in Figure 10.5. The modules are arranged to achieve approximately 50 % water recovery per stage. Thus the membrane area per stage is reduced successively by 50 % and this provides for the flow to each stage, in relation to the number of parallel modules per stage, to remain constant. The basic configuration for a three-stage taper plant is 4/2/1, giving approximately 50; 25 and 12,5 % of the overall water recovery in the three stages respectively. The first stage consists of four parallel modules, the second two and the third one.

Figure 10.5
Basic Configuration of Spiral Elements Showing Flows In Arbitrary Units



Each membrane element has a recommended minimum and maximum flow rate. For example, the 100 mm diameter membrane element has a feed rate specification of 0,03 to 0,04 m³/h.m². The design feed flow is 1,1 m³/h and four spiral elements are required. A 3/1 configuration is the closest to the basic configuration described above. The flow to each element in the first stage is 0,37 m³/h, which is within the manufacturer's specification. The minimum flow to the second stage is 0,2 m³/h. Therefore, the maximum water recovery which can be achieved in the first stage is 82 %. Alternatively, the membranes may be arranged in four parallel sets with a flow rate of 0,28 m³/h to each element.

10.6.4. Overall Performance

The composite permeate quality is a function of membrane rejection and water recovery (equation 5.9). The membrane rejection is a function of:

- 1) *pH*. Variations in pH shift the equilibrium position of the inorganic carbon species, thereby changing the membrane rejection.
- 2) *Concentration*. Rejections of organic molecules and chelated cations can increase at high water recoveries as a result of the removal of most of the permeable fraction during initial concentration.
- 3) *Temperature*. Equilibrium positions, and therefore membrane rejections, are a function of temperature.
- 4) *Foulants*. The accumulation of fouling materials in the vicinity of the membrane surface alters the chemical nature of the rejection surface.

Assuming a 95 % water recovery during cross-flow microfiltration, the overall performance of the nanofilter is predicted in Table 10.7.

10.7. Specification of Electrochemical Recovery Unit

10.7.1. Equipment

Electrochemical cell stacks, in a plate-and-frame construction, are supplied by a number of manufacturers according to their own design and may or may not include ancillary pumps, tanks, piping and power source. When selecting equipment, particular attention should be given to the following aspects:

- 1) Mass transport effects which relate to different aspects of cell performance, including the uniformity of current density over the electrode surface and the limiting current density.
- 2) Fluid mechanics of the pipework between the cells, and between the cell stack and other units to minimise pumping costs.
- 3) Distributor design, such that the fluid enters each cell with minimal creation of dead zones and that flow becomes uniform as quickly as possible.
- 4) The relative positions of the anode and cathode, which determines the uniformity of potential distribution.
- 5) The electrode geometry which, together with the local concentration of electroactive species, determines the current distribution. Electrodes may be constructed with slits or louvers, and from expanded metal or metal sheets in a way which minimises the adhesion of gas bubbles to the surface.
- 6) The availability of a high-voltage direct current which is transmitted around the cell stack with minimum energy loss.
- 7) The inclusion of switches which permit individual cells to be isolated for maintenance without disturbing the rest of the stack.
- 8) The arrangement of cells in a way which ensures that the plant is electrically and chemically safe.
- 9) The choice of electrical connection, monopolar or bipolar. In a monopolar cell, there is an external electrical contact to each electrode and the cell voltage is applied between each cathode and anode in parallel. For bipolar connection, there are two external electrical contacts to the two end electrodes. Table 10.8 compares the two configurations (Motani and Saka, 1980). Where bipolar cells are used, shunt current, or current leaks, should be minimised by installing insulating barriers in the electrolyte flow passage.

Table 10.8
Characteristics of Bipolar Cells In Comparison With Monopolar Cells

Characteristic	Bipolar Cells	Monopolar cells
Conditions of electricity	small current, high voltage	large current, low voltage
Cell-to-cell current distribution	uniform	not uniform
Bus bars	between electrolyser (less)	between electrolyser and between cells
Number of nozzles	more	less
Current leaks	more	less
Capacity of electrolyser	easy to enlarge	not easy to enlarge
Floor area of electrolyser	small	large
Assembly and disassembly of electrolyser	simple	complicated
Electric resistance of conductor	small	large
Switch required	high voltage DC circuit breaker	low voltage, large current bypass switch
Preventing gasket leaks	easy	complicated

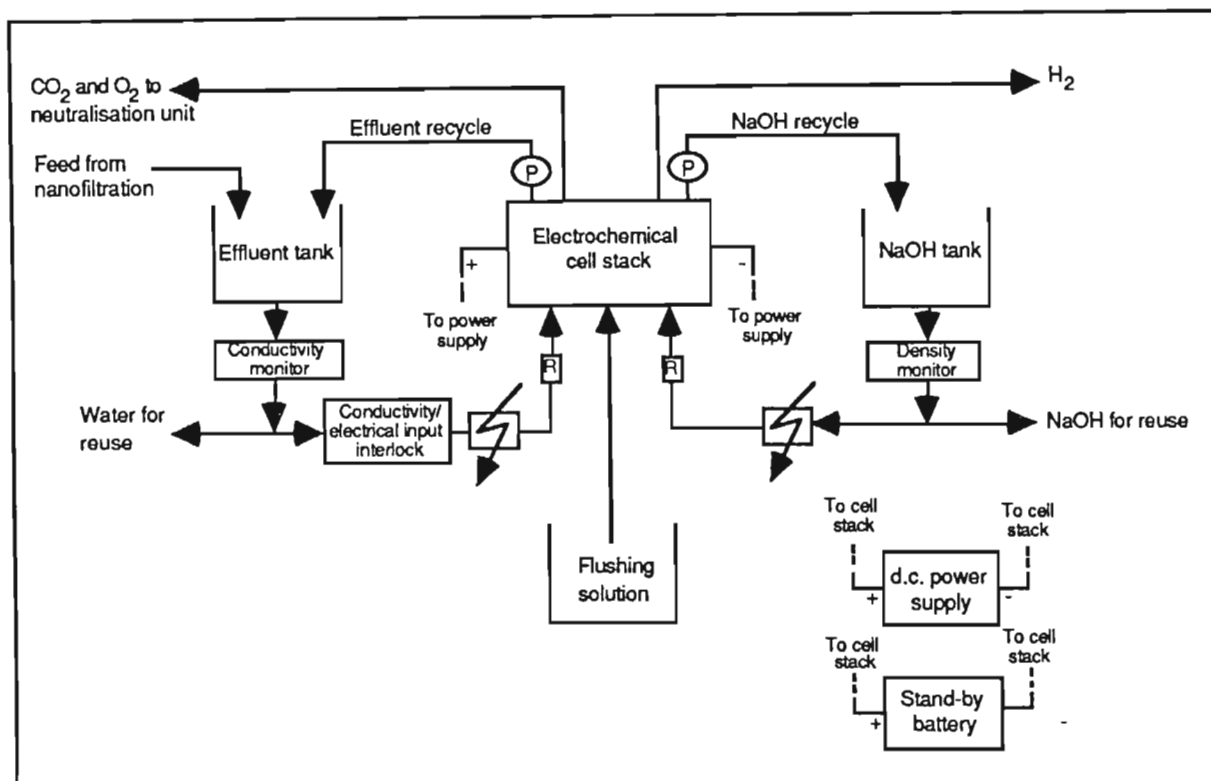
Source: Motani and Saka, 1980

Table 10.9 gives a detailed list of equipment requirements and Figure 10.6 is a schematic of the batch electrochemical recovery unit.

Table 10.9
Batch Electrochemical Unit Specifications

<p><u>Electrolyte transfer and storage</u></p> <p>feed tanks</p> <p>NaOH make-up, storage and batch reticulation tanks</p> <p>depleted brine storage tank</p> <p>concentrated NaOH storage tank</p> <p>flushing solution tank</p> <p>transfer piping for effluent from nanofiltration</p> <p>transfer piping for effluent, NaOH and flushing solution in the electrochemical unit</p> <p>transfer piping to liquid product storage (brine and NaOH) and to factory for reuse</p> <p>transfer piping for carbon dioxide and oxygen gas stream to neutralisation unit</p> <p>transfer piping for hydrogen gas release</p> <p><u>Electrochemical cell stack</u></p> <p>stack frames and gasket assemblies</p> <p>anode, cathode and membrane elements and assemblies</p> <p>electrolyte flow and pressure controllers</p> <p>piping and valves for electrolytes and flushing solutions</p> <p>gas-liquid separation facilities</p> <p>electrical connection points for application of potential</p> <p><u>Electrical power supply</u></p> <p>rectified power facilities sized according to output required</p> <p>ripple prevention facilities, such as tap change, for control on primary side of rectifier</p> <p>battery operated inverter pack for background voltage back-up during power failure</p> <p>electrical output measurement and recording</p> <p>electrical programming to correlate current output to effluent concentration</p> <p>constant voltage operation facilities</p> <p><u>Pumps</u></p> <p>low-pressure pumps for circulation of electrolytes and flushing solutions</p> <p>pumps for transfer of NaOH and depleted brine to storage and factory</p> <p>flow and pressure measurement, indication and control of all streams</p> <p><u>Control</u></p> <p>permeate flow measurement</p> <p>electrolyte flow controllers</p> <p>electrolyte concentration and density controller, with alarms</p> <p>pump motors, starters and interlocks</p> <p>high-pressure alarm</p> <p>low-flow alarm</p> <p>electrical input control with high alarm</p> <p>malfunction and alarm control interlocks</p> <p>electrolyte temperature control with high alarm</p> <p>control panel</p> <p><u>Ancillaries</u></p> <p>sampling ports</p> <p>cooling/heating of electrolytes to maintain temperatures at maximum stable limit of the materials of cell construction</p>

Figure 10.6
Schematic of Batch Electrochemical Unit



Materials of construction must be resistant to the electrolytes. The effluent is not corrosive or abrasive to most materials. However, particular attention should be given to components which come in contact with sodium hydroxide. Rubber components, such as gaskets, may be susceptible to caustic deterioration or embrittlement. The valves and flow meters on the sodium hydroxide line should be carefully selected to function in conditions where solid material may cause blockages. Materials suitable for tanks, piping and cell frames include polypropylene, polyvinyl chloride, poly(vinylidene fluoride) and stainless steel. The former two materials are cheapest, but operational temperatures are restricted to 60 °C. The tank used for storing the flushing and cleaning solutions should be resistant to nitric acid.

The anodes should be constructed from a non-corroding material, stable in the electrolysis environment. They should possess a low overpotential for oxygen generation, with a high current efficiency for water oxidation. Typical materials include titanium substrate, coated with precious metal oxides. Nickel and stainless steel are not suitable for the application. The cathode should be stable under reducing conditions and in the presence of sodium hydroxide. Suitable materials include nickel and stainless or mild steel.

The electromembrane should be stable in sodium hydroxide and selective to the transport of cations in the applicable concentration range.

Electrolyte transfer pumps should perform high-flow, low-pressure duty. The flow rate of the sodium hydroxide in the catholyte compartment should be slightly higher than that of the effluent in the anolyte compartment to maintain a pressure gradient across the membrane.

A cooling system is required to control the temperature of the electrolytes below a maximum limit, dependent on the materials of construction of the unit. If stainless steel is used, the maximum temperature will depend on the electromembrane tolerance. High temperature operation is desirable to increase electromembrane swelling, but temperatures should be controlled to prevent boiling within the structure.

Effluent and dilute sodium hydroxide storage of 6 to 12 h duration is necessary to provide for electromembrane cleaning, minor breakdowns and maintenance. Depleted brine and concentrated sodium hydroxide storage of approximately 12 h are required to allow for factory scheduling. No gas storage facilities need to be provided if the neutralisation unit is operated simultaneously. If the neutralisation unit is shut down, the anolyte gases must be vented to the atmosphere, provided that flue gas is available when the unit becomes operational.

Although various electric current and flow configurations are possible, the design example uses a plate and frame arrangement of individual cells in a cell stack, in which the electrolyte flow to each cell is in parallel and the electric current is in series (bipolar). For this combination, high-flow pumps and a rectifier with a high-voltage, low-current output are required.

Table 10.10 gives the design specifications and operating characteristics of the electrochemical unit. The optimum operating parameters for a given duty are a function of the design of the stack. The specifications in Table 10.10 give typical conditions based on the pilot-plant results, assuming:

- 1) A 95 % water recovery in both filtration stages, or a 90 % overall water recovery in pretreatment;
- 2) A background rinse water concentration of 5 g/l Na;
- 3) The rinsing variables specified in Table 10.2.

Table 10.10
Electrochemical Unit Specifications and Operating Characteristics

Parameter	Units	Value
<u>Design Specifications</u>		
Feed flow	m ³ /day	20,4
	m ³ /h	1,02
	l/kg cloth	1,3
Feed Na concentration	g/l	11,1
NaOH concentration	g/l	150 - 200
Temperature	°C	60
Individual cell area	m ²	1
Electromembrane-electrode gap	mm	2
<u>Operating Characteristics</u>		
Anolyte conductivity	mS/m	3 000 - 5 700
Limiting current density	A/m ²	777 - 1 489
Average anolyte volt drop	V	0,52
Average catholyte conductivity	mS/m	82 000
Average catholyte volt drop	V	0,03
Average cell potential	V	3,6
Electrical requirements	A.s/kg cloth	13,9
Recovered NaOH mass	g/kg cloth (N6)	9,0
Depleted brine flow	l/kg cloth (L7)	1,28
Depleted brine concentration	g/l (C7)	5,86
Area	m ²	9,3
Power	kWh/tonne NaOH	3 169

10.7.2. Sizing

The electrochemical unit is sized according to its predicted performance under defined conditions. Assuming a steady state scouring operation, the performance of the electrochemical unit is a function of many inter-related variables including the:

- 1) Composition and flow of the effluent feed, which in turn depends on the rejection and water recovery of the filtration stages;
- 2) Degree of sodium depletion, which depends on both the selected background concentration of sodium in the wash water and the sodium losses from the system;
- 3) Operating characteristics of the unit including the current density, current efficiency, temperature and voltage which are all related to each other and to the effluent characteristics.

10.8. Synopsis of Design Specifications and Performance

The design example is presented for the case in which the background sodium concentration in the rinse water is 5 g/l and the anolyte is depleted to a sodium concentration of 5,9 g/l. A spread sheet (Appendix 11) was used to compile an example worksheet (Table 10.11) for

the extension of the calculations to include a range of background concentrations, and to illustrate the effect that changing background concentration has on the following parameters:

- 1) *Effluent characteristics.* The effluent and cloth characteristics are a function of rinse water concentration and flow. Figures 4.17 and 4.18 show the effect of rinse water concentration (in the range 0 to 6 g/l) on effluent concentration, and effluent and cloth mass loading.
- 2) *Electromembrane area requirements.* The duty per unit area of electromembrane increases as the final sodium concentration of the depleted brine is increased. Figure 10.7, plotted from data in Table 10.11, illustrates this relationship.
- 3) *Sodium hydroxide make-up requirements.* Sodium losses from the system occur as drag-out in the rinsing process, and retentates from cross-flow microfiltration and nanofiltration. These losses must be balanced by an equivalent input of sodium hydroxide to the impregnator. Although elevated background sodium concentrations are advantageous in terms of the operation of the electrochemical cell, sodium loss from the system (and therefore make-up requirements) increases substantially as the background concentration in the rinse water increases. Figure 10.8 illustrates this relationship. Table 10.11 contains an annex which presents a further extension of the design calculations to cover a range of temperatures between 40 and 100 °C for a background concentration of 5 g/l Na. Figure 10.9 illustrates the relationship between temperature and total electromembrane area requirements.

10.9. Economic Evaluation

Cost estimation of treatment plant is complicated by the variability of the scouring process and effluent composition, and the extent of treatment required. Additional variables include site development costs, exchange rates for imported components, inflation rates and the range of suitable, but different, materials of construction. Cost estimates have been prepared, but are presented for guidance purposes only, to serve as an indication of the cost-effectiveness of the treatment sequence. Table 10.12 presents the cost basis for chemicals and utilities (1987). The design parameters are those specified in Table 10.2.

Table 10.11

Design Example: Process Data on a Dry Fabric Mass Basis, Variable Rinse Water Concentration

Design Parameter		Units	Background Concentration (g/l Na)						
			0	1	2	3	4	5	6
<u>Rinsing Variables</u>									
Moisture content of cloth into range	l/kg cloth	0,5							
Na conc. of moisture on cloth into range	g/l Na	28,8							
Moisture content of cloth out of range	l/kg cloth	0,5							
Na conc. of moisture on cloth out of range	g/l Na	1,3	2,2	3,2	4,1	5,1	6,0	7,0	
Average cloth mass	kg/m	0,3							
Cloth speed	m/h	3000							
Up-time of scouring range	h/d	20,0							
<u>Treatment Plant Variables</u>									
Cross-flow microfiltration water recovery	%	95,0							
Nanofiltration water recovery	%	95,0							
Nanofiltration point Na rejection	%	15,0							
Cell current efficiency	%	75,0							
Cell temperature	°C	60,0							
Cell water transport number	g/g	8,1							
Cell electrolyte length	m	0,002							
Cell catholyte conductivity	S/m	82,0							
Cell decomposition+polarisation+membrane voltage	V	3,0							
Up-time of treatment plant	h/d	20,0							
<u>Rinse Water and Effluent Characteristics</u>									
Na conc. in total rinse water	g/l Na	0,0	1,0	2,0	3,0	4,0	5,0	6,0	
Total rinse water flow	l/kg cloth	1,5	1,5	1,5	1,5	1,5	1,5	1,5	
Effluent flow	l/kg cloth	1,5	1,5	1,5	1,5	1,5	1,5	1,5	
Na conc. in effluent	g/l Na	9,2	9,9	10,5	11,9	11,9	12,6	13,3	
<u>Mass Balance Calculations</u>									
Rinse range:									
Mass Na in on cloth	g/kg cloth	14,4	14,4	14,4	14,4	14,4	14,4	14,4	
Mass Na out on cloth	g/kg cloth	0,6	1,1	1,6	2,1	2,5	3,0	3,5	
Mass Na in effluent	g/kg cloth	13,8	14,8	15,8	16,8	17,8	18,9	19,9	
Cross-flow microfiltration:									
Retentate flow	l/kg cloth	0,1	0,1	0,1	0,1	0,1	0,1	0,1	
Na conc. in retentate	g/l Na	9,2	9,9	10,5	11,2	11,9	12,6	13,3	
Mass Na in retentate	g/kg cloth	0,7	0,7	0,8	0,8	0,9	0,9	1,0	
Permeate flow	l/kg cloth	1,4	1,4	1,4	1,4	1,4	1,4	1,4	
Na conc. in permeate	g/l Na	9,2	9,9	10,5	11,2	11,9	12,6	13,3	
Mass Na in permeate	g/kg cloth	13,1	14,0	15,0	16,0	16,9	17,9	18,9	
Nanofiltration:									
Retentate flow	l/kg cloth	0,1	0,1	0,1	0,1	0,1	0,1	0,1	
Na conc. in retentate	g/l Na	14,4	15,4	16,5	17,6	18,6	19,7	20,8	
Mass Na in retentate	g/kg cloth	1,0	1,1	1,2	1,3	1,3	1,4	1,5	
Permeate flow	l/kg cloth	1,35	1,35	1,35	1,35	1,35	1,35	1,35	
Na conc. in permeate	g/l Na	8,9	9,6	10,2	10,9	11,5	12,2	1,9	
Mass Na in permeate	g/kg cloth	12,0	12,9	13,8	14,7	15,6	16,5	17,4	
Electrochemical cell:									
Mass Na recovered	g/kg cloth	12,0	11,4	10,8	10,2	9,6	9,0	8,4	
Recovered NaOH	l/kg cloth	0,1	0,1	0,1	0,1	0,1	0,1	0,1	
Recovered NaOH conc.	g/l Na	123,5	123,5	123,5	123,5	123,5	123,5	123,5	
Depleted brine flow	g/kg cloth	1,3	1,3	1,3	1,3	1,3	1,3	1,3	
Na conc. depleted brine	g/l Na	0,0	1,2	2,4	3,5	4,7	5,9	7,0	
Na mass depleted brine	g/kg cloth	0,0	1,5	3,0	4,5	6,0	7,5	9,0	
Make-up Na as NaOH	g/kg cloth	2,3	2,9	3,5	4,2	4,8	5,4	6,0	
Make-up water	l/kg cloth	0,2	0,2	0,2	0,2	0,2	0,2	0,2	
<u>Na Losses</u>									
Na loss from drag-out	%	4,3	7,7	11,0	4,3	17,6	21,0	24,3	
Na loss in cross-flow microfiltration retentate	%	4,8	5,1	5,5	5,8	6,2	6,6	6,9	
Na loss in nanofiltration retentate	%	7,1	7,7	8,2	8,7	9,2	9,8	10,3	
Na loss from system	%	16,3	20,4	24,7	28,9	33,1	37,3	41,5	
Savings on existing Na make-up	g/kg cloth	12,0	11,4	10,8	10,2	9,6	9,0	8,4	
	%	83,7	79,6	75,3	70,8	67,0	62,7	58,5	
<u>Water Losses</u>									
Water loss from system	%	16,3	15,9	15,6	15,3	14,9	14,6	14,3	
Savings on existing water make-up	l/kg cloth	1,3	1,3	1,3	1,3	1,3	1,3	1,3	
	%	84,0	84,3	84,7	84,7	85,0	85,3	86,0	
<u>Electrochemical Unit Operating Parameters</u>									
Maximum anolyte conductivity	S/m	4,4	4,7	4,9	5,2	5,5	5,7	6,0	
Minimum anolyte conductivity	S/m	0,0	0,6	1,2	1,8	2,4	3,0	3,5	
Maximum limiting current density	A/m ²	1 137	1 211	1 283	1 353	1 422	1 489	1 555	
Minimum limiting current density	A/m ²	-13	158	322	480	631	777	916	
Average limiting current density	A/m ²	562	685	802	917	1 027	1 133	1 236	
Minimum anolyte volt drop	V	0,5	0,5	0,5	0,5	0,5	0,5	0,5	
Maximum anolyte volt drop	V	0,5	0,5	0,5	0,5	0,5	0,5	0,5	
Average anolyte volt drop	V	0,5	0,5	0,5	0,5	0,5	0,5	0,5	
Average catholyte volt drop	V	0,0	0,0	0,0	0,0	0,0	0,0	0,0	
Average cell potential	V	3,5	3,5	3,5	3,5	3,5	3,5	3,6	
Electrical requirements	V	0,7	0,7	0,8	0,8	0,8	0,8	0,8	
	F/kg cloth								
<u>Electrochemical Unit Area and Power Requirements</u>									
Specific area requirements	m ² /kg cloth	0,002	0,001	0,001	0,001	0,001	0,001	0,001	
Total area requirements	m ²	25,0	19,5	15,7	13,0	10,9	9,3	7,9	
Power requirements for NaOH production	kWh/t NaOH	3 157	3 159	3 162	3 165	3 167	3 169	3 171	

Annexe to Table 10.11

Data calculated for background rinse water Na concentration of 5 g/l.

Design Parameter	Units	Temperature (°C)			
		40	60	80	100
<u>Electrochemical Unit Operating Parameters</u>					
Cell temperature	°C	40,0	60,0	80,0	100,0
Average catholyte conductivity	S/m	55,0	82,0	100,0	130,0
Maximum anolyte conductivity	S/m	4,3	5,7	7,2	8,8
Minimum anolyte conductivity	S/m	2,3	3,0	3,8	4,7
Maximum limiting current density	A/m ²	1 128	1 489	1 863	2 277
Minimum limiting current density	A/m ²	592	777	978	1 222
Average limiting current density	A/m ²	860	1 133	1 421	1 750
Minimum anolyte volt drop	V	0,5	0,5	0,5	0,5
Maximum anolyte volt drop	V	0,5	0,5	0,5	0,5
Average anolyte volt drop	V	0,5	0,5	0,5	0,5
Average catholyte volt drop	V	0,0	0,0	0,0	0,0
Average cell potential	V	3,6	3,5	3,5	3,5
Electrical requirements	F/kg cloth	0,5	0,5	0,5	0,5
<u>Electrochemical Unit Area and Power Requirements</u>					
Specific area requirements	m ² /kg cloth	0,001	0,001	0,000	0,000
Total area requirements	m ²	12,2	9,3	7,4	6,0
Power requirements for NaOH production	kWh/tonne NaOH	3 172	3 169	3 170	3 169

Figure 10.7
Design Example: Dependence of Electromembrane Area Requirements on Rinse Water Concentration (at 60 °C)

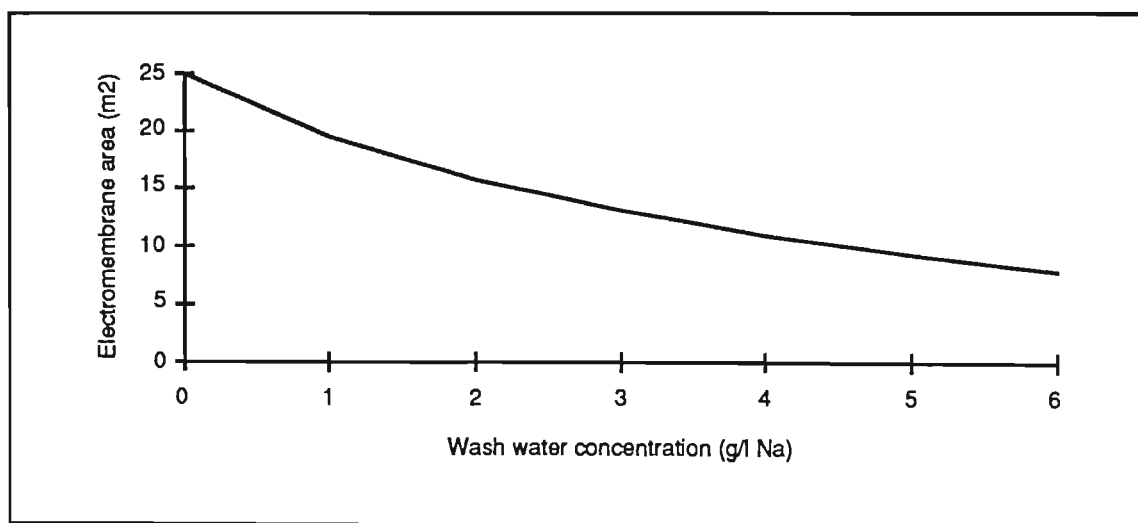


Table 10.12
Typical Costs of Chemicals and Utilities

Chemical/Utility	Cost (1987)
electricity	R0,05/kWh
water	R0,80/m ³
effluent discharge	R0,50/m ³
heat energy	R1,00/m ³ (20 to 100 °C)
sodium hydroxide	R800/tonne 100 % NaOH
limestone	R0,14/kg

Figure 10.8
Design Example: Dependence of Sodium Losses on Rinse Water Concentration

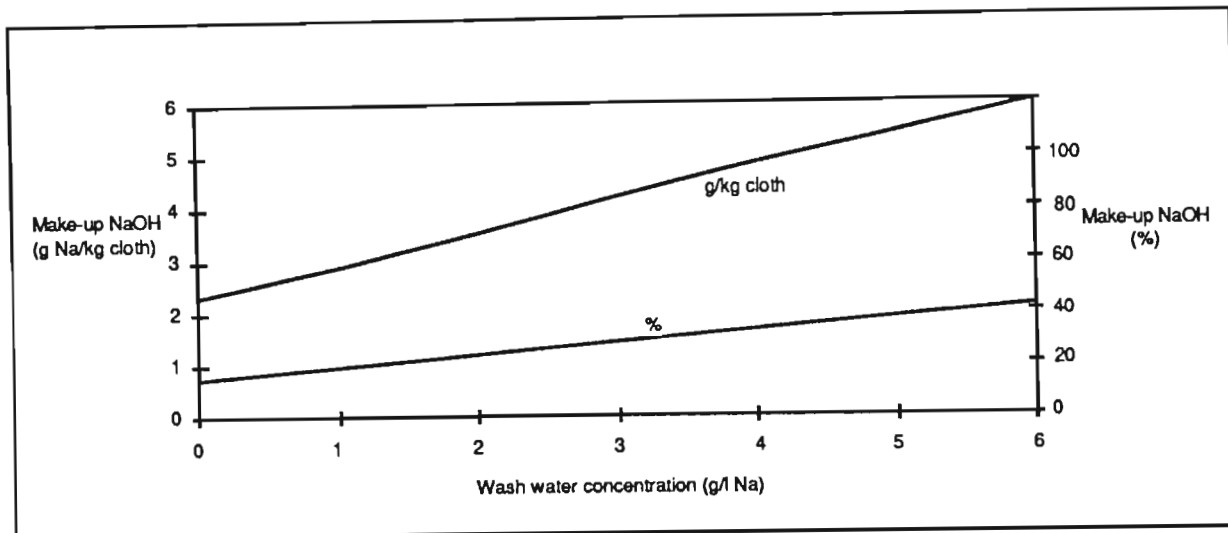
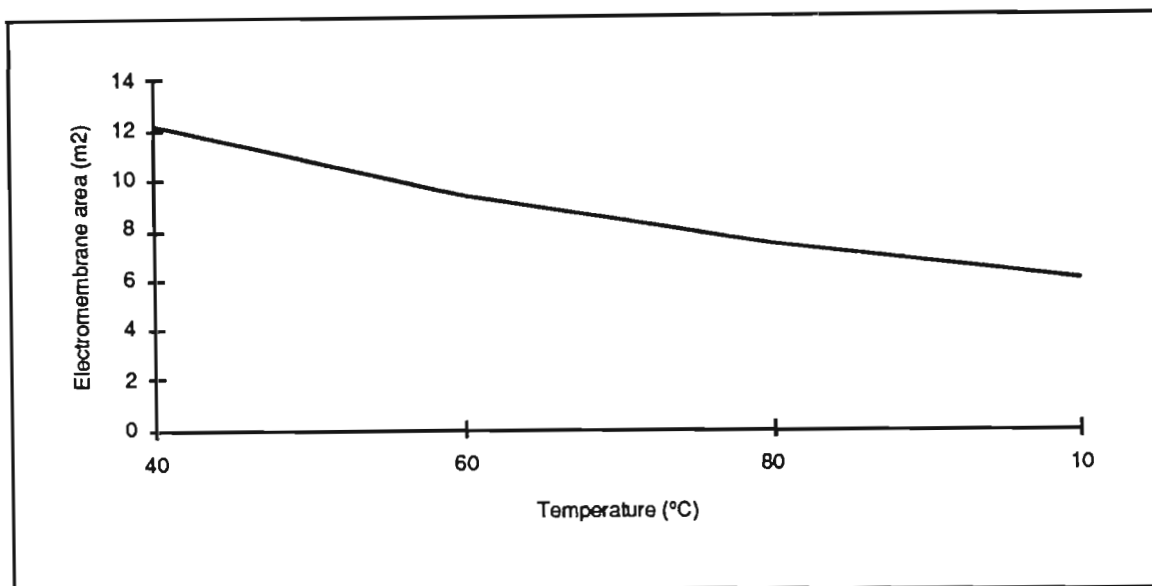


Figure 10.9
Design Example: Dependence of Electromembrane Area Requirements on Temperature



10.9.1. Capital Cost Estimate

Scouring Equipment Modifications

The capital cost for the installation of additional high-expression nip rollers or vacuum extractors is R50 000 to R80 000 per unit (1988). A minimum of two such devices is recommended, the first placed after the impregnator to minimise chemical drag-out, and the second placed after the wash range to minimise impurity and moisture drag-out. It is also

recommended that a third device, installed before the impregnator, would be advantageous in minimising dilution of the padding solution.

Effluent Treatment Plant

The capital cost of the treatment plant depends on various factors as follows:

- 1) Effluent characteristics. For a given chemical loading, a low-volume, high-concentration effluent is desirable when considering plant size.
- 2) Degree of recovery of chemicals and water.
- 3) Means employed for elevating the anolyte sodium concentration in the electrochemical cell. Options include recycling a rinse water which is only partially depleted, or using a concentration technique, such as reverse osmosis or evaporation.
- 4) Materials of plant construction.

Cost estimates of the equipment for the design example (Table 10.2) are summarised in Table 10.13. It is assumed that existing effluent drainage equipment, such as sumps, pumps and pipework, is used.

10.9.2. Operating Costs

A simplistic analysis of the main operating costs is given in Table 10.14. Finance costs and taxation have not been taken into account.

Table 10.13
Capital Cost Estimation (1988)

Equipment	Basis	Cost R
<u>Storage tanks</u>		
8 hour storage of raw effluent	R1 000/m ³	9 600
2 hour storage after neutralisation	R1 000/m ³	2 400
2 hour storage after cross-flow microfiltration	R1 000/m ³	2 400
2 hour storage after nanofiltration	R1 000/m ³	2 400
8 hour depleted brine storage	R1 000/m ³	9 000
8 hour sodium hydroxide storage	R1 000/m ³	1 000
<u>Neutralisation unit</u> pipework, pumps, valves, absorption column, heat exchanger		15 000
<u>Cross-flow microfiltration unit</u> pipework, pumps, valves, controllers, manifolds, filter media	R2 000/m ²	52 000
<u>Nanofiltration unit</u> pipework, pumps, valves, controllers, membranes and membrane holders	R2 000/m ²	52 000
<u>Electrochemical unit</u> DC power supply, pumps, pipework, valves, controllers, electrochemical cell stack	R40 000/m ²	300 000
<u>Scouring machine modifications</u> high-expression nip after impregnator high-expression nip after wash	R 50 000/unit	100 000
Total		545 800

10.9.3. Savings

Table 10.15 summarises the potential savings, based in the cost of utilities given in Table 10.12. The nett savings are calculated as the difference between the total savings and the total operating costs, and amount to R84 870 (1988). Ignoring tax and capital charge considerations, the pay-back time in years, defined as the total capital costs divided by the nett savings is 6,4 years.

Table 10.14
Operating Costs Estimation (1988)

Cost Item	Basis	Total Annual Cost R
<u>Chemicals</u>		
limestone		80
<u>Electricity</u>		
pumping, mixing, etc	0,24 kWh/m ³	430
cross-flow microfiltration	2,2 kWh/m ³	800
nanofiltration	2,5 kWh/m ³	830
electrochemical unit	3 200 kWh/tonne	11 700
<u>Operation</u>		
Plant	2 % of capital	11 000
<u>Maintenance</u>		
absorption column	2 % of capital	300
evaporator	2 % of capital	-
cross-flow microfilter	2 % of capital	1 040
nanofilter	2 % of capital	1 040
electrochemical cell	2 % of capital	6 000
<u>Equipment replacement</u>		
cross-flow microfilter (3 year)	R50/m ² .a	1 300
nanofilter (3 year)	R150/m ² .a	1 275
electromembrane (2 year)	R500/m ² .a	6 000
anode (5 year)	R2 000/m ² .a	12 000
Total		57 170

Table 10.15
Potential Savings (1988)

Savings Item	Basis	Total Annual Savings R
increased nip-expression after impregnator	8,5 g Na/kg cloth	70 960
heat	R1/m ³	6 000
water	R0 80/m ³	4 800
effluent discharge	R0,50/m ³	3 000
sodium hydroxide	R800/tonne	57 200
Total		141 960

SECTION 11

CONCLUSIONS AND RECOMMENDATIONS

The major conclusions of the current work are as follows:

- 1) A broad and multifaceted approach has been successfully applied to solve a real and pressing problem of industrial interest - the development of a commercially viable, legally acceptable, technically feasible and environmentally sound treatment and recovery process for sodium hydroxide scouring effluents from the textile industry. Since these requirements can not be met by any conventional approach, process or operation, the solution had to involve the careful and systematic integration of a series of processing and treatment sub-solutions, which individually do not resolve the problem, but which together combine into a workable and acceptable solution.
- 2) Careful and controlled release of textile waste waters is essential to prevent degradation of the environment by non-biodegradable and mineral components. Waste waters from the scouring of cotton and cotton blends using hot, concentrated sodium hydroxide, have been identified as the most intractable of all effluents from the Textile Industry. The characteristics of these effluents are site-specific, and vary with process parameters, such as water flow, impregnator concentration, rinser design and cloth type. Typically they contribute approximately 25 % of the volume and chemical load of the factory effluent. They are alkaline, containing up to 20 g/l NaOH, have high concentrations of organic materials (up to 20 g/l COD), and contain divalent metal impurities, including calcium and magnesium, at levels typically below 100 mg/l in total. To comply with legal and environmental requirements, these effluents cannot be released directly into receiving water courses.
- 3) Overall management of the scouring process is essential to reduce the impact associated with the disposal of the effluents, and because of escalating costs of purchasing new chemicals and disposing of waste chemicals. The most acceptable overall management system comprises the use of two approaches: waste prevention and minimisation by process-oriented modifications; and waste recycle, treatment and disposal using end-of-line controls. Clearly the latter approach cannot be carried out in isolation. The best practicable solution involves the integration of both approaches, in a way which allows waste handling to be preceded by the comprehensive and effective implementation of a waste minimisation programme. Integration is critical to the success of a treatment process, since the nature of the effluent to be treated, and ultimately its treatability, is dependent on the processing variables.

- 4) The practical application of selected process-oriented waste minimisation considerations can significantly influence scour effluent characteristics and chemical, water and heat consumption. Chemical and water balances over the scouring process, and over the total textile operation, can identify major losses and areas of priority which require attention. Application of rinsing theory to the scouring process allows the most favourable rinsing parameters to be selected and enables rinsing performance and effluent characteristics to be predicted. For example, one case study undertaken indicated that a 77 % savings in water use could be achieved with a reduction in rinsing efficiency of 4,1 %, from 99,8 to 95,7 %, no deterioration in final cloth quality, and a decrease in effluent loading (sodium hydroxide loss) from 22,9 to 13,8 g Na/kg cloth. Annual sodium hydroxide savings were predicted to be 80 tonnes of 100 % NaOH, while effluent volumes were reduced from 38 000 m³ to 8 000 m³.
- 5) While several recycle or treatment technologies are reported in the literature, no commercial installations are known to exist and no researchers have been able to formulate, develop and implement an effective solution, even on a reduced scale. The high sodium ion concentration makes it impossible to treat scouring effluents by conventional processes. The principal methods of handling strong sodium hydroxide scouring effluents include neutralisation prior to disposal to land, water courses, marine environments, or solar evaporation dams. These are considered to be short-term solutions.
- 6) The pilot-plant and supplementary investigations demonstrated the technical feasibility of a four stage treatment sequence of neutralisation, cross-flow microfiltration, nanofiltration and electrochemical recovery to remove colour and impurities, and produce reusable sodium hydroxide and rinse water. The innovation of the process lies not only in the novel way in which four now-commercially available techniques are adapted and applied, but also in the unique way in which they are combined. The chemistry of the individual processes is inter-related, and each stage uses simple adaptations of standard equipment, sometimes operated under non-standard conditions, to achieve the desired recovery and treatment. Since the sequence is a closed-loop recycle system, its operation is closely integrated into the textile process and its performance is dependent on the parameters of scouring and rinsing. The pretreatment stages neutralised the effluent and removed approximately 85 % of the COD, all the colour, 65 % of the organic impurities and calcium compounds, and 50 % of the magnesium compounds. In the final stage, the sodium hydroxide was recovered as a pure solution at a concentration between 100 and 200 g/l. This stream was suitable for reuse in the scouring impregnator. The depleted effluent contained low concentrations of TDS and was suitable for reuse in the scouring rinse range.
- 7) The success and performance of the entire treatment sequence is critically dependent on the chemistry of the inorganic carbon species in solution. Considering carbonate chemistry in the

conventional sense, divalent carbonate ions predominate in solution at high pH values. As the pH of a solution at 25 °C is lowered below 12,8, carbonate ions are converted to monovalent bicarbonate ions, until at pH 8,6 bicarbonate ions predominate. Thereafter, bicarbonate ions exist in equilibrium with carbonic acid. Below pH 4,6, bicarbonate ions cannot exist in significant concentration and carbon dioxide may be lost from the system as carbonic acid dissociates. In practice, this situation is complicated by the fact that a pure sodium carbonate solution will contain eight species in solution, four free ions, two ion complexes and two ion pairs. The addition of small amounts of impurities further complicates the chemistry.

- 8) Carbon dioxide absorption into raw effluent is rapid and complete in the pH range 8 to 14. Efficient recovery of sodium bicarbonate in the nanofiltration stage can only be achieved when the pH of the effluent is lowered to between 8,0 and 8,5.
- 9) Cross-flow microfiltration removed the suspended, particulate and colloidal solids from the neutralised effluent. The reduction in contamination averaged 40 % for COD, 10 % for TS and over 50 % for calcium compounds. The optimum conditions were a feed velocity of 3,0 to 3,5 m/s, with an inlet pressure of 300 kPa, and using a limestone (15 µm) precoat, applied before exposure of the tube surface to the effluent, at a coverage of 100 g/m². Under these conditions, calcium rejections could be increased to above 90 %, and fluxes averaged 50 l/m²h at 20 °C. The most effective cleaning solution for the removal of waxy deposits on the tube surface was a solution containing 20 g/l sodium hydroxide and 1 g/l scouring detergent.
- 10) Although woven cloth cross-flow microfiltration is now commercialised and internationally marketed for a range of water and waste water applications, this work was one of the original studies concerning the use of this membrane technique for treating industrial effluents.
- 11) The nanofiltration stage is critical for removing hardness ion impurities from the pretreated effluent to prolong the life of the electrochemical membrane. Since, in the monovalent form, inorganic carbon species and associated cations readily permeate the nanofiltration membrane and are separated from the effluent contaminants, control of the pH of the feed to the nanofilter is important for successful recovery of sodium. Rejections of sodium decrease from 90 % at pH values above 11 to 15 % at pH 8, and are also dependent on the concentration of ionic species in the feed; rejections of free ionic species decrease with increasing concentration as a result of increased charge shielding of the membrane surface by counter-ions. Rejections of divalent cations follow a similar, but less pronounced, downward trend, with minimum rejections of 60 % at neutral pH. The presence of chelating agents increases rejections by up to 25 %. In the pilot plant trials, COD rejections averaged 90 %. Feed pH is also the most important factor affecting flux. At 25 °C, and at inlet pressures of 1 MPa, fluxes increase sixfold, from 5 to 30 l/m²h, as the

pH of the feed is reduced from 9,7 to 8,0. Membrane cleaning was most effectively achieved using scouring detergent.

- 12) Speciation theory was used to provide details of the species present at thermodynamic equilibrium in the sodium carbonate system at differing pH and concentration, and these details were used to assist in the understanding of the nanofiltration system. Particularly the charged species in solution determine membrane performance during nanofiltration because of the charged nature of the membrane surface. Charge and mass distribution of species are dependent on solution pH and concentration. Using the speciation program, MINTEQA2, it is predicted that, although predominant sodium species is the monovalent cation, Na^+ , it may exist bound in neutral or anionic species. For example, in a sodium carbonate solution, containing 30 g/l Na, 60 % of the Na present exists as a monovalent ion pair, NaCO_3^- at pH 11,5. Similarly bicarbonate and carbonate components exist as neutral species, monovalent anions or divalent anions, the concentration dependent on the pH and overall solution concentration. Of particular importance is the prediction that, in sodium carbonate solutions containing 30 g/l Na at pH 11,5, 80 % of the carbonate component does not exist as a divalent anion, but as a monovalent ion pair, NaCO_3^- . It is predicted that the actual mass and charge distribution therefore has major impact on nanofiltration membrane performance, and that the simple and commonly-used analysis of carbonate solutions presented in 7) above does not adequately describe the nature, charge or concentration of actual species present. Inadequacies are attenuated for solutions of high concentration.
- 13) Speciation adequately predicts the solution chemistry of impure sodium carbonate solutions containing calcium and magnesium salts, with and without the addition of the complexing agent, EDTA. In the absence of EDTA, eight Ca- and Mg-containing species exist at equilibrium, in addition to the eight species in a pure sodium carbonate solution. These are all neutral or positively charged. In the presence of EDTA, an additional eleven EDTA-containing species are predicted to exist, including five metal-EDTA species. The distribution of Ca and Mg between species in the absence of EDTA is very similar, with the free divalent cation dominating at pH below 9 and the ion pairs, CaCO_3 and MgCO_3 , dominating at higher pH values. In the presence of EDTA, there is a marked difference in the chemistry of these two metals. Whereas over 93 % of Ca is bound in the form of the Ca-EDTA complex at all pH values, less than 25 % of Mg is bound in this form. Instead the predominant Mg species at low pH values in Mg^{++} , while MgCO_3 dominants in high pH solutions. These predicted differences in the solution chemistry of Ca and Mg are projected to manifest themselves in the transport characteristics of nanofiltration membranes.

- 14) Qualitative predictions of nanofiltration performance made using speciation and membrane transport modelling were verified experimentally. Osmotic pressure correlations were excellent, and results indicate decreased osmotic pressure of carbonate solutions with decreasing pH and decreasing concentration. This is in accordance with the predictions of speciation theory relating to the colligative properties of solutions.
- 15) The variations of the water permeability constant, A , water fluxes, solute fluxes, and membrane pH gradients with feed pH are explained adequately and accurately by speciation and transport theory. Two important factors for consideration in conditions of changing pH are the variation in chemical species present in solution at equilibrium, and the changes in membrane chemistry, in particular its surface charge density, polymeric structure and permeation properties.
- 16) There is a clear correlation in observed discontinuities of trends in water and solute fluxes with pH, and speciation trends. Discontinuities occur at the cross-over point where the concentration curves of two species of different charges intersect, and are consistent for all solution concentrations. Observations are consistent with solute interaction theories of membrane transport, which predicts that the retention of anions (and associated cations) by a charged membrane increases with the charge on the co-ion, resulting in increased osmotic pressure gradients across the membrane, lower driving forces and lower water and solute fluxes.
- 17) The effects of feed pH on the hydrogen ion gradient across the membrane are dramatic, and discontinuities are again correlated to points of cross-over in the concentration curves of species of different charge densities. Permeate pH values are higher than feed pH values where the feed pH is either very high or near neutral. pH differentials are explained by the tendency of permeating species to re-equilibrate on the permeate side of the membrane to redress the balance between permeating and retained species.
- 18) In the absence of EDTA, slightly increased retentions of Mg above Ca are attributed both to the size of the neutral species and the relative predominance and charge density of the positive species. In the presence of EDTA, Ca retentions are substantially increased at all pH values; although increases in Mg retentions are less, they are still significant. This correlates with the predicted speciation trends - 93 % of Ca exists as a non-permeable species (Ca-EDTA), while only 25 % of Mg exists at this species, and the remaining species either react positively with the membrane (ie are adsorbed) or are neutral and pass freely through the membrane.
- 19) The original study of nanofiltration was one of the first conducted of the nanofiltration process, and resulted in publication of the first paper (Simpson, Kerr and Buckley, 1987) reported in Chemical Abstracts dealing with this technique. This paper has become one of the authoritative

references on the subject. Furthermore, the dual approach of using speciation modelling and transport theory to understand nanofiltration membrane performance is an exciting new approach which offers insight into the quantification of the nanofiltration process.

- 20) The ability of speciation to distinguish between species and quantify the charge and mass distribution is an extremely useful tool in membrane transport modelling. Speciation data, together with experimentally determined parameters were used as input data for developing the transport model PREMSEP. The final model gave very good predictions of water flux and permeate concentration (total species and permeating ions) as functions of feed pressure, flow rate and pH. In particular, the model was able to identify the strong correlation between sodium permeation and feed nitrate ion concentration (the nitrate component had been excluded from consideration in the semi-quantitative examination since it does not speciate significantly into any species other than nitrate ions), predicting similar trends of nitrate concentration, bicarbonate concentration and Na^+ ion and the total sodium concentration as a function of pH. At lower pH values, the nitrate ion is the major anion. Furthermore, of common anions, nitrate ions are least retained by a nanofiltration membrane. Thus, in order to maintain electroneutrality, the passage of nitrate ions enhances the permeation of sodium ions, and especially at lower pH values is the main anion associated with sodium ions in transport through the membrane. In modelling membrane transport of carbonate solutions to simulate accurately actual systems, the model must take consideration of non-speciating nitrate ions.
- 21) The electrochemical recovery stage is considered to be the most critical stage, since the technical and economic viability of the treatment sequence is largely dependent on the ability to recover sodium hydroxide. In addition, little or no evaluation has been undertaken in the past of the application of electrochemical techniques in the current manner. Up to 99 % of the sodium present in the pretreated effluent was recovered as sodium hydroxide. At optimum conditions, current efficiencies are 70 to 80 %, and power consumption 3 500 to 4 000 kWh/tonne 100 % NaOH. The current efficiency for sodium transfer from the anolyte to the catholyte determines the plant size and operational cost. The main sources of current inefficiency result from the passage of current through the electromembrane by cations other than sodium, in particular hydrogen ions, and the migration of anions, in particular that of hydroxides from the catholyte compartment to the anolyte. Hydrogen ion transport is minimised by ensuring that there is a sufficient supply of sodium ions at the electromembrane surface by careful control of current density, current distribution, flow rate and flow distribution. For the pilot plant, concentration polarisation occurred at anolyte flow rates below 20 l/min and when the limiting current density (determined to be $2,6 \times 10^{-3} \times \text{anolyte conductivity}$) was exceeded. Back-migration of hydroxide ions is minimised by maintaining the minimum acceptable concentration gradient across the

electromembrane. Current efficiency and power consumption was also determined to be dependent on electrolyte temperature (and therefore conductivity), the anolyte pH and concentration, and the condition of the electromembrane and electrodes.

- 22) An anode life of four years was predicted if mechanical abrasion by the electromembrane was prevented. Neither nickel nor stainless steel were found to be suitable substitutes for the dimensionally stable anode (DSA), since their rate of corrosion was unacceptably high under the conditions of electrolysis.
- 23) The electromembrane area-resistance was observed to increase with decreasing anolyte concentration. In addition, electromembrane fouling, which occurs as the result of the deposition of insoluble salts of divalent cations, in particular calcium carbonate, on and within the membrane structure, causes increased area-resistance and poor performance. Even in a severely fouled state, however, current efficiencies of 50 % are expected. The ability of calcium carbonate to form on either side of the membrane, and in different crystalline structures (calcite and aragonite) suggests that its formation is controlled by the complex interaction of a number of variables such as current density, temperature, degree of concentration polarisation and back-migration of anions. Formation of scale was accelerated during the pilot-plant trials, since the work was of an investigative nature, conditions were very often non-ideal, and no attempt was made to control or remove deposition as it occurred. Scale loading at the end of the trials was 0,5 g/g electromembrane. Cleaning by soaking the electromembrane in a stirred solution of nitric acid (pH 0,5) for 8 to 10 hours restored current efficiencies to 90 %. It is recommended that in commercial installations, scale formation be minimised by preventing concentration polarisation and controlled by implementation of a routine and effective cleaning cycle.
- 24) Water transport across the electromembrane dilutes the catholyte and reduces the volume of the anolyte. There exists an exponential relationship between the water transport number (or number of moles of water transported per mole of sodium) and the concentration of the anolyte. The water transport number varied from 2 to 35 over the concentration range of the anolyte investigated (0 to 45 g/l Na). No blistering, as a result of a differential of water transport rates across the two polymers comprising the electromembrane, was observed.
- 25) More so than any other factor, the anolyte concentration influences the operation and performance of the electrochemical unit, including current density, current efficiency, water transport, scaling, electromembrane area requirements, and power consumption. Low anolyte concentrations adversely affect operation. Therefore, a system is proposed involving the

closed-loop recycle of rinse water with a background concentration, whereby only pick-up sodium is recovered in the treatment process, and a sodium bicarbonate solution is used for rinsing after scouring.

- 26) The application of electrochemistry to the treatment of scouring effluent is novel in that it uses sodium carbonate solutions in place of sodium chloride, which is itself a previously unexplored diversion from conventional practice, as well as non-conventional operating conditions.
- 27) Because the treatment system is integrated into factory operations, the design of a full-scale treatment plant must consider possible modifications to the scouring process, as well as treatment plant specifications. For the design example, 1,17 m³ of effluent, containing 19 kg of sodium hydroxide, requires treatment every hour. A background concentration of 5 g/l Na is selected, and the rinse range is equipped with high-expression nip rollers before the first bowl and after the last bowl. The plant is designed with 26 m² each of tubular cross-flow microfiltration membranes and spiral wrap nanofiltration elements. Assuming a 95 % water recovery during both prefiltration stages, electromembrane area requirements are 9,3 m². Crude cost estimates indicate that pay-back is 5 to 6 years, with potential savings on heat, water, effluent discharge, and chemicals.

Any future research on this process should address the following objectives:

- 1) Test other cross-flow microfiltration membranes to determine if improved performance (flux and retention of organic compounds and hardness ions) can be obtained.
- 2) Test other nanofiltration membranes to obtain improved separation of sodium salts from organic compounds and hardness ions. It is possible that newer membrane types exist which perform suitably in the presence of suspended and colloidal solids, thus negating the need for a separate cross-flow microfiltration stage.
- 3) Test other electromembranes, anodes and cathodes to determine if higher current efficiencies and current densities can be achieved, at lower power consumptions.
- 4) Carry out long-term, continuous electrolysis trials under conditions which achieve best performance to evaluate the maximum possible lifetime of the DSA coating.

- 5) Test various electromembrane cleaning routines, to develop the best cleaning strategy with respect to chemical use, temperature, current density, frequency and duration which could be implemented at full-scale to ensure prolonged electromembrane life and to control scaling at levels which do not significantly effect cell performance.
- 6) Review existing cell designs as well as designs currently in development to identify the most suitable internal design and flow characteristics for operations involving low concentration anolytes.
- 7) Apply speciation theory to the understanding of the chemistry of anolyte solutions, in particular the behaviour of hardness ions in the presence of complexing agents.
- 8) Investigate more fully two additional process configurations which offer other methods for maintaining a background salt concentration in the closed loop recycle system. One process employs an evaporation stage as the first stage in the treatment process to recover water. This water is combined with the depleted anolyte and returned to the process as waste water. The second process employs a reverse osmosis stage to concentrate the cross-flow microfiltration permeate prior to nanofiltration and electrochemical recovery.
- 9) Determine the feasibility of using the proposed treatment sequence to recover chemicals and water from caustic effluents from other industrial sectors, such as the bottling and pulp and papers sectors, and to treat ion exchange regeneration effluents.
- 10) Investigate the array of new and developing ultrafiltration membranes available to determine the feasibility of using these membranes to directly concentrate the raw scouring effluent (no pH adjustment or cooling) to recover high quality water. The feasibility of the recycling the retentate to the scouring process as padding solution make-up in a diminishing efficiency-multicycle system should be determined and the results compared to those of the treatment sequence presented in this dissertation.

REFERENCES

- Allison, J. D., Brown, D. S. and Novo-Gradac, J. (1991), MINTEQA2/PRODEFA2, A Geochemical Assessment Model for Environmental Systems: Version 3.0 User's Manual. Environmental Research Laboratory, Athens, Georgia, US Environmental Protection Agency.
- Anselme, C., Mandra, V., Baudin, I., Jacangelo, J. G. and Mallevalle, J. (1993), Removal of Total Organic Matters and Micropollutants by membrane Processes in Drinking Water Treatment, *Water Supply*, **11** (3-4, IWSA Specialised Conference on Quality Aspects of Water Supply, 1993), pp. 249 - 258.
- Asawa, T. (1989), Material Properties of Cation Exchange Membranes For Chlor-Alkali Electrolysis, Water Electrolysis and Fuel Cells, *J. Appl. Electrochem.*, **19**(4), pp. 566 - 570.
- ATMI (1973), Recommendations and Comments for the Establishment of Best Practicable Waste Water Control Technology Currently Available for the Textile Industry, Institute of Textile Technology and Hydrosience Inc., USA.
- Austin (1985), J. H., Presented to Third London International Chlorine Symposium of the Society of the Chemical Industry, June .
- Awadalla, F. T., Striez, C. and Lamb, K. (1994), Removal of Ammonium and Nitrate Ions from Mine Effluents by Membrane Technology, *Sep. Sci. Technol.*, **29**(4), pp. 483 - 495.
- BASF Manual (1977), Cellulosic Fibres: Sizing, Pretreatment and Dyeing, Tapp and Toothill Ltd, Leeds, London.
- Bechtold, T., Burtcher, E., Sejkora, G. and Bobleter, O. (1985), Modern Methods of Lye Recovery, *International Textile Bulletin*, Dyeing/Printing/Finishing, pp. 5 - 26, April.
- Benforado, D. M., Ridlehoover, G., and Gores, M. D. (1991), Pollution Prevention - One's Experience, *Chemical Engineering*, pp 130 - 133, Sept.
- Best, H. J. (1984), The Water Amendment Act, 1984, *J. Wat., Sew. and Eff.*, **18**, p. 5, Sept.
- Bhattacharyya, D., Adams, R. and Williams, M. (1989), Separation of Selected Organic and Inorganic Solutes by Low Pressure Reverse Osmosis Membranes, *Biological and Synthetic Membranes*, **292**, pp. 153 - 167.
- Bilstad, T. (1992), Sulphate Separation from Seawater by Nanofiltration, *Environ. Sci. Res.*, **46** (Produced Water), pp. 503 - 509.
- Bleachers Association Ltd, Manchester (1919 - 1920), The Recovery of Caustic Soda from Kier Liquors, Proceedings of Meetings of Managers, etc, Vol I, p. 69.
- Bonomo, L., Bianchi, R., Capra, C., Mezzanotte, V. and Rozzi, A. (1992), Nanofiltration and Reverse Osmosis Treatment of Textile Dye Effluents, *Recent Prog. Genie Proceses*, **6**(20, Technol. Innovantes Epur. Eaux) pp. 327 - 336.
- Brandon, C. A. and Samfield, M. (1978), Application of High-Temperature Hyperfiltration to Unit Textile Processes for Direct Recycle, *Desalination*, **24**, p. 97.
- Brandon, C. A., and Gaddis, J. L. (1977), *Desalination*, **23**, p. 19.
- Brandon, C. A., Gaddis, J. L. and Spencer, G. (1980), Recent Applications of Dynamic membranes, Synthetic Membranes, Vol II, ACS Symposium Series, **154**, American Chemical Society, Washington D. C., p. 435.
- Brandon, C. A., Jernigan, D. A., Gaddis, J. L. and Spencer, H. G. (1981), Closed Cycle Textile Dyeing: Full Scale Renovation of Hot Wash Water by Hyperfiltration, *Desalination*, **39**, p. 301.

Brouckaert, C. A. (1994), Research on the Modelling of Tubular Reverse Osmosis Systems, Draft Final Report to the Water Research Commission (Contract No 325), Pretoria, June.

Brouckaert, C. J., Baddock, L. A. D and Wadley, S. (1994), PREMSEP: A Program for Modelling Pressure Driven Membrane Separation Processes, Pollution Research Group, Dept. of Chemical Engineering, University of Natal, South Africa.

Brouckaert, C. J. (in press), PhD Thesis, University of Natal, South Africa

Brouckaert, C. J., Brouckaert, B. M. and Buckley, C. A. (1993), Prediction of Osmotic Pressure of Inorganic Ionic Solutions from Equilibrium Speciation, Proceedings of the 3rd Biennial Conference of the Water Institute of Southern Africa, pp. 156 - 157, May.

Brown, A. and Buckley, C. A. (1983), Treatment of Cotton Scouring Effluents by Dynamic Membrane Hyperfiltration, Water Research Commission Project No, 122, Report SB 1, Sept.

Brown, D. E. (1983), The Development of Low Overpotential Cathodes, Modern Chlor-Alkali Industry, Vol 2, London, Soc. Chem. Ind., Ch 14.

Buckley, C. A. (1983), Characterisation of Effluents from Scouring and Bleaching of Cotton and Polyester Fibres, Report S7, Department of Chemical Engineering, University of Natal, Sept.

Buckley, C. A. (1984), Literature Survey on the Chlor-Alkali Industry, Department of Chemical Engineering, University of Natal, Durban, Jan.

Buckley, C. A. and Groves, G. R. (1977), Preliminary Report on the Analysis of Washing in the Textile Industry, Report UF1, Pollution Research Group, Department of Chemical Engineering, University of Natal, August .

Buckley, C. A. and Simpson, A. E. (1990a), Closed-Loop Recycle Options for Scouring Effluent, Presented at Symposium on New Technology for Textiles, Port Elizabeth, RSA, 15 - 16 Oct.

Buckley, C. A. and Simpson, A. E. (1990b), Practical Methods in Attaining Reductions in Chemicals, Water and Effluent Loads, Presented at Symposium on New Technology for Textiles, Port Elizabeth, RSA, 15 - 16 Oct.

Buckley, C. A., Bindoff, A., Kerr, C. A., Kerr, A., Simpson, A. E. and Cohen, D. W., The Use of Speciation and X-Ray Techniques for Determining Pretreatment Steps for Desalination, *Desalination*, 66, pp. 327 - 337 (1987).

Buckley, C. A., MacMillan, C. D., Nel, P. F. and Groves, G.R. (1979), Characterisation of the Effluents from the Wet Preparation of Cotton and Cotton/Polyester Fibres, Report S6, Department of Chemical Engineering, University of Natal, Durban, March.

Burney, H. S. and Gantt, G. R. (1983), US Patent 4381230, 26 April.

Butler, J. N. (1982), Carbon Dioxide Equilibria and their Applications, Addison-Wesley Publishing Company, USA, ISBN 0-201-10100-9.

Carleil, C. N. (1993), Biological Degradation of Azo Dyes in an Anaerobic System, MSc (Eng) Dissertation, University of Natal, Durban, South Africa.

CDTRA (1971), Effluent Treatment and Water Conservation, Textile Res. Conf. Leeds, United Kingdom .

Chemex Plc (1991), Pollution Control in Pharmaceutical Production Processes, Draft Report to Her Majesty's Inspectorate of Pollution for Contract No. 7/9/597, Oct.

Cooper, S. G. (1978), The Textile Industry: Environment Control and Energy Conservation, Noyes Data Corp., New Jersey.

- De Witte, J-P. (1992), The Use of FilmTec Nanofiltration Membranes in the Production of Potable Water, Technical Paper, Dow Europe Separation Systems, Springfield House, Cheshire, SK9 5BA, England.
- Department of Planning and the Environment (1978), Energy Utilisation in South Africa, Pretoria.
- Department of Water Affairs (1986), Management of the Water Resources of the Republic of South Africa, ISBN 0 621 11004 3, CTP Book Printers, Cape Town.
- Department of Water Affairs and Forestry (1991), Water Quality Management Policies and Strategies in the RSA, Pretoria, April.
- Department of Water Affairs and Forestry (1993), Water Quality Guidelines for Various Water Uses, Volume 5, Industrial Water Use, Pretoria, ISBN 0-621-15461-X.
- Eilbeck, W. J. and Mattock, G. (1987), Chemical Processes in Waste Water Treatment, Ellis Horwood Ltd., England, ISBN 0-85312-791-3.
- El-Nashar, A. M. (1977), The Desalting and Recycling of Wastewaters from Textile Dyeing Operations Using Reverse Osmosis, *Desalination*, 20, p. 267.
- Eriksson, P. (1988), Water and Salt Transport through Two Types of Polyamide Composite Membranes, *Journal of Membrane Science*, 36, pp. 297.
- Eriksson, P. K. (1988), Nanofiltration, What it is and its Applications, Presented at the 6th Annual Membrane Technology/Planning Conference, Boston, 1 - 3 November.
- Ermakov, P. P., Bakharev, A. V., Striga, S. A. and Goncharenko, S. A. (1990), Electrochemical Removal of Soluble Impurities from Wastewater, *Khim. Prom-st. (Moscow)*, (6), pp. 339 - 340.
- Etablissements Emile Degremont (Associated with Aqua-Aid (Proprietary) Ltd, PO Box 6061, Johannesburg, RSA), Water Treatment Handbook.
- Fane, A. G., Awang, A. R., Bolko, M., Macoun, R., Schofield, R., Shen, Y. R. and Zha, F. (1992), Metal Recovery from Wastewater Using Membranes, *Water Sci. Technol.*, 25(10, Membr. Technol. Wastewater Manage.) pp. 5 - 18.
- Flaschka, H. A. (1964), EDTA Titrations: An Introduction to Theory and Practice, Pergamon Press.
- Fleet, B. (1989), Evolution of Electrochemical Reactor Systems for Metal Recovery and Pollution Control, ACS Symposium Series, 390 (Electrochemistry, Past and Present), American Chemical Society, Washington D. C., 554 - 577.
- Fosberg, T. M. and Claussen, H. L. (1982), *TAPPI*, 65, p. 23.
- Franklin, J. S. Bames, K. and Little, A. H. (1969), Textile Effluent Treatment with Flue Gases, *Ind. Dyer and Textile Printer*, p. 427, Sept.
- Funke, J. W. (1969), A Guide to Water Conservation and Reclamation in Industry, CSIR Guide K9, Pretoria .
- Gaddis, J. L., Spencer, H. G. and Jernign, D. A. (1989), Caustic Recovery and Recycling at a Textile Dyeing and Finishing Plant, Report of National Research Council of Canada, NRCC 29895, Advanced Reverse Osmosis and Ultrafiltration, pp. 347 - 355.
- Gaeta, S. N. and Fedele, U (1991), Recovery of Water and Auxiliary Chemicals from Effluents of Textile Dye Houses, *Desalination*, 83(1-3), pp. 183 - 194.
- Gorzka, Z., Socha, A., Jasinska, K. and Kazmierczak, M. (1991), Electrochemical Purification of Alkaline Solutions After Bleaching of Fabrics, *Environment Science Res.*, 42, pp 621 - 627.

Government Gazette (1984), No. 991, 18 May.

Groves, G. R. and Anderson D. (1977), Characterisation of Effluents from a Small Batch Processing Cotton Textile Mill, Report S1, Department of Chemical Engineering, University of Natal, Durban Dec.

Groves, G. R., Buckley, C. A., Castledon, A., Mercer, H. G., Klug, G. and Hart, O. O. (1983a), Application of Membrane Technology to Industrial Effluent Treatment and Water Recycling, NIWR/IWPC Symposium on Desalination: New Developments in Industrial Applications, Pretoria.

Groves, G. R., Buckley, C. A., Cox, J. M., Kirk, A. R. M., MacMillan, C. D. and Simpson, M. P. J. (1983b), Dynamic Membrane Ultrafiltration and Hyperfiltration for the Treatment of Industrial Effluents for Water Reuse, *Desalination*, **47**, pp. 305 - 312.

Gutman, R. G. (1987), Membrane Filtration: The Technology of Pressure-Driven Cross-Flow Processes, Adam Hilger, Bristol, ISBN 0-85274-522-2

Hagmeyer, G. and Gimbel, R (1993), Rejection of Carbonic Acid Species in (Reverse Osmosis and) Nanofiltration, Conference on Membrane Technology for the Water Industry, Baltimore, Aug 1 - 4.

Harned, H. S. and Davies, R. (1943), The Ionisation Constant of Carbonic Acid in Water and the Solubility of Carbon Dioxide in Water and Aqueous Salt Solutions from 0 to 50 °C, *American Chemical Society Journal*, **65**, p. 2030.

Harned, H. S. and Scholes, S. R. (1941), The Ionisation constant of HCO_3^- from 0 to 50 °C, *American Chemical Society Journal*, **63**, p. 1706.

Hart, G. K. and Messner, S. M. (1991), Iron Removal at the Corkscrew Water Treatment Plant Using Nanofiltration Membranes, *Membr. Technol. Water Ind.*, AWWA Membr. Processes Conf., pp. 139 - 147, American Water Works Association, Denver, Colorado.

Heyde, M. E. and Andersen, J. E. (1975), *Journal of Physical Chemistry*, **79**, p. 1659.

Hiyoshi, T. and Kashiwada, A. (1992), A Method for the Electrolysis of an Alkaline Metal Chloride Using a Cation Exchange Membrane, European Patent Application EP 479392, 8 April.

Hofman, J. A. M. H., Noij, T. H. M., Kruithof, J. C. and Schippers, J. C. (1993), Removal of Pesticides and Other Micropollutants with Membrane Filtration, *Water Supply*, **11** (3-4, IWSA Specialised Conference on Quality Aspects of Water Supply, 1993), pp. 259 - 269.

Holdgate, M. W. (1979), A Perspective of Environmental Pollution, Cambridge University Press.

Hong, Z., Xuan-Rong, Z. and Ji-Fung, L. (1985), The Application of Membr Flash in Reuse of Alkalinous Waste Water, *Desalination*, **56**, p. 121 - 130.

Hora, C. J. and Maloney, D. E. (1977), Nafion® Membranes Structured for High Efficiency Chlor-Alkali Cells, Presented to 152nd National Meeting of the Electrochemical Society, Atlanta, Georgia, 10 - 14 Oct.

Jelen, P., (1991), Pressure-Driven Membrane Processes: Principles and Definitions, New Applied Membrane Processes, 7-14, International Dairy Federation, Brussels, Belgium.

Johnson, J. S., Minturn, R. E. and Wadia, P. H. (1972), Hyperfiltration XXI. Dynamically Formed Hydrrous Zr(IV) Oxide-Polyacrylate Membranes. *J. Electroanal. Chem.*, **37**, pp. 267 - 281.

Jones, A. P. (1974), The Treatment of High Proportions of Textile Effluent in Admixture with Sewage Water Pollution Control, *Wat. Pollut. Control*, p. 551.

Jones, E. L., Alsbaugh, T. A. and Stokes, H. B. (1962), Aerobic Treatment of Textile Mill Waste, *J. Wat. Pollut. Control Fed.*, **34**(5), p. 495.

Jones, H. R. (1973), Pollution Control in the Textile Industry, Noyes Data Corp..

Kennedy, M. (1991), Electrochemical Wastewater Treatment Technology for Textiles, *Am. Dyest. Rep.*, **80**(9), pp. 26, 28, 94.

Kenox Corporation, Wet Oxidation and the Kenox Process; Fundamental Principles and Applications, 350 Consumers Rd, Suite 107, North York, Ontario, Canada.

Kerr, C.A and Buckley, C.A. (1993), A Child's Guide to Chemical Speciation, Presented at the 5th Biennial PC Symposium, SA institution of Chemical Engineers (N-TVL Branch), Conference Centre, University of Pretoria, 21 April.

Kopp, V., Tanghe, N. and Faivre, M. (1993), Tertiary Refining by Nanofiltration of Surface Water in the Paris Region, *Water Supply*, **11** (3-4, IWSA Specialised Conference on Quality Aspects of Water Supply, 1993), pp. 271 - 280.

Lobo, V. M. M. (1984), Electrolyte Solutions: Literature Data on Thermodynamic and Transport Properties, Vol I, Coimbra , Portugal.

Lobo, V. M. M. and Quaresma, J. L. (1981), Electrolyte Solutions: Literature Data on Thermodynamic and Transport Properties, Vol II, Coimbra , pp. 379, 419, Portugal.

Lockwood Greene Engineers Inc. (1975), Textile Industry Water Pollution Abatement Technology: Capabilities and Costs, Report PB 244802, US National Information Service, Aug.

Loewenthal, R. E. and Marais, G. v. R. (1983), Carbonate Chemistry of High Salinity Waters, Water Research Commission Report No. W46, Jan.

Lomax, I. (1994), Dow Europe Separation Systems, Springfield House, Wilmslow, Cheshire, SK9 5BA, England. Personnel communication, 25 May.

Lonsdale, H. K., Pusch, W. and Walch, A. (1975), Donnan-Membrane Effects in Hyperfiltration of Ternary Systems, *Journal of Chemical Society, Faraday Trans.*, **71**, p. 501.

Lozier, J. C. and Carlson, M. (1991), Organics Removal from Eastern US Surface Waters Using Ultra-Low Pressure Membranes, *Membr. Technol. Water Ind.*, AWWA Membr. Processes Conf., pp521 - 544, American Water Works Association, Denver, Colorado.

Maddern, K. N. (1980), Wet Air Oxidation Recovery at Burnie, *ADDITA*, **34**(2), pp. 130 - 134.

Majumdar, A., Singh, V. P. and Thakur, B. D. (1993), Low Cost Treatment of Alkaline Textile Dye Effluent by Flue Gas and Gypsum, *Textile Dyer and Printer*, **26**(5), pp. 23 - 26.

Martin, I. (1991), Cory Puts the Squeeze on Heavy Metals, *Industrial Waste Management*, Feb.

Meissner, W. and Heartel, G (1992), Many Reasons for Electrochemistry in Wastewater Treatment, *Chemical Industry (Dusseldorf)*, **115**(7/8), pp. 17 - 18.

Mickley, M. C. (1985), A Charged Ultrafiltration Membrane Process for Water Softening, *IDA Journal*, **1**(1), pp. 1, March.

Miyake, H., Kaneko, I. and Watakabe, A. (1987), Methods and Electrolytic Cells for Producing an Alkali Metal Hydroxide, European Patent Application EP 229321, 22 July.

Molnar, C. J. and Dorio, M. M. (1977), Effects of Brine Purity on Chlor-Alkali Membrane Cell Performance, Presented to 152nd National Meeting of the Electrochemical Society, Atlanta, Georgia, 10 - 14 Oct.

Morgan, J. E. and Soul, C. M. (1968), The Zimmerman Process in Soda Pulp Mill Recovery System: Development of a Commercial Process, *ADDITA*, **22**, pp. 60 - 70.

Motani, K. and Saka, T. (1980), Modern Chlor-Alkali Technology, Ch 18, The Tokuyama Soda Membrane: Caustic-Chlorine Process, Edited M.O. Coulter, C. Jackson, Ellis Horwood Ltd., UK, Vol 2, pp. 223 - 234, ISBN 0 85312 535 2.

Muldowney G. P. and Runzi, V. L. (1988), A Comparison of the Solute Rejection Models in the Reverse Osmosis Membrane System: Water-Sodium Chloride-Cellulose Acetate, Ind. Eng. Res. Dev., 27, p. 2341.

NCWQ (June 1975), Textile Industry: Technology and Costs of Wastewater Control, NCWQ Contract No. WQ5ACO21, Comm. No. 74391.01.

Neytzell-de Wilde, F. G. (1985), Membrane Fouling in Electrodialysis, Supplement to Water Research Commission Project: Research into the Treatment of Industrial Effluents with High Salinity and Organic Content, University of Natal, March.

Nichols, A. B. (1988), Industry Initiates Source Reduction, *Journal WPCF*, 60(1).

Nielsen, D. W. and Jonsson, G (1994), Bulk-Phase Criteria for Negative Ion Rejection in Nanofiltration of Multicomponent Salt Solutions, *Separation Science and Technology*, 29(9), pp. 1165 - 1182.

Nuortila-Jokinen, J., Luque, S., Kaipia, L. and Nystrom, M. (1993), The Effect of Ultra- and Nanofiltration on the Removal of Disturbing Substances in the Paper Machine Water Circulation System, *BHR Group Conf. Ser. Publ.*, 3(Effective Membrane Processes; New Perspectives), pp. 203 - 213.

Olivier, H. (1980), Our Water Resources in Perspective, *Construction in Southern Africa*, 25(6), p. 71 Sept.

Olthof, H. and Eckenfelder, W. W. (1976), Coagulation of Textile Waste Water, *Textile Chemist and Colourists*, 8(7), pp. 18 - 22.

Parish, G. J. (1965), Continuous Rinsing of Impurities from Textile Fabrics, *Am. Dyest. Rep.*, 54, pp. 402, May.

Patel, R. (1988), Technology Upgradation in Pharmaceutical Production, *Chemical Age of India*, 39(10) .

Pearson, B. (1991), Waste Minimisation and Recycling: Less is More, *Ind. Waste Management*, 1(9), Feb.

Pedersen, S., Cote, P. and Fiessinger, F. (1991), Performance of a Loose RO Membrane for the Removal of Organic Compounds from Fresh Surface Water, *Membr. Technol. Water Ind.*, AWWA Membr. Processes Conf., pp. 603 - 611, American Water Works Association, Denver, Colorado.

Peters, E. J. and Pulver, D. R. (1977), The Commercialisation of Membrane Cells to Produce Chlorine and Caustic Soda, Presented to 152nd National Meeting of the Electrochemical Society, Atlanta, Georgia, 10 - 14 Oct.

Petersen, R. J. (1993), Composite Reverse Osmosis and Nanofiltration Membranes, *Journal of Membrane Science*, 83, pp. 81 - 150.

Pollution Research Group (1983), A Guide for the Planning, Design and Implementation of Waste-Water Treatment Plants in the Textile Industry, Part 1: Closed Loop Treatment/Recycle Systems for Textile Sizing/Desizing Effluents, Report to the Water Research Commission, Pretoria, ISBN 0 908 356 14 5.

Pollution Research Group (1988), A Guide for the Planning, Design and Implementation of Waste-Water Treatment Plants in the Textile Industry, Part 2: Effluent Treatment/Water Recycle Systems for Textile Dyeing and Printing Effluents, Report to the Water Research Commission, Pretoria, ISBN 0 908 356 66 8.

Pollution Research Group (1989), Final Report to the Water Research Commission for the Project "Water Management and Effluent Treatment in the Textile Industry: Treatment of Scouring and Bleaching Effluents", Water Research Commission Project No. 122.

Pollution Research Group (1990), A Guide for the Planning, Design and Implementation of Waste-Water Treatment Plants in the Textile Industry, Part Three, Closed-Loop Treatment/Recycle Options for Textile Scouring, Bleaching and Mercerising Effluents, ISBN 0 947447 80 9, Report to the Water Research Commission (Contract No. 122) , Pretoria.

Porter, J. J. (1971), State of the Art of Textile Waste Treatment, EPA 12090 ECS.

Porter, J.J. and Goodman, G. A. (1984), *Desalination*, **49**, pp. 165.

Pourbaix, M. (1966), Atlas of Electrochemical Equilibria in Aqueous Solutions, Pergamon Press, Oxford.

Prabhu, M. R. (1972), A Theory of Washing and Applications, *Am. Dyest. Rep.*, **61**, p. 53, August.

Raman, L. P., Cheryan, M. and Rajagopalan, N. (1994), Consider Nanofiltration for Separations, *Chemical Engineering Progress*, **90**(3), pp. 68 - 74.

Randall, P. M. (1992), Pollution Prevention Methods in the Surface Coating Industry, *Journal of Hazardous Materials*, **29**, pp. 275 - 295.

Randall, T. L. and Knopp, P. V. (1980), Detoxication of Specific Organic Substances by Wet Oxidation, *J. Wat. Pollut. Control Fed.*, **52**(8), pp. 2117 - 2130.

Rudie, B. J., Ross, G.S., Harrold, S. J. and Paulson, D. J. (1993), Effects of Surface Force Interactions on an NF/UF Membrane, *Desalination*, **90**(1-3) pp. 107 - 118.

Savall, A. and Comninellis, C. (1992), Electrochemical Treatment of Industrial Organic Wastewaters, *Recents Prog. Genie Procedes*, **6**(20, Techol. Innovantes Epur. Eaux), pp. 207 - 214.

Schirg, P and Widmer, F. (1992), Characterisation of Nanofiltration Membranes for the Separation of Aqueous Dye-Salt Solutions, *Desalination*, **89**(1), pp. 89 - 107.

Schoeman, J. J. (1986), Rapid Determination of the Fouling of Electrodialysis Membranes by Industrial Effluents, *Water SA*, **12** (2), pp. 103 - 106.

Schwarzlmüller, A. (1991), Wastewater Neutralisation by Flue Gas: Aspects of Environmentally Friendly and Inexpensive Neutralisation of Alkaline Wastewater in Textile Finishing, *Text. -Prax. Int.*, **46** (5), pp. 450, 453, 454.

Scott, K. (1992), Industrial Waste Water Treatment: An Electrochemical Perspective, Proceedings of the Symposium of the Institute of Chemical Engineers, North West Branch, **3**(3, Integrated Pollution Control Clean Technologies), pp. 6.1 - 6.15.

Sehn, P. (1994), Dow Membrane Technical Engineering Section, Germany. Personal communication, 22 September.

Semenenko I. (1991), Containment in Chemical and Pharmaceutical Processing, *Process Industry Journal*.

Sequeira, C. A. C. and Araujo, L. P. S. (1991), Electrochemical Removal of Environmental Pollutants, *Proceedings of the International Conference on Environmental Pollution*, **2**, pp. 692 - 699.

Sharma, M. S. (1983), *Colourage*, **5**, p. 11.

Shifrin, S. M., Krasnoborod'ko, I. G., Svetashova, E. S., Gubanov, L. N. and Safin, R. S. (1976), Electrochemical Purification of Waste Waters, *Tekst. Prom-st. (Moscow)*, (8), pp. 76 - 78.

Shifrin, S. M., Svetashova, E. S., Krasnoborod'ko, I. G. and Gubanov, L. N. (1975), Improvement in the Electrochemical Decolourisation of Wastewaters from Dyeing-Finishing Plants, *Novye Issled. Setei i Sooruzh. Vodostabzh. i Kanaliz.* (3), pp 94 - 101.

Simmrock, K. H., Griesenbeck, E., Joerissen, J. and Rodermund, R. (1981), Use of Perfluorinated Cation Exchanger Membranes in Electrolysis Processes, Particularly in Alkali Metal Chloride Electrolysis, *Chem; Ing. Tech.*, 53(1), pp. 10 - 25.

Simpson, A. E. and Buckley, C. A. (1987a), The Recovery and Recycling of Sodium Hydroxide Containing Effluents, Presented at the Institute of Water Pollution Control Biennial Conference, Port Elizabeth, South Africa, 12 - 15 May.

Simpson, A. E. and Buckley, C. A. (1987b), The Recovery and Reuse of Sodium Hydroxide from Industrial Effluents, Presented to American Chemical Society, Division of Industrial and Engineering Chemistry Meeting at the Third World Congress of the North American Continent, Toronto, Canada, 5 - 11 June.

Simpson, A. E. and Buckley, C. A. (1987c), The Recovery of Caustic Soda from Caustic Effluents, Presented at the Technology Forum on Effluent Treatment and Chemical Recovery by Electrically Driven Membrane Processes, CSIR Conference Centre, Pretoria, South Africa, 29 June.

Simpson, A. E., and Buckley, C. A. (1987d), The Treatment of Industrial Effluents Containing Sodium Hydroxide to Enable the Reuse of Chemicals and Water, Presented to the 3rd World Congress on Desalination and Water Reuse, Cannes, France, 14 - 17 Sept.

Simpson, A. E., Kerr, C. A. and Buckley, C. A. (1987), The Effect of pH on the Nanofiltration of the Carbonate System in Solution, 3rd World Congress on Desalination and Water Reuse, Cannes, France, 14 - 17 Sept.

Simpson, A. E., Neyzell-de Wilde, F. G. and Buckley, C. A. (1986), Caustic Recovery from Bottling Plant Effluent, Presented to the Coca Cola Water Management Seminar, Rosebank Hotel, Johannesburg, South Africa, 29 Sept. - 2 Oct.

Smart, P. E. (1990), Facing Up to Rising Treatment Charges, *Process Industry Journal*.

Socha, B. (1989), Neutralisation of Alkaline Waste Waters by Flue Gases in a Three-Stage Saturation Process, *Tech. Wlok.*, 38(6), pp. 188 - 190.

Sourirajan, S. and Matsuura, T. (1985), Reverse Osmosis/Ultrafiltration Process Principles, National Research Council, Canada Publications, Ottawa.

Spiegler, K. S. and Kedem, O. (1966), Thermodynamics of Hyperfiltration (Reverse Osmosis): Criteria for Efficient Membranes, *Desalination*, 1, pp. 311 - 326.

Stander, J. v. R. (1987), Fighting SA's Salinity Problem, *SA Waterbulletin*, 13(5), p. 10, Oct.

Strathmann, H. and Kock, K. (1979), Selective Removal of Heavy Metal Ions from Aqueous Solutions, *Recent Developments in Separation Science*, 4, pp. 29 - 38.

Svetashova, E. S., Safin, R. S., Krasnoborod'ko, I. G., Vodop'yan, R. I., Bystrov, V. I., Vasil'ev, E. Y., Yurkov, L. I. and Kubasov, V. L. (1976), *Zh. Prikl. Khim. (Leningrad)*, 49(10), pp. 2244 - 2247.

Textile Federation (1993), Textile Statistics and Economic Review 1992/3, Construction House, Ellis Park, Doornfontein, South Africa.

Timmer, J. M. K., van der Horst, H. C. and Robbertsen, T. (1993), Transport of Lactic Acid Through Reverse Osmosis and Nanofiltration Membranes, *Journal of Membrane Science*, 85(2), pp. 205 - 216.

Treffry-Goatley, K., Buckley, C. A. and Groves, G. R. (1983), Reverse Osmosis Treatment of Textile Dyehouse Effluents, *Desalination*, 47, pp. 313 - 320.

Tsuru, T., Shutou, T., Nakao, S. and Kimura, S. (1994), Peptide and Amino Acid Separation with Nanofiltration Membranes, *Sep. Sci. Technol.*, 29(8), pp. 971 - 984.

Tsuru, T., Urairi, M., Nakao, S. and Kimura, S. (1991), Negative Rejection of Anions in the Loose Reverse Osmosis Separation of Mono- and Divalent Ion Mixtures, Proceedings of the Twelfth International Symposium on Desalination and Water Reuse, Malta, 15 - 18 April.

Uhrich, K. D. and Demmin, T. R. (1988), Electrochemical Treatment of Textile Wastewater, Andco Environmental Processes Inc, Amherst, New York, USA.

US EPA (1974), Economic Analysis of Proposed Effluent Guidelines, Textile Industry, EPA 230/1-73-028, March.

US EPA (1974), Textile Mills: Point Source Category, EPA 440/1-74-022a, June.

US EPA (1978), Environmental Pollution Control: Textile Processing Industry, EPA 625/7-78-002, Oct.

US EPA (1979), Control Technology for the Metal Finishing Industry: Evaporators, Report EPA 625/8-79-002, Developed by the Industrial Environmental Research Laboratory, June.

Van der Vlist, E. (1989), Selective Sequestration and Electrochemical Treatment: Two Novel Methods for Treatment of Industrial Wastewaters, *Eau, Ind., Nuisances*, 129, 69 - 70, 73.

Van Leeuwen, J., Pitt-Pladdy, A., Watson, A., Reddy, P. and Wynne, G. N. (1981), Effluent Treatment at Three South African Textile Mills, NIWR/IWPC Symposium on Industrial Effluent: Control and Treatment, CSIR, Pretoria, Nov.

Von Eysmond, J., Rittner, S., Tapper, A., Holz, J. and Elsner, G. (1993), Purification of the Phosphorus Acid Obtained in the Halogenation of Hydrocarbons, Especially the Chlorination of Fatty Acids, With Phosphorus Trichloride, Ger. Offen.

Voortman, W. J. (1992), An Evaluation of the Technical Feasibility of Removing Ammonium Nitrate from Aqueous Effluents With Electrolysis, MSc (Eng) Dissertation, University of Natal, Durban, South Africa.

Wadley, S. (1994a), Recovery of Brine from Sugar Decolourisation Resin Regeneration Effluent by Nanofiltration, MSc Thesis, Department of Chemical Engineering, University of Natal, King George V Ave, Durban, South Africa.

Wadley, S. (1994b), Applications - Membrane Electrolysis, Presented at African Water Conference, National Exhibition Centre, Johannesburg, 6 - 9 June.

Wadley, S., Brouckaert, C. J., Baddock, L. A. and Buckley, C. A. (1994), Modelling of Nanofiltration Applied to the Recovery of Salt from Waste Brine at a Sugar Decolourisation Plant, Presented at Engineering of Membrane Processes II: Environmental Applications, Il Ciocco, Tuscany, Italy, 26 - 28 April.

Water Research Commission (1976), Master Plan for Water Management and Effluent Treatment, Including Water Recycling and Recovery of Chemicals, Pretoria.

Water Resources Research Institute (1982), Water Conservation Technology in Textiles: State of the Art, Edited by D. M. Hall, W. S. Perkins and J. C. Warman, Report No. WRR 46, May.

Weast, R. C. (1987), CRC Handbook of Chemistry and Physics, First Student Edition, CRC Press Inc, Florida.

Wieslaw, Z. and Bielski, A. (1987a), Neutralisation of Alkaline Textile-Industry Wastewaters Using Carbon Dioxide I, *Przegl. Wlok.*, 41(7), pp. 271 - 273.

- Wieslaw, Z. and Bielski, A. (1987b), Neutralisation of Alkaline Textile-Industry Wastewaters Using Carbon Dioxide II, *Przegl. Wlok.*, **41**(8), pp. 315 - 317.
- Wilcock, A., Brewster, M. and Tincher, W. (1992), Using Electrochemical Technology to Treat Textile Wastewater: Three Case Studies, *Am. Dyest. Rep.*, **81**(8), pp. 15 - 16, 18 - 22.
- WIRA (1973), The Use of Water by the Textile Industry, Textile Res. Conf. WIRA, Leeds, United Kingdom .
- Wissburn, K. F., French, D. M. and Patterson, A. (1954), The True Ionisation Constant of Carbonic Acid in Aqueous Solution From 0 to 45 °C, *J. Phys. Chem.*, **58**, p. 693.
- Yahya, M. T., Cluff, C. B. and Gerba, C. P. (1993), Virus Removal by Slow Sand Filtration and Nanofiltration, *Water Sci. Technol.*, **27**(3-4, Health Related Water Microbiology, 1992), pp. 445 - 448.
- Yeager, H. L. (1982), Transport Properties of Perfluorosulfonate Polymer Membranes, ACS Symposium Series, **180** (Perfluorinated Ionomer Membranes), American Chemical Society, Washington D. C., pp. 41 - 63.
- Yeo, R. S., Chan, S. F. and Lee, J. (1981), Swelling Behaviour of Nafion and Radiation-Grafted Cation Exchange Membranes, *Journal of Membrane Science*, **9**(3), pp. 273 - 283.
- Zaidi, A., Buisson, H., Sourirajan, S. and Wood, H. (1992), Ultra- and Nanofiltration in Advanced Effluent Treatment Schemes for Pollution Control in the Pulp and Paper Industry, *Water Sci. Technol.*, **25**(10, Membr. Technol. Wastewater Manage.) pp. 263 - 276.
- Zimmerman, F. J. (1958), New Disposal Process, *Chemical Engineering*, **56**, pp. 117 - 120, Aug.
- Zimmerman, F. J. and Diddams, D. G. (1960), *TAPPI*, **43**(8), pp. 710 - 715.

NOMENCLATURE

<u>Symbol</u>	<u>Units</u>	<u>Description</u>
A	$\text{l/m}^2\text{h.MPa; l/s.Pa}$	membrane water permeability
a	m^2	area
a_w	-	activity of water
\bar{a}	-	constant reflecting reflection coefficient and potential
B	$\text{kg}^{1/2}/\text{cm.mol}^{1/2}$	parameter in osmotic pressure predictions
b_q	kg/mol	ion specific parameter
C	g/l, kg/m^3	impurity concentration (on fabric or in solution)
c	-	charge number
D	-	diffusion coefficient
d	m	distance
DP	kPa, MPa	pressure drop at ambient temperature
E	V	half cell potential or equilibrium potential
E^0	V	standard electrode potential
F	coulombs/mol	Faraday's constant (96 485)
f	l/kg cloth	specific water use
G	$\text{kg}^{1/2}/\text{mol}^{1/2}$	constant in osmotic pressure predictions (0,509 at 25 °C)
I	mol/kg	ionic strength
i	A	current
J_{sol}	$\text{mol/m}^2\text{s}$	solute flux through membrane
J_v	$\text{mol/m}^2\text{s}$	permeate volume flux
J_w	$\text{m/s; l/m}^2\text{h}$	solvent flux
k	-	rinsing parameter, defined in equation 4.6
k_1, k_2	-	acid dissociation constants
L	m	length
M	m/s	mass transfer (by diffusion) co-efficient (solution diffusion theory)
m	kg/kg cloth	fabric moisture content
m	mol/kg	molality (Section 5)
N	kg/h	sodium mass flow
n_e	-	number of electrons transferred
n	-	number of rinsing bowls ($n = 1, 2, 3...$)
n_w	g water/g sodium	water transport number
ΔP	Pa	transmembrane pressure
p_q	cm	ion size parameter of charged species q

Q	m^3/h	flow
q	-	constant which includes the reflection co-efficient and
potential R	joules/K-mol	universal gas constant 8,314 l.kPa/mol.K
R_{mem}	Ωm^2	electromembrane area resistance
r	-	rinse ratio (refers to rinsing)
r_{diff}	$\text{mol/m}^2.\text{s.n}$	rate of migration of a reactant by diffusion in diffusion layer
r_{mig}	$\text{mol/m}^2.\text{s.n}$	rate of migration of ions
r_{total}	$\text{mol/m}^2.\text{s.n}$	total rate of ion delivery across a diffusion layer
	Ω	electrical resistance
S	g/l	impurity concentration in rinse water or effluent
T	K	absolute temperature
t_+	-	cation transport number
u	$\text{C/m}^2.\text{J.s}$	mobility of species in solution
V	m/s	velocity
v_w	l/mol	molar volume of water (0,018067 at 25 °C)
WR	%	water recovery
X	-	mole fraction
x	m	membrane thickness
x, y, z, a, b	-	dummy variables in matrices for analysis of scour ranges
Z	mol/m^3	membrane charge density
z	-	valence on species
α	-	constant for predicting activity co-efficient of neutral species
β	-	convective coupling co-efficient
δ	m	thickness of the diffusion layer
γ	-	activity coefficient
γ_q	-	activity co-efficient of charged species q
γ_u	-	activity co-efficeint of neutral species u
ϕ	V	potential at any point in the nanofiltration membrane
φ	-	ratio of dissociated functional groups on membrane to fixed ones
σ	%	membrane point retention
θ	m	effective thickness of nanofiltration membrane
Λ	mS/m	conductivity
η	%	current efficiency
π	Pa	osmotic pressure
$\Delta\pi$	MPa	osmotic pressure differential across the membrane
ψ	V	electric potential
{ }	mol/l	activities

Subscripts

0, 1, 2, 3....n, n + 1

a

b

ca

c

cc

d

e

f

in

mem

nc

o

out

p

q

r

s

sol

u

v

w

Description

order of rinse bowl in rinsing sequence

anode/anolyte

bulk solution

cathode/catholyte

concentrate stream (refers to filtration)

cross-flow microfiltration concentrate

drag-out

at electrode surface

feed stream (refers to filtration)

into unit operation

of membrane

nanofiltration concentrate

exchange (current)

leaving unit operation

permeate stream (refers to filtration)

charged species

rinsing water (referring to flow, S)

padding solution/saturator/impregnator

solute

neutral species

permeate volume

water